The cause of coastal erosion on a nourished beach in Kololi, The Gambia

Report M.Sc. Thesis

February 2011

The cause of coastal erosion on a nourished beach in Kololi, The Gambia

Eelco Bijl

M.Sc. Thesis

February 2011

Graduation Committee

Prof. dr. ir. M.J.F. Stive

ir. A.P. Luijendijk

dr. J.E.A. Storms

D. Heijboer MSc.

ir. H. de Vroeg

Haskoning Nederland B.V.
Coastal & Rivers

ROYAL HASKONING

TU Delft Delft University of Technology

PREFACE

The final section of the Master Study program at Delft University of Technology consists of an individual master thesis on a subject related to the specialisation of the student. This Master of Science Thesis was carried out Delft University of Technology and Royal Haskoning from April 2010 to February 2011. The study included two visits to The Gambia in April and September 2010 for the collection of data, introduction to the government of The Gambia and to perform bathymetric and topographic surveys along the coast. These visits were partly sponsored by the Nedeco Fund.

I would like to thank Royal Haskoning and Dirk Heijboer for the opportunity to graduate on such an interesting subject with many different aspects. I would also like to thank the Nedeco Fund for their financial support for the missions to The Gambia for the collection of data. I am also grateful to Royal Haskoning for arranging the accommodation, flights and everything else for my stay in The Gambia.

Furthermore I owe a special thanks to:

My graduation committee, Prof. dr. ir. M.J.F.Stive (Delft University of Technology) for his support and interest in my graduation work; ir. H. de Vroeg (Deltares) and ir. A.P. Luijendijk (Deltares) for their help with the modelling study and reviewing the report; Dr. J.E.A. Storms for his support, interest and help with the sediment characteristics and D. Heijboer MSc. for his support during the study and expertise on the Gambian coast.
Marco Westra for all his technical help and assistance for Matlab and Swan. Salomon Chune and Modu Gaye for all their help and assistance in The Gambia and to introduce me to the Gambian government for the collection of data. Claartje Hoyng and Martijn Lips as my mentors at Royal Haskoning and all my other colleagues at Royal Haskoning for the pleasant time I had during my graduation.

And last but not least I would like to show gratitude to all my friends and family for their support and the good times during my years as a student.

Eelco Bijl,

Delft, February 2011

SHORT SUMMARY

The erosion problem at the Senegambia area (The Gambia) is the subject of this thesis. In November 2003 Royal Haskoning has constructed a beach nourishment of 1,000,000 m^3 as an erosion buffer with a lifetime of 10 to 15 years. In 2010 this nourishment has been eroded almost completely. The processes that drive this high ongoing erosion are not known; therefore two research questions have been defined: (i) What happened to the nourished sand, where has it been transported to? and (ii) Which processes cause the high erosion rate at Kololi Beach?

To gain insight in the coastal processes in front of the Senegambia area field data have been collected and analysed, the nearshore wave climate has been modelled using SWAN and sediment transport capacities and shoreline movements along the coast have been computed using DHI software. The most important results are:

- Nourished sediment contains 10-20% of shell fraction with a maximum of 30% for the lowest quality of sediment. These shell fractions wash out very easily and do not contribute to the total volume of the sediment in case of erosion, increasing the erosion rate.

- Shoreline movement for the 2004-2009 periods has qualitatively the same trend as the shoreline movement for the undisturbed period 1964-1983, however a factor 5 to 8 larger. According to the computations two direction reversal points are present along the coast causing a large area of small accretion and a small area of large erosion.

- The computed net sediment transport is southerly directed between Sheraton and the Senegambia area, north of this area the sediment transport is northerly directed. The water level and a changing wave climate for the period 2007-2009 have a large influence on the sediment transports. These transports have been computed for the recent bathymetry and wave data, which can differ from the conditions between 1964 and 2000.

These results lead to the following conclusions:

- The largest part of the nourishment has been transported to the stretch south of the Senegambia area. The accreted volume along the coast is approximately 50% of the total nourished volume; sediment characteristics of the nourished area and the accreted area are approximately the same when the shell fractions have been disregarded.

- The cause of the high erosion rate at Kololi Beach is an enumeration of multiple processes. The combination of a large amount of shell fractions in the nourished sediment, spatial placement of the nourishment, sand deficit due to sand mining and the effect of sea level rise as the water level has a high influence on sediment transport. A possible changing reef bathymetry and changing wave climate have probably enforced the erosive processes.

- The modelling study on which the conclusions have been based is performed using the present bathymetry and the wave climate from 2000 to 2009. It is possible that both the bathymetry and wave climate have changed over time; this could have large influence on the sediment transport along the coast.

- A Combination of a “hard” structure with initial nourishment in front of the Senegambia area may be considered as a mitigation measure for the present erosion. Re-nourishment in combination with a “hard” protection scheme would solve the short-term erosion problem and the interruption of the alongshore sediment transport could maintain a stable beach.

SUMMARY

PROBLEM

Along the coast of the Gambia there is a trend of slight erosion caused by sediment loss due to alongshore transports. Because of human interference, erosion rates are higher at certain locations such as tourist areas and the capital city Banjul. From 1983 to 1996 volumes up to 150,000 m^3 of sand have been mined from the beaches in front of Bijilo, see Figure 1 for the research area. In 2000 Royal Haskoning executed a Feasibility Study on the erosion problem, based on this study a beach nourishment was constructed at Kololi Beach in front of the Senegambia area. This area contains the largest tourist beach resort in The Gambia, which contribute significantly to the economy of The Gambia. Numerical modelling during the Feasibility Study indicated that a nourishment of 650,000 m^3 would act as an erosion buffer with a lifetime of 10 to 15 years; eventually 1,000,000 m^3 has been nourished. After 7 years the largest part of the nourishment has already been eroded. The erosion rates did not decrease as expected and the stretch in front of the Senegambia area is still eroding with a large rate. If no measures are taken, the beaches in front of the beach resorts will disappear again. The processes which caused the high erosion rates during the last years are not known; a detailed study on the erosive processes is necessary to substantiate short and long term solutions.

Figure 1: Overview research area: from Bald Cape to Kotu

RESEARCH GOALS

To find out why there is such a high erosion rate the following questions will be answered:

- What happened to the nourished sediment, where has it been transported to?
- Which processes cause the high erosion rate at Kololi Beach?

With the knowledge derived from answering the questions more insight will be gained into the processes that drive the ongoing erosion and historical evolution of the coast. Using the research results a prediction will be made on the performance of measures in front of Senegambia area to mitigate the erosion problems.

RESEARCH APPROACH

To answer the research questions and achieve the goals as presented, (historical) field data has been collected, partly in The Gambia. Aerial photographs for different years are available from previous research; hydraulic conditions have been obtained, bathymetric measurements carried out and sediment samples have been taken from the beach in front of Senegambia. These field data have been analysed to determine trends in shoreline movement, sediment budgets, and coastal processes along the coast. Computational models have been used to simulate the nearshore wave climates and morphological processes. The applied models are the SWAN and LITPACK software by DHI. LITPACK has been used to model the sediment transport capacities along the coast; these results have been interpreted and calibrated based on the observed trends in shoreline movement.

RESULTS

Conclusions on the field data analysis are presented below:

- Shoreline movement for the 2004-2009 periods has qualitatively the same trend as the shoreline movement for the undisturbed period 1964-1983, see Figure 2. The trends in 2004-2009 are however a factor 5 to 8 larger, this is for a large part due to the nourishment in 2003. Observed trends show erosion north of Bald Cape and inside the nourishment area and accretion between Sheraton and Bijilo. There is a sediment loss out of the total area between Bald Cape and Kotu of approximately 30,000 m^3/y.

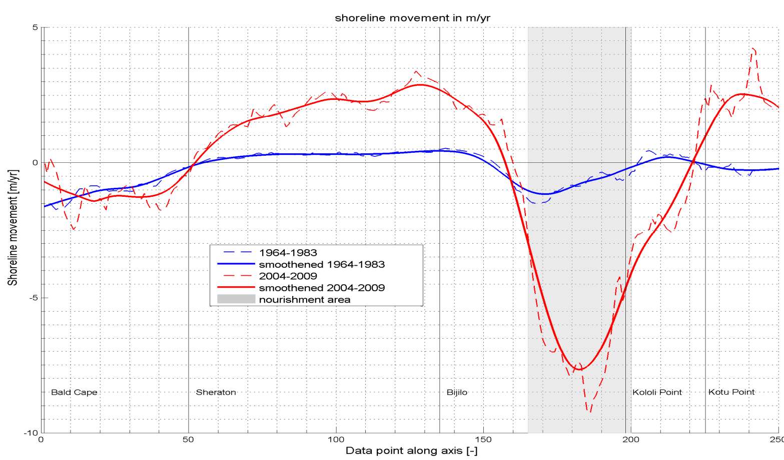

Figure 2: Measured shoreline movement for 1964-1983 and 2004-2009, the nourishment area is in front of the Senegambia area

- Sieve analyses show that the nourished sediment contains a lot of shell fractions which is also clearly visible. The sediment contains 10-20% of shell fraction with a maximum of 30% for the lowest quality of sediment. These shell fractions wash out very easily and do not contribute to the total volume of the sediment in case of erosion, increasing the erosion rate with the same percentage as the volume of shells inside the nourishment.

- Northwest of the Senegambia area off-shore reefs are present in front of Kololi and Kotu points; these outcrops have been created by the presence of the reefs. The reefs contain two distinct very shallow points and some less shallow areas so a complex bathymetry is present in front of Senegambia which influences the nearshore wave climate and resulting sediment transports.

The conclusions on the nearshore wave climates are as presented below:

- Swell waves coming from the south are partially blocked by the large reef in front of Bald Cape. Due to refraction and wave dissipation on the Bald Cape reef a large amount of energy has dissipated and therefore the wave height has decreased behind the reef; see Figure 3 (a) for the wave climate at the reef. Hence the reefs at Bald Cape have a sheltering effect on the research area for swell waves from the south.

- Swell waves coming from the north can propagate freely to The Gambian coast without any obstructions, see Figure 3 (b) for the wave heights behind the reef area. Off-shore swell waves refract yet far away from the coast due to limited water depths; therefore the wave incidence is close to normal on arrival.

- Wind generated waves, which are coming from the north, have a large angle of wave incidence within the research area.

- During low water waves with less energy arrive at the coast due to additional friction caused by the terrace in front of the coast. Also the reef area has a more sheltering effect as the reefs become very close to the sea level, during high water the reefs have less influence on the incoming waves and the wave climate near the coast behind the reef area is rougher.

- Complex refractive patterns are present within the reef area caused by the complex bathymetry. This causes local relatively large differences within the nearshore hydrodynamics. Large alongshore transport gradients can arise behind or at the reefs which are very difficult to model with a 1 Dimensional approach, if possible at all.

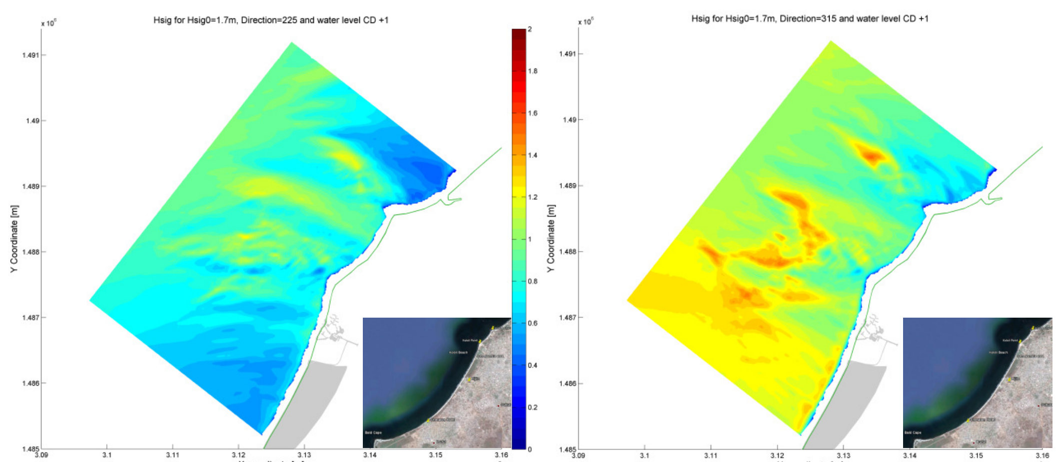

(a) (b)

Figure 3: Significant wave heights in front of the Beach resorts and at the reef area for southern waves (a) and northern waves (b)

The conclusions on the sediment transport analysis are as presented below:

- Interpretation and calibration of the model results is required to account for the effects of reef features and interpolation perturbations of the bathymetry in the area. This is especially the case northeast of Bald Cape, inside the nourishment area and around Kotu and Kololi Point, see Figure 4.

- The computed net sediment transport for swell waves and sea waves is southerly directed between Sheraton and the beach resorts. North of the Senegambia area the sediment transport capacities are northerly directed; the occurring sediment transports behind the reef area are much lower than the transport capacities due to a hardened seabed.

- A higher water level causes higher sediment transport along the coast and also higher erosion and accretion rates, see Figure 5. The erosion rate during high water is more than 1.5 times the erosion rate for mean sea level. This can be of large influence in case of sea level rise, especially for longer periods. The reef area looses a part of its sheltering effect during high water and the bottom friction on waves is less, causing higher erosion rates. This effect would also be present or even larger when the reefs would be slowly eroding or subsiding.

- A so-called 'morphological zero point' is computed in front of the Senegambia area. The modelling study shows that the sediment transport direction changes from southerly to northerly transport in front of the Senegambia area. Further calibration for of the sediment transport direction by adjusting the coastline equilibrium orientation causes this transport reversal point to move along the coast.

- A changing wave climate for the years 2007 – 2009 causes more northerly directed transport along the entire coast, in front of Senegambia this northern transport is less and north of Kololi Point the northern transport is clearly higher again, causing larger gradient as can be seen in Figure 6.

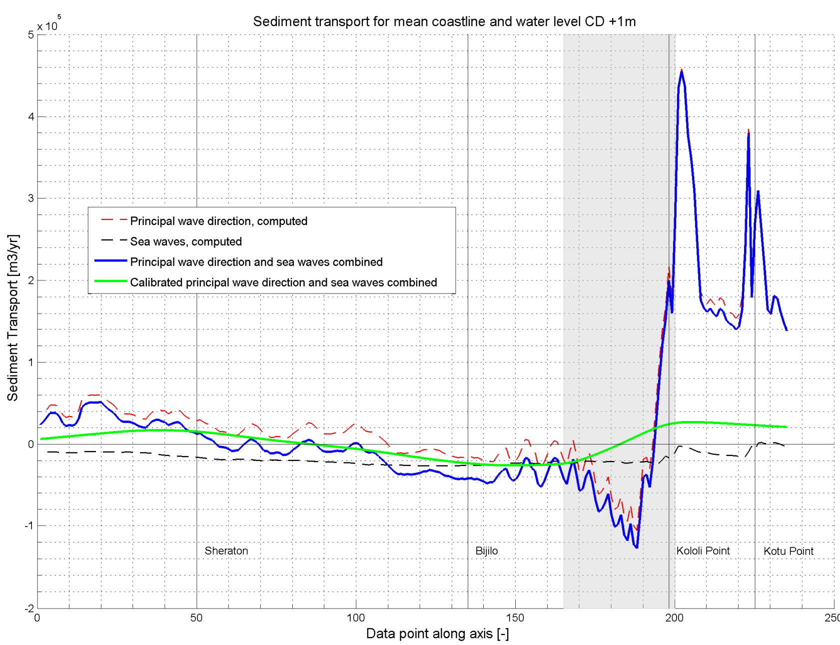

Figure 4: Sediment transport for mean coastline and water level CD+1

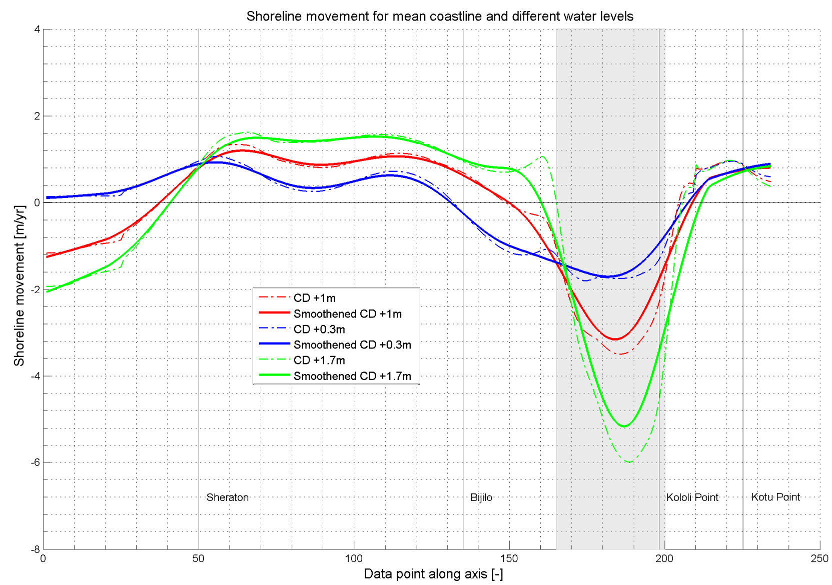

Figure 5 Shoreline Movement for different water levels

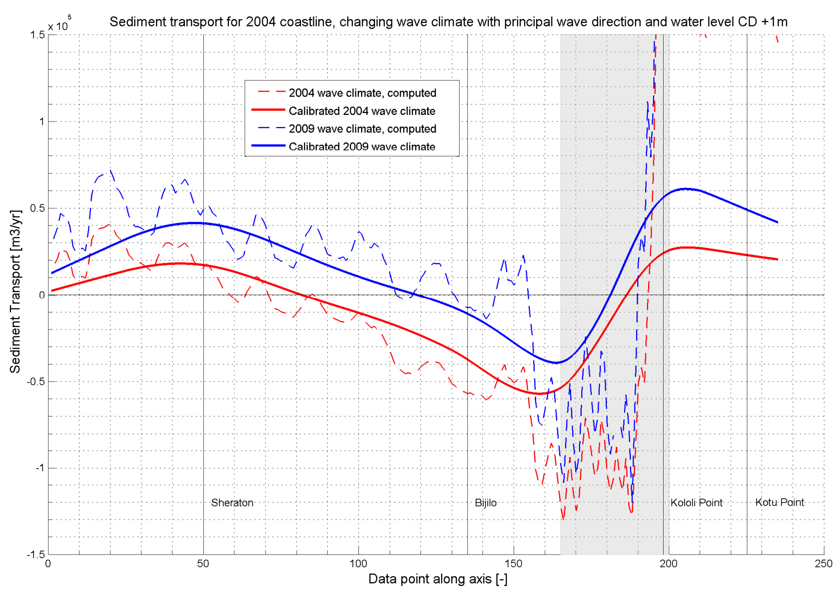

Figure 6: Sediment transport for different wave climates

Conclusions

These results lead to the following conclusions:

- The sediment transport modelling substantiates the observed trends in shoreline movement in a qualitative way; not in a quantitative way. A small trend of erosion is present north of Bald Cape, dependent on the outlet of the Tanji River. From Sheraton the northerly alongshore transport decreases and turns gradually to a southern alongshore transport causing accretion between Sheraton and Bijilo Park. Inside the nourishment area the alongshore transport changes to the northern direction again, causing erosion in front of the Senegambia area.

- The largest part of the nourishment has been transported to the stretch south of the Senegambia area. The accreted volume along the coast is approximately 50% of the total nourished volume; sediment characteristics are approximately the same when the shell fractions have been disregarded. Initially also large accretion was present north of Kololi Point due to local flow patterns caused by the reef area and the outcrop; this effect has been reinforced due to the a high amount of sediment in the northern part of the nourishment.

- The cause of the high erosion rate at Kololi Beach is an enumeration of multiple processes. The combination of a large amount of shell fractions in the nourished sediment, shape of the nourishment, sand deficit due to sand mining and the effect of sea level rise as the water level has a high influence A possible changing reef bathymetry and changing wave climate have probably enforced the erosive processes.

- Erosion inside the nourishment area is very high for the 2003 coastline orientation; namely of the order of -25 m/yr. This erosion rate is already much smaller for the 2004 coastline orientation. The averaged computed erosion rate for the calibrated 2004 and 2009 coastline orientation is approximately 7 m/yr. The computed present erosion rate in front of Senegambia is of the order of 3 m/yr. The 2003 and 2004 coastline orientations furthermore show relative large accretion south of the nourishment area.

- The modelling study on which the conclusions have been based is performed using the present bathymetry and the wave climate from 2000 to 2009. It is possible that both the bathymetry and wave climate are changing over time. This would have a large influence on the sediment transport along the coast.

- A Combination of a “hard” structure with initial nourishment in front of the Senegambia area will probably be a good mitigation measure for the present erosion. Re-nourishment in combination with a “hard” protection scheme would solve the short-term erosion problem; interruption of the alongshore sediment transport could maintain a stable beach.

RECOMMENDATIONS

- Secondary flows and local wave climates inside the reef area are of a great importance on the erosion in front of the Senegambia area. Therefore it is advised to use a 2-Dimensional model to investigate these nearshore hydrodynamics and gain quantitative insight in the sediment transports in front of the Senegambia area. This model can then be used for more research on the application of a protection scheme.

- To gain more quantitative insight into the alongshore sediment transport it is suggested to collect more data along the coast and from the reef area at fixed times throughout the year. By measuring the location of the coastline, cross-shore profiles along the coast and the reef are, the state of the beaches and the reefs can be closely monitored and the data is very useful for future research.

- The nourished sediment contains a lot of shells and shell fractions. These shell fractions wash out of the sediment and do not contribute to the stability, no further information on shells in nourished sediment is present. The beach scarp at Kololi Beach has also been caused by cementation of the shell fractions. More research is needed on the influence of the shells on the erosion and stability of a beach.

CONTENTS

1. Introduction 1

1.1 General introduction 1

1.2 Erosion problem 2

1.3 Coastal Protection Project 3

1.4 Problem Definition: 6

1.5 Research Questions 7

1.6 Hypotheses 7

1.7 Methodology 8

1.8 Thesis Outline 9

2. Previous related studies and projects 11

2.1 Feasibility Study 2000 11

2.1.1 Introduction 11

2.1.2 Coastal erosion 11

2.1.3 Numerical modelling during the Feasibility Study 12

2.2 Sand search campaign 16

2.3 Design and construction Kololi Beach 17

2.3.1 Design 17

2.3.2 Construction 19

3. Site Conditions 21

3.1 General 21

3.2 Rivers in The Gambia 23

3.3 Wind and wave data 24

3.3.1 Wind 25

3.3.2 Waves 26

3.4 Tide 30

3.5 Bathymetry 31

3.6 Coastal Processes 35

3.6.1 Nearshore wave processes 35

3.6.2 Sediment transport processes 36

3.6.3 Other processes 37

4. Field data analysis 39
4.1 Trends in shoreline movement 39
4.1.1 Method 40
4.1.2 Results 43
4.1.3 Comparison with the 2000 Feasibility Study 46
4.2 Sediment budget 48
4.3 Sediment characteristics 50
4.4 Observed coastal processes 52
4.4.1 Coastal profiles 52
4.4.2 Construction of the nourishment 54
4.4.3 Rip current 55
4.5 Conclusions 56
4.5.1 Conclusions on observed trends and coastal processes 56
4.5.2 Design modelling study 57

5. Nearshore Wave Climate 59
5.1 Model set up 59
5.2 Results 66
5.2.1 Swell Conditions 66
5.2.2 Wind Conditions 71
5.2.3 High and low water level 74
5.3 Conclusions 75

6. Sediment Transport Analysis 77
6.1 Modelling software and theory 77
6.2 Model Set-up 79
6.2.1 Model settings 79
6.2.2 Modelling runs 84
6.3 Results 85
6.4 Discussion 94
6.4.1 Calibration for alongshore sediment transport calculations 94
6.4.2 Influence of different processes 97
6.4.3 S-ϕ curves 105
6.5 Conclusions 105

7. Mitigation measures 107
7.1 Zero option 107
7.2 "Hard" Solutions 107
7.2.1 Groynes 108
7.2.2 Near shore or Detached Breakwaters 109
7.2.3 Revetment or sea wall 110
7.3 "Soft" Solutions 111
7.4 Recommendations 112

8. Conclusions and recommendations 115
8.1 Conclusions based on the research questions 115
8.2 Conclusions on the hypotheses 116
8.3 Recommendations 118

Bibliography 121
List of Figures 123
List of Tables 128

Appendix A: Bathymetric Survey 131
April 2010 131
September 2010 134
Appendix B: Sand search campaign locations and results 135
Appendix C: Wave data 141
Appendix D: SWAN Results 153
Appendix E: Report Figures 161

1. INTRODUCTION

1.1 GENERAL INTRODUCTION

The Gambia is a country located on the western side of Africa, see Figure 1-1. It is the smallest country on the African mainland and is bordered by Senegal in the north, east and south and has a small coast on the Atlantic Ocean in the west. The Gambia is very narrow and the borders follow the meandering Gambia River.

Figure 1-1: Map of Africa

The country is less than 50 km wide at its widest point and approximately 325 km long. The coastal zone stretches from Buniada Point in the north to the mouth of the Allahein River in the south. The open coastline measures approximately 70 km and consists of sandy shores, cliffs and to lesser extent mangrove wetlands. Just some 20 km of the coastline is significantly developed including Banjul (capital city), Cape Point, Bakau, Fajara and the Tourism Development Areas (TDA) around Kololi and Kotu, see Figure 1-2. The locations which are indicated in the figure will be used as points of reference in the remainder of the report. The largest TDA is the Senegambia area with adjacent Kololi Beach. The Senegambia area houses the largest tourist resorts and a district with restaurants, bars and shops. Elsewhere the coastline is largely underdeveloped, except for some fish landing sites and cold storage infrastructure for fisheries.

The coastal zone contributes significantly to the economy of The Gambia. From October to May, The Gambia receives more than 100,000 tourists; all the beach resorts are operational and the industry employs about 7,000 persons. The climate of The Gambia is sub-tropical; from June till October is the period of hot weather and a rainy season. From November until May, it is dry and the temperatures are cooler, this climate is very attractive and therefore this period is high tourism season in The Gambia.

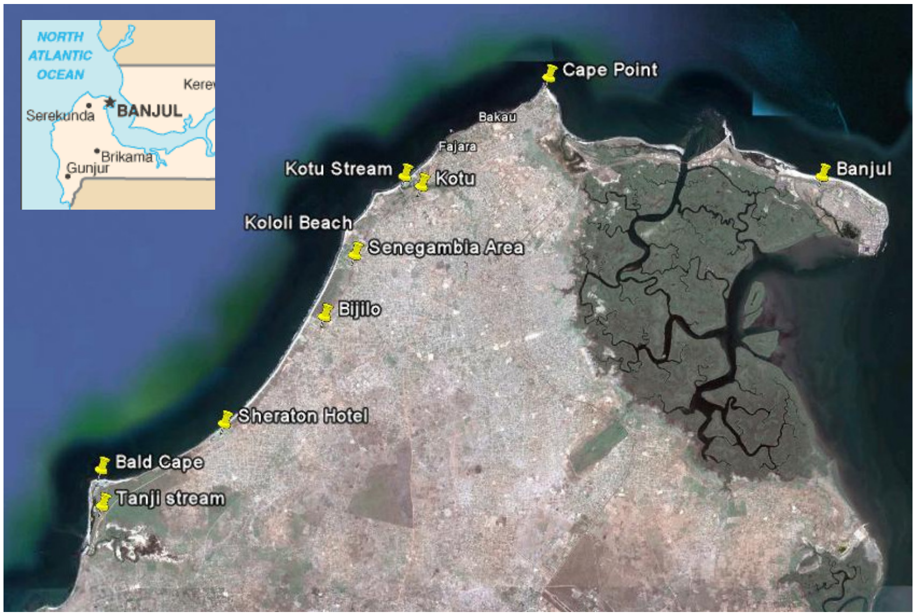

Figure 1-2: Map of west-Gambia

1.2 EROSION PROBLEM

There is a trend of slight erosion along the coast of The Gambia caused by sediment loss by alongshore transport to the south, to the river Gambia which acts as a sediment trap and on the other hand by sea level rise. The natural erosion rate due to above mechanisms is generally small. However, because of human interference different coastal processes explained later in this report, erosion rates are higher at certain locations such as tourist areas and the capital city Banjul.

Measures to combat the coastal erosion have been implemented since the mid-fifties. Most of them, implemented either by the private sector or by the Government, were on ad-hoc basis. In 1957 groynes, constructed with rhum tree piles and concrete panels were constructed west of Banjul. Later, similar protection measures have been placed at several places along the coast between Cape Point and Banjul. Most of them have become ineffective, if not already from the start, then due to lack of maintenance.

In the nineties, coastal erosion of The Gambia coast becomes more and more a serious threat. Delft Hydraulics raised the matter in 1994 with DHI, in 1996 with the Department of Water Resources in Banjul, and also with UNEP/FAO/PAP in 1998. Especially Banjul and the Senegambia area suffer from the erosion problem. The erosion is clearly visible at the beaches which have almost completely vanished. As tourists especially come for the climate during winter, the beaches are of utmost importance for The Gambia. The condition of the beaches in 2002 can be seen in Figure 1-3.

Figure 1-3: Kololi Beach in front of Senegambia Beach Resort (2002)

ENVIRONMENTAL ACTION PLAN

In 1992 The Gambian Government, with the assistance of the United Nations Development Program (UNDP) and the Government of the Netherlands, launched an Environmental Action Plan (GEAP), emphasizing the importance of the tourist industry and the need to safeguard the country's beaches and coastal infrastructure. The GEAP represents the commitment of the Government of The Gambia to sound environmental management and is an integral component of the Government's Program for Sustained Development (PSD). In 1996 the Government issued the draft of an Integrated Coastal Area Management Plan, emphasizing the importance to ensure cross-sector considerations to the coastal erosion issue.

In 2000 Royal Haskoning executed a Feasibility Study of the erosion problem of The Gambian Coast. Based on this Feasibility Report a detailed design of protection works has been carried out for several locations. The project locations were based on an assessment of economic, social and cultural coastal values. The extend of the protection works to be implemented was based on available funds. Construction of the works was started in July 2003 and was completed in April 2004.

1.3 COASTAL PROTECTION PROJECT

Based on the Feasibility Study of 2000, a detailed design of protection works has been carried out for the Banjul area, Cape Point, Bakau and Kololi Beach. These works consisted of beach nourishment and redistribution of a sand spit at Banjul, placing 5 groynes at Cape Point, a T-groyne at Bakau and beach nourishment at Kololi Beach. The completed works at the Banjul area and Cape point area are performing very well. The beach nourishment at Kololi on the other hand, is still suffering from high erosion rates. For this reason, the nourished beach at Kololi will be discussed in this study, see Figure 1-4 for the research area.

Figure 1-4: Location Kololi Beach

KOLOLI BEACH

The main function of the beach nourishment was to protect the infrastructure behind the beach; the nourished beach should act as an erosion buffer. The nourishment has been designed for the protection of the Kairaba and Senegambia beach resort, the 2 largest tourist hotels in the Senegambia area. Adjacent hotels and bars will also benefit since the nourishment will spread out and feed the adjacent coastal stretches. The nourishment was designed on the basis of a recurrence of 10 to 15 years. An initial nourishment of 650,000 m^3 was recommended but because of the high initial costs, 1,000,000 m^3 was nourished. The nourishment extended over a distance of approximately 1,500 m, see Figure 1-5. During the first year the beach width would be approximately 80 m. It should be noted that immediately after nourishment the beach width might be considerably wider, since the nourished profiles are placed under a slope considerably steeper than the natural profile. This implies that relatively more sand is placed in the upper part of the profile, which will rapidly be transported by the waves to deeper parts of the profile to restore the natural profile. At the southern and northern transition of the nourishment to the existing coast, relatively large transport gradients will occur. To create a smooth connection to the beach, the nourishment has been extended on both sides of the main facilities that must be protected.

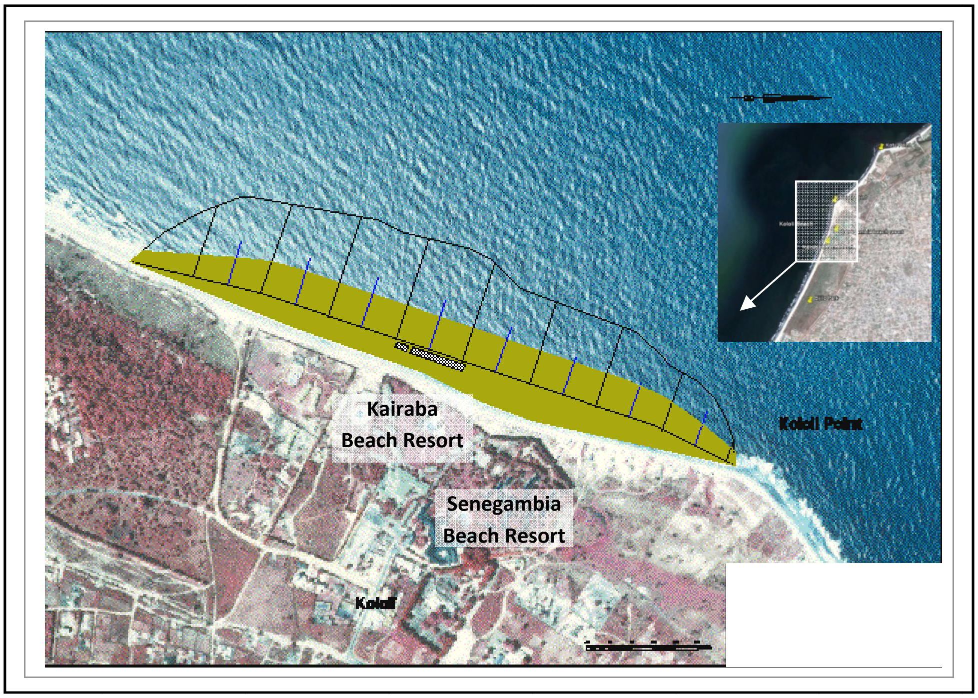

Figure 1-5: Design nourishment at Kololi Beach

Figure 1-6: Finished nourishment at Kololi beach, Senegambia Beach Resort (December 2003)

1.4 PROBLEM DEFINITION:

The high erosion rates at Kololi Beach which occurred in the first years after the nourishment were as predicted in the design. The expectation for the next years was that the erosion would decrease to a stable and low erosion rate. The expected lifetime of the nourishment was 10 to 15 years. After 7 years however, the largest part of the nourishment has been eroded and a beach width of only 25m is still present. The erosion rates did not decrease as expected and especially the stretch in front of the Senegambia area is still eroding with a high erosion rate. The adjacent stretches next to the Senegambia area have no erosion problems.

Early 2010 The Gambian government indicated the erosion problem at Kololi Beach as an urgent matter. If no short-term measures are taken and long-term measures are examined, the beaches in front of the largest tourist area will disappear. This will have a large impact on tourism and the economy of The Gambia. Before solutions can be devised, the cause of erosion has to be researched extensively. The Feasibility Study in 2000 was conducted for the entire Gambian coast; a more detailed study on a smaller scale is necessary.

Figure 1-7: Kololi Beach in front of Senegambia Beach Resort (April 2010)

1.5 RESEARCH QUESTIONS

During the Feasibility Study in 2000 the erosion rates for the complete Gambian coast have been determined by WL Delft; also the expected erosion rates were calculated. The occurred erosion rate at the Kololi beach however, is higher than expected. To find out why there is such a high erosion rate and to investigate possible solutions, the following questions will be answered:

- What happened to the nourished sand, where has it been transported to?
- Which processes cause the high erosion rate at Kololi Beach?

With the knowledge derived from answering the previous questions, short term and long term solutions can be substantiated.

1.6 HYPOTHESES

The hypotheses for the study have been set up after a first visit to The Gambia in April 2010 and a first evaluation of the available data.

1. The waves which attack Kololi Beach are rougher than in the surrounding areas. North of Kololi Beach two reefs are present and the wave climate is calmer there. Because of direct wave impact from the sea and a steep foreshore, the waves break close to the coast and therefore the breaker zone is rough and the rate of erosion is high.

2. Between approximately 1980 and 1996 high volumes of sand have been mined from coastal stretches south of Kololi. Because of this, the coast has a shortage of sand. Nourished sand has been transported south with the alongshore current to supplement the deficit.

3. The amount of shells in the nourished sediment has a negative effect on the beach stability and will therefore erode more easily. The nourished sand contains a large amount of broken and sometimes whole shells. These shell fractions have a negative influence on the sediment characteristics.

4. During the rainy season a large portion of the precipitation in the hinterland is drained on Kololi Beach by two drainage points. Because of the intensity of the rain, deep and wide gullies arise on the beach. They wash away the sand and leave a gap on the beach which is filled up again. This will have effect on the erosion rate, although not to a large extent.

5. During the first days of construction, the sediment used for the nourishment was dredged in front of Kololi. Changes in bathymetry which arose during these activities could have influence on the waves, wave conditions and cross shore transport. A pit in the sea bottom that arises can cause nourished sediment to fill up that pit again, losing sediment to the ocean.

6. Checking the amount of nourished sediment was done by counting the hopper capacities. Some sediment remains in the hopper causing a deficit in the total amount of nourished sediment. Also the porosity of the sediment inside the hopper, just after the nourishment and after settlement can be different, causing a volume change.

7. The reefs in front of Kololi and Kotu influence the nearshore wave climates which have caused the outcrops along the coast at Kololi and Kotu. Erosion or subsiding of these reefs would have a large effect on the area behind them which could cause locally high erosion rates.

1.7 METHODOLOGY

To find the cause of high erosion at Kololi Beach, an extensive analysis of (historical) field data of the research area has been performed. This analysis gives insight into the long-term processes along the coast, the effect of human interference and other observed processes which influence erosion or accretion. Computational models will be used to substantiate the observations and show the influence of different processes on the alongshore sediment transport. The computational model used for the determination of the nearshore waves is SWAN. The alongshore sediment transport will be modelled using the LITPACK software by DHI.

Using aerial photographs and satellite data over the period 1964 – 2010, the behaviour of the coast is investigated with and without human interference for different periods. Based on the aerial photographs and satellite images, coastlines are drawn for different years and the shoreline movement for the periods are determined. Then sediment budgets are assessed which will give insight in the behaviour of the coast for the different periods. With this insight the first ideas about the cause of high erosion are formulated. The analysis is also used to calibrate and validate the models to be used.

To obtain up-to-date bathymetric data, a bathymetric survey has been conducted in The Gambia. Together with surveys from 2000 and 2003 and off-shore data from C-map (DHI), the seabed is mapped. The measurements from 2003 and 2010 are conducted in the same area; profiles from both periods and in the same track will be compared.

Relatively large amounts of shells and shell fractions in the nourished sediment can have a negative effect on the sediment properties and therefore cause higher erosion rates. The amount of shells for several samples will be determined and the effect on the erosion rates investigated.

Because of the complex bathymetry near Kololi Beach and the large influence of waves on erosion, a detailed nearshore wave climate has to be obtained for the Kololi area. Sediment transport capacities along the coast will be modelled using the LITPACK software. The shoreline movement will then be determined by the gradients in sediment transport. As the modelling area is very complex, interpretation and calibration of the results is required to account for the effects of the reef features in the area. Modelling results will be calibrated using the observed trends in shoreline movement and corresponding sediment budgets.

Based on the conclusions of the sediment transport modelling, the effect of several mitigation measures will finally be explained.

1.8 THESIS OUTLINE

After an introduction to The Gambia and the erosion problem at Kololi Beach in this Chapter, the reader is informed about the Feasibility Study conducted in 2000 and subsequently the design of the nourishment project in Chapter 2. An overview of the site conditions of The Gambia are given in Chapter 3. Observed trends in shoreline movement and other processes are shown and compared in Chapter 4. Based on these trends, sediment budgets are drawn and a design for the further modelling is made. The set-up and results of the nearshore wave modelling are described in Chapter 5. Results of the nearshore wave fields and directions are used in the sediment transport modelling. The design, results, discussion and calibrated results of the sediment transport modelling is shown in Chapter 6. Possible mitigation measures and their influence on the present situation are explained in Chapter 7. The final conclusions and recommendations are summarized in Chapter 8.

2. PREVIOUS RELATED STUDIES AND PROJECTS

The following Chapter describes studies and calculations which have been performed during previous research in The Gambia. Royal Haskoning performed a Feasibility Study in 2000, including the calculation of expected erosion rates. On the base of this Feasibility Study, several sand search campaigns have been conducted and a design for the nourishment in front of Kololi has been made. The following Chapter is a summary of the previous studies and modelling study.

2.1 FEASIBILITY STUDY 2000

2.1.1 INTRODUCTION

In October 1999 a contract was signed between the Department of State for Works, Communications and Information, The Gambia and Haskoning B.V. The contract called for studies to be carried out and engineering designs to be made in relation to the coastal erosion problems. The objectives of the study were to determine the causes of beach erosion and sedimentation along the coastline and to recommend protective measures to mitigate the problem. The study also determined the technical feasibility, economic viability and environmental impact of the protective measures. After this, detailed engineering designs and tender documents were prepared.

2.1.2 COASTAL EROSION

During the Feasibility Study trends in shoreline movement have been determined on the basis of aerial photographs for the years 1946, 1964, 1972, 1983 and 1993 for the complete Gambian coast. Special attention was paid to the average trend in the period 1972-1993, since for this period the most complete sets of photographs were available at that time. The position of the water line could not be identified accurately from these images due to inaccuracies in the overlays of the different photographs and to inaccuracies in the definition of the water line on the photographs. Also water levels were not known so no corrections on the water lines could be made. Therefore, only the larger scale trends over the last decades could be identified. Erosion rates smaller than 1 m/yr should be considered with caution.

Future erosion rates were predicted for characteristic points along the coast. It should be noted that erosion rates computed for the coast south of Bald Cape were all well below 1 m/yr. (in the period 1972 - 1993), it could therefore be concluded that erosion south of Bald Cape is small. The sand balance as assessed on the basis of these trends is displayed in Figure 2-1.

There is a natural trend of erosion along the coast of The Gambia, caused by alongshore gradients in the longshore transport and the effect of sea level rise. The natural erosion rate due to above mechanisms is generally small, and the trends along the largest part of The Gambia coast can be explained by these mechanisms. However, for the large erosive trends between Kololi Point and Bald Cape and along the Banjul-Serrekunda highway west of Banjul, other mechanisms dominate.

Along the Atlantic coast, the alongshore transports and the natural gradients hereof are small to moderate. The observed large erosive trends between Kololi and Bald cape in the last decades are for a large part (more than 50%) caused by sand mining from the beach. The deficit due to sand mining was created very locally, over a stretch of several kilometres around Bijilo. This has locally increased the natural sand deficit by a factor 3 to 4, resulting in erosion rates of the order of 4 to 5m per year in this area.

Based upon the understanding of the coastal processes a numerical model that was used to predict future erosion rates was developed.

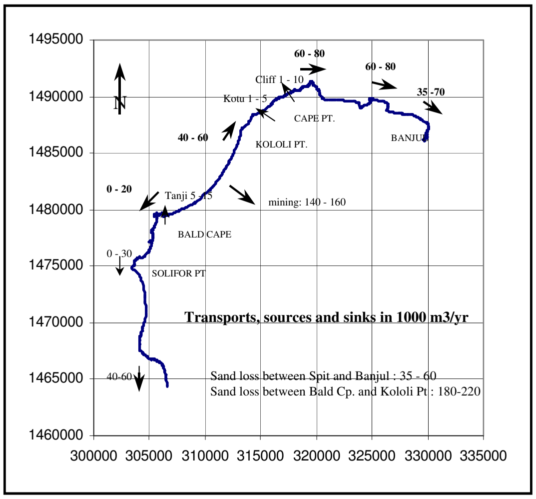

Figure 2-1: Sand balance 2000 (Source: CZM Handbook)

2.1.3 NUMERICAL MODELLING DURING THE FEASIBILITY STUDY

WAVE MODELLING

During the modelling for the Feasibility Study in 2000, wave propagation modelling with mathematical models was carried out to assess the nearshore wave climate at several locations along the coast. For the translation of the waves from the offshore location to the CD -10 m depth contour the 1D wave propagation model WATRON was used. For the wave propagation from the CD -10 m to the CD -5 m contour the 1D wave propagation model ENDEC was selected. The wave propagation computations were carried out for mean sea level. The wave output locations at the CD -10 m and the CD -5 m contour are indicated in Figure 2-2.

SEDIMENT TRANSPORT MODELLING

At the output locations indicated in Figure 2-2 by the numbers 1-13, the alongshore sand transports have been computed with the mathematical model UNIBEST. The main input for this model is the local wave climate, the local coastal profile, the sediment characteristics and the local tidal currents (if relevant). The transport computations were carried out for mean sea level. The transports were computed with the Bijker sand transport formula with standard parameter settings. The computations were carried out with sediment D_{50}= 0.22 m and D_{90}= 0.35 mm for the area north of Bald Cape.

With the model the alongshore transport (S) is assessed for a range of coast orientations (ϕ). In this way spatial variations of the shoreline orientation and changes of the shoreline shape through the years can be taken into account. The relationship between the net alongshore transport (S) and the coast orientation (ϕ) is presented in a so-called S-ϕ curve. For most of the output locations the S-ϕ curves are different, since the local wave climate varies along the coast.

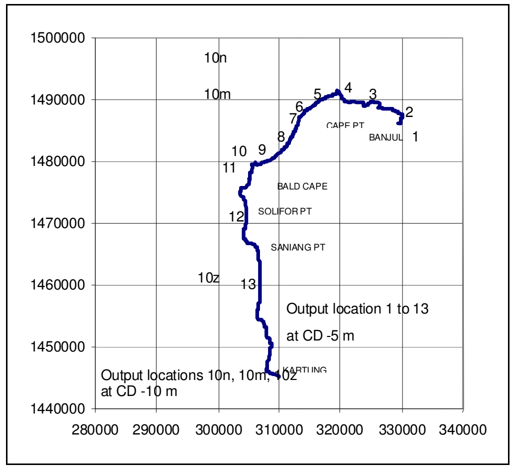

Figure 2-2: Wave output locations

Some of the S-ϕ curves demonstrated interesting features of The Gambian coast. In general, the S-ϕ curves show that along the Atlantic coast west of Cape Point, the deviation of the actual coast orientation from the equilibrium coast orientation is small. East of Cape Point the difference between the actual coast orientation and the equilibrium orientation is considerable. For location 8, between Kololi Point and Bald Cape, the actual shoreline orientation is similar to the equilibrium orientation; location 7 gives a small northern transport while location 9 gives a small southern transport, see Figure 2-3. This indicates that a zero point for the net alongshore transport (in fact a turning point) is located at or close to location 8. Due to year-to-year variations of the wave climate the zero point will move within a certain area along the coast.

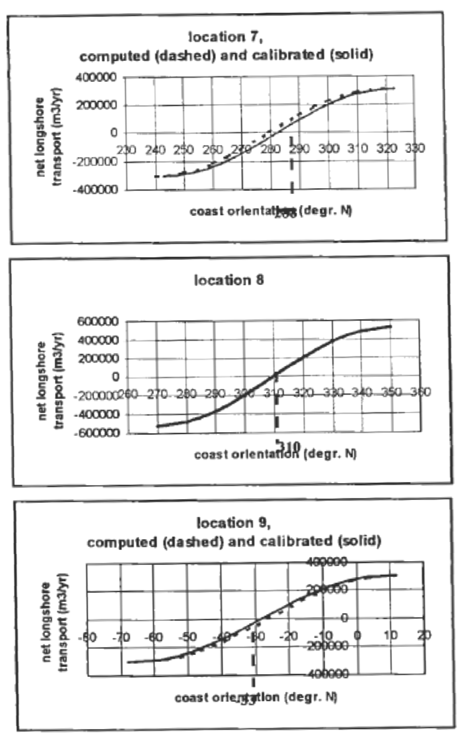

Figure 2-3: S-phi curves for location 7, 8 and 9.

SHORELINE MODELLING

The objective of the shoreline modelling was to make a prediction of the autonomous trend and to evaluate possible morphological effects of proposed measures on the sediment balance. The shoreline in the model has been derived on the basis of the 1993 situation. Some smoothing of the shoreline shape has been carried out in order to obtain a representative alignment of the breaker zone along the coast. The shoreline in the model should be interpreted as the alignment of the coastal profile between CD +2 m and CD - 3 m. With the shoreline models a prediction was made for the future development of the shoreline for a period of 25 years. Since the coastline shape of 1993 formed the basis of the shoreline model, a computation of the coastline was first made from 1993 to 2001. Next the prediction of the autonomous development was made for the period 2001-2026. The results are shown in Figure 2-4.

From Fajara to Kotu Point the autonomous trend is extrapolated. From Kololi Point to Bijilo Park the trends of erosion slowly decrease in time due to the adjustment of the shoreline to the unbalance created by sand mining in the past. The Senegambia area is predicted to have the largest erosion rate of the cells situated along the Atlantic coast.

From Bijilo to Bald Cape, where the turning point of the alongshore transport is located, there is a rather steady trend of erosion. All trends are based on the assumption that no sand mining will take place in the future, though illegal sand mining is likely to continue.

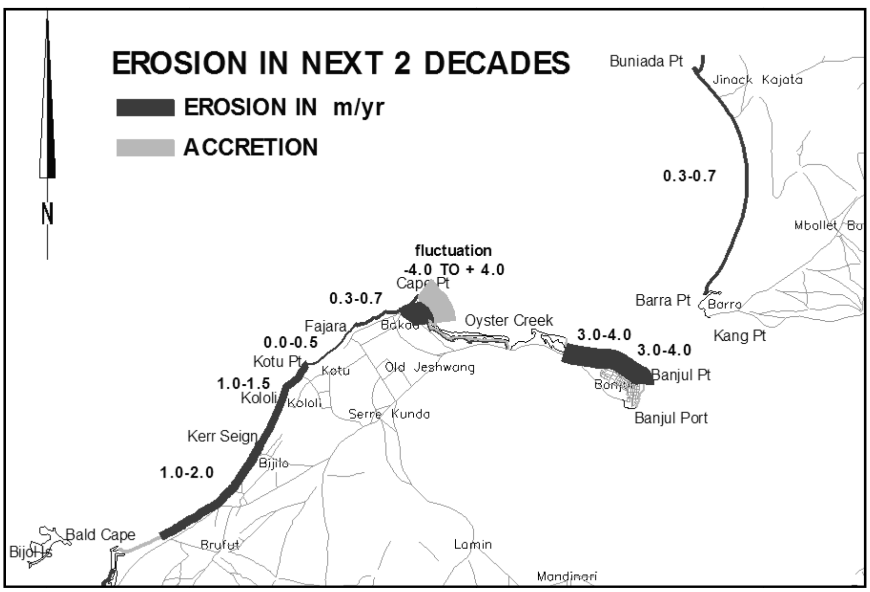

Figure 2-4: Prediction of coastal development

From the Kololi area sand is being eroded and distributed along the coast. It can be expected that if the northward supply of sand along Kololi Point is blocked, this will have adverse effects on the down drift coastal sections (north of Kololi Point). Therefore, from a morphological point of view, a protection with structures was not recommended here. Sand nourishment is considered to be the most suitable option. Since alongshore transports in this area are only moderate, sand nourishment can be effective for a long period of time, provided sand mining should be strictly prohibited and prevented. In addition, adding sand to the coastal system will be beneficial for a large part of the coast in the long term. The Senegambia Beach Resort, the Kairaba Beach Resort, the Holiday Beach Club Hotel and the Kololi Beach Club Hotel will for sure benefit immediately from the beach restoration.

CHANGE OF TRENDS DUE TO COASTAL PROTECTION MEASURES

It should be noted that the shoreline model is used primarily to test the performance of the functional design. The actual design (to be tested in the model) is based on insight in the coastal system, the local S-ϕ curves and insight in the functioning of coastal protection schemes.

The proposed beach nourishment south of Kololi was tested in the model. The results in Figure 2-5 show that a nourishment of 600,000 m^3 over a distance of 1200 to 1500 m is predicted to prevent erosion of the present shoreline in the protected zone for a period of 10 to 15 years.

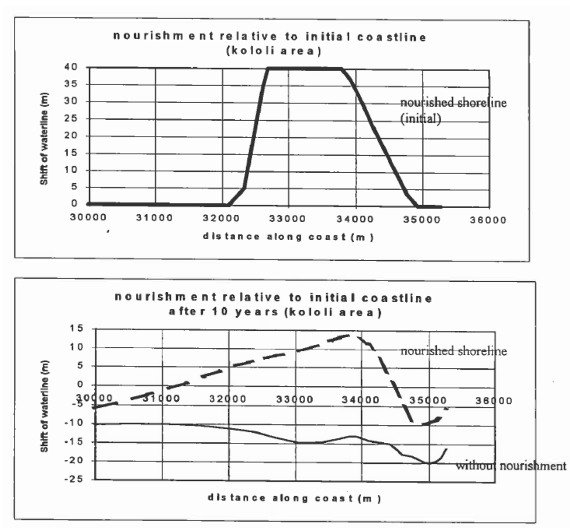

Figure 2-5: Prediction of coastal development after nourishment

2.2 SAND SEARCH CAMPAIGN

Most of the beaches from The Gambia consist of medium to fine quartz sand. In order to obtain more information on available sediment for the nourishment, several sand search campaigns have been conducted in 2000 (Haskoning), 2001 (Deep) and 2002 (Blankevoort).

See Appendix B for drawings of the sample locations and the results of the sand search campaigns.

SAND SEARCH CAMPAIGN 2000 (HASKONING)

Along the entire Gambian coast seabed samples were taken at 75 locations close to the coast in May 2000, see Figure B-1. Close to Kololi a total of 3 samples were taken with two samples having a D_{50} of 0.12 mm and one sample a D_{50} of 0.22 mm.

SAND SEARCH CAMPAIGN 2001 (DEEP)

The coastal area in front of Kololi, north of Cape Point and in the close vicinity of Banjul was surveyed in 2001 using a side sub bottom profiler to find areas with suitable sand in adequate volumes for the nourishments. Also a corer was available to take seabed samples up to 3 meters in depth. This sand search was conducted more offshore than the sand search campaign in 2000. Results of sand sieving on the samples show very high medium grain sizes, which do not reflect the actual situation, see Table B-2in Appendix B. This is mainly caused by the large amount of crushed shell content. The contents of the cores collected at Kololi did not prove to be a source of suitable material when inspected visually. The sub-bottom profiles suggested that the material was unlikely to be sand and indicated that the bed material was consistent for some depth. In the close vicinity of Banjul there is a source of suitable sand available at water depths over 7 to 8 meters.

SAND SEARCH CAMPAIGN 2002 (BLANKEVOORT)

After awarding the contract for the coastal protection projects to D. Blankevoort, an additional soil investigation has been organized to extend investigation of the coastal area for sand reserves. The research locations were based on the previous research conducted in 2001. The sampling was performed by use of a pneumatic hammer with 3 meter core barrels and liners. Referring to the previous sand search the area in front of Kotu has been examined; these results were disappointing, the available sediment was not suitable for the nourishment. North of Cape Point 3 samples were taken; neither the available sediment here is suitable for the nourishment. In front of Kololi Beach the results of the sand search were good: fine clean dark gray sand on top with medium yellowish brown sand below 0.5 - 3 meter. From this sand search could be concluded that 2 areas have been identified as areas with suitable sand in enough quantities for both Kololi and Banjul. This conclusion is in contradiction to the outcome of the sand search campaign in 2001, although the 2001 samples have been taken closer to the shore at Kololi; see Figure B-3 in Appendix B

2.3 DESIGN AND CONSTRUCTION KOLOLI BEACH

2.3.1 DESIGN

The nourishment is designed on the basis of a recurrence of 10 to 15 years, meaning that initial nourishment and a re-nourishment (after 10 to 15 years) are planned within the next 25 years. An initial nourishment of about 600,000 m^3 and a re-nourishment of 600,000 m^3 are recommended. This calculation was based on the coastline for 2000. But if the nourishment is carried out several years later, the coast has by then eroded further and this aspect has not been taken into account. Because of this, the high mobilization and demobilization costs and the positive influence of nourishment, it has been decided to nourish a total amount of 1,000,000 m^3.

The height of the nourishment will be selected in such a way, that it is smoothly connected to the present adjacent surface plane, which is about CD +4.00 m. The seabed in front of the nourishment has a depth of approximately 6 meters. The restored beach will, after reaching its equilibrium profile, have a minimum width of approximately 75 m. The baseline has been set around the location of the sand bag revetment, which means that the beach will be even wider at most locations, namely 80 to 85 m. The final equilibrium seaside slope will be about 1:30 to 1:50, depending on the grain size of the imported sand. Initially, the beach will be constructed significantly wider and the seaside slopes will be much steeper, i.e. in the order of 1:10, but the wave climate will rapidly alter its cross-sectional shape into a natural equilibrium profile. The total amount of sand placed on the beach per meter stretch of coastline is in principle the governing parameter for the design.

On the basis of results of the bathymetric and the beach profile surveys, 6 cross-sectional profiles have been selected with intervals of 250 m in which the nourishment profiles have been inserted, see Figure 2-6 and Table 2-1. Probably the nourishment has been constructed over a somewhat larger area then in the design, which was first based on the nourishment of 650,000 m^3. Therefore the final beach widths are somewhat smaller then indicated in Table 2-1.

Profile no.	Shoreline Elevation	Horizontal Beach width	Seaside Slope	Fill Volume	Representative Width
1	CD+4.00m	60.0 m	1:30	600 m^3/m^1	125 m
2	CD+4.00m	80.0 m	1:30	800 m^3/m^1	250 m
3	CD+4.00m	90.0 m	1:30	900 m^3/m^1	250 m
4	CD+4.00m	90.0 m	1:30	900 m^3/m^1	250 m
5	CD+4.00m	100.0 m	1:30	1,000 m^3/m^1	250 m
6	CD+4.00m	55.0 m	1:30	550 m^3/m^1	125 m

Table 2-1: Nourishment design profiles

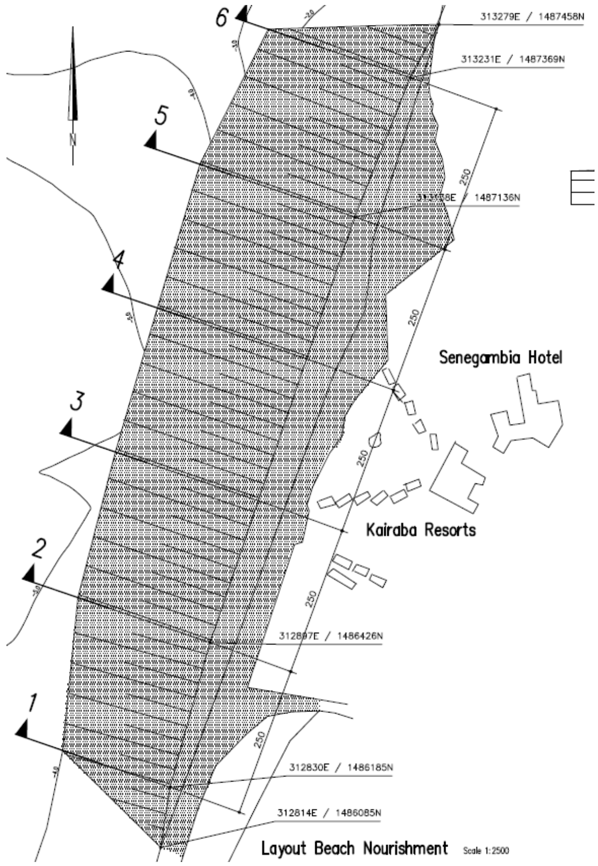

Figure 2-6: Beach nourishment profiles

According to this overview, the total amount of sand needed to nourish the beach is estimated to be approximately 1,000,000 m^3 for a D_{50}-criterion of at least 200 micron, which can be found offshore in adequate volumes according to sand search campaigns, see also Appendix B. The initial situation of Kololi beach is shown in Figure 2-8, the design of the nourishment is shown in Figure 2-7

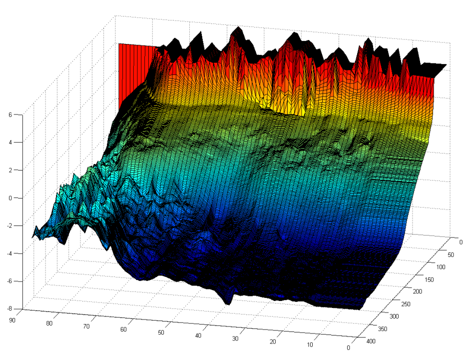

Figure 2-8: Kololi area before nourishment

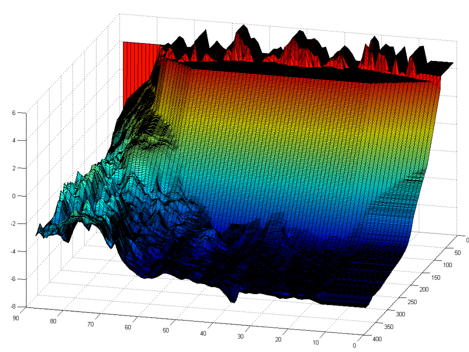

Figure 2-7: Design of the nourishment

2.3.2 CONSTRUCTION

Beach nourishment at Kololi has been carried out from the 22nd September 2003 until the 21st November 2003. For the supply of sand, a sinker pipeline of 1 km length was installed in front of the Senegambia hotel. First the area within the concrete wall in front of the Kairaba Hotel was filled. Then sand was nourished in north-eastern direction towards Kololi Point, thereafter in south-western direction towards Bijilo. The total amount of sand to be nourished according to the design is 1 million m^3. This amount was monitored by counting the number of hopper capacities; the nourished volume was calculated by subtracting the residual sediment from the content of the hopper for each cycle. The porosity of saturated sediment inside the hopper is higher than the porosity of consolidated sediment at the beach. During the dredging and nourishment, the sediment can be slightly oversaturated due to the large amount of water in the sand mixture. This difference in porosity between sediment inside the hopper and the final beach state makes the nourished amount of sediment considerably less. This can cause a change in total volume of approximately 5-10%; also errors in calculating the exact amount of hopper capacities can cause a deficit.

The beach nourishment was started by dredging sand in front of the Kololi Beach, according to the dredging plan shown in Figure B-4 in Appendix B for the locations of the borehole locations. The Contractor had made an offer to reduce the rate for the supply and placement of sand at Kololi Beach when sand was found nearby. After a few days of dredging nobody at the construction site was satisfied with the dredging process and the quality of sand, although within the specification. It contained a lot of shells and was grey coloured. Sufficient suitable sand could be dredged north of Cape Point.

Sand was placed at the average level of CD+4.0m. At the hotel area the levels have been locally adjusted to connect with local levels of each of the hotels. At two drains, near the Senegambia and Kairaba hotels, the beach level has been lowered to allow the storm water to flow freely towards the sea during the rainy season.

Unfortunately no sufficient data are present on the final construction of the nourished beach to determine the exact final shape of the nourishment and the total amount of nourished sediment. An Auto-CAD drawing of the out-survey is available, this is shown in

Figure 2-9: Construction of Kololi Beach

3. SITE CONDITIONS

Chapter 3 describes the site conditions in The Gambia, general information is given in section 3.1; section 3.2 describes the presence and influence of rivers. Wind- , wave- and tidal conditions are given in section 3.3 and 3.4. The bathymetric surveys and following bathymetric data and profiles are shown in section 3.5. Section 3.6 shows the present sediment characteristics which were determined by samples from the beach. The governing coastal processes in The Gambia are finally described in section 3.7.

3.1 GENERAL

CLIMATE

The climate of The Gambia is sub-tropical and is characterized by two distinct seasons: a short and hot rainy season from June to October and a long dry season from November to May. In spite of the existence of a sub-tropical climate, the coastal zone generally benefits from the ocean's tempering effect. The dry season coincides with the coolest part of the year. Figure 3-1 shows The Gambian climate with temperature, precipitation and humidity.

The temperature varies little throughout the year, but January and February are the coolest months of the year, whereas the highest temperatures are registered at the end of the rainy season around September/October. Average maximum and minimum monthly temperatures are shown in Table 3-1.

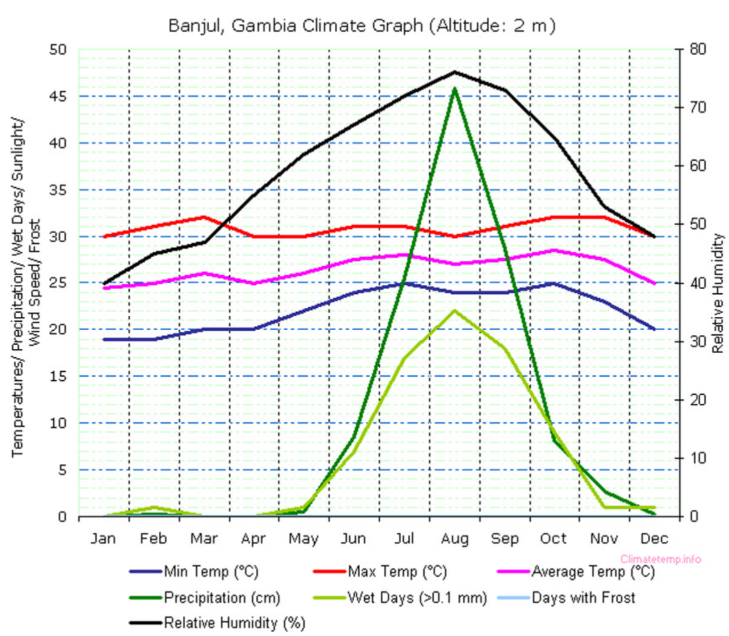

Figure 3-1: Climate graph

	Jan	Feb	Mar	Apr	May	Jun	Jul	Aug	Sep	Oct	Nov	Dec
Min	30	31	32	30	30	31	31	30	31	32	32	30
Max	19	19	20	20	22	24	25	24	24	25	23	20

Table 3-1: Minimum and maximum temperature

Rainfall during the wet season is short but very intense. Rainfall figures recorded in the past 50 years range from 500 to 1150 mm annual rainfall. Rainfall computed for the last 20 years up to 2009 shows a yearly average of 850 mm. Humidity is at his highest during the months of July to October, when rainfall is at its maximum; during this period humidity levels may exceed 75 %. In January the mean relative humidity reaches a minimum of 40 %. Along the coast, however, humidity rarely falls below 50 %.

CHART DATUM

Chart Datum is the lowest low sea level and is 0.15 m below Gambia Precise Level Datum (GPLD). The Mean Sea Level is approximately Chart Datum +0.98 meter. Chart Datum is related to the fixed tide gauge at Banjul Port, located halfway the jetty opposite to The Gambia Ports Authority Offices. Tidal predictions made by The Gambian Port Authority are related to Chart Datum.

All depths and heights which are reported in this project are with respect to Chart Datum, unless otherwise stated.

SEDIMENT CHARACTERISTICS

The coastal zone in the research area consists of fine to small quartz sand. Inside the research area almost no sediment is deposited by rivers, only during the period 1972-1993 and 2000-2008 the Tanji River deposited sediment northeast of Bald Cape. During this research several sediment samples have been taken and analysed for different locations along the nourished stretch. The analysis of these sediment samples and the sieving curves of the present sediment in front of the Senegambia area are shown in section 4.3.

SAND MINING

Sand mining from the beaches has taken place at several locations along the coast, mainly between Kololi and Bijilo. Sand mining from the beach is prohibited since 1996. It was estimated during the 2000 Feasibility Study that volumes of 100,000 to 150,000 m^3/yr have been mined decade(s) before; this may even have been more. Before the restriction was imposed mining may have been more intense (first near Kololi and later near Bijilo), and also in the period of the above limitation it is likely that some additional illegal sand mining has taken place. Especially in the small coastal cells sand mining from the beach may result in significant shoreline changes. Sand deficit created by sand mining will be spread over adjacent coastal cells, resulting in overall shoreline changes, see Figure 3-2.

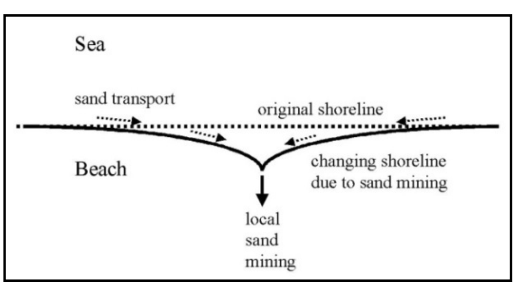

Figure 3-2: Effect of sand mining

COASTAL DEFINITIONS

The coastal definitions used during this research are shown in Figure 3-3.

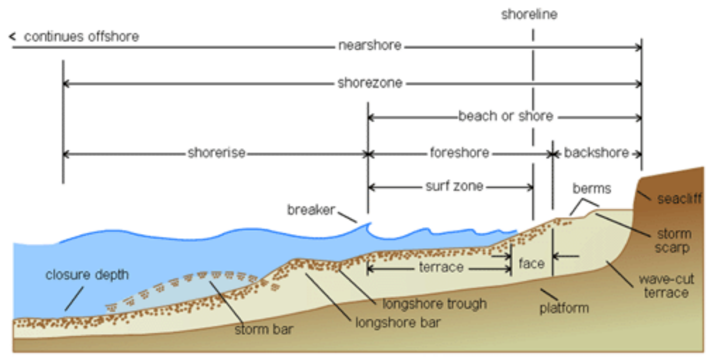

Figure 3-3: Coastal definitions

3.2 RIVERS IN THE GAMBIA

The Gambia River, with a catchment area of 77,000 km^2 and a length of about 1150 km runs through Guinea, Senegal and The Gambia. The mean annual discharge at 490 km from the mouth was in the order of 250 m^3/s between 1953 and 1981. The once in ten years flood reaches a discharge of about 2000 m^3/s. These river discharges are small compared with the peak tidal discharges, which vary between 2,500 m^3/s and 4,000 m^3/s 200 km from the river mouth, and 30,000 m^3/s to 45,000 m^3/s at the river mouth of the estuary at Banjul.

The dominance of the tidal discharges over the river discharges indicates that the lower 200 to 250 km of the system is much more an estuary than the lower part of a river. The total sediment yield from the river Gambia is estimated to be smaller than the virtual loss of sand to the estuary due to sea level rise. Since this virtual loss exceeds the sand load coming from the river, the estuary acts as a sediment sink for sediments coming from the river and the coast. As a result, no significant volumes of sediment transported by the river reach the coast. The above consideration of the estuary having a hunger for sand instead of supplying sand to the coast fits the geological history of the estuary being a drowned valley which is now filled up both by sediment of the river and the sea.

The small streams along the coast of The Gambia bring small volumes of sediment to the coast. The contribution of river sediment yield to the coast is estimated at 25,000 to 70,000 m^3/yr of total load. Only a part of this sediment will be sandy and thus contribute to the nearshore coastal dynamics. The fine sediments (silt) will be distributed over the deeper (offshore) area. The sand supplied to the nearshore coastal region by the streams is estimated to be several thousands of m^3/yr only.

Near the research area two streams are present: Kotu Stream north of Kololi at Kotu and Tanji River near Bald cape, see Figure 3-4. The outlet of the Tanji River fluctuates between northeast and southwest of Bald Cape. In the period 1972 – 1993 and 2000 – 2008 the outlet was directed to the north and inside the research area before 1972; from 1993 until 2000 and from 2008 on the outlet is directed to the west and does not influence the research area. During the period 1972 – 1993 accretion is clearly visible northeast of Bald Cape. The sediment yields of the rivers inside the research area are summarized in Table 3-2.

Stream	Catchment area (km^2)	Transport (m^3/yr)
Gambia river	77,000	1 - 3 x 10^6
Kotu stream	65	4,5000 - 9,000
Tanji river	145	10,000 - 30,000

Table 3-2: Sediment supply to the coast by rivers in the research area (Source: CZM Handbook)

Figure 3-4: Streams near the research area

3.3 WIND AND WAVE DATA

Offshore wind and wave data for a 10-year period (1999 – 2009) are obtained through BMT Argoss. 3-Hourly time series of wave and wind parameters were generated with the use of model data from the BMT Argoss hindcast database. These model data are routinely calibrated by means of nearby satellite observations.

Wave parameters are integrated from at most two dominant peaks of the wave spectrum (high frequency tail included). A wave steepness criterion (wave steepness>0.03 for wind-sea) is used to distinguish the wind-sea and swell components in the wave spectrum. Note that this "engineering" definition does not consider the wind; only wave steepness. For sea states without a peak classified as wind-sea, height of wind-sea becomes zero and its period and direction undefined. Similarly, if all spectral peaks are classified as wind-sea, height of swell will be zero with undefined period and direction[1]

[1] Delivery fact sheet, BMT Argoss

The data are available for two locations offshore, labelled “Point N” and “Point S” respectively, and are marked by a yellow pin, see Figure 3-5. The data from the two locations are fairly the same; therefore only one of the two locations, Point N, is used during this research. This is also due to difficulties of using two data points in the wave modelling. This will be explained later in section 5.1. All directions are given in the nautical convention, which means that for wind and waves the direction refers to the direction where the wind or waves are coming from and are measured positive in degrees from true north.

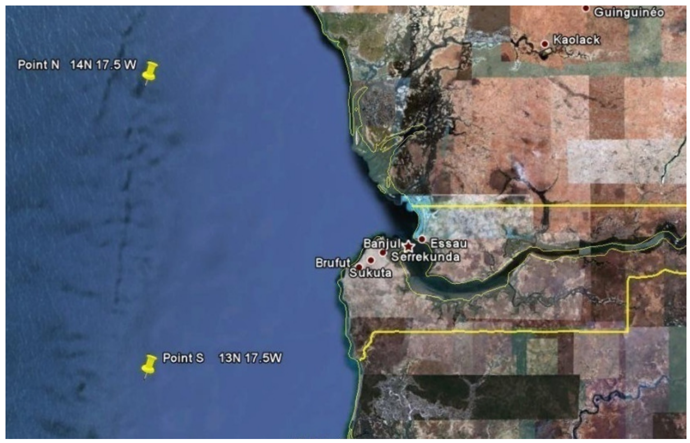

Figure 3-5: Available wind/wave points

3.3.1 WIND

The movement of the Inter-Tropical-Front largely determines seasonal variations. This is a belt separating the trade winds circulation of the northern and the southern hemispheres. Its position fluctuates between January and August. (CZM Handbook, 2004)

The wind rose for the all year climate (average of the 10-year period) is presented in Figure 3-6. Monthly wind roses show a dominance of the northern to north-eastern wind directions in the period November-March and wind from west-north-western direction in the period June-August. This corresponds with wind data measured inland of The Gambia. The highest wind speeds occur in the first 5 months of the year, from January to May. Wind velocities in the study are generally small; indicated wind speeds are in m/s.

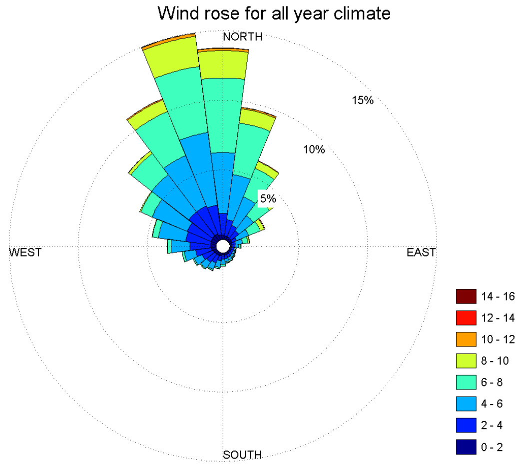

Figure 3-6: Wind rose for all year climate

3.3.2 WAVES

SEA WAVES

For waves at sea a distinction can be made between sea waves and swell waves. Sea waves are generated by the local winds at the sea. The all year sea wave climate is shown in Figure 3-7. Keep in mind that sea waves are only defined if a separate spectral peak for wind waves is present. For 80% of the available data no separate peak is classified as wind-sea. These data have been eliminated and only the remaining values have been used for the wave rose. The main direction of the sea waves is in line with the wind direction.

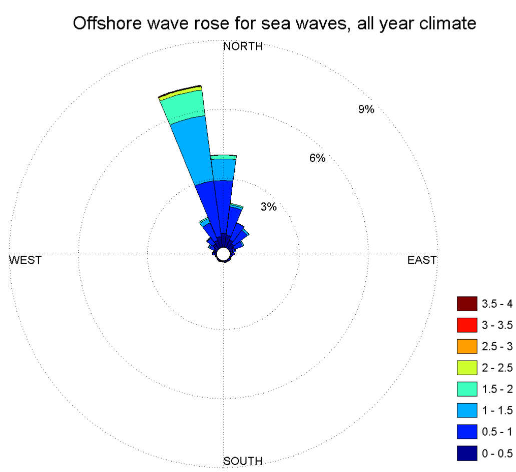

Figure 3-7: Offshore wave rose for sea waves

SWELL WAVES

Swell waves are low frequency waves which have left the area in which they were generated. Swell waves are long-crested, uniformly symmetrical and can travel long distances. Due to the location of The Gambia in western Africa, swell waves arrive both from the North- and South Atlantic Ocean at the coast of The Gambia. This means that two swell systems dominate the wave spectrum. A wave pattern at sea consists of multiple waves, each with their own height, period and direction. Translated to wave data, this can be shown by a 2-Dimensional spectrum where the wave energy is shown for the directions and frequencies. In time-series the parameter of the wave direction is given by 1 value. Hereby two different wave direction parameters have been distinguished; the principal wave direction (mean wave direction) and the peak direction (direction of the highest wave).

Because swell waves coming from two different directions can arrive at The Gambia simultaneously, there is a large difference between the two wave direction parameters, see Figure 3-8 and Figure 3-9. These images show the swell wave roses for the significant wave height and the two different direction parameters, for an average of the 10 year period. See Appendix C for annual and monthly wave roses. The significant wave heights of the wind roses are shown in meters.

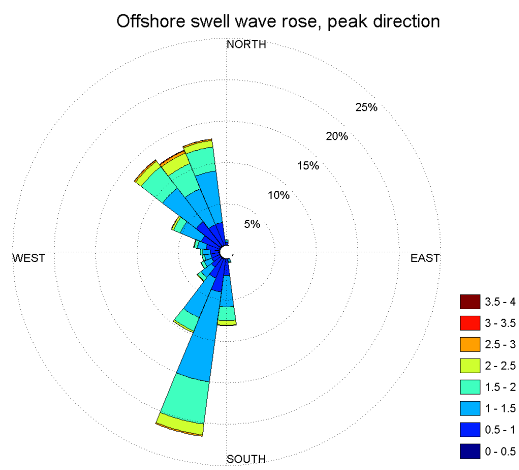

Figure 3-8: Offshore swell wave rose, peak direction

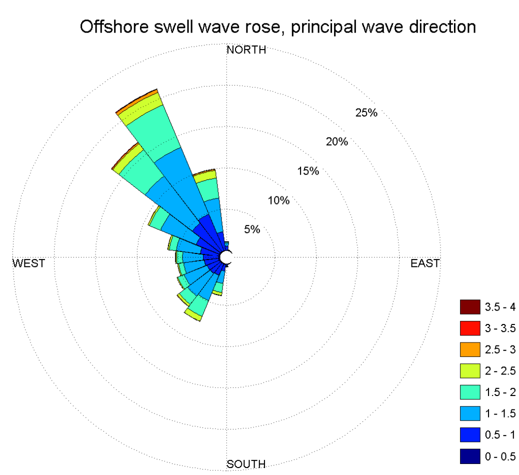

Figure 3-9: Offshore swell wave rose, principal wave direction

For the principal wave direction, see Figure A-1, the waves are clearly coming from the northwest in the period November until May (dry season). During August and September the waves are coming from the southwest. In June, July and October, the intervening months, waves are distributed between northwest and southwest. During these periods waves arrive at the Gambia both from the north as from the south, the principal wave direction gives the mean direction of all these waves combined.

For the peak direction, see figure A-3, the waves are coming from the northwest from December until March. From July until September the waves are coming from the south/south-western direction. During the intervening months, waves are coming both from southwest and northwest. The direction of the waves is random in that period, which means that swell waves arrive at The Gambia from both directions, as well from the north as from the south. Alternately swell waves from each direction are higher and therefore the directions are fluctuating for the peak direction parameter.

So from November until March waves from the northwest are present for both direction parameters. This is winter season in the northern hemisphere and therefore more storms occur on the North Atlantic Ocean. From July until September, which is the wet period and winter season in the southern hemisphere, waves are mainly coming from the southwest. This can be distinguished for both the available wave direction parameters. During the transition months between the wet and dry season, waves are coming both from the north and from the south. Given the tendency for west/north-western waves for the principal wave direction in this period, it can be concluded that if waves are coming from both directions, the southern waves are generally higher than the northern waves because the peak direction has a more southern tendency while the mean direction has a north-western tendency.

The wave roses for the total wave heights of the two different direction parameters are shown in Figure 3-10 and Figure 3-11. These wave roses show the total off-shore wave conditions from where separate swell waves and sea waves have been distinguished. As can be seen the peak direction does hardly differ from the swell wave rose, see Figure 3-8 and Figure 3-9. Swell waves with the principal wave direction are shifted slightly to the west. This is because the total wave height represents both swell waves and sea waves have been taken into account for the. The principal wave direction represents the average direction of all the waves, swell waves are almost always the highest waves and therefore the peak direction for the total climate is nearly the same as the peak direction for swell.

The differences between the two directional parameters can cause differences in alongshore littoral drift. For the Feasibility Study in 2000 only the peak direction was available, therefore the wave and coastline modelling was performed with the peak direction for that study. During this study the effect of the directional parameter is investigated by comparing the corresponding alongshore sediment transports.

Figure 3-12 shows the wave heights against the peak periods. Clearly the dominance of swell waves over sea waves can clearly be seen.

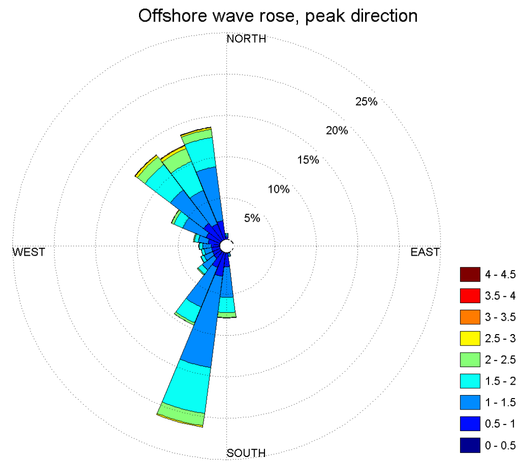

Figure 3-10: Offshore wave rose (total), peak direction

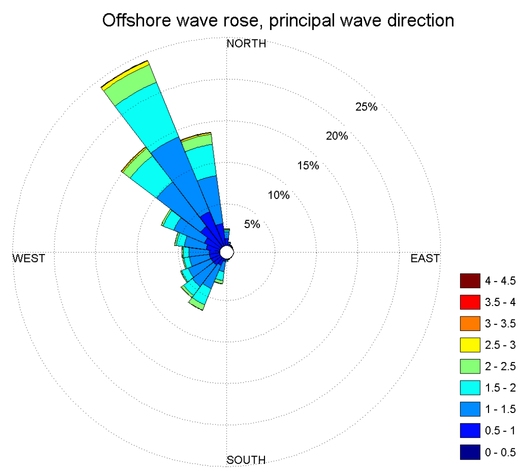

Figure 3-11: Offshore wave rose (total), principal wave direction

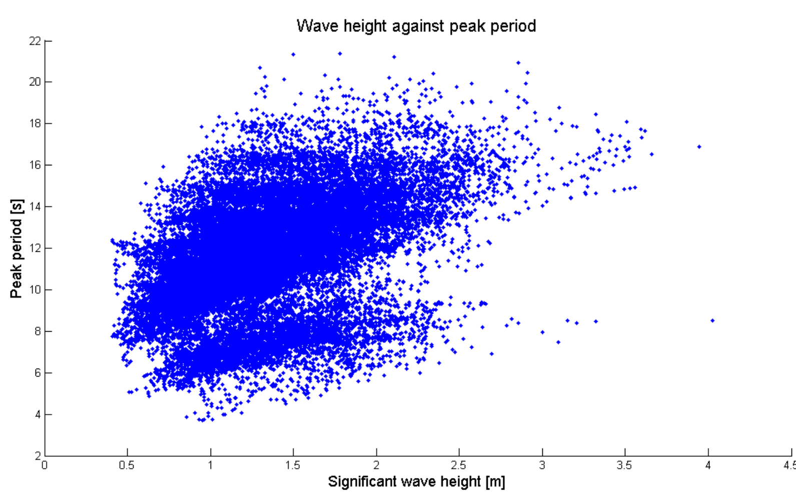

Figure 3-12: Wave height against peak period

3.4 TIDE

The tide at Kololi beach is semi-diurnal and has a daily inequality. Tidal data have been gathered from The Gambia Ports Authority (GPA) as a tide table for 2010 and by global tide model data (DHI). The data table from GPA gives times and water levels for high and low water at the Port of Banjul for 2010. These values have been calculated by the GPA and are referred to Chart Datum.

Although the data from the GPA give a good estimation, some of the highest and lowest values are unreliable and the data are representative for the Banjul Port, situated inside the mouth of the estuary. The global tide model data give more reliable results but does not refer to Chart Datum but to mean sea level. Mean sea level is Chart Datum + 0.98 m, see general site conditions. The predicted tide level from the global tide model data is shown in Figure 3-13.

Characteristic water levels at Kololi are shown in the Table 3-3.

Tidal currents run northward during rising tide and southward during falling tide. The tidal currents along The Gambia coast are in the order of 0.1 m/s according to DHI (1993).

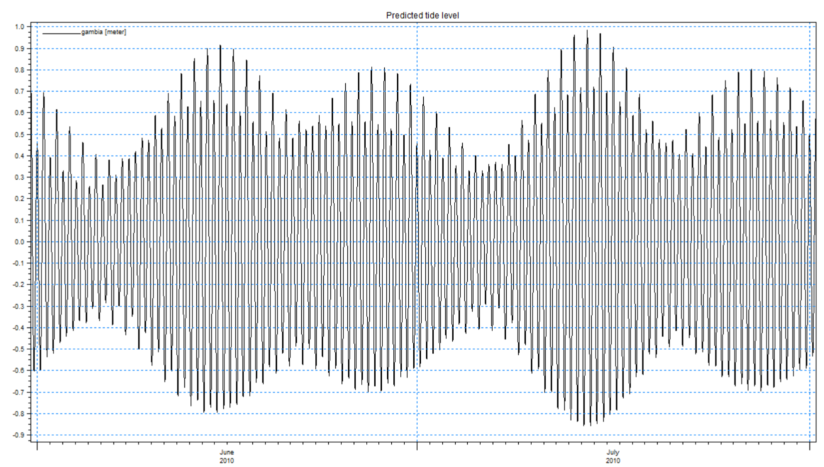

Figure 3-13: Tide level in front of the Senegambia Area

MHWS = CD + 1.70m
MHWN = CD +1.43m
MSL = CD + 0.98m
MLWN= CD +0.53m
MLWS = CD +0.2m

Table 3-3: characteristic tidal water levels at Kololi (MHWS/N = Mean High Water Spring/Neap tide)

3.5 BATHYMETRY

The definitions used for the coastal zone are shown in Figure 3-3. The Atlantic Ocean in front of The Gambia has a depth of approximately 4 kilometres. 80 Kilometres offshore, this depth decreases quickly to a depth of 100 meters, after which the depth decreases slowly to a plateau near shore that is approximately 20 km wide with an average depth of 10 meter. The (interpolated) offshore bathymetry is shown in Figure 3-14. On the terrace in front of the research area the depth decreases slowly to the beach face where a much steeper beach profile is present. The terrace slope in front of the Senegambia Beach resorts contains multiple reefs, shallow and deeper parts see Figure 3-16. Between Bijilo and Bald Cape the terrace is much smoother and has a slope of 1:1000. In front of Bald Cape a large and shallow reef can be seen.

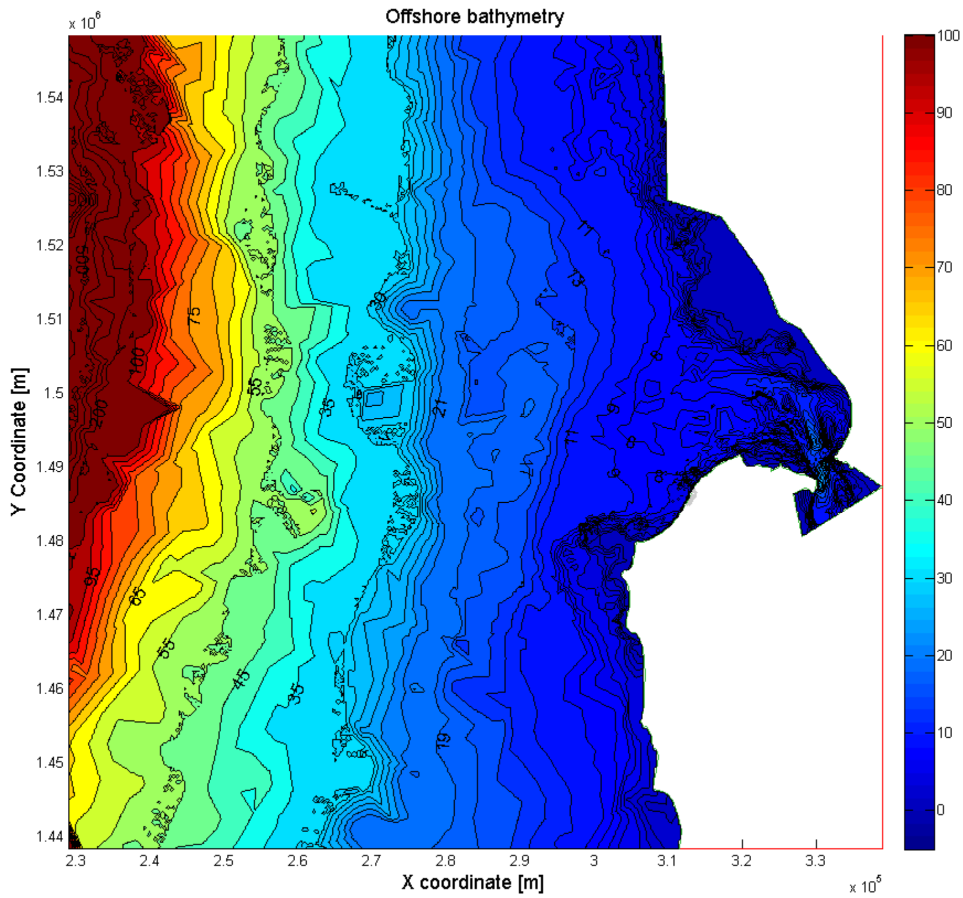

Figure 3-14: Offshore Bathymetry

For the determination of the bathymetry in front of The Gambia, measurements were available from 2000, 2003 and off-shore data from C-map by DHI. The 2000 measurement has been conducted during the Feasibility Study and stretches from Bald Cape until the northern coast. Measured lines are up to 5 km offshore, intervals of approximately 1 km with smaller intervals at interesting points like Kololi Point, Cape Point and the Banjul Area. The measurement of 2003 has been conducted in front of the Senegambia area for the protection works in 2003 and is therefore much more detailed. The measurement stretches from Kololi point to Bijilo Park and approximately 600 meters offshore with intervals of 25 meter. See Figure 3-15 for the measured points and values.

SURVEYS

For this study, two more bathymetric surveys have been conducted in 2010. The first one was conducted in April 2010 on a low-budget basis; this measurement covered a 1.5 km wide stretch in front of Senegambia and was measured up until 1.2 km offshore. See Appendix A for the implementation and results of this survey. Further study made clear that the nearshore area in front of Kololi is very complex and of great influence on the wave modelling. This area has not been measured yet; the conducted surveys were too close to the coast. The data of the complex area were interpolated between the lines from the 2000 measurement making these data unreliable. To obtain more reliable bathymetric data for the modelling, an extra bathymetric survey was conducted in September 2010 together with DEEP BV. The measured lines have a length of 3 km and intervals of 100 m between Kotu Stream and Bijilo Park; from Bijilo Park to Bald Cape the measurement continued with intervals of 500 m. see Figure 3-16 for the results of this bathymetric survey. Together with both measurements in 2010, associated profiles have been measured along the beach to complete the survey.

The nearshore profile is locally very different within the research area; in front of Kololi Point and Kotu Point reefs are present and towards the south the terrace is less deep. From the beach and the boat it was clear that the reefs are rocky. Behind the reefs outcrops are formed in the coastline, forming Kotu Point and Kololi Point.

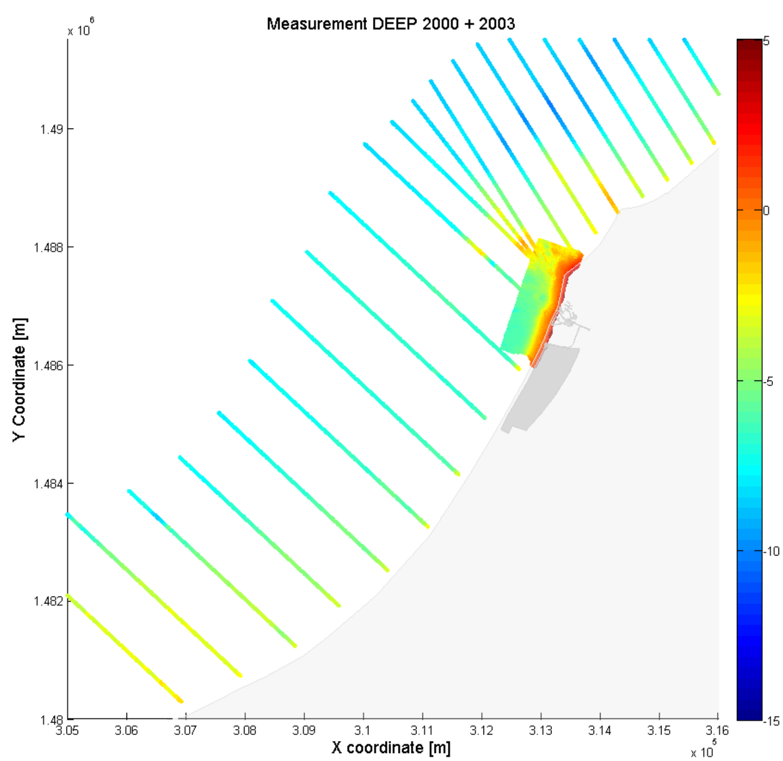

Figure 3-15: Data point measurement 2000 + 2003

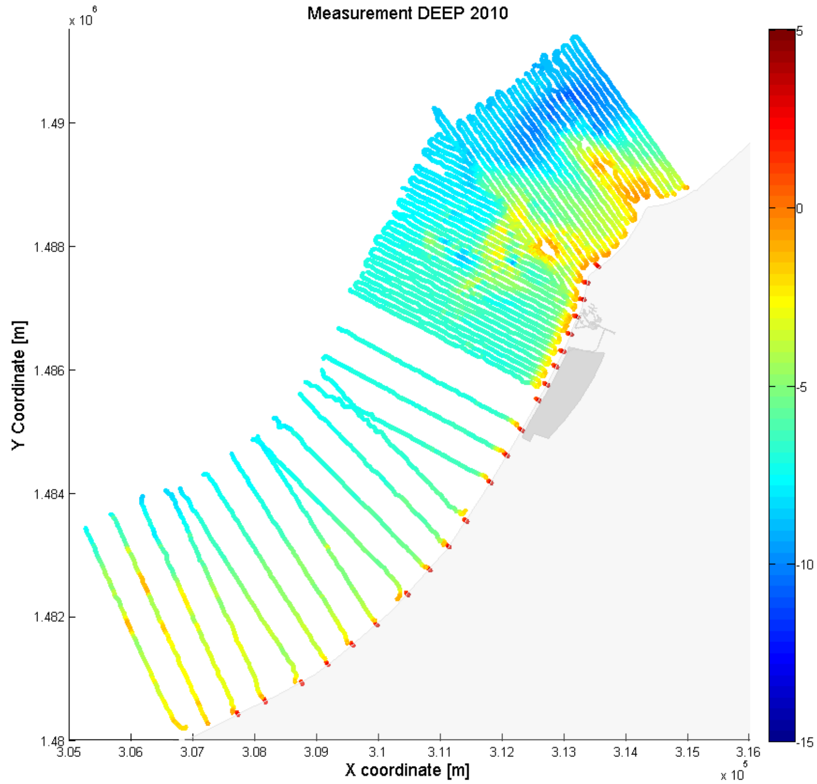

Figure 3-16: Data point measurement September 2010

BEACH PROFILES

See in Figure 3-17, just north of the Sheraton hotel at Point 1, the beach slope runs from CD +4 m to CD -3.30 m over a length of 180 m giving a slope of 1:25. In front of Coco Ocean, point 2, the beach slope runs from CD +4 m to CD -6 m over a length of 300 m giving a slope of 1:30. The beach slope in front of the Senegambia hotel, Point 3, runs from CD +2 m to CD -5 m over a length of 280 m giving a slope of 1:40. The very steep part of the beach in front of the resorts, from CD +2 until CD +5 has been disregarded. See Figure 3-18 for the profiles.

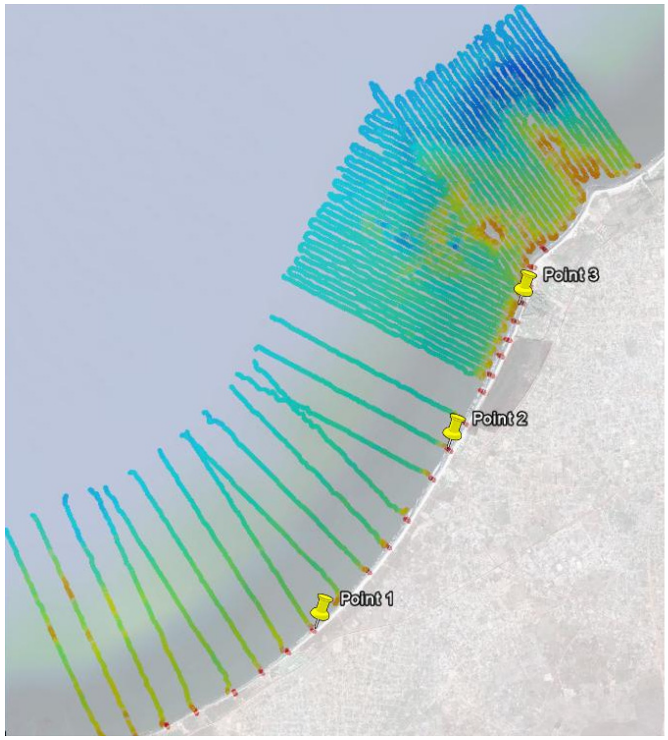

Figure 3-17: Location of beach profiles

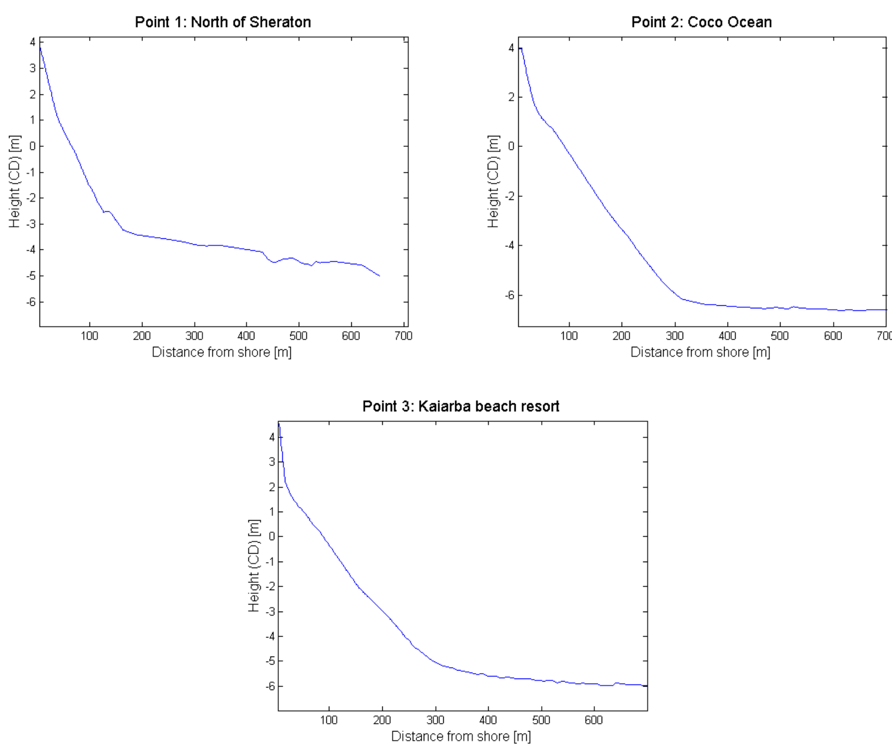

Figure 3-18: Beach profiles

PROJECTION

The bathymetric data are shown in the Universal Transverse Mercator projection using the WGS'84 reference system. Available data with different local projections have been converted to this globally standard reference system.

3.6 COASTAL PROCESSES

In deep water the waves are not influenced by limited water depths. Waves entering coastal waters will be affected in their amplitude and direction by these limited water depths. The relevant nearshore wave processes are described below.

3.6.1 NEARSHORE WAVE PROCESSES

SHOALING

As waves propagate into shallower water, group velocity decreases with water depth. This decrease in transport speed is compensated by an increase in energy density, making the wave height increase. Shoaling waves retain their frequency while the wavelength decreases and wave height increases.

REFRACTION

If a harmonic wave approaches a coast under an oblique angle, the wave will slowly change its direction as it approaches the coast. This is due to variation in depth along the wave crest with a corresponding variation in phase speed. The crest moves faster in deeper water than in shallower water so in deeper water waves travel over a larger distance in a certain time interval. This causes waves to turn towards regions with shallower water. Oblique waves approaching a coast will turn towards the coast. Propagating waves over a complicated bathymetry will change their direction because of this refraction

BOTTOM FRICTION

For continental shelf seas with a sandy seabed, the dominant mechanism for bottom dissipation appears to be bottom friction. Bottom friction is the mechanism in the relatively thin, turbulent boundary layer at the bottom that is created by the wave-induced motion of the water particle. It is a transfer of energy from the orbital motion of the water particle just above the thin layer to the turbulent motion in that layer, decreasing the wave energy. A smooth and sandy bottom may develop ripples under certain wave conditions, which could enhance the bottom friction.

WAVE BREAKING

Nearshore the approaching waves steepen by the effect of shoaling, the phase speed slows down and wave height increases. As depth decreases, the bottom of the wave decreases speed a point where the top of the wave overtakes the bottom and the wave becomes unstable and starts to break causing large amounts of wave energy to be transformed in turbulent kinetic energy. In general a wave will start to break when it reaches a water depth of 1.3 times the wave height.

3.6.2 SEDIMENT TRANSPORT PROCESSES

In general, the sediment balance of a section determines the behaviour of a coastal section. If more sand is transported into an area than out of it, the area accretes. In the opposite case the area erodes. This implies that shoreline movement is determined by gradients in sand transport. Such gradients can be generated in an alongshore or in a cross-shore direction.

Sand can be transported in or out of an area by the following main mechanisms:

- Wave-induced longshore transport
- Tide-induced longshore transport
- Aeolian (wind-induced) transport
- Wave-induced cross-shore transport

WAVE-INDUCED LONGSHORE TRANSPORT

Wave-induced longshore transport is considered to be the dominant sediment transport mechanism along the greatest part of the coast in The Gambia. Wave-induced longshore currents are generated by the shore-parallel component of the stresses associated with the breaking process for obliquely incoming waves, the so-called radiation stresses. Radiation stress is the flux momentum which is carried by the propagating oceanic waves. When the waves break, the momentum is transferred to the water column, causing water level set-up and currents in case of oblique waves. In the breaker zone relatively much sand is stirred up by the breaking waves. The combination of considerable current velocities and high sediment concentrations results in relatively large sand transports in and around the breaker zone. Due to the strong curvature of the coastline between Kololi and Bald Cape, the angle of wave incidence relative to the coast varies considerably and gradients in the net wave-induced long shore transports can be expected.

TIDE-INDUCED LONGSHORE TRANSPORT

Tidal currents running parallel to the coast move sand along the coast, in combination with stirring-up of the sand by wave action. Material that comes into suspension, for instance in the breaking zone under influence of breaking waves, can be transported parallel to the coast under influence of the tidal currents. Along the research area tidal currents in the nearshore area are small (<0.1 m/s) and the wave-induced currents dominate them.

AEOLIAN TRANSPORT

Aeolian transport is considered to play just a minor role in the sediment balance of the research area. The strip of sand remaining dry during High Water is narrow, especially in the erosive zones. Large parts of the beach are wet most of the time, with the result that picking-up and transportation of sand by wind is limited. In addition, wind velocities in the study area are most usually low to moderate. It is even possible that sand from the hinterland is deposited on the beach on some places. The upper layer of the beach in front of Senegambia consists of fine, brown sand which is also present in large parts of the land. Probably this is sand from the Sahara desert which is deposited in The Gambia by Aeolian transport.

WAVE-INDUCED CROSS-SHORE TRANSPORT

Wave-induced cross-shore transport causes fluctuations of the beach profile. During severe wave conditions some sand will be transported from the upper part of the profile to the lower part. Where the average coastal profile is in equilibrium, this sand will be transported back to the upper part during mild wave conditions. Only if the average profile is not in equilibrium, a net cross-shore loss (or gain) affects the sediment balance.

3.6.3 OTHER PROCESSES

SEA LEVEL RISE

The effect of sea level rise is considered to be the only cross-shore process which affects the sediment balance along The Gambian coast. As no information is available on sea level rise at The Gambia, global sea level rise scenarios that have been widely adopted (IPCC 1990, Pepper et al. 1992) are used. These scenarios include the current rate of sea level rise of 0.2 m per century (no acceleration) and possible future sea level rise of 0.5 m and 1m per century. The apparent loss due to sea level rise, for the area between Banjul and Bijilo Beach, is roughly estimated at 20,000 to 50,000 m^3/yr according to the CZM Handbook (2006). This corresponds with a tendency of shoreline retreat of 0.1 to 0.2 m/yr. This is only a fraction of the trends observed in the problem areas with larger erosive trends of 1 m/yr. or more. However, for the slowly eroding areas (approximately 0.5 m/s) the contribution of sea level rise of 0.1 to 0.2 m/yr is significant.

DRAINAGE

During rainfall the precipitation of the Senegambia hinterland is drained on the beaches in front of the Senegambia beach resorts. Rainfall can be very intense, causing the roads and the Senegambia area to flood. This flood of water is then drained by 3 drains in front of the Hotels. The outlet of the drains are approximately at CD +2m, while the beach height is CD +4m to CD +5m causing large gaps on the beach, see Figure 3-19. Sand is washed away from the beach and becomes a part of the sediment balance in the sea. After the rainfall the gaps are filled up again, possibly with sediment from the adjacent coast. The sediment that has been washed away and has come in suspension becomes part of the total sediment balance and can be transported alongshore. It is not clear if this causes a sediment loss on the small stretch in front of the hotel area due to the drainage on the beach.

More research is necessary to investigate the effect of drainage on the beach on the erosion rates.

Figure 3-19: Gaps in the beach due to drainage problems

RIP CURRENTS

Rip currents are strong, narrow currents which flow seaward from the surf zone. They are fed by the longshore currents that turn seaward to form a rip current. These longshore currents are generated by set-up differences and run from the position of the highest set-up towards the position of the lowest set-up. Such a situation will only be able to develop for nearly normal wave incidence; in case of oblique incident waves a longshore current by gradients n radiation stress will overshadow the more subtle effects of set-up differences. A combination of the two effects may occur for slightly oblique wave incidence, see Figure 3-20 for the circulation patterns for these cases. In case of high sediment concentration inside the surf zone, the suspended sediment flows offshore out of the surf zone.

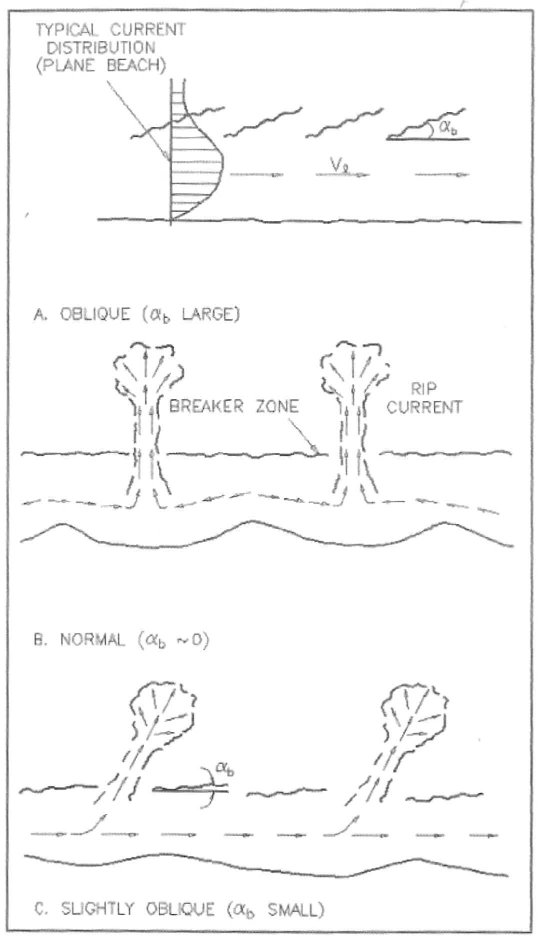

Figure 3-20: Circulation patterns for different angles of wave incidence, A: typical longshore transport due to obliquely incident waves, B: rip current pattern in case of approximately normal wave incidence, C: combination of previous two cases for slightly oblique waves.

4. FIELD DATA ANALYSIS

To gain insight in the coastal processes and historical evolution of the coast the research area has been analysed with the evaluation of field data. For this research photographic data of several years, bathymetric measurements in 2003 and 2010, sediment samples and visual observations by executing staff are available. Using this data trends in shoreline movement and the corresponding sediment budgets, profiles along the coast, sediment characteristics and visible coastal processes have been analysed. The analysis results give an indication of the occurring sediment transports along the coast and processes within the research area which influence erosion or accretion rates. Modelling results will be used to possibly substantiate the observations and give an indication of the influence of different processes.

Trends in shoreline movement for several periods have been determined by comparing the corresponding coastlines. Based on these trends, sediment budgets have been assessed for the corresponding periods. The observed trends in shoreline movement and corresponding gradients in littoral drift along The Gambian coast will be used for the calibration of the modelling study. On the basis of the layout and results of this observation analysis, a set-up for the wave and sediment modelling has been made.

The method to determine the trends in shoreline movement and their results are explained in section 4.1. Sediment budgets for different periods are drawn and shown in section 4.2. The sediment characteristics of the nourished sediment is defined and discussed in section 4.3. Section 4.4 contains the remaining field data analysis and their results. Conclusions on the observed trends in shoreline movement and coastal processes are shown in section 4.5, as the design of the wave and sediment modelling study.

4.1 TRENDS IN SHORELINE MOVEMENT

The historical evolution of the coastline and trends in shoreline movement for several periods has been analyzed with available photographic data. Aerial photographs are available for the years 1964, 1972, 1983 and 1993 from the Feasibility Study in 2000. Google Earth contains satellite images of December 2004 and April 2009. Furthermore satellite images from 2002 have been purchased to obtain data of the coastline just before the nourishment. Using the images, coastlines for the corresponding years have been drawn. Trends in shoreline movement for different periods are then determined based on these coastlines. During the 2000 Feasibility Study, trends in shoreline movement have been determined for the periods from 1964 to 1993 and these results have been compared with the recent study.

Photographs taken from airplanes for the coastline before and after the nourishment and for the present situation are shown in Figure E-1 to Figure E-3. This already shows the erosion on front of the Senegambia area and accretion in front of Bijilo.

4.1.1 METHOD

RESEARCH AREA

Trends in shoreline movement have been determined from Bald Cape to Fajara, see Figure 4-1. North of Fajara coastal cliffs are present without any beaches in front of them so shoreline movement will be close to zero; the cliffs north of Fajara are slowly eroding. At Bald Cape the coast makes a 90 degree angle; west of Bald Cape the sediment transport will be directed southerly and is not of any influence on the shoreline movement of the research area. Sediment transport modelling will be based on the same data points along the coast as the determination of the coastlines so they can be compared directly. Due to limitedly available bathymetric and topographic data, the area where the coastlines are determined is somewhat smaller than the area between Fajara and Bald Cape; the used data points are represented by the red line with green points in Figure 4-1. The areas where no sufficient bathymetric data are present, north of Bald Cape and north of Kotu, are not included in the determination of the coastline and sediment transport modelling. For the assessment of the sediment budget these two areas do have been taken into account.

At Fajara, where the coastal cliffs start, shoreline movement will be close to zero. For the sediment budget, the shoreline movement will be extended from the last data point to Fajara. The outlet of the Tanji River fluctuates between northeast and southwest of Bald Cape, therefore the area just northeast of Bald Cape is very dynamic. For the periods in which the outlet of the river is northeast of Bald Cape and inside the research area, the river deposits 10.000 – 30.000 m^3/year of sand, see section 3.2. While the Tanji River outlet is inside the research area and shortly after, accretion is clearly visible as well as erosion when the outlet has moved again to the west. The shoreline movement and corresponding sediment budgets in the area just northeast of Bald Cape have been determined manually and taken into account for the sediment budget of the total research area.

The coastline positions for different years and trends in shoreline movement are determined for the data points as shown by a red line and green data points for every 10^{th} point in Figure 4-1. As 245 points are situated along the coast, separate points are too small to distinguish. The locations of the data points will be used during the complete research, so also as output data for nearshore wave climates and sediment transport calculations. The data points are generated as point’s perpendicular to a baseline along the coast, the black line in Figure 4-1, with a fixed step size of 50 meters.

As the aerial images are very large, these images have not been added to this report. When observations in aerial pictures are mentioned in the report, these observations have been made during the research. Only when reference is made to a figure, the images have been added to the report.

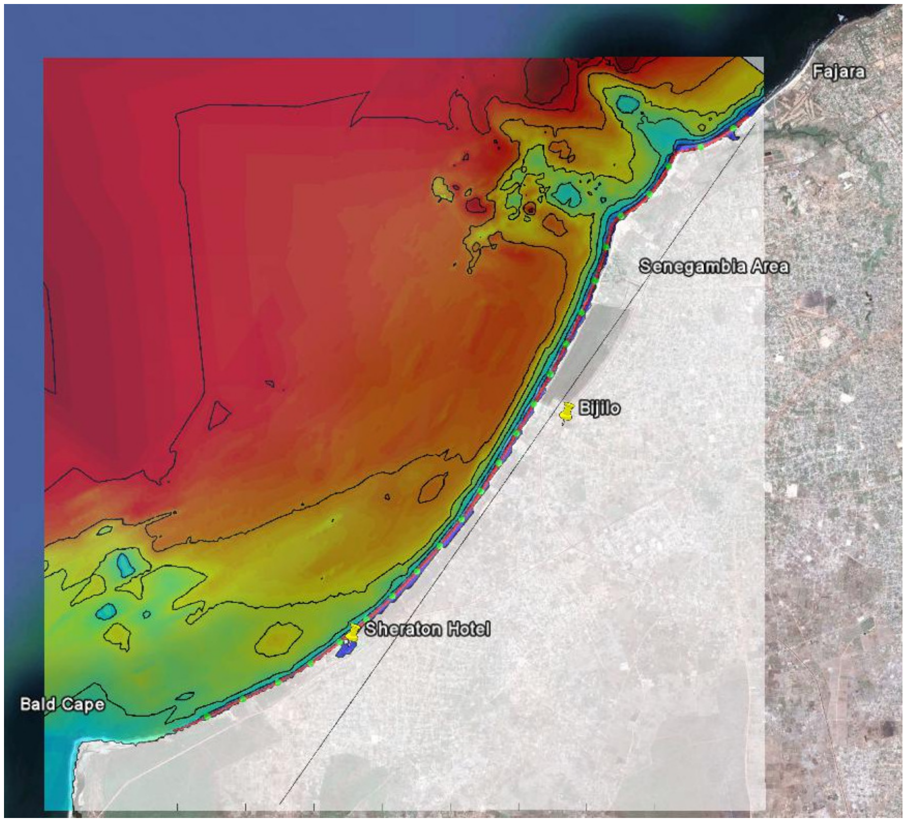

Figure 4-1: Coastline data points along research area

PERIODS

The analysis of shoreline movement between 1964 and 2009 has been carried out for 4 different periods. These periods have been chosen so that a distinction can be made between undisturbed periods without human interference and different kinds of human interference. The boundaries of the periods are given by the availability of aerial photographs. The first period is between 1964 and 1983. In this period no or almost no sand mining has taken place. This period can be seen as historically the most undisturbed period without significant human interference.

In the aerial photographs of 1993 the effect of mining was clearly visible. As illegal sand mining is prohibited since 1996, the end of the second period has to be after 1996. Therefore the second period is between 1983 and 2002. During this period a high volumes of sediment have been mined illegally at the coastal stretch in front of Bijilo.

In November 2003 the beach nourishment at Kololi has been carried out, so the third period is very short and between 2002 and 2004. In this period the human interference consisted of the construction of the beach nourishment at Kololi Beach in front of Senegambia.

The last period is between 2004 and 2009. This period started only 1 year after the nourishment so it describes more or less where the sand has been deposited. We should keep in mind that the spread of the nourishment per year is the largest in the first year after nourishment.

For the above 4 periods the trends in shoreline movement are determined separately. Only the first and the last period will be used for the calibration of the sediment transport modelling. The periods with human interference of sand mining and nourishment will not be used for the modelling but they give a good insight in the effects of local interference which has an impact on a far larger area.

METHOD FOR DETERMINING SHORELINES

The locations of the coastlines of 1964, 1983, 2002, 2004 and 2009 have been determined on the basis of the available aerial photographs and satellite images. The definition of coastline is rather broad; the coastline is often defined as the boundary between sea and land at mean sea level. It is almost impossible to determine the coastlines like this by aerial photographs. For this study the coastline is defined as the high water level mark. This was best visible on the aerial photographs by the difference in sand colour, breaking of the waves and sometimes a clear beach scarp.

The aerial photographs and the satellite image from 2002 have been loaded into Google Earth. Using image overlay, images can be loaded into Google Earth, resized, rotated and placed into a certain position by hand. Placing the pictures in the right position is done by choosing fixed points through the years, like roads and building, and overlapping the aerial photograph based on these points. Multiple available photographs along the coast have been used to determine the coastline for each year. It is difficult to place the pictures in the right position. The main problem is that the aerial photographs are taken under different angles making it impossible to compare the different photographs exactly. Furthermore the images are placed by hand which can give errors because of the large scale of the images. Despite these shortcomings this method is very useful to draw reliable coastlines when the effects of the problems are taken into account. The results will have a certain bandwidth where the uncertainties of the results are included.

By inserting a path in Google Earth the coastline can be estimated according to the aerial photographs, see Figure 4-2. The green line represent the 1983 coastline, the pink line represents the 2009 coastline. While drawing the coastlines, the position of the aerial photographs are compared with the fixed satellite images from 2004 and 2009 and adjusted so that the position of the coastline is as accurate as possible. Small irregularities along the coastline have not been taken into account and the coastlines have been smoothened so trends in the shoreline movement match with visually observed trends from the aerial photographs.

Figure 4-2: Coastline estimation in Google Earth

The assessment for the trends in shoreline movement has a limited accuracy. This is mainly due to the inaccuracies in the overlays of the different photographs and in the definition of the water line on the photographs due to high or low tide. Taking into account these inaccuracies it should be realized that only the larger trends, say of more than 0.5 to 1 m/yr. can be substantiated.

Trends smaller than 1 m/yr. should be considered with caution, but due to the comprehensive analysis the direction of the trend is reliable. For every coastline data point the coastline angle is determined by the previous and following data point. Using this angle, the shoreline movement of the coast has been determined for a certain period.

4.1.2 RESULTS

The results of the trends in shoreline movement and corresponding sediment budgets are shown in the following section. The x-axes of the figures correspond with the coastline data points as defined in Figure 4-1, the distance between 2 data points is approximately 50m. The y-axes display the coastline trend in meter per year. Along the x-axes the location of the Sheraton Hotel, Bijilo and Kololi and Kotu point are indicated as points of reference. The figures show the exact coastline changes as they have been derived from the aerial photographs and a smooth line as average coastline change. It should be kept in mind that the coastline trends are based on the aerial photographs, creating an uncertainty of approximately 0.3 – 0.5 m/year.

UNDISTURBED PERIOD 1964 – 1983

The shorelines from 1964 and 1983 were relatively difficult to distinguish as the quality of the aerial photographs was not that good for those years. Global trends in shoreline movement were yet good to distinguish. The shoreline movement in meter per year is shown in Figure 4-3. The area just northeast of Bald Cape, which is not shown in this picture, has an accreted area as the Tanji River deposited sediment inside the research area before 1983. This accretion is large but very local, after which erosion is present which is visible in Figure 4-3. The erosion rate is relatively large from point 0 to Sheraton; unfortunately this trend is unreliable due to bad image quality. Between Sheraton and Bijilo a small trend of accretion is present with an overall trend of 0.3 m/yr. From Bijilo Park to Kololi Point an erosive trend is present. It is plausible that illegal sand mining took place in this small area before 1983. In the nourishment area the average trend in this period was -0.5 to -1.5 m/yr.

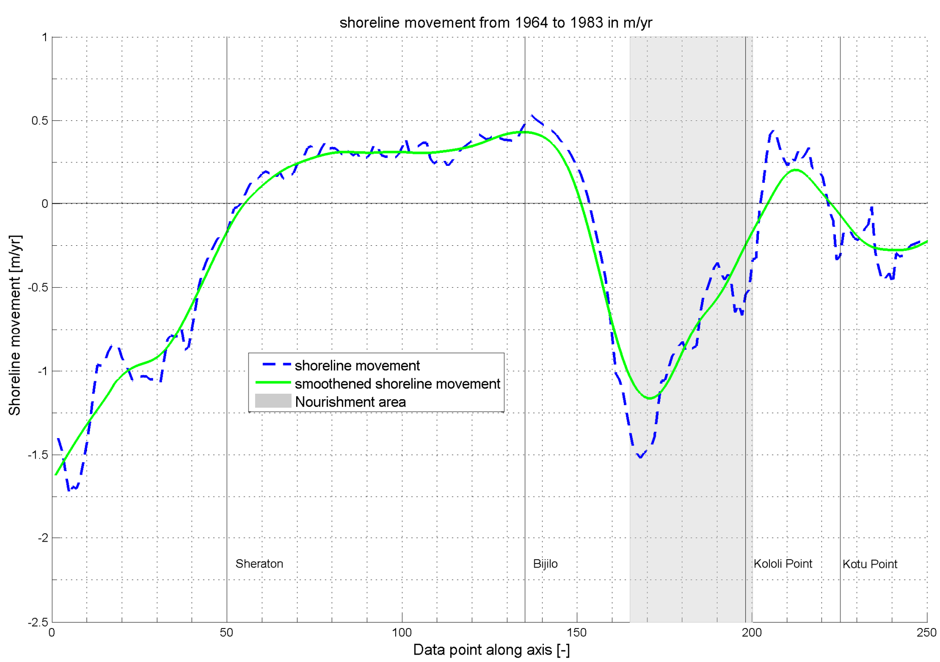

Figure 4-3: Shoreline movement from 1964 to 1983, derived from aerial photographs

ILLEGAL SAND MINING, 1983 – 2002

The shoreline movement in meter per year for the period 1983-2002 is shown in Figure 4-4. From 1983 to probably 1996 sand was mined from the coastal stretch in front of Bijilo. The size of the stretch and the locations where the sand was mined is not known precisely. Probably volumes up to 150.000 m^3/year have been mined from the beaches. The area where erosion was present stretches from Sheraton to Kotu Point as adjacent coastal cells suffer from the illegal sand mining as explained in section 3.1. Illegal sand mining has been prohibited since 1996. Because this period (1983-2002) stretches until 2002, the erosive trends were higher in front of Bijilo and less in the surrounding areas till 1996. Just northeast of Bald Cape no large change in shoreline is present. The outlet of the Tanji River was southwest of Bald Cape in 1993 and again northeast in 2002. East of Kotu until Fajara the change in shoreline is small and goes to 0. Inside the nourishment area the average trend was -1.5 to -2.5 m/yr.

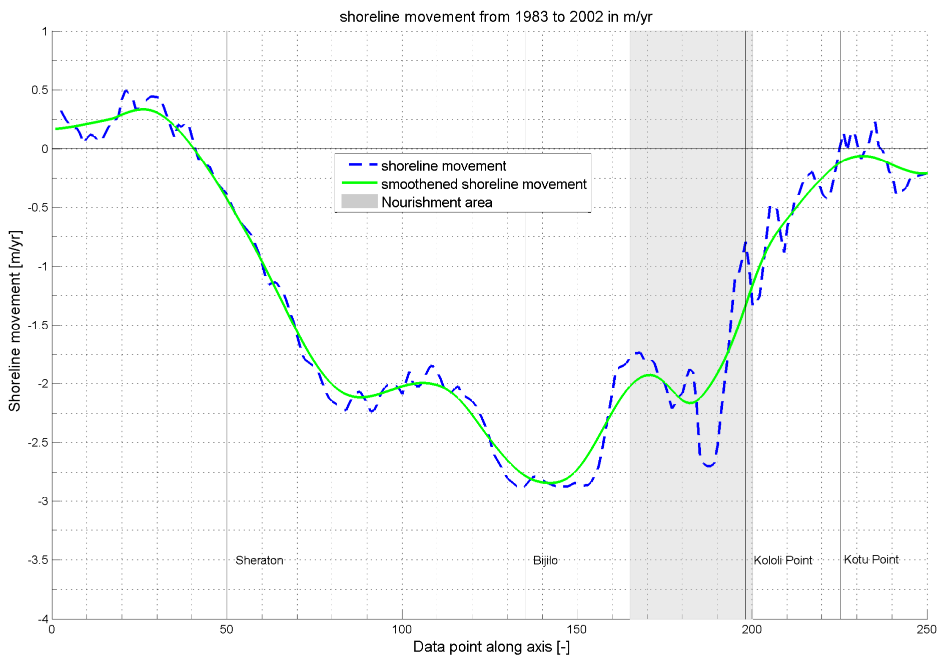

Figure 4-4: Shoreline movement from 1983 to 2002, derived from aerial photographs

BEACH NOURISHMENT, 2002 – 2004

The effect of the beach nourishment is shown in Figure 4-5. The gray area represents the nourishment area according to the design. The 2004 coastline dates from December 2004, one year after the completion of the nourishment. The spreading effect of nourishment is clearly visible as the coast has also accreted in front of Bijilo Park and between Kololi and Kotu Point. Remarkable is the large area of accretion between Kololi Point and Kotu; this is partly because this is a shallow area so the active zone smaller. The first design of the nourishment was made for 650.000 m^3 but eventually approximately 1.000.000 m^3 has been nourished; it is possible that the nourishment was constructed somewhat wider than the first design. The seaward movement of the coastline in front of Senegambia 1 year after construction had a maximum of approximately 65 meters in the middle and 30 meters at the edges of the nourished area. This indicates that the initial erosion after the first year of construction was relative large, this can also be seen by the large accreted area south and north of the nourishment.

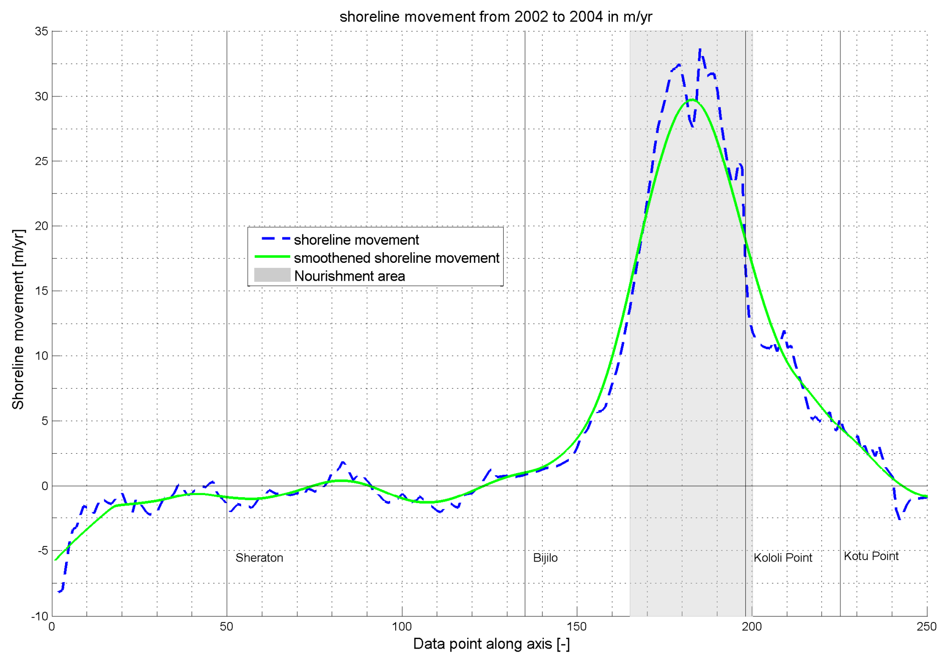

Figure 4-5: Shoreline movement from 2002 to 2004, derived from aerial photographs

AFTER NOURISHMENT, 2004 – 2009

The shoreline movement between the nourishment and the April 2009 situation is shown in Figure 4-6. A large erosive trend of -4 to -8 m/yr. is visible at the nourishment area; between Kololi Point and Kotu Point an average erosive trend of -2 m/yr. can be seen where initially accretion was present after the nourishment. A large area between Sheraton and Bijilo Park (point 160) has been accreting with approximately 2.5 m/year. This was clearly visible in the satellite images and on these locations along the beach of The Gambia in reality. North of Kotu Point the beach is accreting and the accretion gradually decreases until Fajara. Northeast of Bald Cape accretion is present, due to the presence of the Tanji River outlet inside the research area between 2004 and 2008.

Qualitatively the trend in shoreline movement, apart from rates per year, is similar with the shoreline movement between 1964 and 1983: small accretion between point 50 and 150 and erosion in front of the Beach Resorts area in Senegambia.

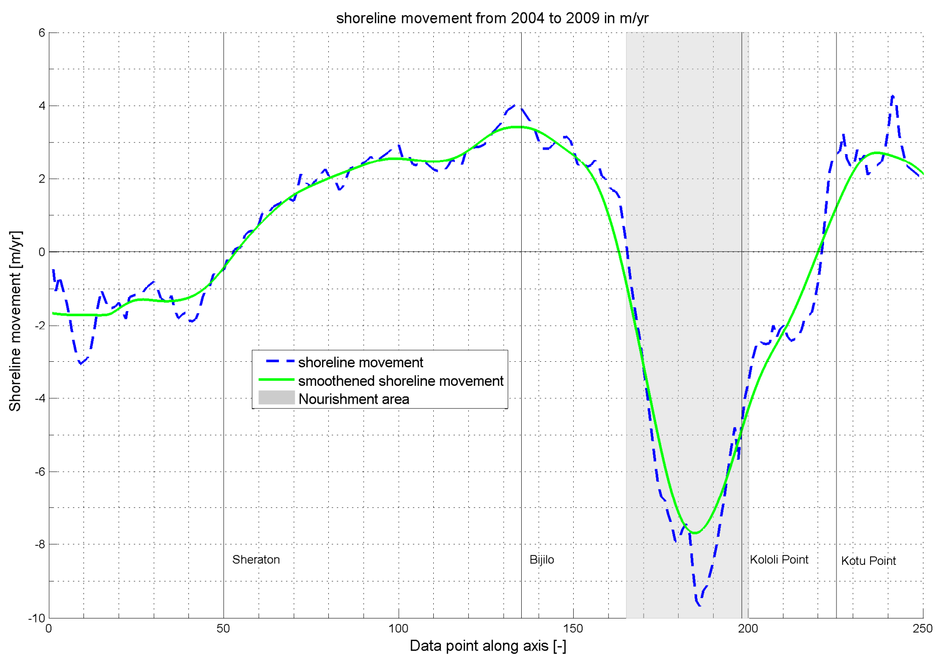

Figure 4-6: Shoreline movement from 2004 to 2009, derived from aerial photographs

4.1.3 COMPARISON WITH THE 2000 FEASIBILITY STUDY

For the Feasibility Study in 2000, trends in shoreline movement have been determined on the same aerial photographs as used during this study. Trends from 1964 are hardly available in the 2000 study as the data were too insufficient to use at that time. For the current study especially the coastlines from 1964 and 1983 have been compared because for this period the coastlines could be best compared. The 1972 aerial photographs were taken during high water and were difficult to compare with those of 1964 and 1983.

The shoreline movements in m/yr according to the 2000 Feasibility Study (FS 2000) and according to this study (MSc. Thesis) are shown in Table 4-1. Shoreline movement according to this study is also shown in Figure 4-7 for the period 1964-1983 and Figure 4-8 for the period 1983-1993.

Area	1964-1972 FS 2000 m/yr.	1972-1983 FS 2000 m/yr.	1964-1983 MSc Thesis m/yr.	1983-1993 FS 2000 m/yr.	1983-1993 MSc Thesis m/yr.
Between Kotu stream and Kotu Pt (average)	0	0	-0.2	0.3	0.4
Between Kotu Pt and Kololi Pt, max in Centre	-0.2	1	+0.2	-2	-0.5
Kololi Pt	-0.1	0	0	-1.5	-1
Area 2000 m south of Kololi Pt	*	-0.5	-1	-1.5	-1.5
2000 m to 4000 m south of Kololi Pt, average	*	-1	+0.2	-5	-5
4000 m to 5500 m south of Kololi Pt, average	*	*	+0.3	-5	-4.5
5500 m to 9000 m south of Kololi Pt, average	*	-0.5	-0.5	-1.5	-1.5
Area 2000 m north of Bald Cape	*	0	-1	1.5	2

Table 4-1: Shoreline movement according to 2000 Feasibility Study

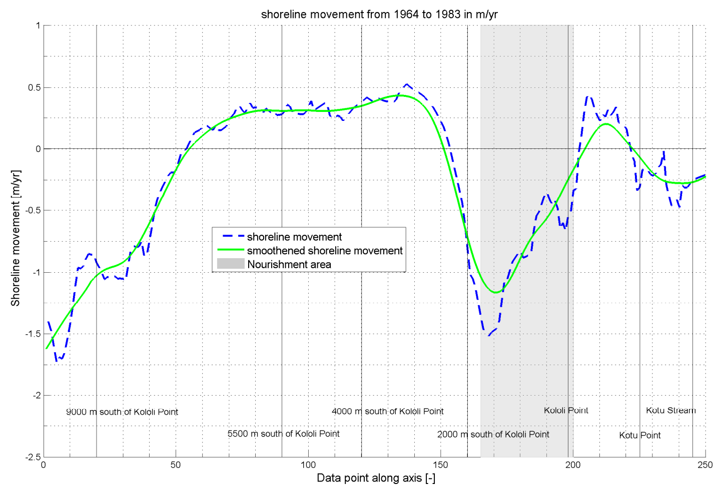

Figure 4-7: Shoreline movement from 1964 to 1983, derived from aerial photographs

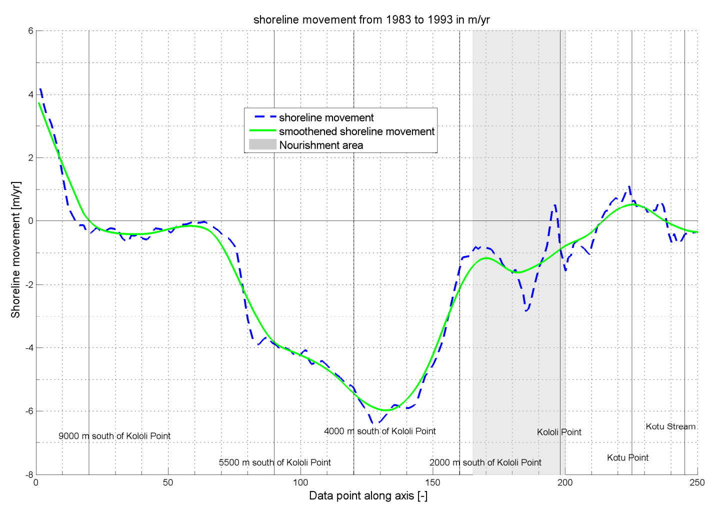

Figure 4-8: Shoreline movement from 1983 to 1993, derived from aerial photographs

For both periods the derived trends in shoreline movement agree very well, except for the accretion between point 50 and 150 in the period 1964-1983. During the Feasibility Study in 2000 no trends could be derived for the period 1964-1972; this could be the cause of the difference. According the Feasibility study in 2000 small erosion was present between Sheraton and Bijilo while the recent study shows small accretion inside this area. This has a large influence on the sediment budgets to be assessed and therefore also on the calibration of a modelling study.

4.2 SEDIMENT BUDGET

Considering the single line theory by Pelnard-Considère (1956), the profile (shape) remains the same during accretion or erosion. The equation of the single line theory for shoreline movement can be rewritten to define change in sediment transport for a given shoreline movement, see equation 4.1:

$$\partial S_x = -\frac{\partial Y}{dt} \cdot d \cdot \partial x \qquad \textbf{(4.1)}$$

Where ∂S_x is the change in alongshore sediment transport over a given distance, $\partial Y / dt$ is the shoreline movement over time, d is the height of the active zone and ∂x is the given distance, in this case the distance between data points which is 50m. Based on the calculations of change in alongshore sediment transport for every data point, the sediment budget for the research area has been estimated for different periods. As the coastline definition and definition of active zone height has uncertainties, the sediment budgets are shown as a bandwidth between which the occurred transports will take place. The active zone height is the depth of closure plus the berm height of the beach. The berm height of an eroding or accreting beach is often different; this effect has been taken into account for the estimation of the sediment budget. The overall berm height of the coastal stretch along the beach is approximately CD +4m .

DEPTH OF CLOSURE

The depth of closure of a cross shore profile is defined as the seaward limit of the littoral zone, where intense bed activity is caused by extreme nearbreaking waves and breaker-related currents (Hallermeier (1978)). This author also introduced a predictive formula for the Depth of Closure (4.2):

$$d_l = 2.28 \cdot H_e - 68.5 \frac{H_e^2}{gT_e^2} \qquad \textbf{(4.2)}$$

in which d_l is the annual Depth of Closure below mean low water (MLW), H_e is the nonbreaking significant wave height that is exceeded 12 hr per year (0.137% of the time),T_e is the associated wave period, and g the acceleration due to gravity. As the Depth of Closure is used for the estimation of the sediment budget, the determination of values can be simplified for the 245 data points. In Figure 3-18 a clear transition between the shore face and terrace in front of the coast can be seen. These depths have been taken as an approximation of the Depths of Closure. For several profiles the Depth of Closure has been calculated and the results correspond very well.

The sediment budget for the period 1964-1983 and 2004-2009 is shown in Figure 4-9 and Figure 4-10. The sediment budgets for periods in between are shown in Appendix E.

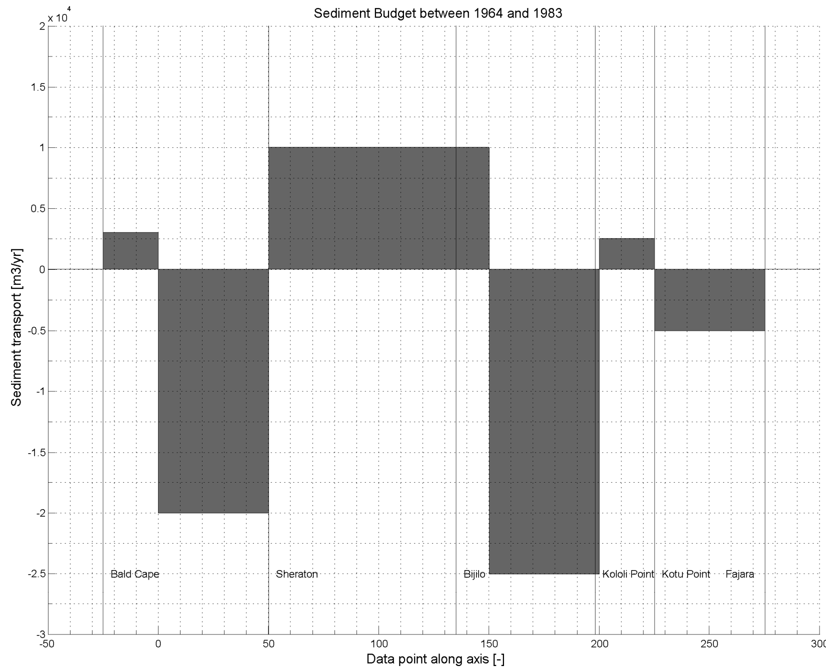

Figure 4-9: Sediment budget between 1964 and 1983

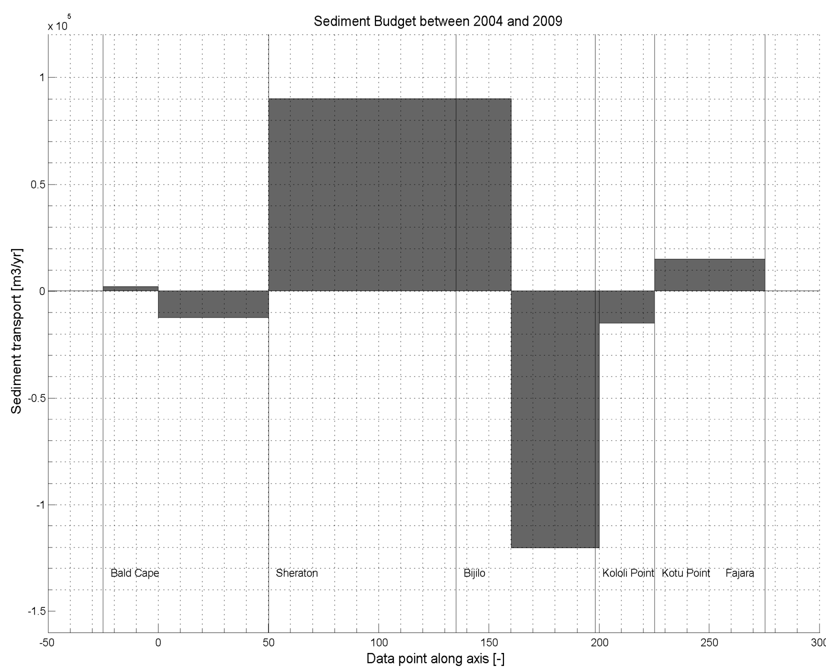

Figure 4-10: Sediment budget between 2004 and 2009

The total sediment loss over the complete research area between 1964 and 1983 is of the order of -30.000 m^3/year. The bandwidth of this loss is relatively large, approximately between -15,000 and -55,000 m^3/year. The sediment loss between 1983 and 1993 is in the order magnitude of -170,000 m^3/year, between 1993 and 2002 the sediment loss is in the order magnitude of -60,000 m^3/year. This is due to the illegal sand mining between 1983 and approximately 1996. On average, volumes of the order of 140,000 m^3/year have been mined from the beaches in front of Bijilo. The sediment loss between 2004 and 2009 is in the order magnitude of -40,000 m^3/year. This higher loss of sediment is due to the shell fractions within the nourished sediment; they wash out, break apart and do not contribute to the alongshore sediment transport as they are transported away from the breaker zone like fine sediments, resulting in a sediment loss.

4.3 SEDIMENT CHARACTERISTICS

Striking on Kololi Beach is the amount of shells in the beach sediment on the nourished stretch. In front of the Senegambia Beach resort on a stretch of 400m the current sediment in 2010 is gray coloured with a high amount of shell fractions. South and north of this stretch the sediment is browner but still contains a lot of shell fractions. This is due to the two different borehole locations where sand has been dredged for the nourishment. The dredged sediment from the borehole in front of Kololi with low sediment quality was placed first in front of the Senegambia Beach resort. The rest of the nourishment was constructed with material dredged from the borehole location near Cape Point. The low quality, grey coloured sediment in front of the Senegambia Beach resort has not been placed over the complete width of the nourishment. In September 2010 the poor quality of gray sediment was visible in front of the Senegambia Beach resort, whereas it was not as clear as that in April 2010. Along the nourished stretch, layers of different sediment qualities were clearly visible; all the layers contained shell fractions although some layers clearly more than others. All this sediment was brown coloured and originates from the borehole at Cape Point. See Figure 4-11 for the difference in nourished sediment which is clearly visible in September 2010. A high beach scarp is present at the nourished stretch due to these shell fractions and cementation of the sediment.

To investigate the current present sediment properties, samples have been taken from different places at Kololi Beach; two samples in front of the Senegambia Beach resort, two samples 200 m north of the beach resort and three samples 200 m south of the beach resort, in front of the Kairaba Hotel. One of the samples in front of the Kairaba hotel is from the wet part of the beach; one of the samples is taken on top of the beach scarp behind a sea wall and one on the beach. Also in front of Coco Ocean beach resort, see Figure 1-4, and 2 km more to the south, samples have been taken from the beach. This beach has clearly been accreting after the nourishment. All the sediment samples have been taken at a depth of approximately 0.5 -1m, except for the wet sample which was taken close to the surface. The names and locations of the sediment samples are listed in Table 4-2.

Name	Location
Senegambia	In front of Senegambia
Senegambia North 1	200 m north of Senegambia
Senegambia North 2	200 m north of Senegambia
Senegambia South	200 m south of Senegambia
Senegambia South wall	200 m south of Senegambia, above sea wall
Senegambia South wet	200 m south of Senegambia, wet part of the beach
Coco Ocean	In front of Coco Ocean Hotel
Beach South	2 km south of Coco Ocean

Table 4-2: Locations sediment samples

Figure 4-11: Kololi beach September 2010

Sieve analysis has been performed on all the samples as named in Table 4-2. For every sample location 2 sieve analyses have been carried out while for each analysis the sample has been sieved three times and the average was taken. Figure 4-12 shows the results of the sieving analysis. The two samples from Senegambia consisted of gray sediment and both were almost exactly the same; therefore only one sample is shown. Senegambia South, South Wall and North 1 have almost the same properties; visibly less shell fractions were present in these samples. The Senegambia North 2 sample visibly contained a larger amount of shell fractions. The Senegambia South wet sample had almost exactly the same properties as the sample from Coco Ocean, where the beach has been accreting for the last 5 years. This wet sample was taken in front of the location where the Senegambia South Wall sample was taken where clearly more shell fractions were present. This indicates that the shell fractions wash out of the sediment due to breaking waves in the surf zone.

For all the cases except Coco Ocean, Beach South and the Senegambia South wet sample, the last sieves consisted almost completely of shell fractions. These small shell fractions wash away into the ocean very easily, together with the fine particles, due to the shape and mass of the shell fraction. Larger shell particles diminish due to the force of breaking waves, after which the fragmented particles wash away. Therefore the shell fractions have a negative influence on the sediment characteristics. The larger grain diameters of the shells disturb the sieving curves and can therefore be removed as the shells have no influence on the stability. Modelled shoreline movements are approximately 15-20% higher when the effect of shell fractions washing away is taken into account. For the stretch in front of the Senegambia Beach resort and other locations with low quality of sediment, this effect can cause additional erosion up to 35% due to the presence of fine sediments.

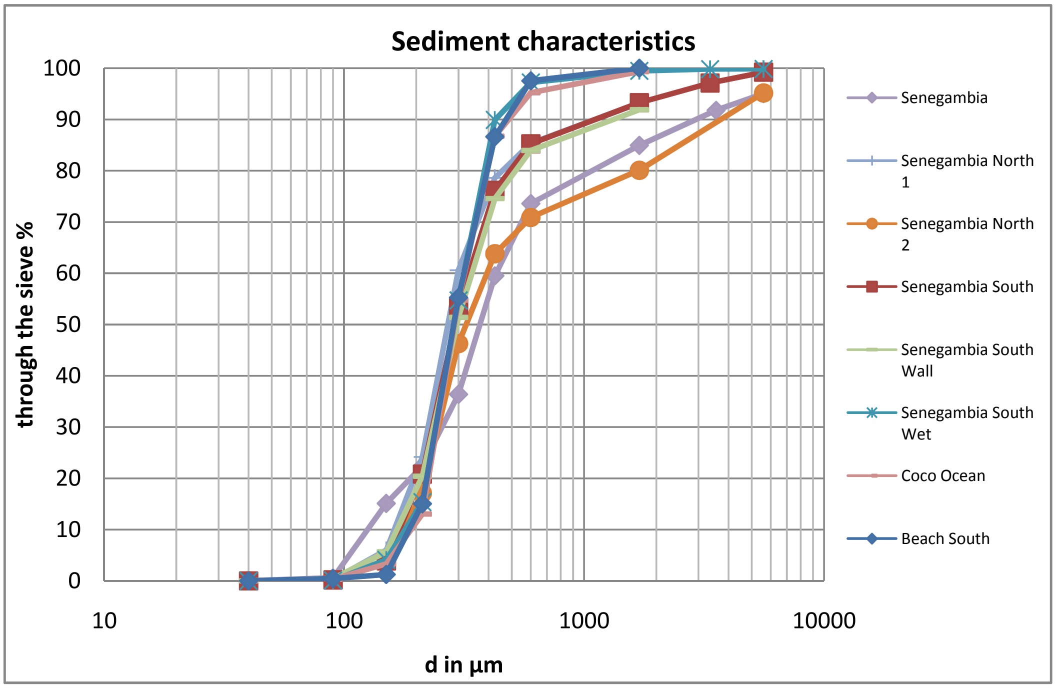

Figure 4-12: sediment characteristics

4.4 OBSERVED COASTAL PROCESSES

4.4.1 COASTAL PROFILES

Along the lines of the 2000, 2003 and 2010 measurements with the same track, profiles can be directly compared. This has been done for the measurements of 2000 and 2010 and for the measurements of 2003 and 2010. The 2000 measurement was performed from the beach to 5 km offshore while the 2003 measurement reaches until 600 meters offshore; the 2003 measurement does include topographic measurements. The measured lines and compared profiles are shown in Figure E-5 to Figure E-8 in Appendix E. The compared profiles for the Kololi reef are shown in Figure 4-13.

Along the coastline and at Kololi reef only small variations within the profiles are visible. Therefore the cross-shore profiles maintain more or less the same shape, which is on of the assumptions in the single-line theory. The reefs at Kotu show large differences in the profiles see Figure E-7. These large differences can be caused by measurement errors in 2000, the locations of this measurement contained some errors in the first place. As the reefs are very close to the measured lines a small location shift causes large differences in the profiles. The other possibility is that the reef bathymetry is subjected to changes due to erosion. The reefs consist of rocky material with sand and shell particles in between, over the years small changes can occur but mayor changes are unlikely. Therefore this change has not been taken into account during this research. Further research on the bathymetry of the research area is recommended. A changing bathymetry due to eroding reefs would have large influence on the wave climate behind the reef area.

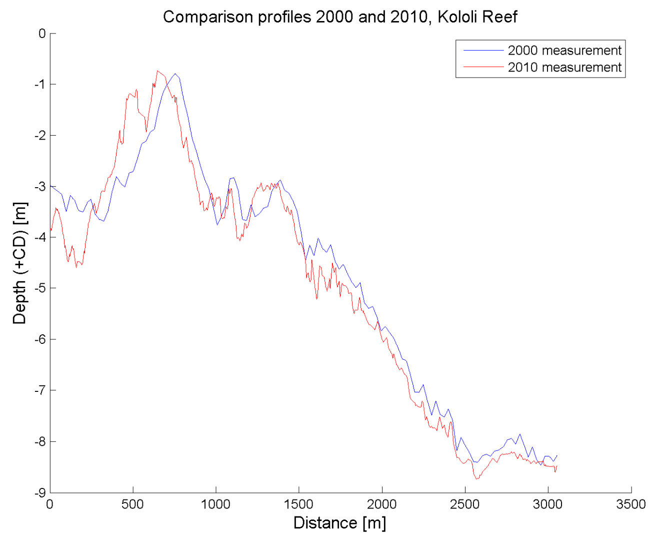

Figure 4-13: Comparison profiles 2000 and 2010

During the first visit in April 2010, bathymetric measurements were performed along with 5 profile measurements in front of the beach resorts. The location of the profile measurements are not very accurate and have to be looked at with caution, but they give a good indication of the difference between the summer and winter profile in 2010. The 2003 measurements have also been performed around April; the second 2010 measurements have been performed in September. Profiles from the 2003, April 2010 and September 2010 measurement in front of Senegambia are shown in Figure 4-14. The other profiles in front of the Senegambia area are shown in Figure E-8.

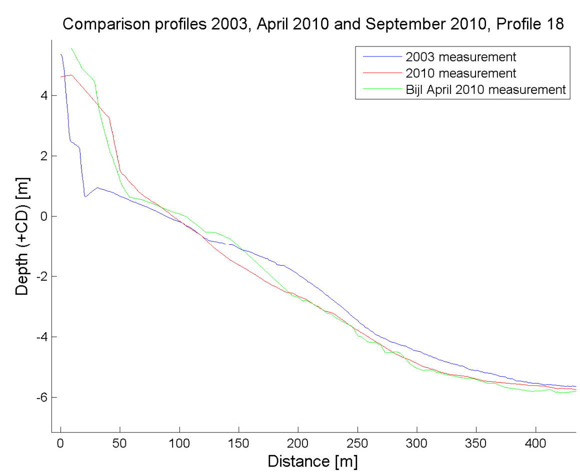

Figure 4-14: Comparison profiles 2003, April 2010 and September 2010

During a rough season with higher waves, sand is deposited cross-shore to the lower part of the profile, which is (partly) transported back again to the upper part during a calm season. April is approximately after the rough winter season while September is after the calmer summer season. The difference in summer and winter profile is clearly visible between the April and September 2010 measurement. The 2003 measured profile also has the shape of a summer profile but the difference with the September 2010 profile is larger. This difference can be caused by a combination of various reasons such as a change in sediment characteristics due to the nourishment or a rough wave climate before the 2003 measurement. The overall profile shape is approximately the same. Clearly almost all the nourished sediment has been eroded in 2010.

4.4.2 CONSTRUCTION OF THE NOURISHMENT

For the construction of the nourishment only an AutoCAD drawing of the out-survey and visual observations of executive staff of the nourishment are available. The complete in- and out-surveys are shown in Figure E-11and Figure E-12 respectively. The out-survey contains some location-shift errors so the location of Kololi Point (the white outcrop) in both figures cannot be compared directly. Characteristic depth contours where no nourishment took place can be indicated in both figures and on the basis hereof, both figures can be compared. The northern area of the nourishment in- and out-survey is shown in Figure 4-15.

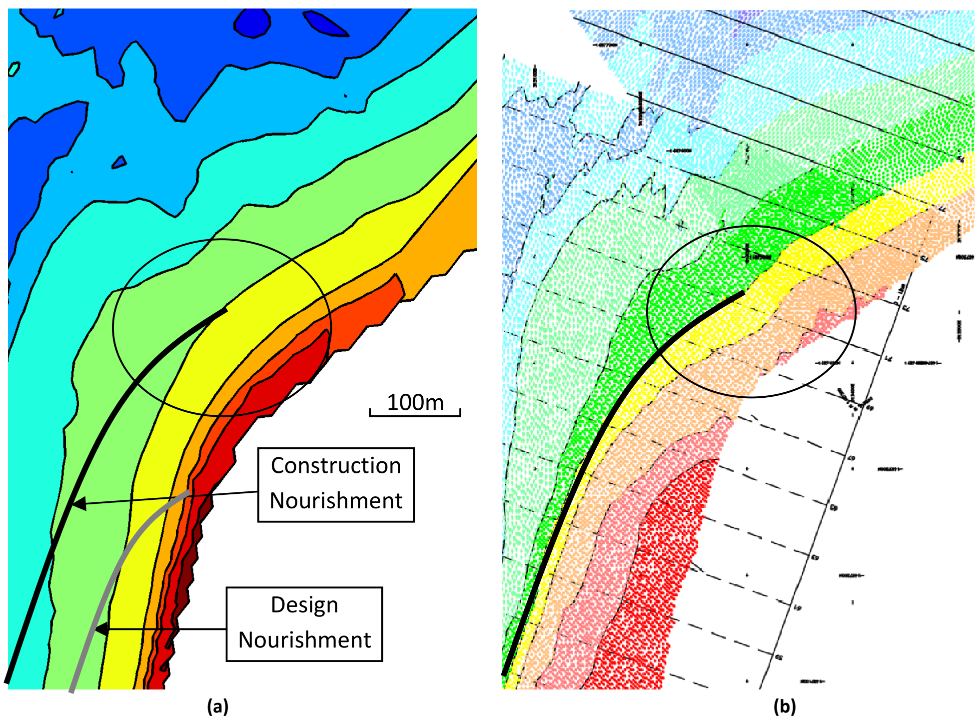

Figure 4-15: Northern part of the (a) in-survey and (b) out-survey

When comparing the in- and out-survey of the northern part of the nourishment, it can be concluded that the nourishment starts just north of Kololi Point. According to the design the nourishment should connect to the shoreline south of Kololi Point. Also visual observations indicate that a relatively large amount of sediment was placed on the northern part of the nourishment close to Kololi Point. After the construction of a nourishment, the nourished sediment spreads out according to Figure 4-16. The nourishment will spread over the adjacent area; therefore the construction of the nourishment has to be relatively narrow with a large beach width. When the nourishment is constructed with a higher spread, the horizontal beach width will be smaller and the nourishment already spread out over a larger area. The lifetime of the nourishment as erosion buffer becomes less due to this initial spread.

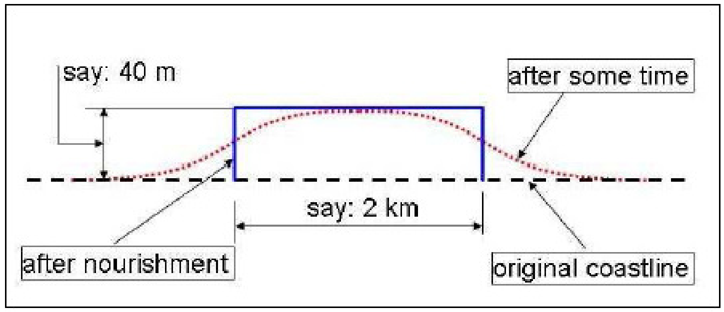

Figure 4-16: Spreading of a nourishment

Because of the location of Kololi point with corresponding currents and wave climate, nourished sediment around Kololi Point is transported to the north very easily. During and after construction the high amount of nourished sediment close to Kololi Point has leaked to the north causing the beach between Kololi Point and Kotu Point to accrete with a high rate. This can be seen in the shoreline movement for the period 2002-2004, see Figure 4-5. This rate is very high and caused some doubts, but also visual observations during and after construction confirms this trend of accretion.

During and shortly after the construction of the beach, erosion is very high as the constructed steep slope alters its cross-sectional shape into a natural equilibrium profile. Visual observations indicate that also after this settling of the beach profiles, the erosion at the nourished beach was very high. Therefore the beach width after nourishment in front of the Senegambia area is only 65m, see Figure 4-5, while the design width for the 1,000,000 m^3 nourishment was considerably larger.

4.4.3 RIP CURRENT

Along the coastline in front of the Senegambia area a dent and a bulge are present, see Figure 4-17. This shape in the coastline is visible in aerial photographs for several different years, before and after the nourishment. It is caused by a rip current which is clearly visible by a sediment plume in front of the beach resorts for the 2004 situation. The local shape can also be seen in the depth contours, see Figure E-11, this coastline shape indicates the possibility for a local rip current, see section 3.6.3. The presence of the rip-current is very likely due to secondary flows and wave refraction caused by the bathymetry of the reef area. This indicates that the wave climate and flow patterns behind the reefs are very complex.

The presence of a rip-current can cause suspended sediment to flow offshore out of the surf zone for high sediment concentration inside the surf zone. Also secondary flows caused by the rip current can have a large influence on the local flow patterns if the alongshore currents due to waves are small.

Figure 4-17: Rip-current in front of the Senegambia area

4.5 CONCLUSIONS

4.5.1 CONCLUSIONS ON OBSERVED TRENDS AND COASTAL PROCESSES

The trends for the period 2004-2009 are roughly the same as the trends between 1964 and 1983; however the erosion and accretion rates are however very different. Probably some illegal sand mining already took place in front of Bijilo Park around 1983, causing a relatively large erosion rate between data point 160 and 180. The total erosion or accretion was small between 1964 and 1983 as the yearly rates shown in Figure 4-3 are low. Erosion and accretion in the southern part near Bald Cape depends on the presence of the Tanji River output inside the research area. When the outlet is inside the research area, the river deposits sediment north of Bald Cape and the area starts accreting. Some years after the outlet switched to the west of Bald Cape the local accretion was smoothened out over the adjacent area after which the total area started eroding until the outlet moved to the north again. Between Sheraton and Bijilo the beach was slowly accreting in case of no human interference; between 2004 and 2009 the rate was much higher than between 1964 and 1983. Probably this is caused by the sand deficit in this area due to the illegal sand mining till 1996. The bad condition of the beaches in the research area can clearly be seen in Figure E-1, even in front of Bijilo Park. Figure E-2 shows the nourishment, large amount of nourished sediments are indeed present in the northern part of the nourishment. Figure E-3 shows the present situation, clearly the beach in front of Bijilo Park has benefited from the nourishment; the beach in front of Senegambia is almost gone and the strange coastline shape can been seen again.

Erosion at Kololi beach was also present from 1964 on, although with a smaller rate than from 2004. After the illegal sand mining the coast in front in Kololi was eroding partly due to effect of the mining in adjacent cells. The average rate of sand mining was 130,000 m^3/year, with even higher maximum rates. The erosion rate between 2004 and 2009 is relatively high, partly due to the effect of the spreading of the nourished sediment during the first years after the completion of the works. There is a general trend of sediment loss to the adjacent areas of approximately 30,000 m^3/year, independent of the input of the Tanji Stream. The adjacent areas are southwest of Bald Cape and north of Kotu, the direction of the sediment loss is not exactly known. If the outlet of the Tanji Stream is inside the research area, the stream contributes to the sediment budget with approximately 10,000 to 30,000 m^3/year.

There is a small difference in the trends in shoreline movement between the recent study and the 2000 Feasibility Study for the period 1964-1983, namely for the stretch between Sheraton and Bijilo. Although the rest of trends for this period agree well, this difference in observed erosion and accretion results in a different sediment budget for the research area. This can have a large influence when the observed trends are used for the calibration of sediment transport modelling.

Sieve analyses show that the nourished sediment contains a lot of shell fractions which is also clearly visible. The sediment contains 10-20% of shell fraction with a maximum of 30% for the lowest quality of sediment. These shell fractions wash out very easily and do not contribute to the total volume of the sediment in case of erosion, increasing the erosion rate with the same percentage as the volume of shells inside the nourishment.

No large differences are visible between the measured profiles of 2000, 2003 and 2010, except for the Kotu reef. These large differences in measured profiles can be causes by the uncertainty of the measurements and measurement locations or could indicate changes in the reef area in front of Senegambia. There is not enough data available to draw conclusions on the possible eroding or subsiding of the reefs, therefore the eroding reefs have not been taken into account.

In front of the Senegambia area a rip-current is present. A rip current is often generated by set-up differences and run from the position of the highest set-up towards the position of the lowest set-up. In case of high sediment concentration inside the surf zone, the suspended sediment flows offshore out of the surf zone. The presence of a rip-current indicates complex secondary flows and the presence of locally curved coastline.

4.5.2 DESIGN MODELLING STUDY

Due to the large time scale of several years to decades, the morphological study is performed using the single line theory which is a 1-Dimensional sediment transport modelling approach. Longshore transport is the dominant mechanism so the problem can be simplified using the single line theory while it gives a valuable insight into the principle of coastline dynamics. Due to the reef area, strong curvature of the coastline and the reefs in front of Bald Cape, the research area is too complex to simplify as 1-Dimensional model; these models are usually suitable for quasi uniform beaches. Using a 2- or 3-Dimensional model is neither possible as the available time scale is too short for the period of interest. Therefore 1-Dimensional modelling is applied while keeping in mind the shortcomings of the model. Therefore the results of the sediment transport modelling have to be interpreted an calibrated manually to correct effects caused by the shortcomings of the model.

The nearshore wave climates and the sediment transport capacities will be calculated for the same data points that have been used to determine the shoreline movements. As explained in section 4.1 this area has been chosen on the availability of bathymetric and topographic data to generate profiles which are used in the calculation. For sediment capacity calculations the nearshore wave climate and a local profile perpendicular to the coast are needed. The length of the profiles has been chosen to be 400 meters. In this way the sediment transport is within the complete profile and the input wave climate is close to the coast for accurate results but the wave climate is not largely influenced by interpolation errors in the nearshore bathymetry. Profiles have been generated for each point where also topographic measurements have been carried out on the beach during the measurement campaign in September 2010; see the pinks lines in Figure 4-18. The wave output data points have been generated perpendicular tot the coastline for each coastline data point. For each coastline data point the coastline angle has been determined by the previous and following data point, and perpendicular to this coastline angle the wave input data point is determined by a fixed distance from the coast, see Figure 4-18. This gives 245 wave climate data points for which the nearshore wave climates will be calculated.

This design for the sediment transport calculations depends largely on the nearshore wave climates as the sediment transport will be calculated for a nearshore wave climate very close to the coast. In this way the reef area is included within the calculation of the waves, still the results of the shoreline modelling behind the reefs have to be interpreted with caution. Using wave climates more off-shore and longer profiles, was not possible due to the curvature of the coast and the presence of the reefs.

For all the wave climate data points in Figure 4-18 the complete time series of the nearshore wave climate will be calculated using the SWAN model, see Chapter 0. This will happen for the mean wave direction, peak wave direction and for the wind generated waves for 3 different water levels: mean water level, mean high water and mean low water level during spring tide:

Using these nearshore wave climates the sediment transport capacity will be calculated using the LITPACK software, see Chapter 6. This is applied for all the data points as during the first calculations it became clear that the calculations are sensitive and results can be different for data points close to each other. As the resulting transport is almost zero, small differences can have a large effect. This could cause errors in the sediment transport for the complete coast and therefore results will not be interpolated between large areas.

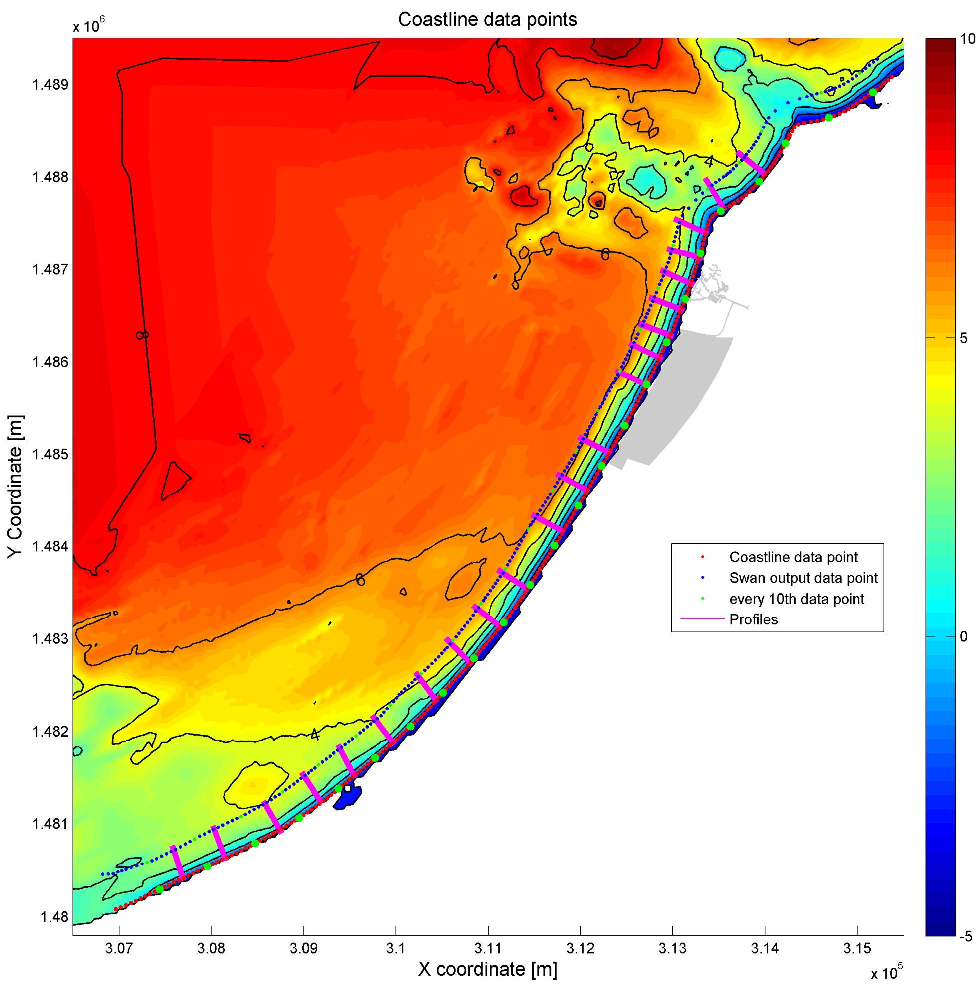

Figure 4-18: Used profiles, Coastline and Swan data point

5. NEARSHORE WAVE CLIMATE

In order to investigate morphological behaviour along the coast of The Gambia, the nearshore wave climate has to be known. To simulate the evolution of off-shore swell waves and wind-generated waves off The Gambian coast, the nearshore wave climate will be calculated using the SWAN package. SWAN stands for Simulating WAves Nearshore.

SWAN is a third-generation wave model for obtaining realistic estimates of wave parameters in coastal areas, lakes and estuaries from given wind, bottom and current conditions. The model is based on the wave equation with sources and sinks. The SWAN package computes wave propagation, wave generation by wind, nonlinear wave-wave interactions (quadruplet and triads), white-capping, bottom friction, depth-induced wave breaking and wave induced set-up for a given bathymetry, wind- and wave data, water levels and current field in waters of deep, intermediate and finite depth. For further information regarding the SWAN package the reader is referred to the SWAN Manual.

The nearshore wave conditions will be based on the transformation of the off-shore time series of wind- and wave records from BMT Argoss, see section 3.3. Because of the difference in wave direction parameters, both the peak direction and the principal wave direction for swell waves are calculated using the model. Wind generated sea waves have been determined separately. To investigate the effects of the tide, the nearshore wave climate for swell and sea waves is determined for the mean sea level and the mean high and low water level at spring tide.

To determine the nearshore wave climate for the further morphological computations the setup of the model is explained in section 5.1. Here the model grids, boundary conditions and model settings are described. The results are shown and discussed in section 5.2; the conclusions are drawn in section 5.3.

5.1 MODEL SET UP

MODEL GRIDS

For the modelling of the nearshore wave climate at the research area, a model area was first defined. Therefore an area larger than the area of interest is defined to simulate the propagation of the swell waves and to stimulate the development of waves under wind conditions. The selection of the size of this area depends on the locations of the available boundary conditions, see Figure 3-5 for the location of the off-shore wind- and wave data. It is also important that possible error data from the boundary conditions do not penetrate into the research area. Therefore the largest grid has to be large enough, preventing the error data to penetrate in the research area. To introduce the areas of interest to a model area, rectangular grids are placed over the area. Between the grid cells wave energy and momentum are transferred. To save computational time, initially a large grid is defined to transfer the off-shore wave data to a nearshore grid. This finer sub grid is nested inside the coarse grid, see Figure 5-1.

The idea of nesting is to compute the waves on a coarse grid for a larger region first and then on a finer grid for a smaller region. The computation on the fine grid uses boundary conditions that are generated by the computation on the coarse grid. The first nested grid runs from North of Kotu Point to Bald Cape, which is the research area.

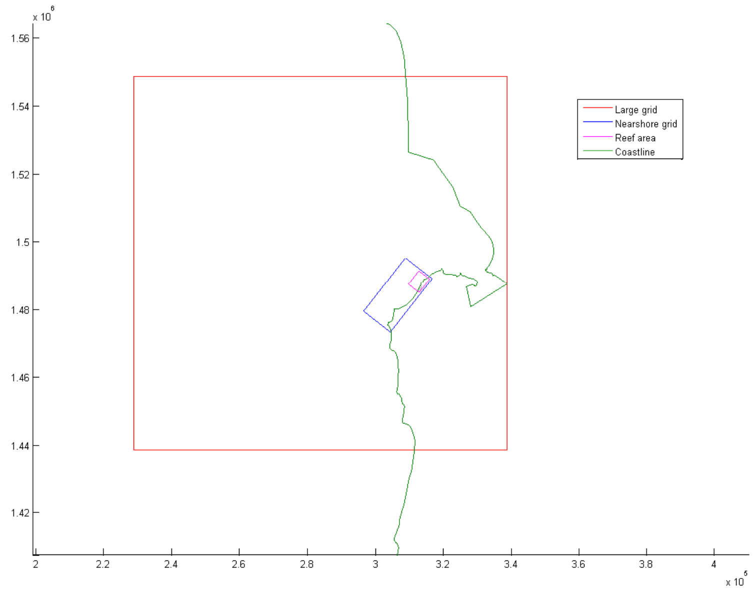

Figure 5-1: computational grids

Because of the complex nearshore bathymetry and the importance of the Senegambia area, a finer grid is once more applied around this area, see Figure 5-1. The boundary conditions for the nested grids are automatically obtained from the coarser model. All the grid and cell sizes and hence the computational resolutions can be found in Table 5-1.

Grid	Grid points [-]	Cell size [m]
Coarse grid	200 x 220	500 x 500
Nearshore grid	200 x 100	100 x 100
Reef area (Senegambia)	250 x 200	20 x 20

Table 5-1: Computational resolution

BATHYMETRY

The bathymetry used for the computation is composed of the DEEP BV 2010 measurement, C-Map offshore data and measurement points from 2000 which fall outside the 2010 measurement area. On all the grid points, depths are calculated by means of interpolation of the available, nearby data points. The C-map data have some unreliable points off-shore causing unexpected plateaus in the coarse grid, see Figure 5-2a. The specific points which cause these irregularities have been deleted from the C-Map data points, and lead to the bathymetry shown in Figure 5-2b.

The bathymetry for the nearshore grid is shown in Figure 5-3

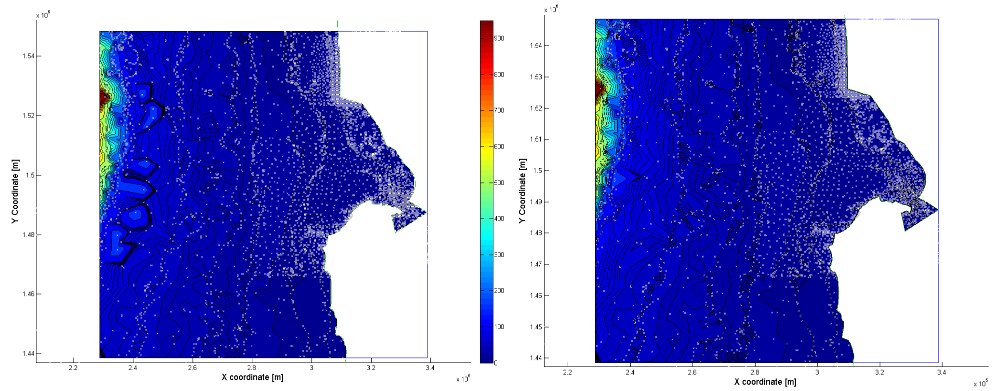

(a) **(b)**

Figure 5-2: (a and b): Off-shore bathymetry

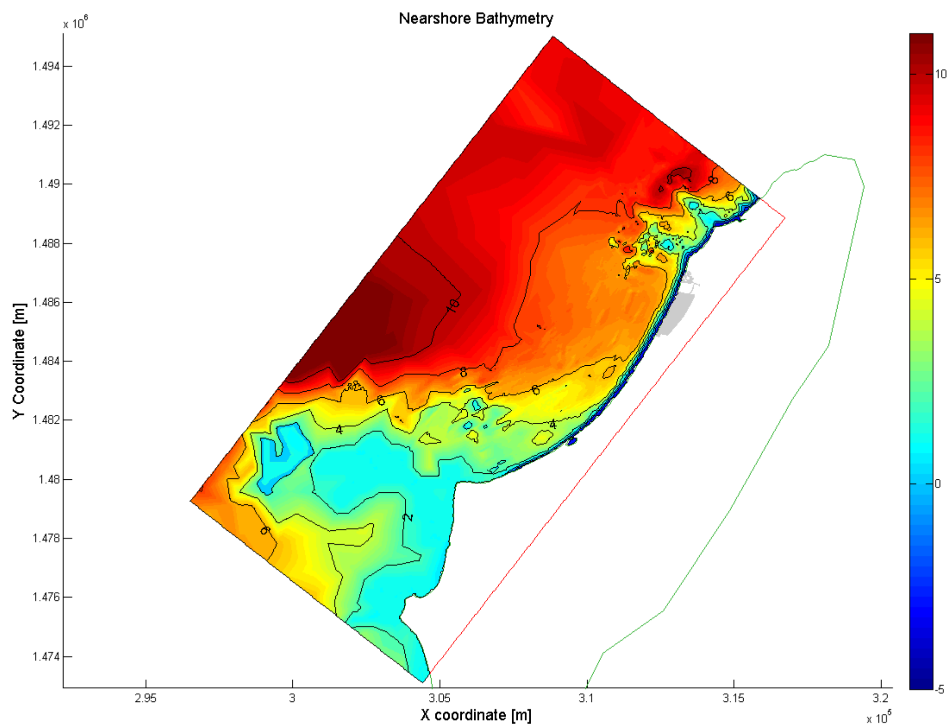

Figure 5-3: Nearshore bathymetry

BOUNDARY CONDITIONS

The boundary conditions used for the nearshore wave modelling are based on one of the two available data points by BMT Argoss. The western, northern and southern boundaries of the large grid will be formed by data point N. The data from point N and point S are almost identical, there is only a slight difference in wave heights and directions but the overall wind and wave climates are the same. Because of the transformation from off-shore waves to a nearshore climate, this small difference will have almost no effect on the nearshore climate. Two different data points make the calculation more complicated and time consuming, therefore only point N is used.

The nearshore climate will be calculated both for swell conditions, as for wind generated waves separately. Swell waves are present for 99.9% of the time in the time series. Because of bad classification of the separate swell wave data from Argoss, the total wave height is used as input for swell conditions. For the swell conditions no wind input and wind generation of waves is used for the calculation.

Sea waves are only classified when two different peaks in the spectrum could be distinguished. These wind generated waves were present for 20% of the total time series. The direction of the wind waves is in line with the direction of the wind, see Figure 5-4. Therefore the wind direction has the same input as the wave direction during the calculation. In view of the method of calculation this saves a lot of computational time.

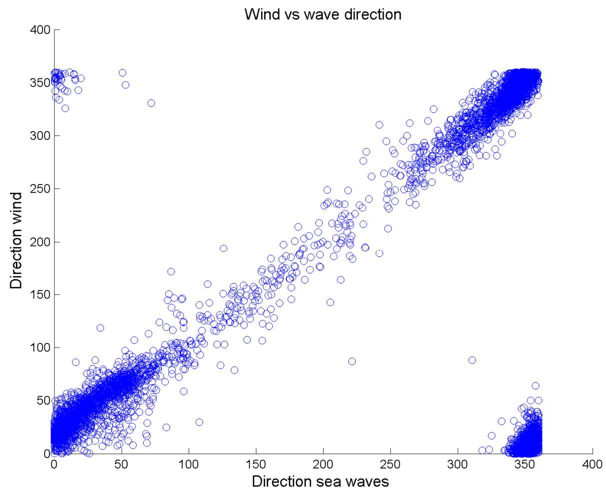

Figure 5-4: Wind direction versus wave direction

METHOD OF CALCULATION

The nearshore hydrodynamics will be calculated for the complete 10 year time series with 3-hourly wind and wave data. As the translation of long time series is very time consuming, the method of transformation matrices have been used for the translation to nearshore waves. For this method, nearshore wave climates are modelled for a selection of combinations of offshore wave heights, -steepness, and -directions and as far as wind waves are concerned also for wind speed and direction. Nearshore wave climates for every time step in the off-shore wave climate are then determined by means of interpolation between the modelled wave climates using transformation matrices. The combination of conditions is selected in such a way that they give an optimal coverage of the offshore wave data, see Figure 5-5 for the combination of swell wave conditions and Figure 5-6 for the combination of wind-wave conditions. The combination of boundary conditions are described in terms of wave height, direction and steepness as presented in Table 5-2 for swell conditions, and for wind-wave conditions in Table 5-3 with wind speed. Table 5-2 shows the matrix dimensions of the wave simulations for swell conditions that have been carried out: 8 wave heights x 7 steepnesses x 13 directions gives 728 simulations in total. Table 5-3 shows the matrix dimensions of the wave simulations for wind-wave conditions that have been carried out: 6 wave heights x 4 steepnesses x 6 directions x 4 wind speeds gives 576 simulations. One should keep in mind that the direction is used both for the wind direction and wave direction. Because of the difference in the wave direction parameters for swell waves, both the peak direction and the principal wave direction will be calculated for the complete time series using the transformation matrices.

The wave steepness for each wave period and wave height at the boundaries is calculated based on the simple deep water formula for the wave height and period:

$$s_o = Hs * 2 * \pi/(9.81 * T_p{}^2) \qquad \textbf{(5.1)}$$

Parameter	Range of values for boundary conditions												
H_s [m]	0.4	0.8	1.2	1.7	2.2	2.7	3.4	4.1					
s_o [-]	.0018	.003	.005	.008	.012	.021	.045						
Dir [°N]	180	195	210	225	240	255	270	285	300	315	330	345	360

Table 5-2: Range of values for boundary conditions for swell conditions

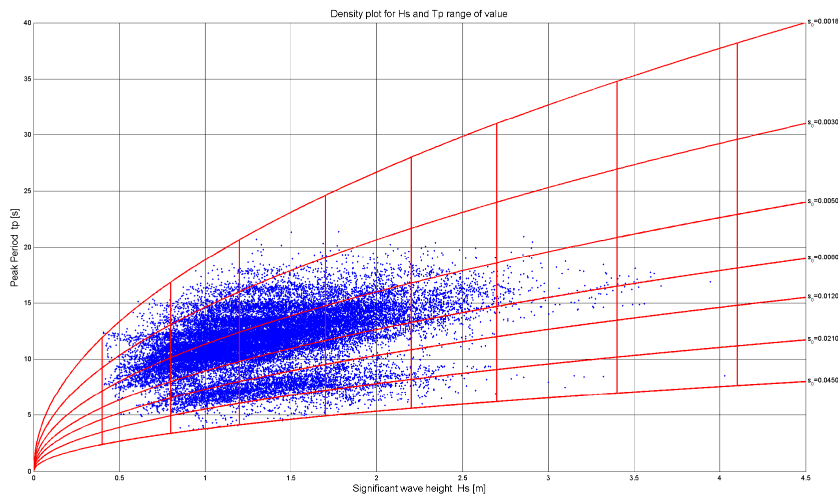

Figure 5-5: Density plot for swell conditions

Parameter	Range of values for boundary conditions									
H_s [m]	0.15	0.7	1.2	1.8	2.5	3.7				
s_o [-]	.012	.022	.032	.08						
Dir [°N]	330	345	360	15	30	60				
U_{10} [m/s]	2	6	10	15						

Table 5-3: Range of values for boundary conditions for wind conditions

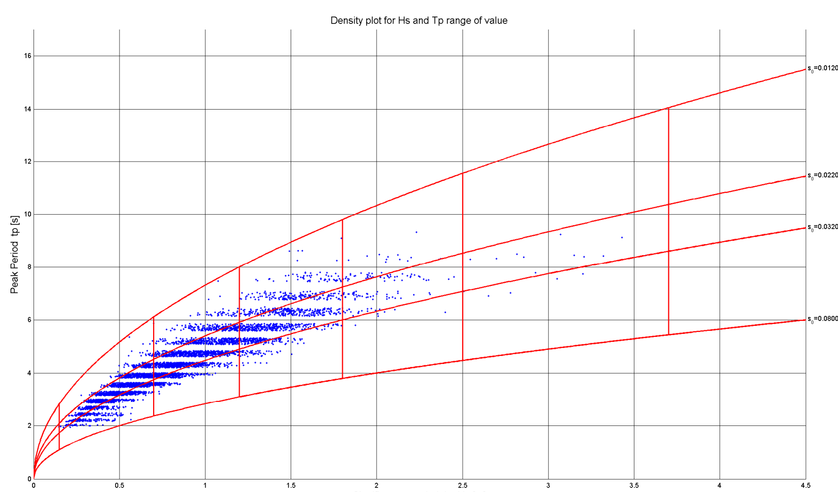

Figure 5-6: Density plot for wind0wave conditions

MODEL SETTINGS

The swell conditions will be calculated for the total significant wave height without wind and wave generation by wind. Swell waves are the waves that are governing the total wave heights originating from the south to north. The wind and corresponding sea waves are coming from the north. For the computation of sea waves, wind and wind growth has been taken into account.

The absence of available nearshore wave data makes it impossible to calibrate the model to increase the accuracy. Therefore the physical model settings are modified for this specific area and corresponding conditions. The water levels used are Mean Sea Level, mean high and mean low spring tide; which is approximately CD +0.3m, CD +1m and CD +1.7m. First of all the model settings for the swell conditions are given in the next paragraph.

The Gambia lies at the Atlantic Ocean so no limited fetch is present for swell conditions, giving a fully developed sea state. Therefore the spectral space is given by the Pierson-Moskowitz shape. The following formulas originate from the 'environmental conditions and environmental loads' by Det Norske Veritas. See the scatter data in Figure 5-5 for wave heights with corresponding peak periods, for these values and equation 5.2 it follows that γ = 1, giving the Pierson Moskowitz shape.

$$\begin{aligned} &\gamma - 5 \quad \text{for} \quad T_P/\sqrt{H_S} \leq 3.6 \\ &\gamma = \exp(5.75 - 1.15\frac{T_p}{\sqrt{H_s}}) \quad \text{for} \quad 3.6 < T_P/\sqrt{H_S} < 5 \\ &\gamma = 1 \quad \text{for} \quad 5 \leq T_P/\sqrt{H_S} \end{aligned} \qquad \textbf{(5.2)}$$

The used period is the Peak period and the directional spreading is given in Degrees. Because of swell waves which have a very limited spreading, the number of degrees has been selected to be 5. The water density in front of The Gambia is 1025 kg/m^3; this was measured during the bathymetric survey in September 2010.

All relevant shallow water processes are taken into account: refraction, nonlinear interactions (quadruplet and triads), bottom friction, white-capping and depth induced breaking. The empirical Johnswap model will be used with the coefficient = 0.038 for waves with Tp>12 and 0.076 for waves with Tp<8. For waves with peak periods between 8 and 12 seconds, the coefficient is linearly interpolated between the two previous values. The depth induced breaking is described by the Battjes and Janssen model. The default values for this parameter are α=1 and γ=0.73. The breaker index γ is not a universal constant, 0.73 is an average of a large number of experiments. For instance, Battjes and Stive (1985) suggested a formula for γ which is widely used, based on the steepness of the wave:

$$\gamma = 0.5 + 0.4tanh(33s_o) \qquad \textbf{(5.3)}$$

Where s_o is the incident wave steepness ($s_0=H_{rms}/L_{peak,\ deep\ water}$). For the different conditions and corresponding steepnesses, the breaker index has been calculated and used as an input coefficient.

The maximum number of iterations has been set to 20 and the accuracy to 95% to get accurate results with limited time consumption.

The physical model settings used for swell conditions are summarized in Table 5-4:

Parameter	Settings
Directional spreading (spectral space)	Pierson Moskowitz
- Period	Peak period
- Degrees	5
Water density	1025
Depth induced breaking (α)	1
Depth induced breaking (γ)	0.58 – 0.83
Bottom friction	JonSwap
- coefficient	0.038 – 0.076
Wind growth	Not activated
White-capping	Activated
Quadruplets	Activated
Nonlinear triad	Activated
Refraction	Activated
Max number iterations	20
Accuracy	95%

Table 5-4: SWAN Physical parameter settings for swell conditions

For the SWAN calculation of wind generated wave conditions the Jonswap spectrum has been used with γ = 3.3, which is the default value for wind generated waves. Generated sea waves have larger spreading than swell waves and therefore the degree of directional spreading has been selected to be 30. The coefficient for depth induced breaking has been calculated with equation 5.3 for the different wave steepnesses. The bottom fraction is given by Jonswap; due to the higher wave steepness the Jonswap coefficient has been chosen to be 0.076. All other processes have been activated and this time also the wind growth has been activated.

Parameter	Settings
Directional spreading (spectral space)	Jonswap (γ = 3.3)
- Period	Peak period
- Degrees	30
Water density	1025
Depth induced breaking (α)	1
Depth induced breaking (γ)	0.65 – 0.89
Bottom friction	JonSwap
- coefficient	0.076
Wind growth	Activated
White-capping	Activated
Quadruplets	Activated
Nonlinear triad	Activated
Refraction	Activated
Max number iterations	20
Accuracy	95%

Table 5-5: SWAN Physical parameter settings for wind conditions

5.2 RESULTS

SWAN computations have been performed for a large number of input combinations as described above. Therefore only SWAN results for common wave directions and for high and low water are shown in the following section. This is done for as well the swell conditions as for wind generated wave conditions. In Appendix D SWAN results are shown for different wave directions, wave heights and wave steepnesses.

5.2.1 SWELL CONDITIONS

The significant wave height for an offshore significant wave height of 1.7m from the southeast (direction 225° North) is shown in Figure 5-7 and the same wave coming from the northeast (direction 315° North) is shown in Figure 5-8 for the large and the nearshore grid. One should keep in mind that the southern boundary for southern waves and the northern boundary for the northern waves are not representative. The input conditions at the northern and southern boundary, between the off-shore point and the land, are the same as the off-shore condition, which is not the case in reality. The waves near the land are lower and have different properties than the off-shore waves. These error data are far enough away from the research area so that they do not penetrate into the nearshore hydrodynamics.

The refraction of the waves around Bald Cape and dissipation in front of Bald Cape can clearly be seen for southern waves. This refraction pattern is also shown in Figure 5-9. Therefore these waves have less energy at the research area than waves coming from the north. For the northern waves a strip of higher wave heights is visible towards the hotel area. The higher wave heights north of the hotel area are caused by the reefs. As a result of shoaling the waves become higher and dissipate energy on the reefs, creating waves with less energy behind these reefs. See also Appendix D for significant wave heights for western waves and for the wave heights and the refraction pattern inside the reef area.

The limited off-shore depths, approximately 100 m see Figure 5-2, for the long swell waves cause some energy dissipation by bottom friction. This can also be seen in Figure D-5 and Figure D-6 for waves with different steepness. Steeper waves are less influenced by bottom friction off-shore due to limited length and therefore less energy is dissipated offshore. Because these steeper waves have a higher bottom friction coefficient nearshore, the energy dissipation is higher there than for less steep waves.

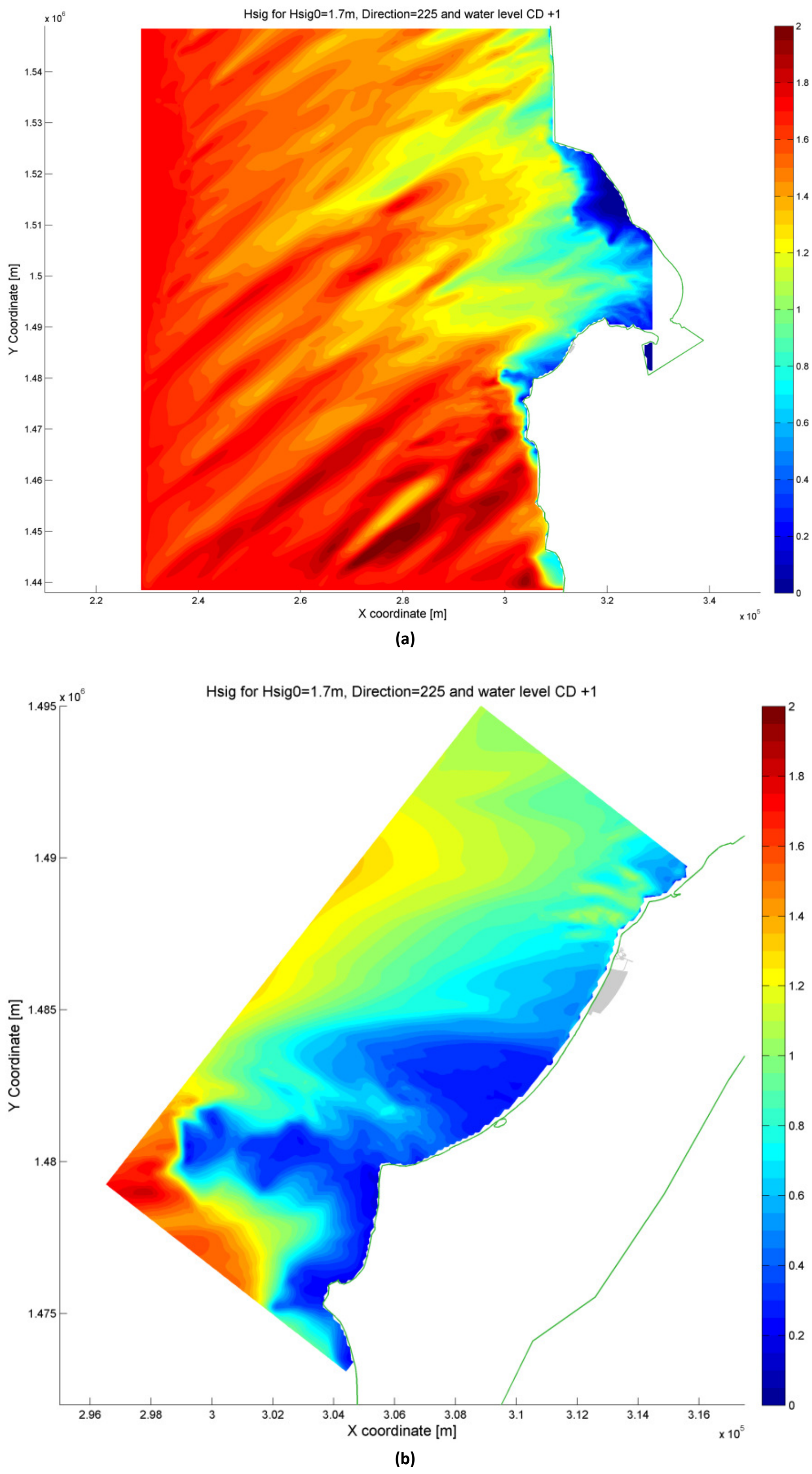

(b)

Figure 5-7: Significant wave height for south-western waves for large grid (a) and nearshore grid (b)

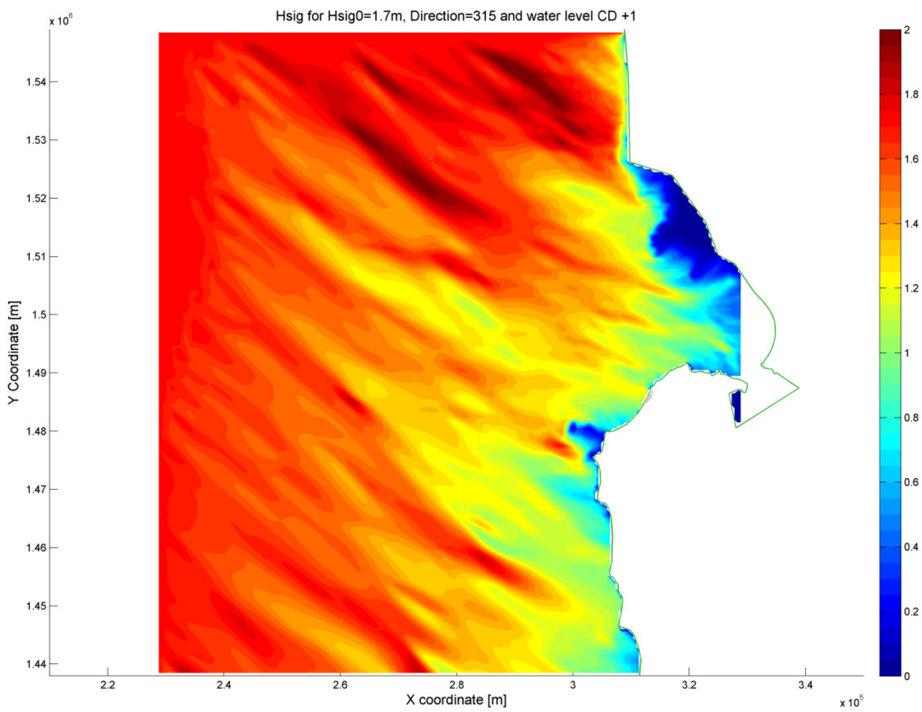

(a)

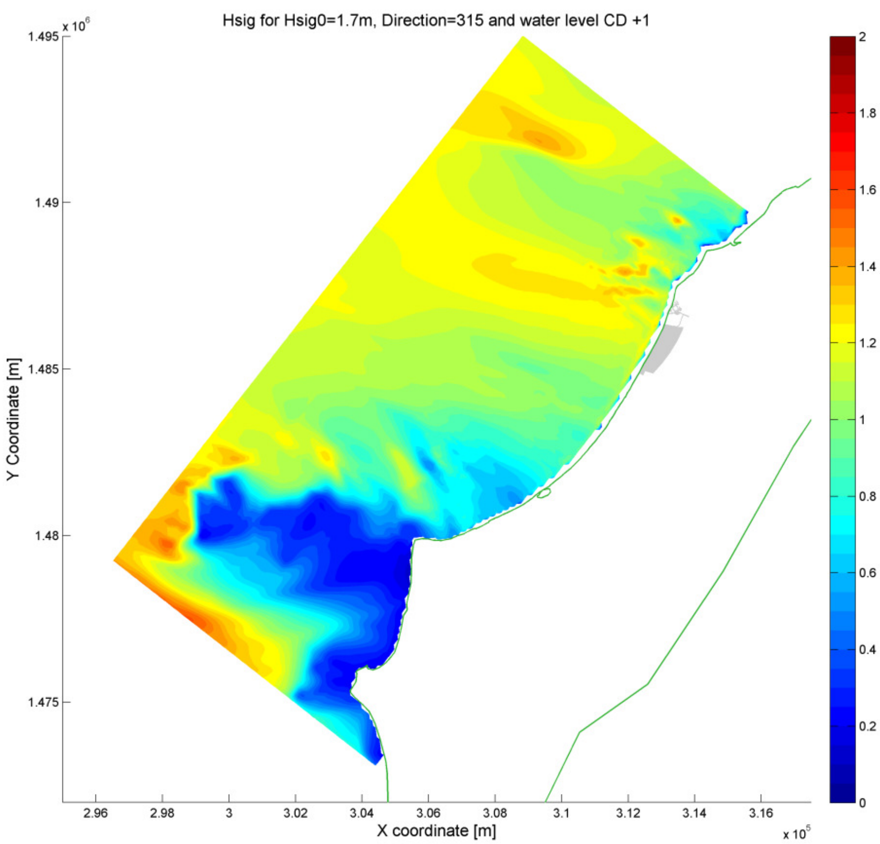

(b)

Figure 5-8: Significant wave height for north-western waves for large grid (a) and nearshore grid (b)

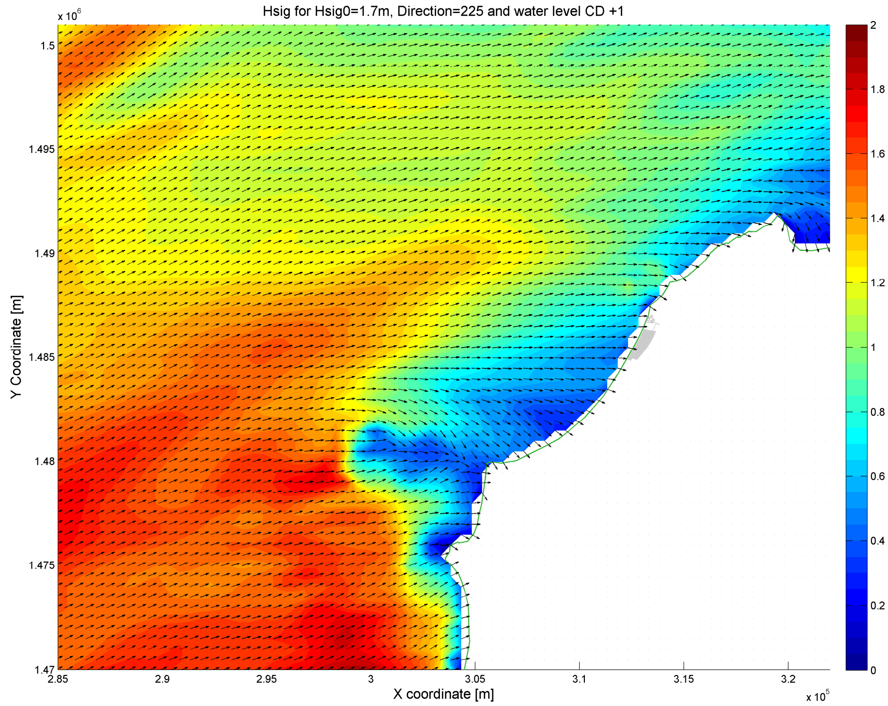

Figure 5-9: Refractive pattern for south-western swell waves

The 10 year time series for both the wave direction parameters has been generated for several nearshore locations. The wave roses for both direction parameters in front of the Senegambia area are shown in Figure 5-10. Several nearshore wind roses in comparison with the coastline, added to Google Earth, are shown in Figure 5-11 for the principal wave direction and Figure 5-12 for the peak direction.

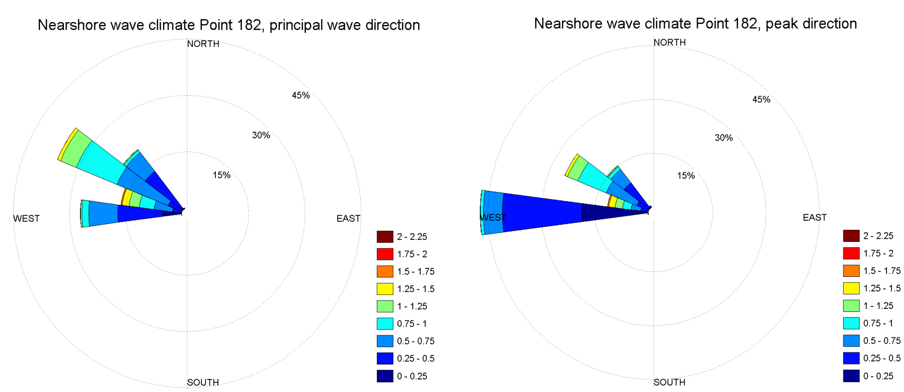

(a) **(b)**

Figure 5-10: Nearshore wave roses in front of Senegambia (a) principal wave direction and (b) peak direction

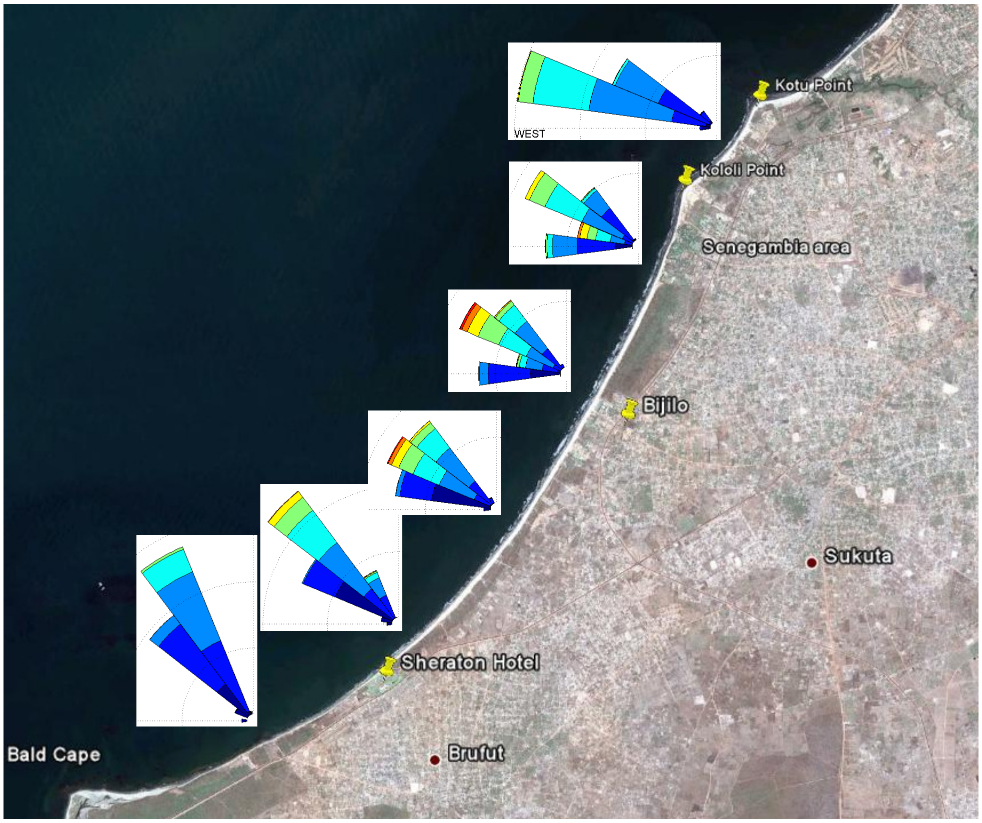

Figure 5-11: Nearshore wave roses for principal wave direction

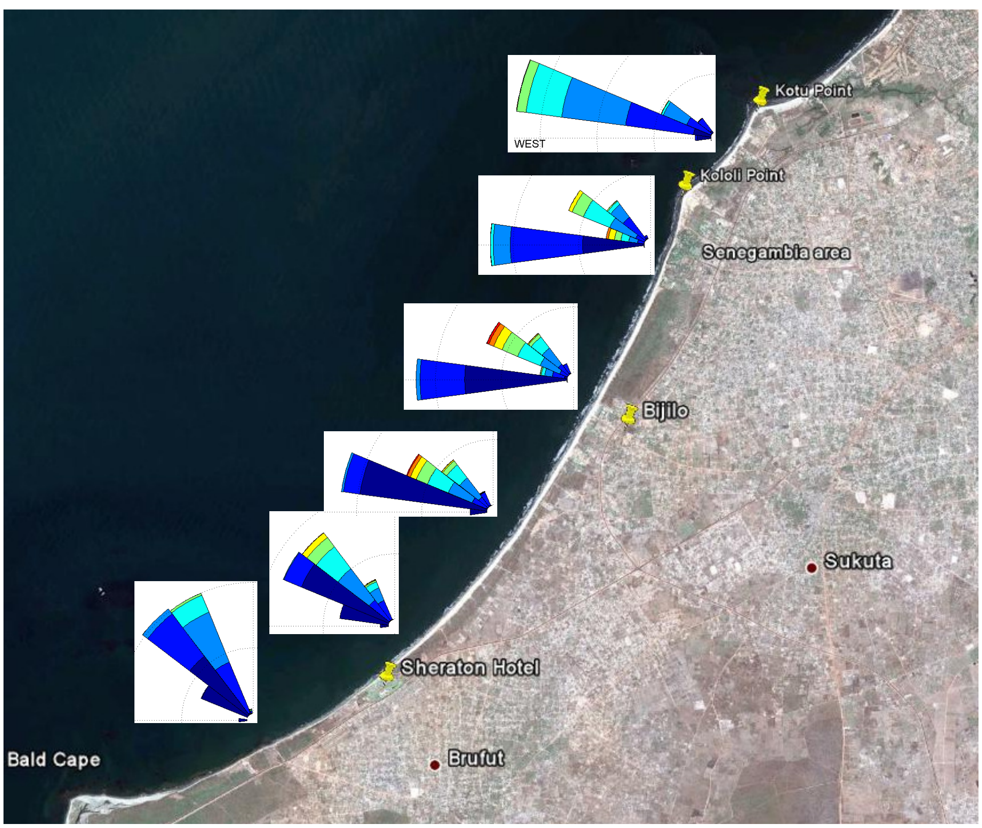

Figure 5-12: Nearshore wave roses for peak direction

5.2.2 WIND CONDITIONS

For the wind generated wave conditions again the error data from the northern boundary can clearly be seen, see Figure 5-14. These data are corrected relatively quickly and do not penetrate into the research area. The generation of waves can be seen by the higher wave heights in front of the research area where a larger fetch is present for the northern wind. The bottom friction coefficient is higher for steep wind waves than for swell waves, which can be seen by the large energy dissipation nearshore. The wave heights and frequency of occurrence are lower than swell waves but the wind-generated waves have a large wave incidence, possibly causing relatively larger alongshore transport. This can be seen by the refractive pattern in Figure 5-15.

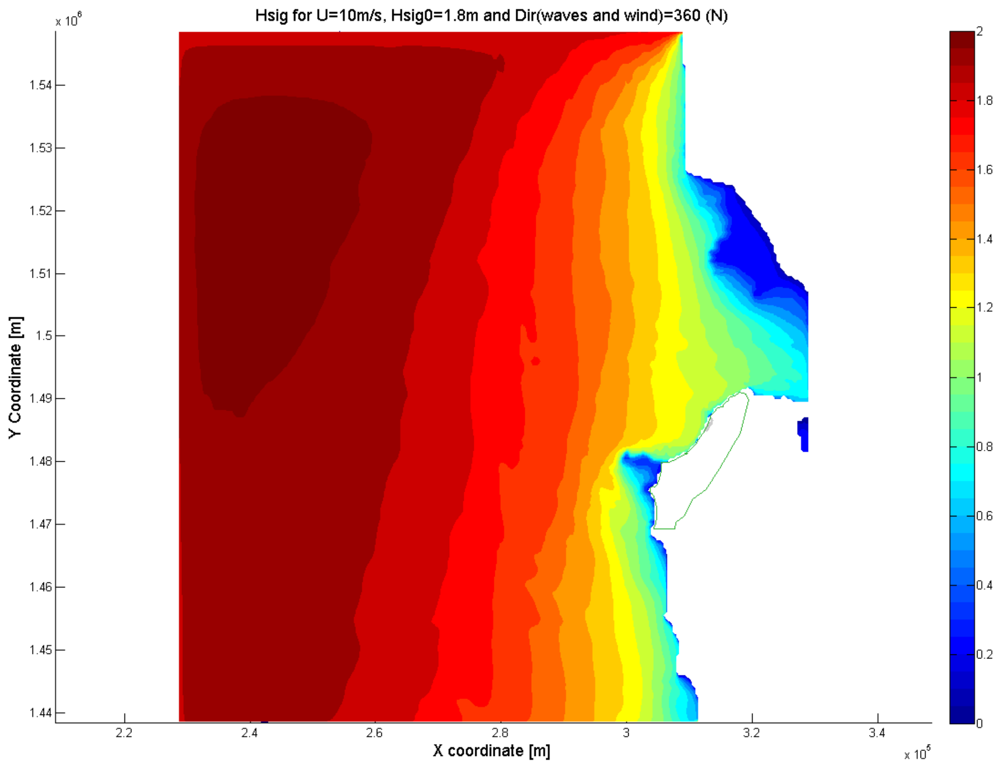

Figure 5-13: Significant wave height for wind generated waves for the large grid

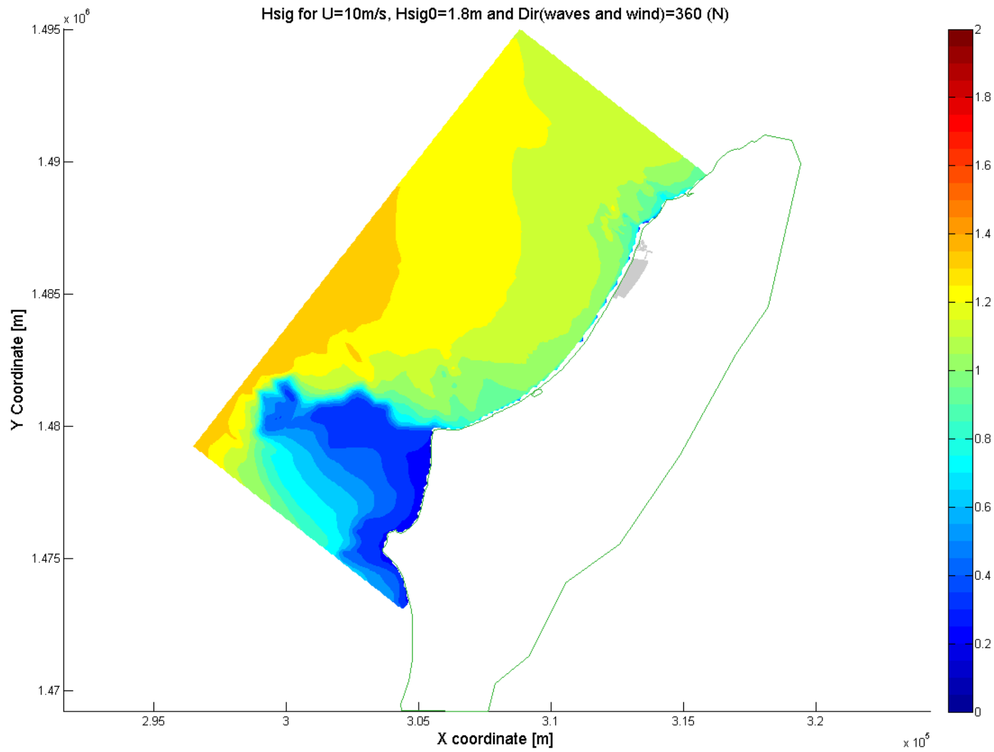

Figure 5-14: Significant wave height for wind generated waves for the nearshore grid

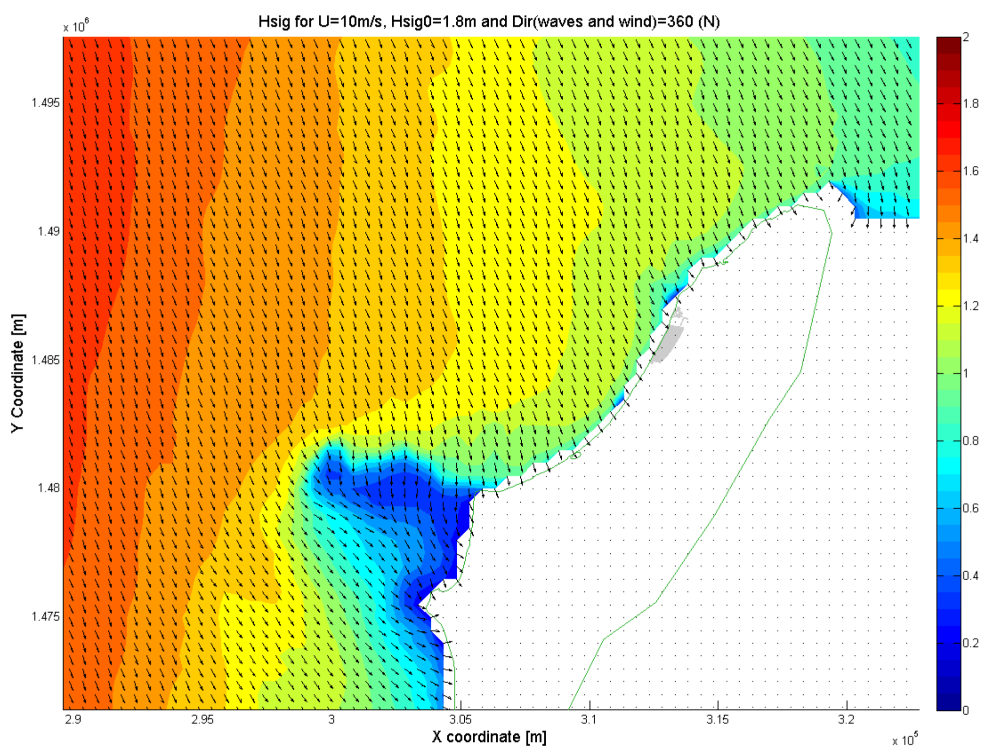

Figure 5-15: Refractive pattern for wind generated waves.

Also for the wind generated waves the nearshore wave climate can be described by the two different wave direction parameters. Because the wind waves are distinguished by a separate spectral peak with a high frequency within the spectrum, the principal wave direction and the peak direction are practically the same. Also along the coast the annual wave climate hardly changes. The wave roses for two different locations are shown in figure XX.

The percentage of occurrence for the wind waves is much lower than for the swell waves. This is because only approximately 20% of the total time series a separate spectral peak for wind waves is distinguished. Also about 90% of the wind waves lies within the boundaries for which the wind waves are calculated.

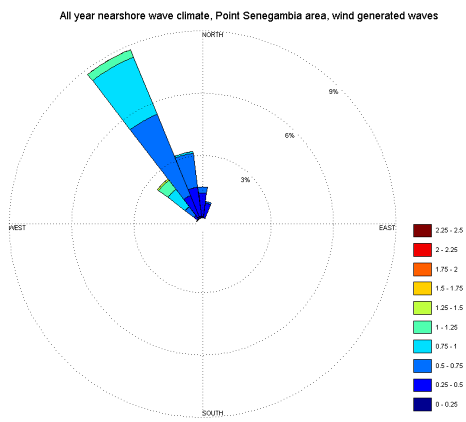

(a)

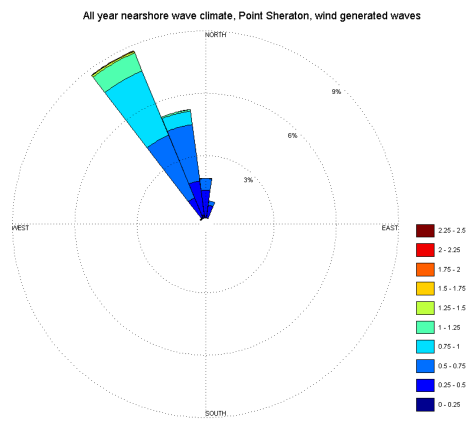

(b)

Figure 5-16: Wave roses for wind generated waves at (a) Senegambia area and (b) Point Sheraton

5.2.3 HIGH AND LOW WATER LEVEL

To investigate the influence of the tide for the sediment transport modelling, the nearshore wave conditions have also been calculated for the mean high water level and the mean low water level at spring tide; which are respectively CD +1.7m and CD +0.3m respectively. The differences are at its best to be seen inside the reef area. The significant wave heights for the different water levels are shown in Figure 5-17 and Figure 5-17.

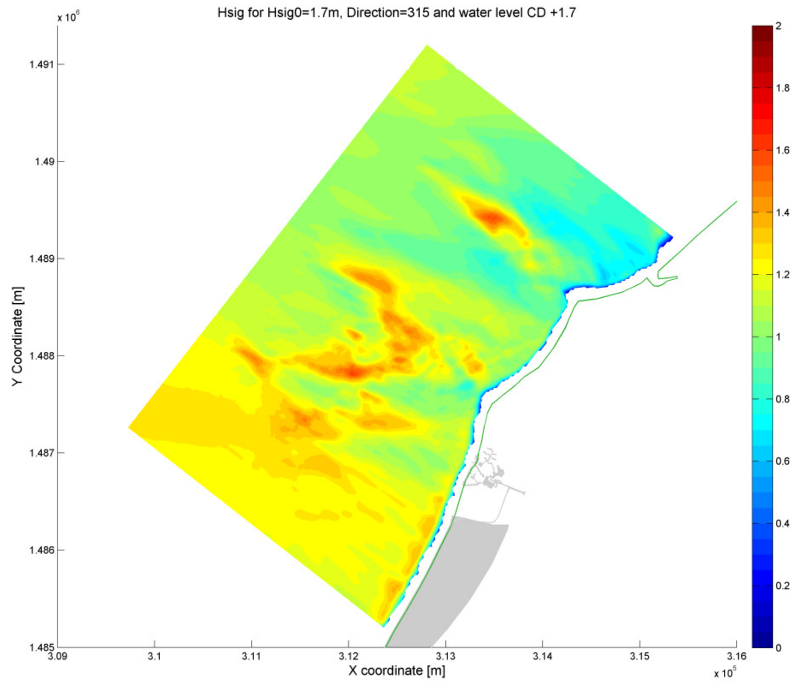

(a)

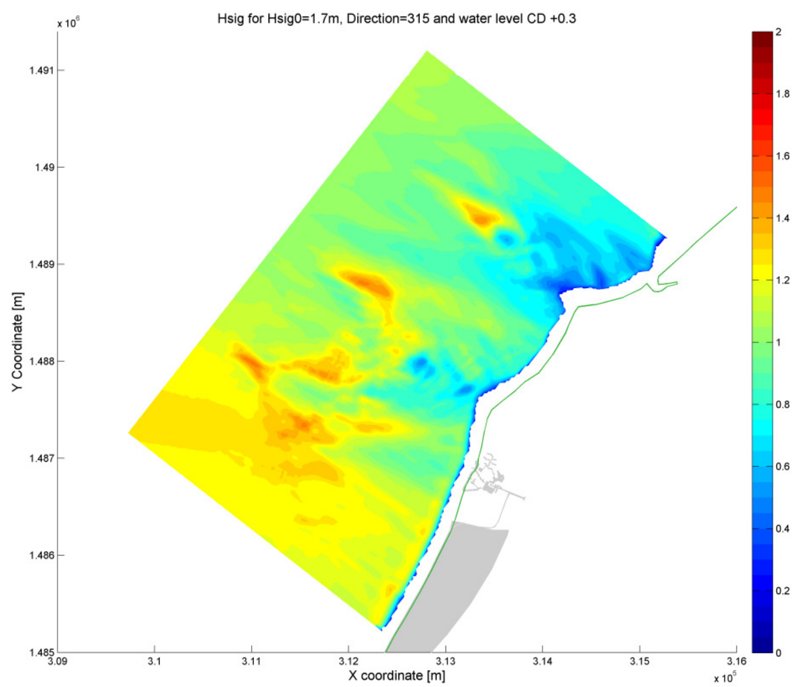

(b)

Figure 5-17: Significant wave height for high water level (a) and low water level (b)

During low water the reef area is very shallow and therefore the waves break on the reefs causing less wave energy behind the reefs. Also the friction on the incoming waves is higher as the depth is lower on the terrace in front of the research area, causing the waves having less energy; this can be seen in the figures by decreased significant wave heights. Along the coastal stretch the nearshore waves are lower and carrying less energy during low water. This is visible for waves both from the south and from the north.

5.3 CONCLUSIONS

The determination for the nearshore wave climates in front of The Gambia has been done for swell wave conditions and for wind generated wave conditions. Observations and analysis of the nearshore climate have led to the following conclusions:

- Swell waves coming from the south are partially blocked by the large reef in front of Bald Cape. Due to refraction and wave dissipation on the Bald Cape reef a large amount of energy has dissipated and therefore the wave height has decreased behind the reef. Hence these reefs have a sheltering effect on the research area for swell waves from the south.

- Swell waves coming from the north can propagate freely to The Gambian coast without any obstructions. Off-shore swell waves refract yet far away from the coast due to limited water depths, see Figure 3-14. Therefore the wave incidence is close to normal on arrival. These swell waves do have large wave-energy due to higher wave heights and long wave periods, so even with a small angle of wave incidence the alongshore sediment transport can be relatively large.

- Wind generated waves, which are coming from the north, have a large angle of wave incidence within the research area. This will cause alongshore sediment transport to the south. These waves are, however, wind generated with short periods and are subjected to larger bottom friction near the coast and are much more dispersive than swell waves. Therefore the wave-energy is lower than that of well waves when arriving at the breaker zone.

- As can be seen in section 3.3.2 there is a large difference between the two directional parameters which describe the offshore wave direction. This large difference in directional parameter is also translated into the nearshore hydrodynamics. The main difference is a large frequency of southern waves for the peak direction, but these waves have a very low wave height. For the principal wave direction a large percentage of these, eventually, western waves are shifted towards the north increasing the frequency of waves coming from the northeast. This difference in frequency for wave directions can cause a large difference in alongshore sediment transport for both directional parameters.

- For swell conditions the waves arrive at the coast for nearly normal wave-incidence. During the year, the direction of the incoming waves varies with the seasons causing alongshore sediment transport in both directions ending with a net transport. The direction of this transport is calculated in Chapter 6.

- Complex refractive patterns are present within the reef area caused by the complex bathymetry. This causes local relatively large differences within the nearshore hydrodynamics. Large alongshore transport gradients can arise behind the reefs which are very difficult to model with a 1 Dimensional approach, if possible at all.

- During low water waves with less energy arrive at the coast due to additional friction caused by the terrace in front of the coast. Also the reef area has a more sheltering effect as the reefs become very close to the sea level, the waves break and the wave climate behind the reef area is calmer. During high water the reefs have less influence on the incoming waves and the wave climate near the coast behind the reef area is rougher.

6. SEDIMENT TRANSPORT ANALYSIS

Sediment transport and shoreline modelling has been carried out to obtain better insight into erosive transport gradients, which contribute to (rapid) erosion of the nourishment. Using the SWAN results and measured bathymetry, alongshore sediment transport and corresponding instantaneous coastline evolution have been modelled with the LITPACK software by DHI. The nearshore wave conditions that are defined in Chapter 5 are used to model the sediment transport capacity for every data point. Gradients in sediment transport indicate a change in alongshore transport along the coast; this can then be transformed into an instantaneous coastline change.

The observed trends in shoreline movement indicate low sediment transports with changing directions. The coastline orientation and bathymetry of the research area varies inside the research area, causing the input parameters to change considerably along the coast. As sediment transport modelling is (very) dependent on these input parameters, the results will be sensitive to small differences in the input parameters along the coast. Together with wave incidence close to shore normal it implies that results along the coast can fluctuate which is not a representation of reality where the sediment transport changes gradually along the coast. Therefore the results will be smoothened to indicate the trends in sediment transport along the coast.

Furthermore due to the presence of the reef area in front of Kololi Point, Kotu Point and Bald Cape, the bathymetry and wave climates are locally complex which influences the occurring alongshore sediment transport. This cannot be represented properly by the modelling as this is a coarse schematization of reality. Therefore the results will be calibrated manually based on observed trends in shoreline movement and knowledge on the area and local processes.

A description of the modelling software LITPACK is given in section 6.1. The program input and output parameters are defined and shown in section 6.2. The raw results of the sediment transport capacity calculations will be shown first in section 6.3. A discussion on the raw results and the calibration of the results is done in section 6.4. The conclusions are drawn in section 6.5

6.1 MODELLING SOFTWARE AND THEORY

LITPACK, developed by DHI, is a software package for simulating non-cohesive sediment transport in waves and currents, littoral drift, coastline evolution and profile development along quasi uniform beaches. LITPACK consists of different modules to describe these processes. During this modelling study the LITDRIFT module for longshore currents and littoral drift has been used. The sediment Transport Program (STPQ3D) is the core of the modelling system and solves the vertical diffusion equation on an intra-wave period grid. STPQ3D accounts for waves and currents at arbitrary angles, breaking/non-breaking waves, plane/ripple-covered bed, uniform/graded bed material, effect of bed slope and effect of streaming.

LITDRIFT

LITDRIFT is a deterministic numerical model which consists of a hydrodynamic and a sediment transport model. The hydrodynamic model includes a description of propagation, shoaling and breaking of waves, calculation of the driving forces due to radiation stress gradients and momentum balances. The sediment transport is dominated by contributions from areas where wave breaking occurs. The longshore and cross-shore momentum balance equation is solved giving the distribution of sediment transport across the profile which is integrated to obtain the total longshore sediment transport rate. Input parameters are integrated within the profiles and wave climates, as will be explained in the following section. The sediment transport model within LITDRIFT is based on the sediment transport formulae by Deigaard (1985).

Further information on the modelling software can be found in the DHI manuals for LITPACK and LITDRIFT.

For a given coastal profile with corresponding wave climate and coastline orientation, LITDRIFT calculates the sediment transport capacity. The transport capacity indicates the possible amount of sediment to be transported across the coastal profile. If for some reason the sediment is blocked or no transportable sediment is present across the coastal profile, the occurring sediment transport can be considerably less than the transport capacity.

Coastline modelling has not been performed for this study as the reef area is not suited to be represented within a 1-Dimensional coastline model. Due to 2-Dimensional processes and a hardened seabed inside the reef area, which are not possible to be represented adequately by a 1-Dimensional model, a coastline model will give unreliable results. Therefore coastline changes will be determined as instantaneous shoreline movements using the single line theory, based on the sediment transport modelling results.

SINGLE LINE THEORY

The single line theory is a coarse schematization where the coast is mapped into a single line. Because of the assumption that the profile itself does not change over time, the coastline can be schematized as one single line which moves seaward or landward. The single line theory has also been used for the estimation of the sediment budget. The presence of sediment transport does not lead to either erosion or accretion; the coastline will remain stable as long as the incoming sediment transport (S_{in}) is equal to the outgoing sediment transport (S_{out}) over a stretch. When there is a difference between S_{in} and S_{out} (δS_x) material must be eroded or deposited in the area in order to maintain a sediment mass balance.

Gradients in sediment transport therefore give shoreline movement. This process is shown in Figure 6-1, the shoreline movement is calculated by the equation of the single line theory (6.1) by Pelnard-Considere (1956):

$$\frac{\partial Y}{dt} = \frac{-1}{d}\frac{\partial S_x}{\partial x} \tag{6.1}$$

Where ∂S_x is the change in alongshore sediment transport over a given distance, $\partial Y/dt$ is the shoreline movement over time, d is the height of the surf zone and ∂x is the given distance. The height of the surf zone is given by the Depth of Closure and the berm height. See section 4.2 for the definition of the Depth of Closure as used during this research.

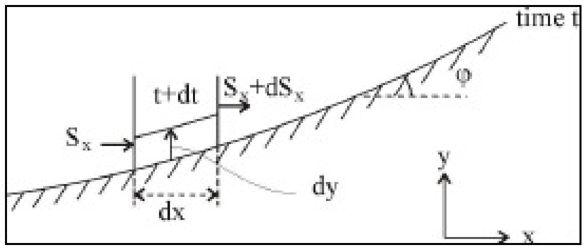

Figure 6-1: Single line theory

Modelling results will give an indication for the alongshore sediment transports and gradients within the research area. As the modelling study is based on a coarse schematization of the coast and input parameters, the model will not be possible to exactly reproduce the occurring transports in reality. A modelling study is a tool to gain understanding on present processes and substantiate observed trends.

6.2 MODEL SET-UP

6.2.1 MODEL SETTINGS

For the coastline data points as defined in Section 4.5.2, the sediment transport capacity has been modelled using LITPACK. Each data point uses the corresponding wave climate, the closest profile and the local coastline orientation as input for the modelling; see Figure 4-18 for the definition of the data points and profiles. The properties and parameter settings of the profiles and wave climates are explained in the following section, as the definition and generation of used coastline orientations.

PROFILES

The cross-shore profiles describe the bathymetry of the modelling area. Figure 6-2 shows the bathymetry of profile 14; the origin is positioned off-shore, approaching the shoreline along an axis which is perpendicular to the depth contours. The off-shore depth has to be at least the depth of closure as sediment transport has to be within the complete profile. All used cross-section profiles are of the same length and described by a line series with 5 items: bathymetry, bed roughness, mean grain diameter d_{50}, fall velocity and the geometrical spreading.

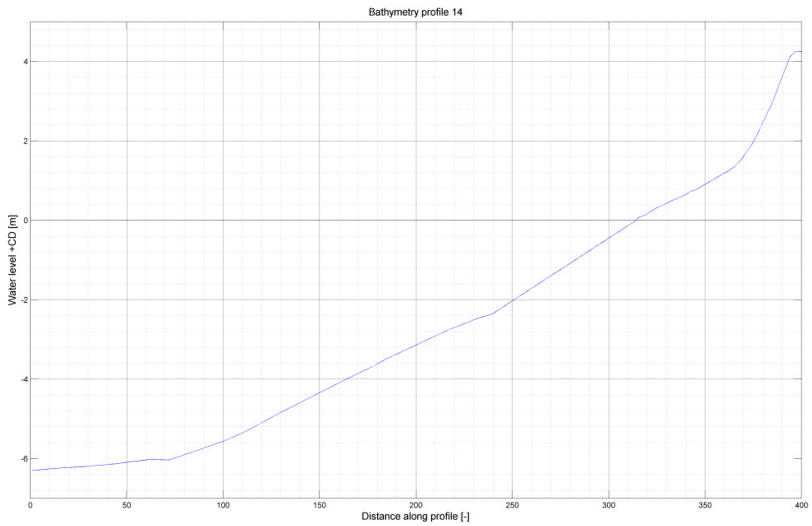

Figure 6-2: Bathymetry of profile 14

The bathymetry is based on measured lines from the September 2010 measurement. The mean grain diameter d_{50} is based on the sieving curves of the sediment samples, see Figure 6-3 and Figure 4-12. After removing the shells fractions from the samples the d_{50} can be read as 0.26 mm. This can be done as the large grain diameters of the shell-fractions do not contribute to the stability of the sediment. Furthermore the shell fractions wash away very easily from the sediment so they do not contribute to the total volume of the nourishment. Using this assumption, you should keep in mind that these shell fractions will erode from the beach but will not become a part of the alongshore sediment transport. The same value for the grain diameter has been used for the across the complete profile.

The bed roughness to be defined includes bed ripples. Without bed ripples the bed roughness is usually 2 a 3 times d_{50}. As a first estimate, 10 times d_{50} has been used; this resulted in too large sediment transports compared with the 2000 Feasibility study and the first analysis of the results. Therefore the default value for UNIBEST by WLDelft, 5 cm, has been used; which is a good approximation of the bed roughness in a coastal area. This value gave reliable results and is therefore used during the rest of the study. After the model produced satisfactory results, no more calibration has been performed on the input parameters.

The fall velocity can be described by Rubey's formula (1933), see equation 6.2. In literature, other formulae can be found. Computed fall velocity's as a function of the grain diameter for 2 formulae are plotted in Figure 6-4. From both equation 6.2 and Figure 6-4 the fall velocity becomes 0.038 m/s.

The geometrical spreading is given by $\sqrt{(d_{84}/d_{16})} = \sqrt{(400/200)} = \sqrt{(2)}$, see Figure 6-3: the geometrical spreading is small as the sediment is rather uniform.

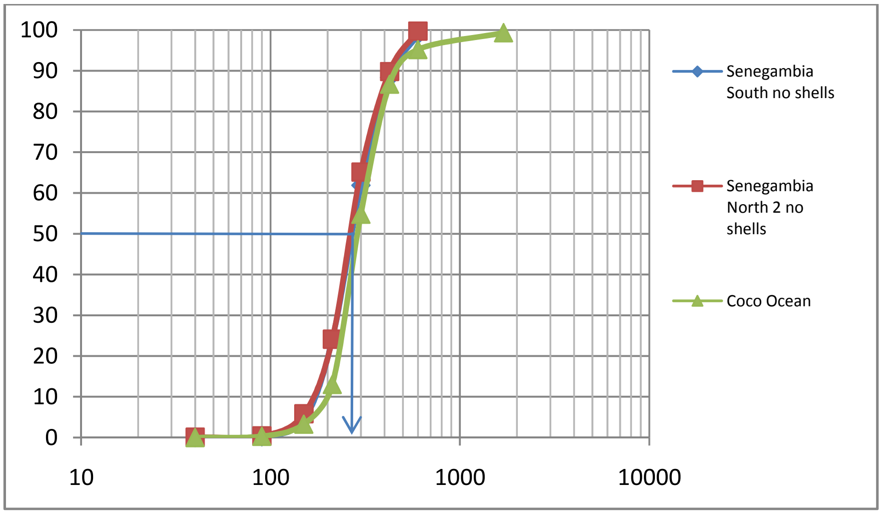

Figure 6-3: Sieving curves for sediment in front of Beach resorts

$$w = \sqrt{g(s-1)d} \cdot \left(\left(\frac{2}{3} + \frac{36\nu^2}{g(s-1)d^3} \right)^{1/2} - \left(\frac{36\nu^2}{g(s-1)d^3} \right)^{1/2} \right) \quad (3.87)$$

.2)

where s is the relative sediment density, g is gravity and ν is kinematic viscosity found by Eq. (3.88).

$$\nu = (1{,}78 - 0{,}0570812T + 0{,}00106177T^2 - 8{,}27141 \cdot 10^{-6}T^3) \cdot 10^{-6} \quad (3.88)$$

where T is the water temperature in degrees Celsius.

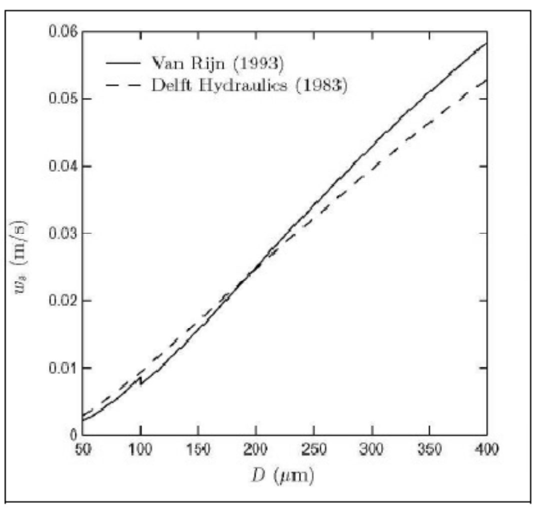

Figure 6-4: Computed fall velocities as function of the grain diameter

WAVE CLIMATE

The important parameters of a wave climate are represented by the wave height, wave angle, wave period, water level and the current velocity at a reference depth in the profile. As the sediment transport is calculated according to the mathematical model for littoral drift by Deigaard (1985), the used wave height is the root-mean-square wave height. Available wave data are given in significant wave height; the estimated relation between the significant wave height and the root-mean-square wave height is given by $H_{rms} = 1/2\sqrt{(2)} \cdot H_s$. (Holthuijsen (2007)).

The reference depth for each wave climate originates from the depth given by the SWAN output for each data point. This depth includes the given water level in SWAN; this water level is also added within the wave climate, therefore the input water level is subtracted from the depth given by SWAN. The current velocity is 0 for all the calculations.

A wave climate in LITPACK is represented by a number of events, each described by its duration in % per year. For this study the greater part of the modelling runs is performed with the probability of occurrence for the nearshore wave climates to save computational time. A 10 year time series contains 29,224 conditions where a probability of occurrence contains a maximum of approximately 500 conditions, dependent on the distribution of waves. The probability of occurrence calculations provide results with an accuracy of 95% and higher. This has been checked for multiple profiles along the coast. For some locations along the coast the total time series has been calculated to show the year-to-year distribution of sediment transport.

A nearshore time series is converted into a probability of occurrence for different wave height and -direction classes. For both swell and sea waves the significant wave heights are divided with a step size of 0.1 meter and the directions are divided with a step size of 2.5 degrees. The total time series is subdivided into these classes, where the probability is defined by the number of waves in a class divided by the total number of waves. The wave height and direction of each class is determined by the weighted average of the wave heights and -directions. After the determination of the probability of occurrence, the wave heights are converted to root mean squared wave heights.

The duration in % per year is given by the probability of occurrence times 100 %. For a year within the total time series, the duration in % per year is given by $(1 / (365.25 \cdot 8)) \cdot 100 = 0.0342466$ %. A calculation for the probability of occurrence then gives the cumulative total of net transport capacity per year, while a total time series gives the sediment transport capacity for every 3 hours with a cumulative total of sediment transport capacity for 10 years.

The probability of occurrences has been determined for the 10 year total time series. During the study it became clear that the calculated transport capacities change over the 10 year period, see Figure 6-12. Especially the years 2007, 2008 and 2009 are different from the first years. Therefore the probability of occurrence has been determined for the 2004 and 2009 wave climate separately to investigate the influence of the changing wave climate.

COASTLINE ORIENTATION

The coastline angles for the modelling study are based on coastlines drawn in Google Earth on the basis of aerial photographs and satellite images. Due to the sand mining and the nourishment in 2003, the coastline locations have changed through the years for different periods. Therefore the coastline orientations for these years change slightly. A large part of the calculations have been performed for an average of the 1964, 1972, 1983 and 2009 coastlines, which are the coastlines for the most undisturbed years. This average has been smoothened out; see Figure 6-5 for the used angles. This coastline orientation is named the mean coastline for the remainder of this report. Alongside the mean coastline, the 2004, 2009 and 2003 coastline shortly after the nourishment have been used as input for the sediment transport modelling. The 2003 coastline is based in the 2002 coastline including the design of the nourishment. The shown coastline orientations are defined as the direction of the seaward directed shore normal, relative to the north..

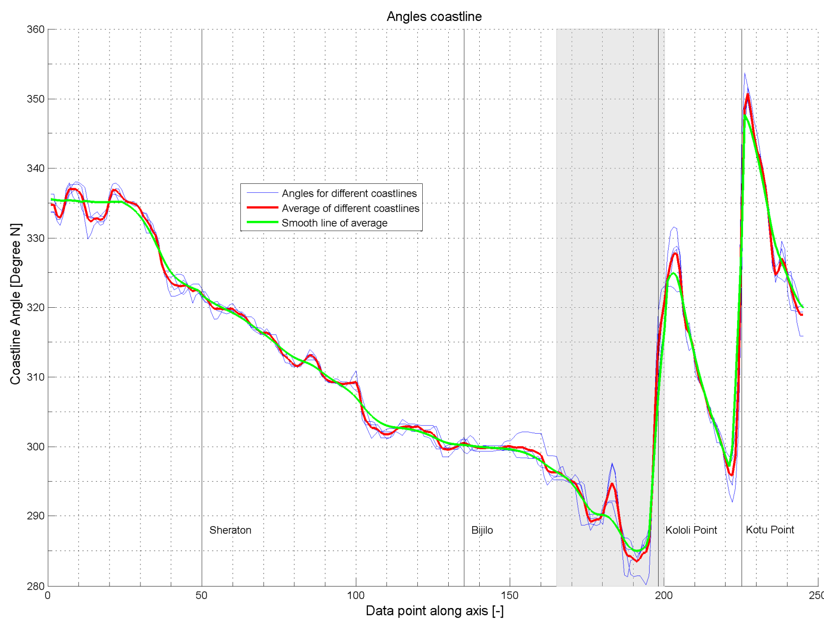

Figure 6-5: Used coastline angles

The peaks from point 0 to 30 and between point 180 and 190 have been smoothened out to obtain a gradually changing coastline orientation along the coast. Due to the local bathymetry these irregularities can be present on the shoreline but this will not be taken into account during the complete transport modelling along the coast. Using calculated S-ϕ curves, see section 6.3, the sediment transport which corresponds with the actual coastline angle can be derived after the modelling.

6.2.2 MODELLING RUNS

The sediment transport capacities along the coast have been modelled for all 245 data points as defined in Figure 4-18 for different combinations of coastlines, water levels and wave climates to investigate their influence on the alongshore sediment transport and gradients. The wave climates consist of the mean and peak direction for swell waves and of the sea waves. Used water levels are mean sea level, mean high and mean low water level at spring tide: CD +1m, CD +1.7m and CD +0.3m. As described above, sediment transport modelling has been performed for the mean, 2003, 2004 and 2009 coastline orientation.

For the mean coastline and mean sea level, the sediment transport has been calculated for the given coastline angle, as well as for the given coastline angle +5° and -5°. The relationship between the net alongshore transport (S) and the coast orientation (ϕ) is presented in a so-called S-ϕ curve. Using the sediment transport for the extra angles, S-ϕ curves for the data points along the coast have been drawn. S-phi curves show the effect of the angle of wave incidence on the longshore sediment transport. Using the S-ϕ curves the C-value can be calculated, which represents the change in sediment transport per coastline angle. The C-value indicates the rate of sensitivity of the alongshore sediment transport.

All modelling runs, except for the total time series, are performed with a probability of occurrence. The sediment transport for the total time series has been calculated for 8 profiles distributed along the coast. The following runs have been done for the list of combinations as shown in Table 6-1:

Coastline Orientation	Wave climate	Water Level (m +CD)
Mean Coastline	Principal wave	1
Mean Coastline	Peak	1
Mean Coastline	Sea	1
Mean Coastline	Principal wave	0.3
Mean Coastline	Peak	0.3
Mean Coastline	Sea	0.3
Mean Coastline	Principal wave	1.7
Mean Coastline	Peak	1.7
Mean Coastline	Sea	1.7
2003	Principal wave	1
2003	Sea	1
2004	Principal wave	1
2004	Sea	1
2009	Principal wave	1
2009	Sea	1
Mean Coastline	Total time series, Principal wave	1
Mean Coastline	Total time series, peak	1
2004	2004 WC Principal wave	1
2004	2004 WC peak	1
2004	2009 WC Principal wave	1
2004	2009 WC peak	1
2009	2009 WC Principal wave	1
2009	2009 WC peak	1

Table 6-1: Overview of sediment transport calculations

6.3 RESULTS

The first results presented are the raw results from the alongshore sediment transport modelling. These results have not been modified and calibrated; the results have solely been smoothened for the presentation. Shoreline movements in the following figures are based on the smoothened sediment transport as the determination by gradients of the sediment transport is very sensitive. In nature the shoreline movement is gradually along the coast; therefore only trends in the shoreline movement modelling results are of importance. Keep in mind that the nearshore wave climate could not be calibrated and therefore the wave climates contain an uncertainty. This is mainly the case on the stretch north of Bald Cape and around the reef area where the wave climate is strongly influenced by the complex bathymetry. The bathymetry has been interpolated between measured lines which are up to 1 km apart around Bald Cape.

Positive sediment transport is transport to the north and negative transport is directed southerly.

SWELL WAVES AND SEA WAVES

The modelled sediment transport capacity for the principal wave direction and peak direction for swell waves and for sea waves is shown in Figure 6-6. Modelled sediment transport capacities for the principal wave and peak direction are represented by the red and blue line respectively, sediment transport capacity due to sea waves is represented by the green line in the figure. The used coastline orientation is the mean orientation at mean sea level, CD +1m.

The modelling results show northerly directed sediment transport northeast of Bald Cape, which decreases and turns to southerly transport before Bijilo; inside the nourishment area another transport reversal point is present after which the transport is northerly directed again. This is the case both for the principal wave direction as for the peak direction. Although the computed trends for both the different wave direction parameters are exactly the same, the peak direction gives 10-30 % lower transport. The sea waves cause a relatively large transport which is always directed southwards and the computed net transport, caused by swell and sea waves, is southerly directed from the Sheraton Hotel until the Senegambia area. Large gradients and transports are computed around Kololi Point and Kotu Point which are not present in reality, see Figure 6-6. Also inside the nourishment area the transport capacities become relative large southerly directed. This is very remarkable due to the expected sheltering effect of the reef area. This will be discussed and modified in the following section.

The instantaneous shoreline movement corresponding to the un-calibrated sediment transport is shown in Figure 6-7. From point 0 to 50, an area with erosion and accretion is determined; from point 50 an overall trend of small accretion exists according to the modelling results. In front of the beach resorts area a very high erosion rate is determined with areas of accretion north and south of the erosion area. These high gradients are caused by the very high computed sediment transport capacities around Kololi Point. In reality, the occurring transports are considerably less so the erosion and accretion rates in reality are not as high as shown in the figures. The high computed transports are caused by the waves breaking and being refracted on the reefs. Large wave driven currents, due to the angle of wave incidence, and stirring is present behind the reef area. No or limited sediment availability at the reefs causes the actual transport to be considerably smaller then the computed capacity.

Positive sediment transport is northern directed and negative transport is directed southerly.

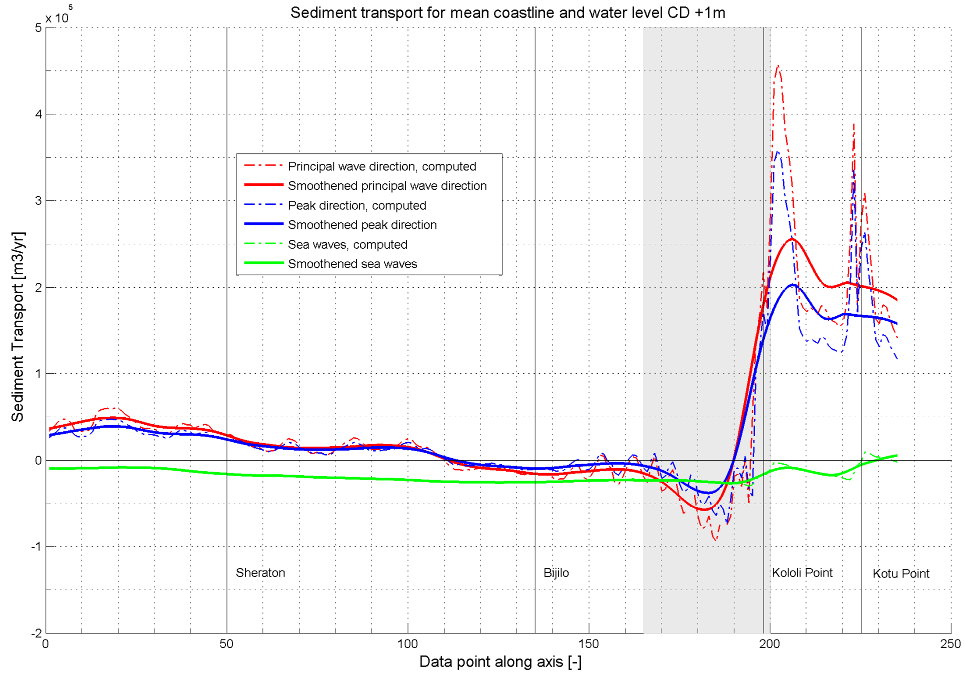

Figure 6-6: Computed Sediment transport capacity for mean coastline and water level CD +1m, note that the results presented have not been calibrated

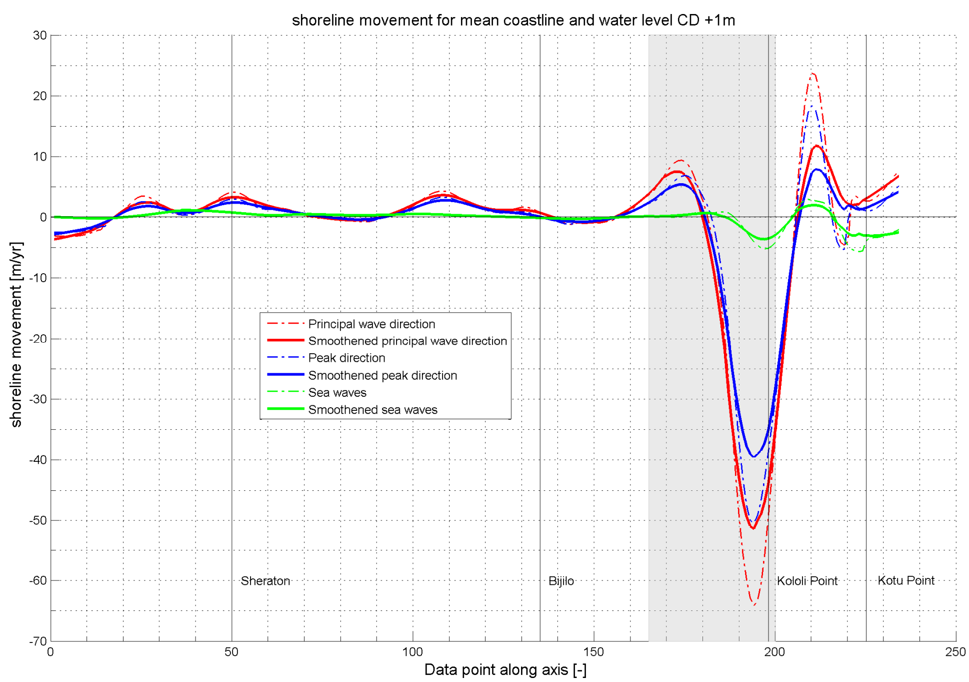

Figure 6-7: Computed Shoreline movement for mean coastline and water level CD +1m, note that the results presented have not been calibrated

For the presentation of the remaining sediment transport modelling results the principle wave direction has been used as input direction. The modelling results for both direction parameters give the same trends. The principal wave direction is being used because the sediment transport capacities of the different water levels has been computed for only the principal wave direction and sea waves when writing the report.

INFLUENCE WATER LEVELS

The raw results of sediment transport capacities along the coast for different water levels are shown in Figure 6-8. Mean sea level is represented by the red line, high water level (CD +1.7m) by the green line and the low water level (CD +0.3m) is represented by the blue line in the figure. Clearly the water level has a large influence on the sediment transport for similar wave conditions. A high water level causes a larger computed transport north of Bald Cape and inside the nourishment area than for mean sea level and low water. Remarkable is the very low computed transport for the low water level, especially inside the nourishment area. This is partly due to the additional bottom friction at the terrace in front of The Gambia due to the lower water level. The transport is relative small along the entire coast until Kololi Point from where the computed transport is northerly directed. The reef area has a clear sheltering effect on the nourishment area during low water, which can also be seen in the SWAN results, see Figure 5-17.

As low water and high water is present for approximately the same time during a tidal cycle, the influence of the water level has no effect on the sediment transport for a short period of time. For longer periods the effect of sea level rise or a subsiding or eroding reef area has influence on the (relative) water level causing a change in sediment transport gradients along the coast.

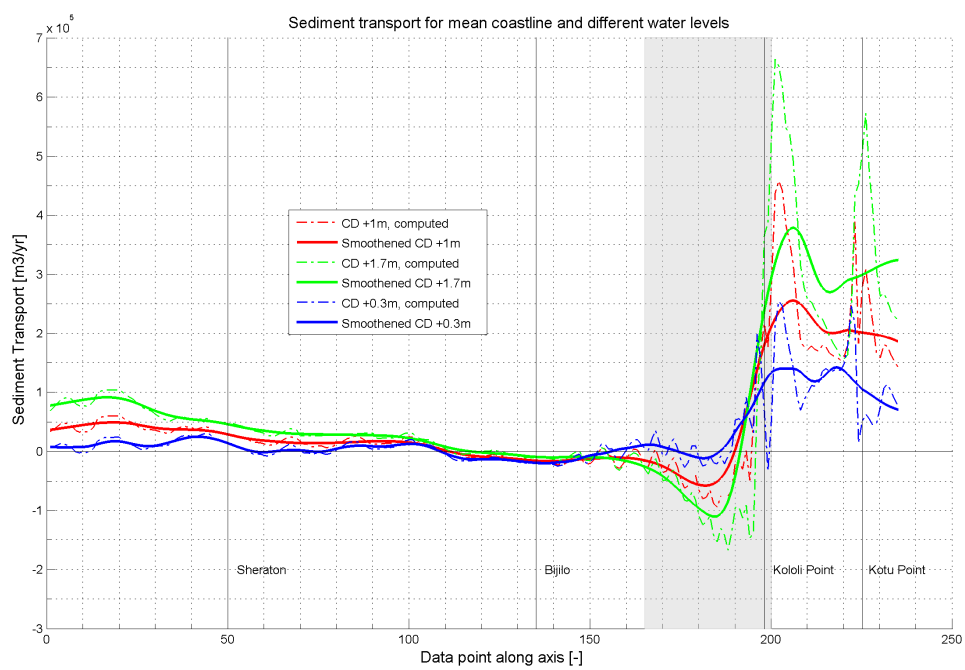

Figure 6-8: Computed Sediment transport capacity for mean coastline and different water levels, note that the results presented have not been calibrated

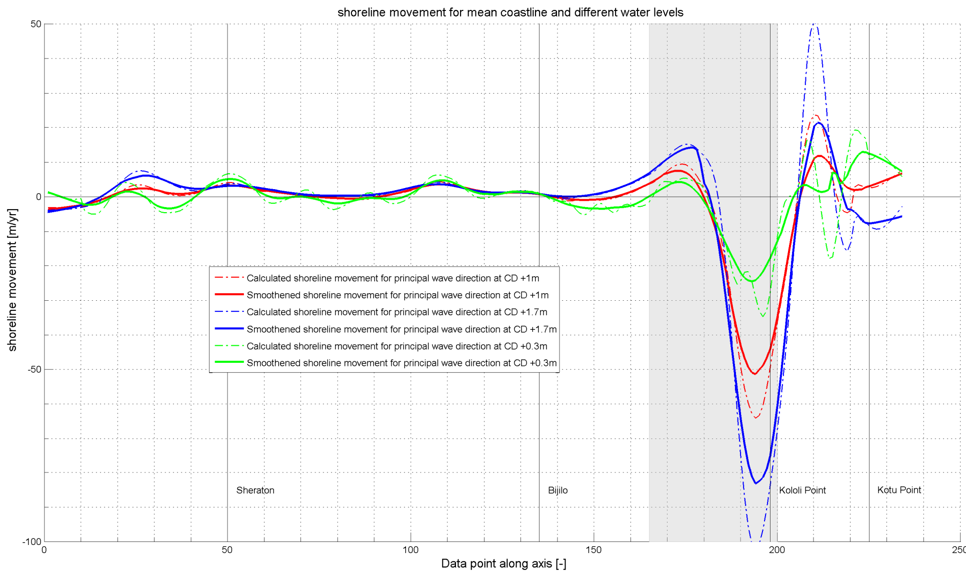

Figure 6-9: Computed Shoreline movement for mean coastline and different water levels, note that the results presented have not been calibrated

INFLUENCE DIFFERENT COASTLINE ORIENTATIONS

Computed sediment transport capacities for the mean coastline and the 2009 coastline are very similar as shown in Figure 6-9. The 2003 coastline orientation is represented by the black line, the 2004 coastline orientation by the green line, the 2009 coastline orientation by the blue line and the mean coastline orientation is shown by the red line in the figure. Computed sediment transport capacities for the 2003 and 2004 coastline are very different than for the mean and 2009 coastlines; this is caused by the nourishment in 2003. The sediment transports and corresponding gradients are large at the both ends of the nourishment, which is also represented by this figure.

The raw shoreline movement in Figure 6-11 shows a large area of erosion in 2003, namely the complete nourishment area. Accretion north and south of the nourishment area is very high and spreads during the next years over the adjacent coastal cells. Also in 2004 a high accretion rate is present between point 140 and 170 which is going to spread out in southern direction. The areas of accretion for the 2009 and mean coastline angle between point 170 and 180 and between point 205 and 220 are aberrant as no clear constant shoreline propagation is present in reality. This is present for almost every modelling run and is caused by the large southerly transport inside the nourishment area and large peak of northerly transport at Kololi Point. This will be discussed and modified in the following section.

Although the local erosion and accretion rates are not representative, the effect of the nourishment for the 2003 and 2004 coastlines is clearly visible. The overall pattern around the nourishment seems to confirm the observed distribution of the nourished sediment to the north and south as discussed in Chapter 4.

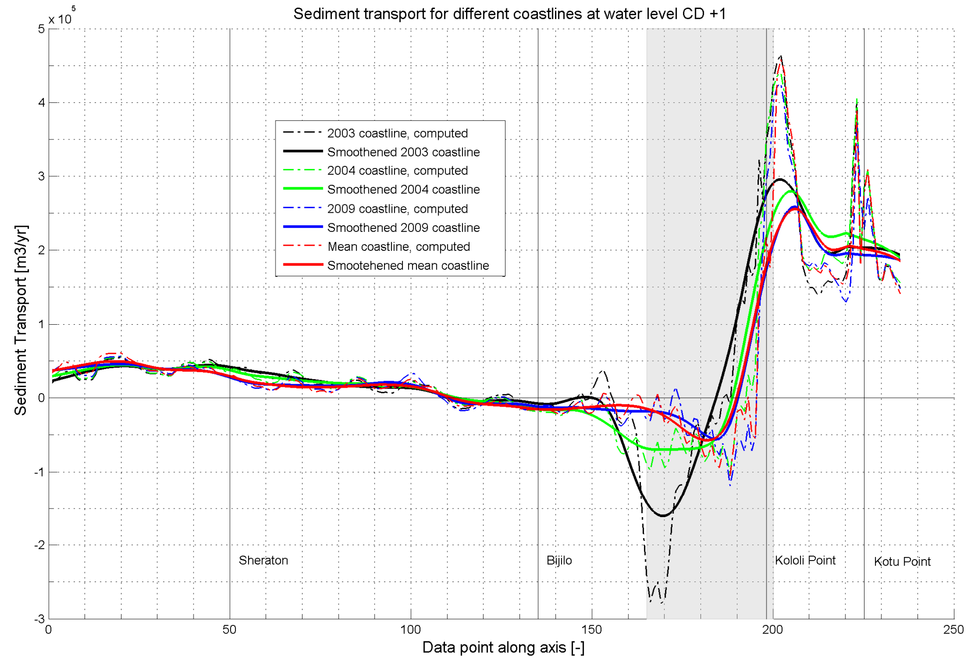

Figure 6-10: Computed Sediment transport capacity for different coastlines at mean sea level, note that the results presented have not been calibrated

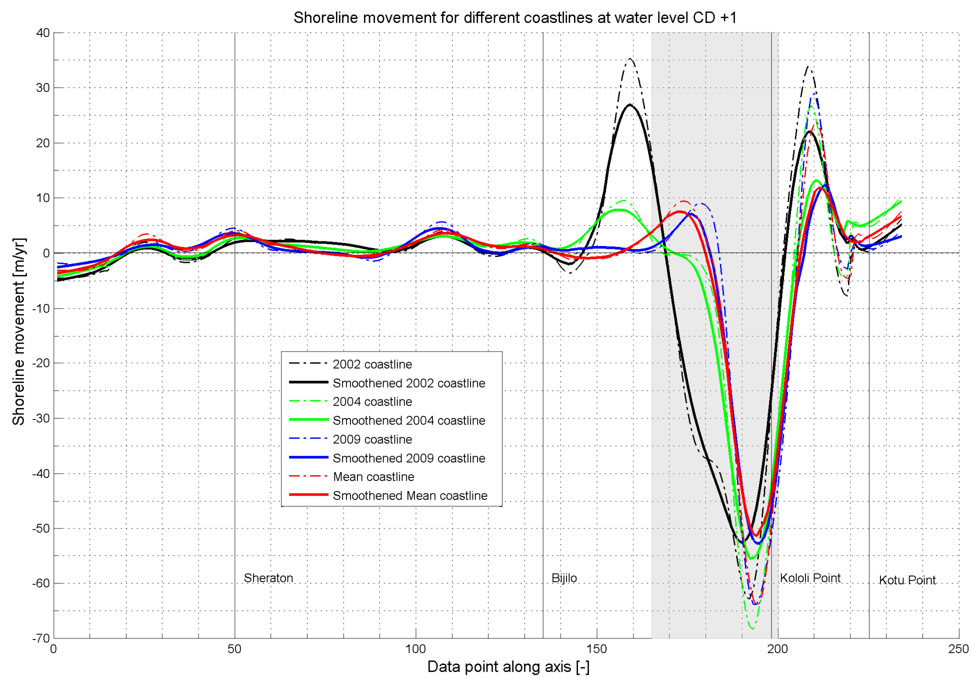

Figure 6-11: Computed Shoreline movement for different coastlines at mean sea level, note that the results presented have not been calibrated

TOTAL TIME SERIES

The accumulated sediment transport for the total time series of 10 years is shown in Figure 6-12 for several profiles along the coast as defined in Figure 4-18. The time series for the peak direction is shown in Figure E-13. Clearly the year-to-year sediment transport has changed in the years 2007, 2008 and 2009, both for the principal wave direction and for the peak direction. This means that the wave climate is changing; this could be part of a long-term cycle or a recent phenomenon. This change in wave climate is not visible in the wave roses, see Appendix A. This is also the case for the nearshore wave roses which are not shown in this report. Unfortunately no extensive wave data are available to analyse the wave climate for a longer period.

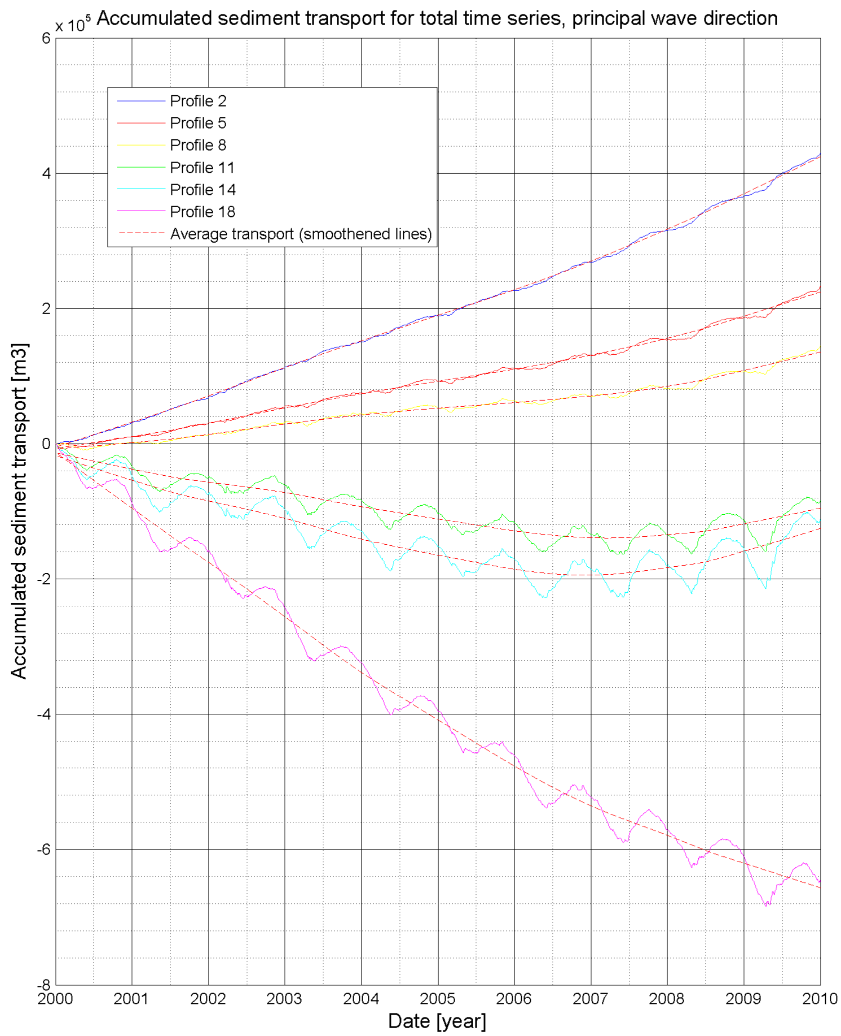

Figure 6-12: Accumulated sediment transport for total time series

The influence of the changing wave climate is investigated by comparing the effect of the 2004 and 2009 wave climate on the 2004 coastline orientation see Figure 6-13. The 2004 wave climate is represented by the red line, the 2009 wave climate by the blue line. The 2009 and overall wave climate have also been compared for the 2009 coastline orientation; see Figure E-14 and Figure E-15. The 2009 wave climate causes a larger northerly directed transport than the 2004 wave climate. Using the transport for both wave climates, a bandwidth for the sediment transport along the coastline can be defined due to year-to-year variations in the wave climate. It is also possible that more than 30 years ago the climate was different from the recent climate of the last couple of years.

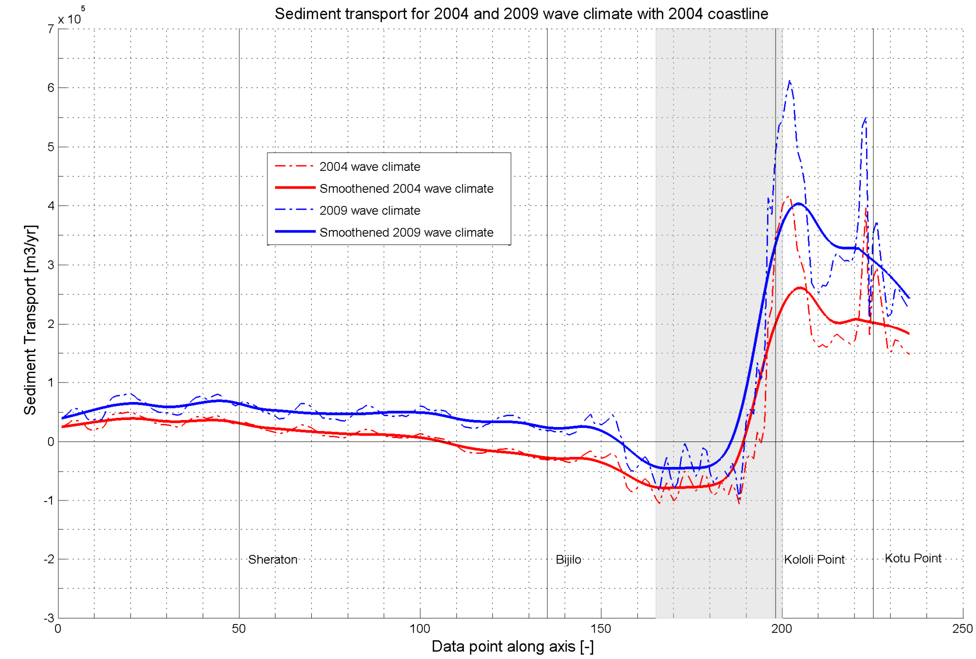

Figure 6-13: Sediment transport capacity for 2004 and 2009 wave climate, note that the results presented have not been calibrated

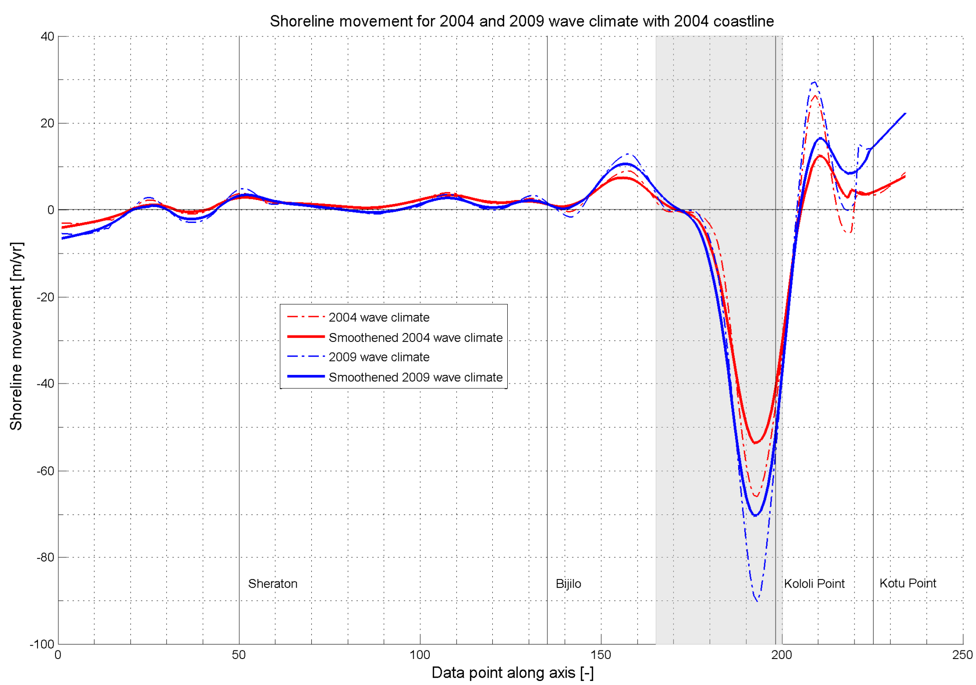

Figure 6-14: Shoreline movement for 2004 and 2009 wave climate, note that the results presented have not been calibrated

CROSS-SHORE DISTRIBUTION OF THE ALONGSHORE TRANSPORT

The distribution of the alongshore sediment transport along the profile for mean sea level is shown in Figure 6-15. The shown transport is the net transport for the probability of occurrence of the total time series in m^3 per year per meter. Figure E-18 and Figure E-19show the cross-shore distribution of sediment transport for mean high and low water levels. Figure 6-15 shows that the main part of the generated above CD -4m.The sediment transport is well within the profile, also for the low water level.

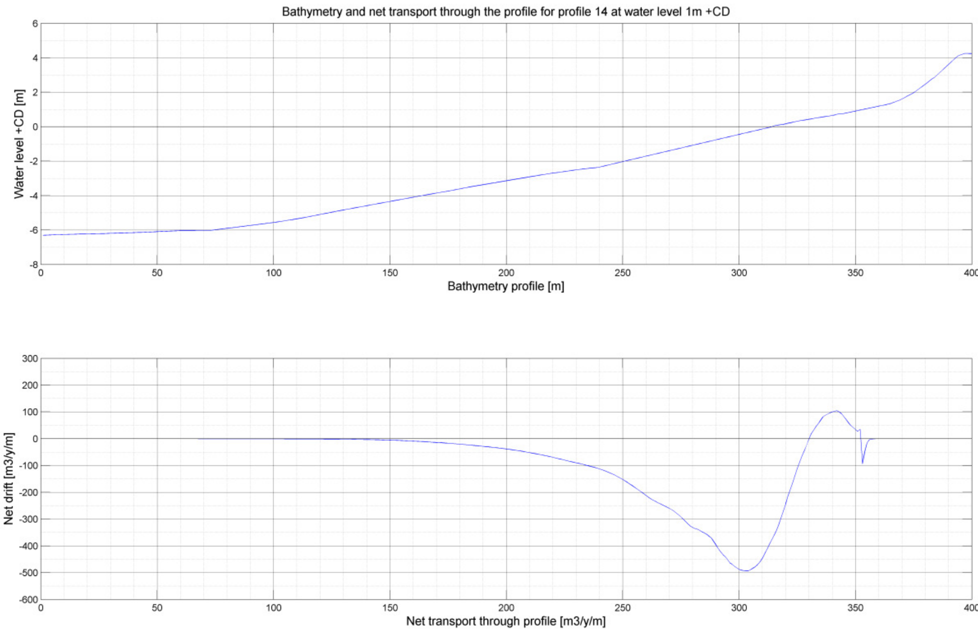

Figure 6-15: Cross-shore distribution of the alongshore transport for MSL

S-ϕ CURVES

The relation between the net longshore transport and the coast orientation is presented in a so-called S-ϕ curve. The S-ϕ curves are different along the coast since the local wave climate and the coast orientation vary along the coast. The S-ϕ curves for several locations along the coast are shown in Figure 6-16. Profiles 5, 8, 11, 14 and 19 are close to their dynamic equilibrium orientation because the transports are very close to zero. The wave climate in the southern part, as can be seen from profile 2, is calmer than the wave climates in the north as the sediment transport per degree coastline angle change is smaller than the profiles in the north. S-ϕ Curves are used to analyse the change in sediment transport for a change in coastline orientation. The alongshore transport for a profile can easily be read from the S-ϕ curve as coastline angles can be different along the coast.

This can also be shown by a so called C-value which is defined as the difference in sediment transport per degree coastline angle change, see Figure 6-17. In reality, the C-values change smoothly along the coast, such as the smoothened lines in Figure 6-17. The C-values and S-ϕ curves are often used for the calibration of a shoreline model as they give relevant information of the behaviour of the system.

S-ϕ Curves are often used to calibrate modelling results according known transport directions or known transports at a certain location. By adjusting the coastline equilibrium orientation for every profile along the coast, the sediment transport will be influenced while the transport gradients stay approximately the same. The coast orientation for which the net longshore transport is zero, is called the equilibrium angle.

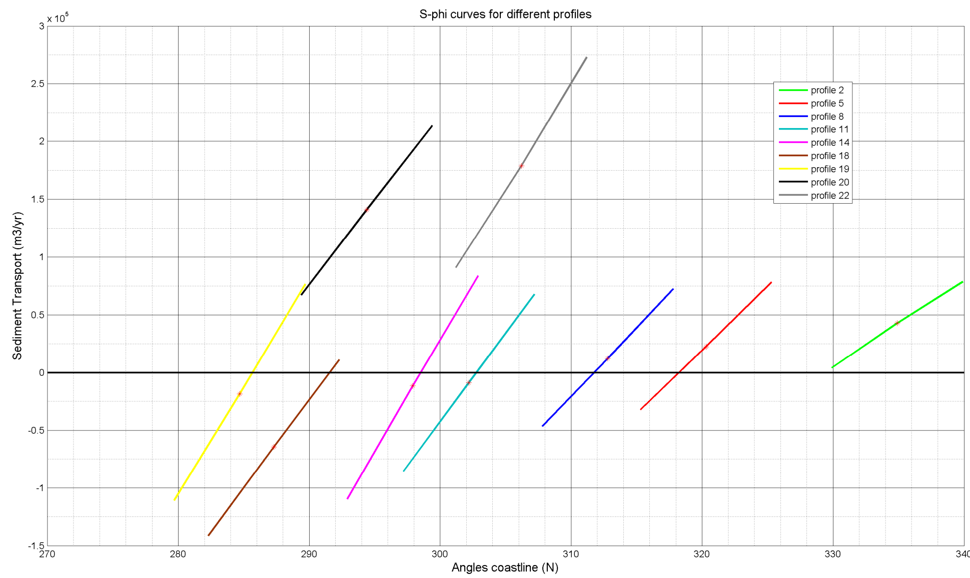

Figure 6-16: S-ϕ curves for different profiles along the coast, note that the results presented have not been calibrated

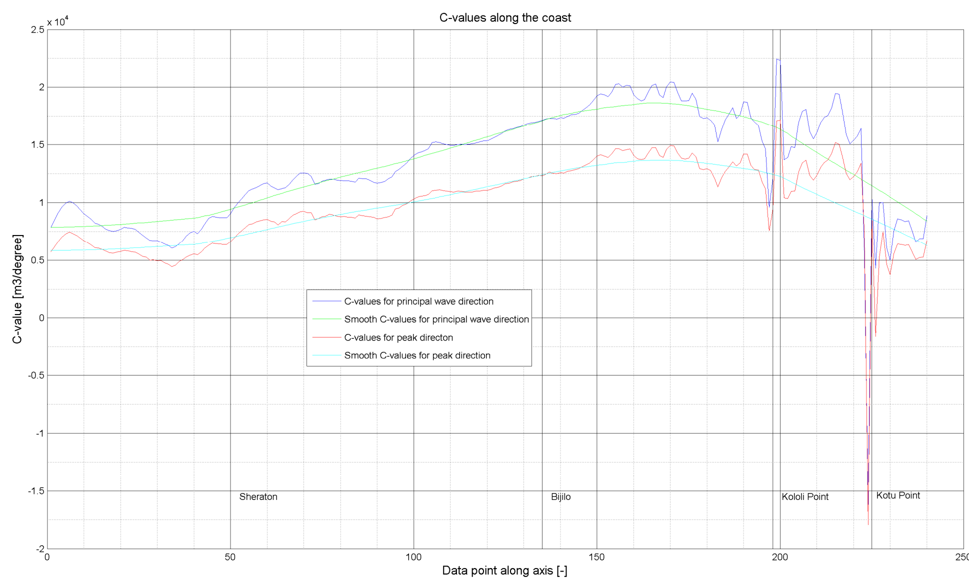

Figure 6-17: C-values along the coast, note that the results presented have not been calibrated

6.4 DISCUSSION

The raw computational results presented in the previous section indicate shoreline change rates which are considerably larger than the observed shoreline changes as presented in Chapter 4. It can therefore be concluded that the occurred sediment transports with corresponding shoreline movement are different from the raw results, although the overall trend corresponds well. For the interpretation of the raw results it should be realised that the sediment transports can only be computed with a limited accuracy. Possible deviations between the computed and the actual computations may occur due to inaccuracies in the offshore wave climate data, the schematisation of waves, some inaccuracies in the wave propagation modelling and inaccuracies in the profiles and coastline orientation. This can cause the sediment transport along the coast to be irregular and sometimes give too high or too low alongshore sediment transports. Inside the reef area and north of Bald Cape, rocky areas are present due to the reefs influencing the occurring sediment transport over the profiles.

Therefore the results of the sediment transport calculations are discussed in this section. Aberrant results have been indicated along the coast and the cause of these results will be explained. Furthermore the modelling results have been compared with the observed shoreline movement and corresponding sediment budgets as estimated in Chapter 4. Based on this comparison, the sediment transports are calibrated to give insight into the observed trends and the influence of the coastal processes. The modelling results for the mean coastline orientation and the net transport of swell waves and sea waves at mean sea level is calibrated first, based on the field data analysis for the 1964-1983 and 2004-2009 periods. This is then the reference for the calibration of the remaining modelling results. The principal wave direction for the swell waves is used because the different wave climates have been modelled only for this direction parameter. As can be seen in Figure 6-6 the trends for principal wave and peak direction are similar and after calibration the calibrated transport will be the same for both direction parameters.

The large difference between the sediment budgets of 1964-1983 and 2004-2009 already indicate changes in the erosive processes over the long period. The direction of shoreline movements are approximately the same but sediment budgets are a factor 5 times larger for the area between Sheraton and Kololi Point. This is for the greatest part due to the nourishment in front of Senegambia and the sand deficit between Sheraton and Bijilo, but high erosion trends were still visible around 2009 while the coastline orientation is almost similar. Furthermore there is a possibility that the bathymetry, the reef area and the wave climate are subject to changes over the years, see section 6.3 and section 4.4.1. This has been taken into consideration during the calibration process.

6.4.1 CALIBRATION FOR ALONGSHORE SEDIMENT TRANSPORT CALCULATIONS

The modelling results of the net transport capacity for swell and sea waves and the mean coastline at mean sea level will be discussed and calibrated in the following section. Calibrated results have been smoothened so only interpreted trends for sediment transport and shoreline movement are indicated. The goal of this study is to investigate the influence of different processes on the erosion and accretion rates, which can be done for these general trends.

BALD CAPE TO BIJILO

From point 0 to point 30, the original coastline orientations have been smoothened out as can be seen in Figure 6-5. In reality, the coastline orientations are generally lower than schematized for the calculations. In Figure 6-16 it can be seen that for profile 2 a smaller coastline angle causes lower northern transport. Off-shore in front of this area the Bald Cape reef is present which consists of rocky material; even on the beach some rocky material is visible. This means that the occurring sediment transports are lower if hardened seabed is present across the profile. Therefore the sediment transport along the stretch north of Bald Cape has been decreased according to observed shoreline trends.

Around point 40 the northern transport decreases to a small southern transport around Bijilo according to the modelling results. The results contain some fluctuations which will be smoothened out to a slight decrease in sediment transport. Since the natural sediment transport and shoreline movement changes smoothly, the sediment transport calculations can be smoothened out to give general trends. The trend for 1964-1983 indicates a shoreline movement of approximately +0.3 m/yr along this stretch while the 2004-2009 trend shows a shoreline movement of +2.5 m/yr, caused by the higher transports shortly after the nourishment. The calibrated trend between Sheraton and Bijilo Park is based mainly on the 1964-1983 sediment budget, but wither higher rates as large erosion is still present in 2009. Furthermore the 1964-1983 period is based on old aerial images which causes a larger uncertainty than the Google Earth satellite images; also changes between 1964 and 2009 on large scale processes can be present, like a changing wave climate or bathymetry or sea level rise.

BETWEEN BIJILO AND BALD CAPE

From point 150 the modelling results along the coast contain large fluctuations see Figure 6-6, probably caused by irregularities in nearshore wave climates and small differences in the used profiles. Inside the nourishment area the computed sediment transports are getting much larger in southern direction; this would indicate accretion which is definitely not present in reality. The off-shore reefs in front of the Senegambia area, see Figure E-4daily cause a complex refractive wave pattern; furthermore a rip current is present along this coastal stretch caused by a dent and a bulge in the coastline. This coastline shape has been smoothened out during the determination of the shoreline orientation for the modelling, see section 6.2.1. This local disturbance is relatively large and also influences the wave climate; therefore the coastline angles in reality have to be taken into account. Figure 6-16 shows the S-ϕ curve for Profile 18: a larger coastline angle causes lower sediment transport. Both the off-shore reefs and the coastline shape indicate that the area in front of Senegambia contain very complex wave and current patterns, enforced by secondary flows caused by breaking waves on the shallow reefs. This is not possible to represent in the 1-Dimensional model. The computed sediment transport capacities inside the nourishment area have been disregarded and the calibration is based on observed shoreline movement.

The reefs present in front of Kololi and Kotu Point are shallow, hardened areas where large sediment transport capacities have been computed. This is due to waves breaking and being refracted by the reefs causing large wave driven currents and stirring behind the reef area. Therefore the transport capacitates are large but due to the hardened seabed only little transport is possible. Therefore the occurring transport is much lower than the computed sediment transport capacities. The calibrated sediment transports will therefore turn gradually to the north from the south end of the nourishment causing erosion inside the nourishment area.

Based on the observed shoreline movement and sediment budgets for the complete research area the sediment transport along the coast has been calibrated according to the above considerations, which is shown in Figure 6-18 and Figure 6-19. The net transport for swell and sea waves is represented by the blue line, the calibrated sediment transport by the green line.

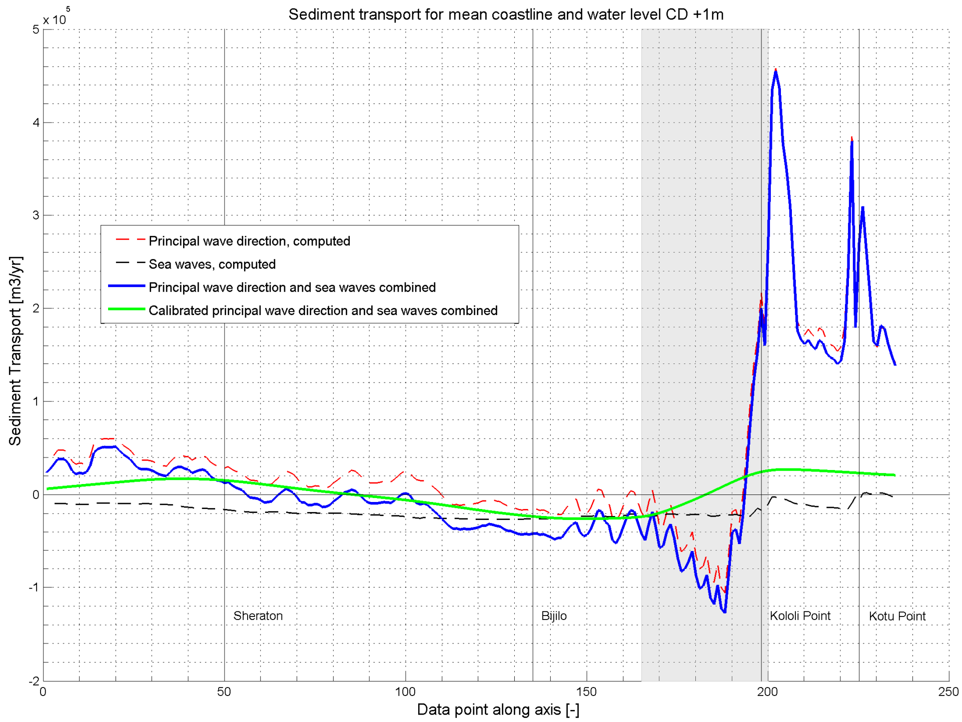

Figure 6-18: Sediment transport for mean coastline and water level CD+1

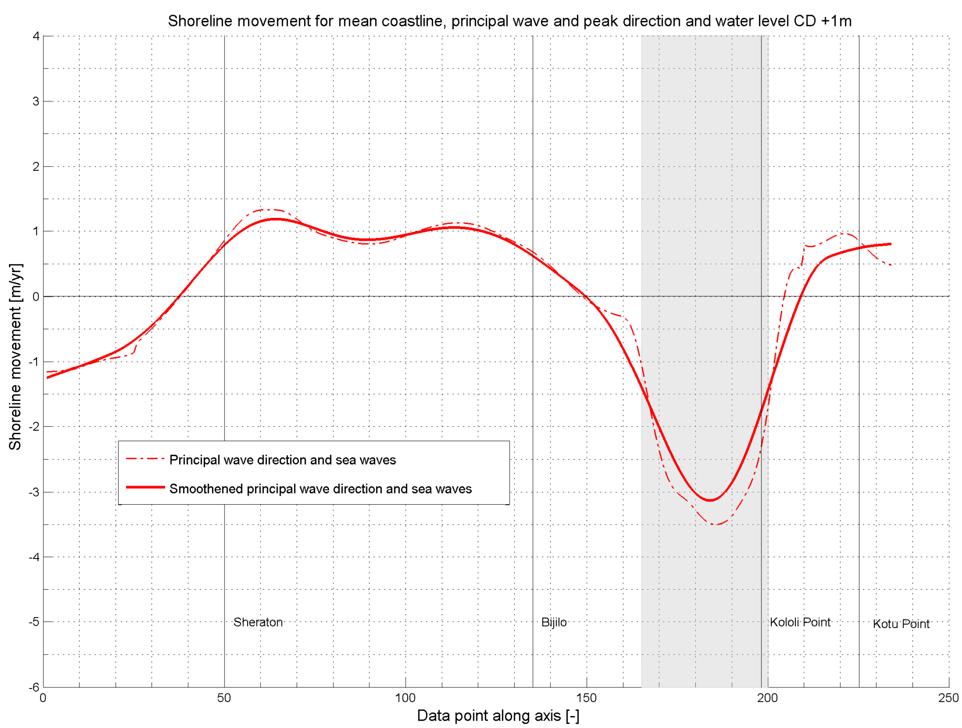

Figure 6-19: Shoreline movement for mean coastline and water level CD+1

6.4.2 INFLUENCE OF DIFFERENT PROCESSES

The influences of different processes on the alongshore sediment transport and gradients is investigated by the comparison of both the raw results and the calibrated results. The processes which can have influence on the sediment transport rates and have been computed are: water level, coastline orientation and the changing wave climate. Computational results of these processes have been calibrated based on the calibration above for the mean coastline with net transport of swell and sea waves at mean sea level. The limits of the y-axis in the figures have been changed for the presentation, high sediment transport capacities no longer determine the limits of the y-axis; these limits are now based on the occurring sediment transports. The presented shoreline movements are instantaneous movements: peaks in shoreline movement will be smoothened out over the adjacent coast over time.

WAVE DIRECTION PARAMETER

The wave direction for a time series is represented by two different wave direction parameters: the principal wave direction and the peak direction. Both direction cause different nearshore wave climates as shown in Figure 5-11 and Figure 5-12. The effect of the different wave direction parameters is shown in Figure 6-6 for the raw results. The peak direction computations produce lower sediment transport capacities than the principal wave direction; however the trends are qualitatively the same along the coast. When calibrated, both wave direction parameters should produce the same results. Both wave direction parameters have been calibrated based on the shoreline movement and sediment budget of the periods 1964 -1983 and 2004-2009. The sediment transports for the principal wave direction had to be lowered more than the sediment transports for the peak direction. The peak direction therefore gives a better transport indication; this does depend on the input parameters. The calibrated alongshore sediment transports and shoreline movements for both wave directions are shown in Figure 6-20 Figure 6-21. The principal wave direction is represented by the red line, the peak direction by the blue line.

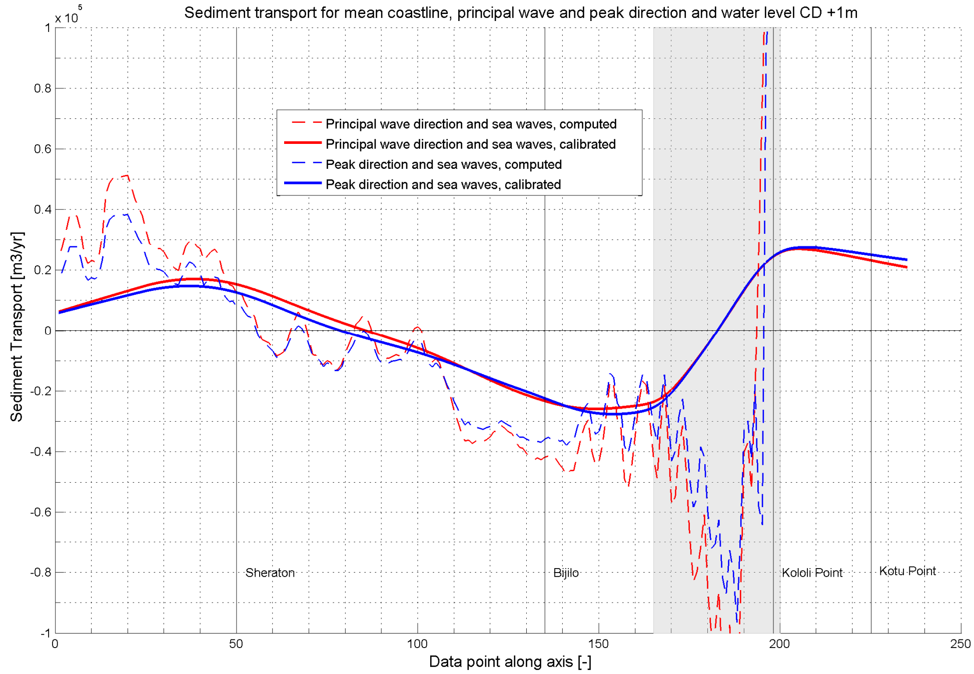

Figure 6-20: Sediment transport for principal wave and peak direction

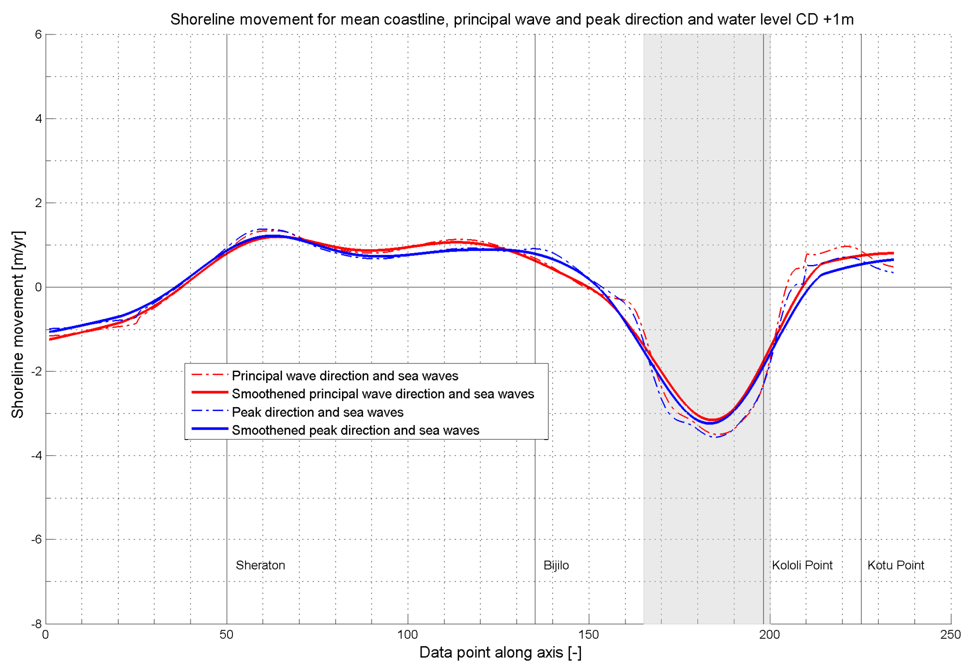

Figure 6-21: Shoreline movement for principal wave and peak direction

WATER LEVEL

The tide at The Gambian causes different water levels during the day along the coast. The influence of these different water levels on the alongshore sediment transport are large as can be seen in Figure 6-8. The used water levels are mean sea level and the mean high and low water during spring tide. The low water level causes almost no transport along the coast as the alongshore transports are almost 0 and the corresponding gradients are very low as can be seen in Figure 6-22 and Figure 6-23. Mean sea level is represented by the red line, high water level (CD +1.7m) by the green line and the low water level (CD +0.3m) is represented by the blue line in the figure. Behind the reef area the wave climate is much calmer causing less transport, see Figure 5-17; waves along the coast are lower for the low water level as bottom friction on the terrace in front if The Gambia is higher. The high water level causes a much larger alongshore sediment transport, especially before Sheraton, inside the nourishment area and north of Kololi Point. The erosion is within the complete nourishment area and not only in the northern part, as shown by the raw result in Figure 6-9. Also the areas of accretion north and south of the nourishment area are not present anymore for the calibrated results.

The High water level causes higher alongshore transport and also clearly higher erosion and accretion rates along the coast. Due to sea level rise, the alongshore transports and erosion rates inside the nourishment will become higher. The short-term influence of sea level rise is small but for larger periods, say some decades, the influence can be relatively large. The current rate of sea level rise is approximately 0.2 m per century but this can be as large as 0.5 to 1m per century, see section 3.6.3. No reliable data are available on the stability of the reef. If the reef would be slowly eroding this would have a similar effect as an increased water level.

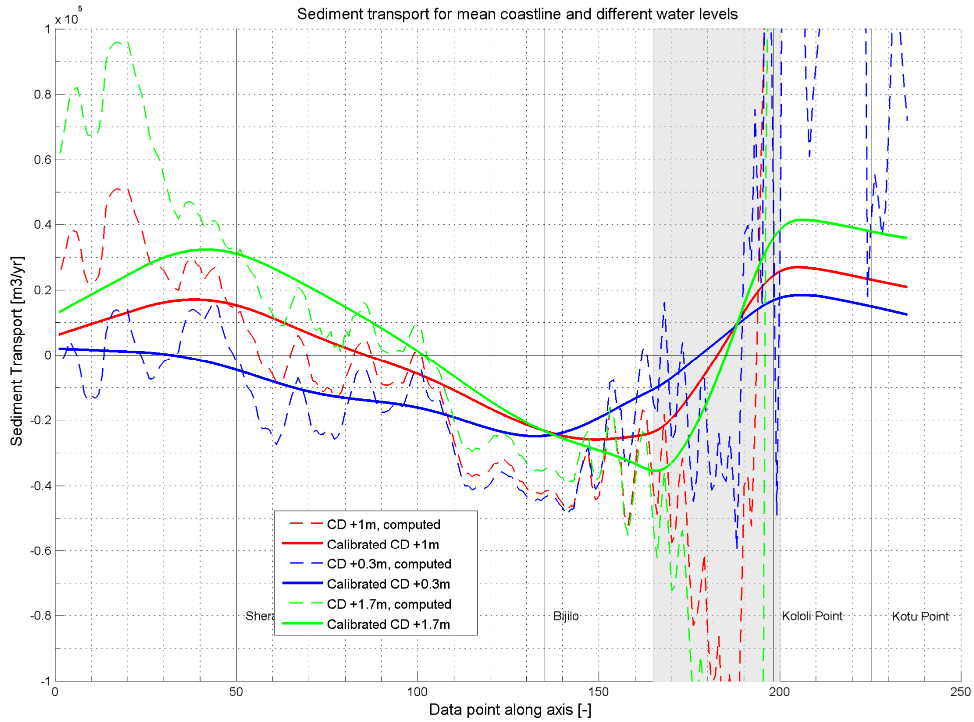

Figure 6-22: Sediment transport for different water levels

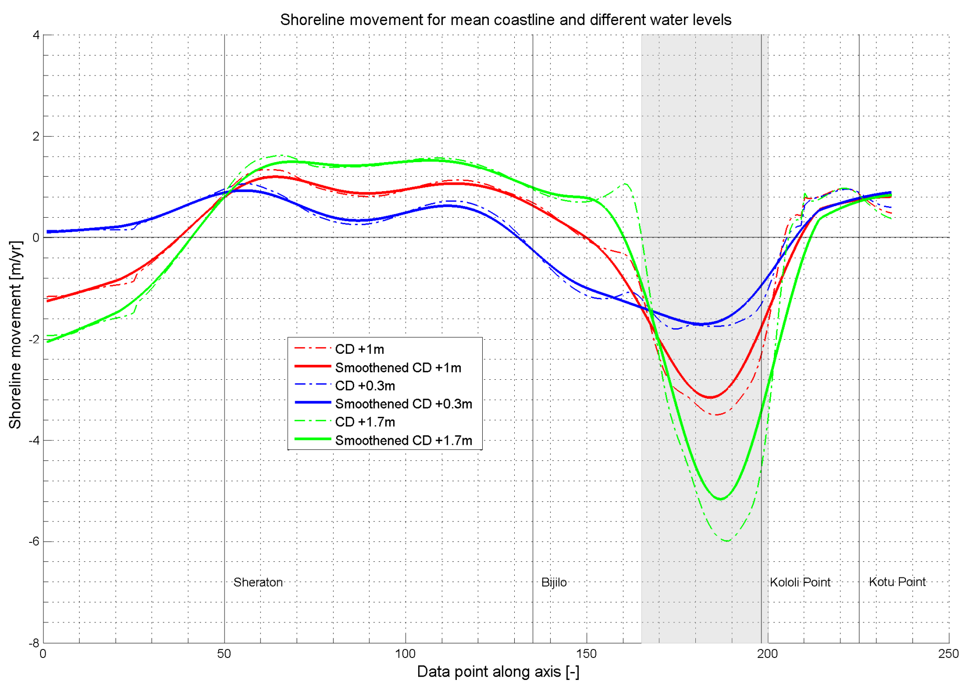

Figure 6-23: Shoreline movement for different water levels

COASTLINE ORIENTATIONS

The 2009 coastline orientation is very close to the mean orientation, this is also shown by the raw results of the alongshore sediment transport capacity, see Figure 6-10. The 2003 coastline orientation is based on the design of the nourishment and is therefore representative for the alongshore transport directly after the construction. The 2004 coastline orientation is only 1 year after nourishment so the first spread of the nourishment is included in this coastline. Figure 6-10 shows the very high southern sediment transport on the southern border of the nourishment (point 175) for the 2003 and 2004 coastline. Especially the 2003 coastline causes high erosion rates on the southern and northern corner of the nourishment. These high shoreline movements are spread out over the adjacent area as the given shoreline movements are instantaneous. The calibrated sediment transports with corresponding shoreline movements are shown in Figure 6-24 and Figure 6-25. The 2003 coastline orientation is represented by the black line, the 2004 coastline orientation by the green line, the 2009 coastline orientation by the blue line and the mean coastline orientation is shown by the red line in the figure.

The 2003 and 2004 transports have been smoothened but still give large erosion inside the nourishment area and accretion south of the nourishment. The shoreline movement for 2003 which has not been smoothened, shows accretion north of the nourishment which was also present in reality. The accretion rate is not very high; this is due to the smoothening effect of the calibration. The high northern sediment transport of the 2003 coastline orientation inside the nourishment area in Figure 6-24 does already indicate a large transport to the north which will be deposited there. This accretion was not present anymore in 2004; erosion is present there from that moment.

The shoreline movement for the period between 2004 and 2009 will be a combination of the shoreline movement results of the 2004 and 2009 coastline orientation. The observed trends for both accretion and erosion are an average of the 2004 and 2009 erosion and accretion rates.

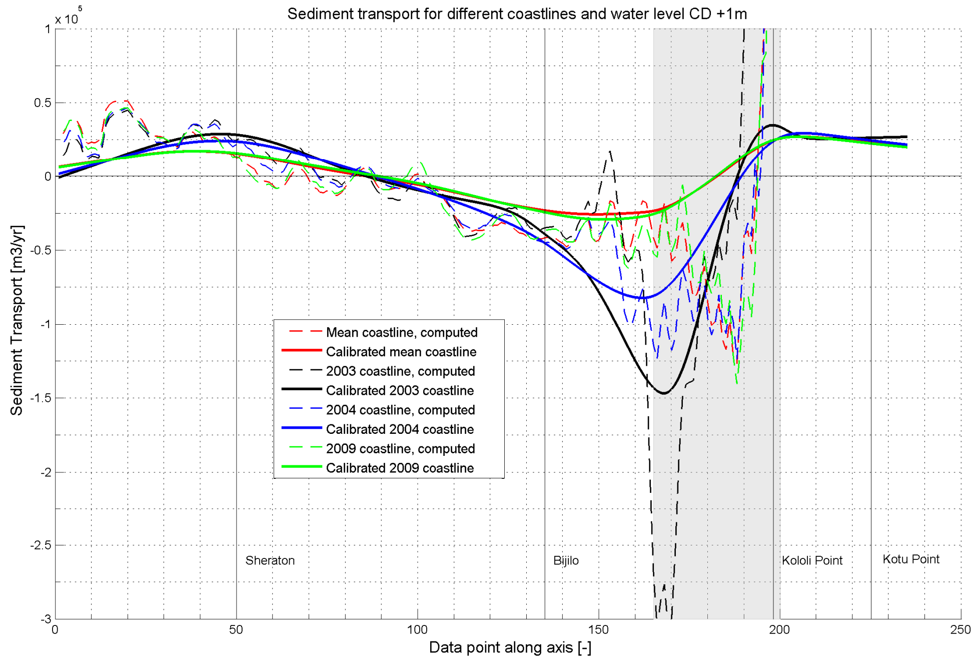

Figure 6-24: Sediment transport for different coastlines

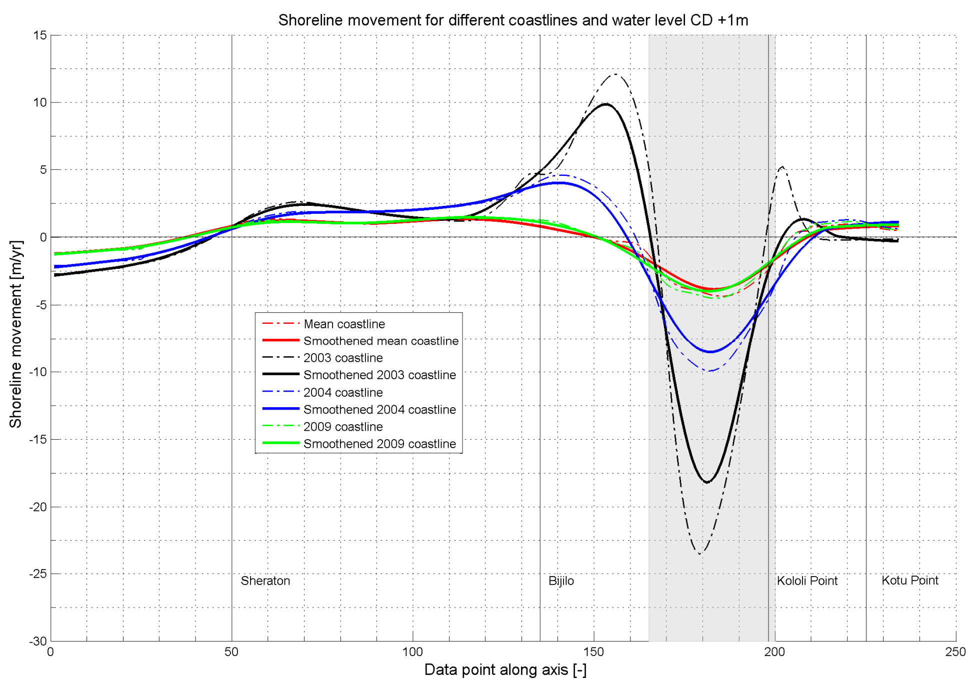

Figure 6-25: Shoreline movement for different coastlines

CHANGING WAVE CLIMATE

According to the accumulated sediment transport for a complete time series the wave climate has been changing for 2007, 2008 and 2009. This is not clearly visible by the annual wave roses in Appendix A but can clearly be seen by the cumulative transports as shown in Figure 6-12. From 2007 the sediment transport has changed to more northerly directed transport for all the calculated profiles. Therefore the probability of occurrence has been determined for the years 2004 and 2009 separately to investigate the influence of the changing wave climate. Figure 6-13 shows a large difference in raw sediment transport between the 2004 and 2009 wave climates. The calibrated sediment transport and shoreline movement are shown in Figure 6-26 and Figure 6-27. The transports have been shifted to more northerly transports for the 2009 wave climate; this doesn't imply that erosion or accretion is higher, this is only a fact if there is also a change in gradients for the sediment transport along the coast. As can be seen in Figure 6-26 the sediment transport capacity of the 2009 wave climate is close to the 2004 wave climate sediment transport before Kololi Point and much higher behind Kololi Point. The transport gradient is thus higher for the 2009 wave climate causing a larger erosion rate as can be seen in Figure 6-27. See also Figure E-16 and Figure E-17 for calibrated sediment transport and shoreline movement for the 2009 coastline orientation. Also for these situations alongshore sediment transports are more northerly directed and the erosion in front of Senegambia is higher than for the 2004 wave climate.

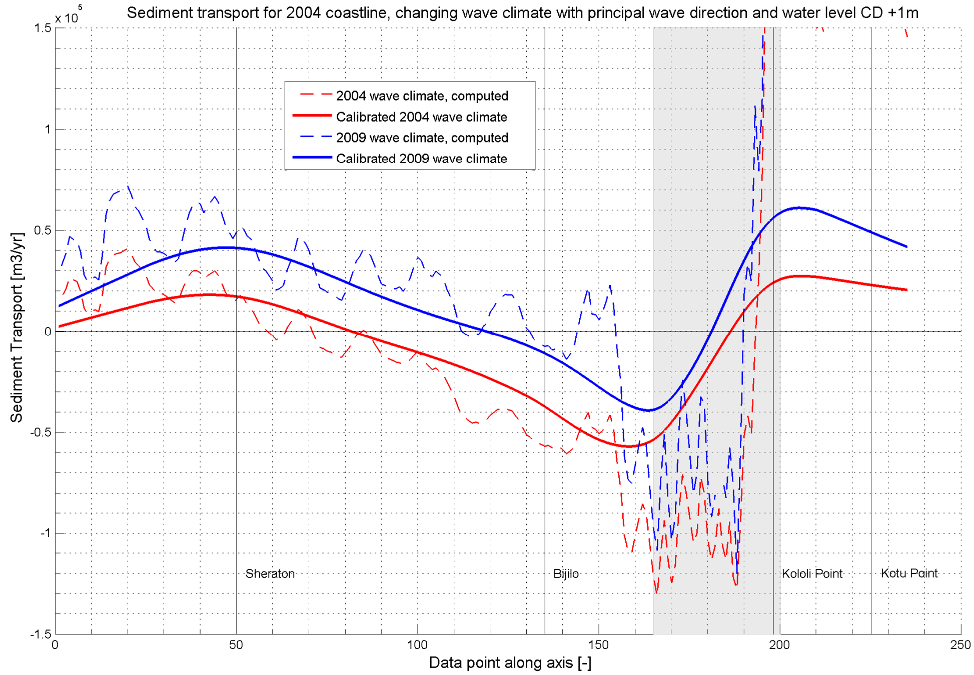

Figure 6-26: Sediment transport for 2004 coastline with changing wave climates

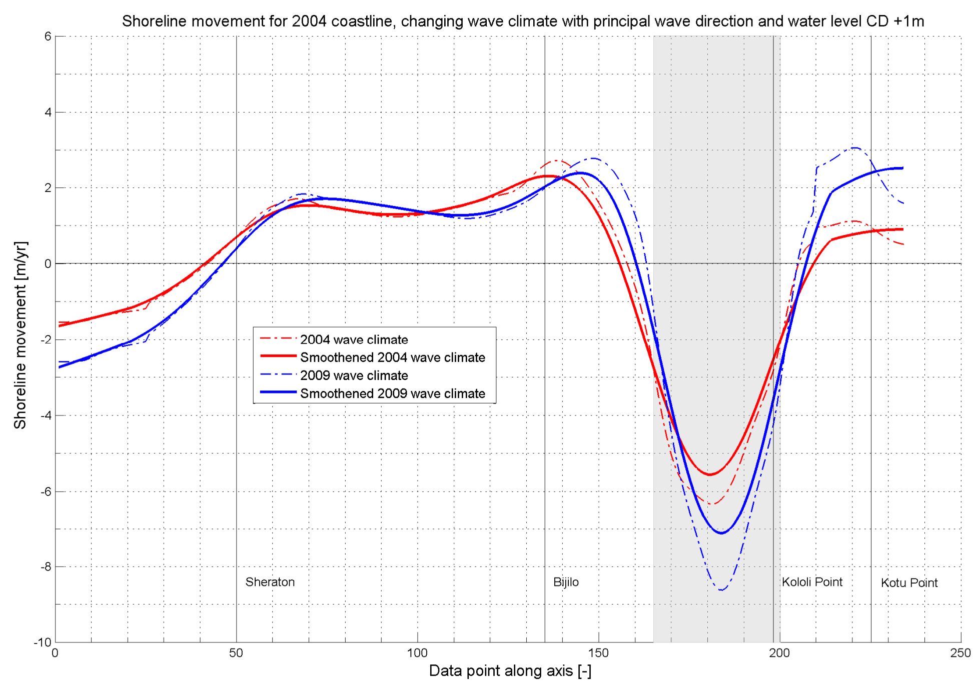

Figure 6-27: Shoreline movement for 2004 coastline with changing wave climates

6.4.3 S-Φ CURVES

The limited accuracy of the modelling results due to inaccuracies in the nearshore wave climates implies that the equilibrium angle can only be determined with a limited accuracy of a few degrees, say +/- 5°. The S-ϕ curves present the relationship between the net longshore transport and the coast orientation; see Figure 6-16 for the curves along the coast of The Gambia. These results can be fine-tuned by adjusting the coastline orientations along the complete coast with a few degrees, based on the sand balance as derived from the observations. Adjusting the coastline orientations causes the equilibrium angle to move along the computed lines of the S-ϕ curves for the profiles. This allows the transports along the coast to become more northerly or southerly directed, causing the transport reversal point to move along the coast or not to exist anymore; local transport directions can then be different than computed. As the transports change approximately consequently along the coast, the transport gradients stay the same causing the erosion and accretion rates to be unchanged. Adjusting the equilibrium angle along the coast is thus used to calibrate the transport directions based on the observed sediment balance.

Due to the sharp transition of the coast at Bald Cape, no (large) sediment transports will enter the research area at that point. Only when the Tanji River outlet is inside the research area sediment is deposited, this has also been observed on the aerial photographs. Therefore the sediment transport would be close to zero in data point 1 near Bald Cape. The computed transport are relative large and northerly directed at that area, therefore the transport along the coast would rather shift more to southern transport than to northern. The computed southerly directed transport from the nourishment area to approximately Sheraton is thus reliable, as the computed 'morphological zero point' inside the nourishment area.

6.5 CONCLUSIONS

Based on the calibrated sediment transport analysis and the raw results of the sediment transport computations, the following conclusions can be drawn.

- General trends in shoreline movement as determined for observed shoreline movement are roughly confirmed by the raw sediment transport calculations in a qualitative way; not in a quantitative way. A small trend of erosion is present north of Bald Cape, dependent on the outlet of the Tanji River. From approximately point 40 the northerly alongshore transport turns gradually to a southern alongshore transport causing accretion between Sheraton and Bijilo Park. Inside the nourishment area the alongshore transport changes to the northern direction again, causing erosion in front of the Senegambia area.

- Interpretation and calibration of the model results is required to account for the effects of reef features and interpolation perturbations of the bathymetry in the area. This is especially the case north of Bald Cape, inside the nourishment area and around Kotu and Kololi Point

- The computed net sediment transport for both the principal wave direction and the peak direction combined with sea waves is southerly directed between Sheraton and the beach resorts for the 2003, 2004, 2009 and mean coastline orientations.

- Using the peak direction as wave direction input parameter gives slightly lower results for sediment transport capacities than the principal wave direction. This should not be a problem when the results of the used parameter will be calibrated.

- Erosion inside the nourishment area is very high for the 2003 coastline orientation, namely of the order of -25 m/yr; this could have been more shortly after nourishment. This erosion rate is already much smaller for the 2004 coastline orientation. The averaged computed erosion rate for the calibrated 2004 and 2009 coastline orientation is approximately 7 m/yr. The computed present erosion rate in front of Senegambia is of the order of 3 m/yr. The 2003 and 2004 coastline orientations show large erosion inside the nourishment area and relative large accretion south of the nourishment area; in 2003 also large accretion is present north of the nourishment. Small erosion is present in this coastal stretch from 2004.

- A higher water level causes higher sediment transport along the coast and also higher erosion and accretion rates. The erosion rate during high water is more then 1.5 times the erosion rate for mean sea level. This can be of large influence in case of sea level rise, especially for longer periods. The reef area looses a part of its sheltering effect during high water and the bottom friction and the waves is less, causing the higher erosion rates. This effect would also be present or even larger when the reefs would be slowly eroding or subsiding.

- A changing wave climate causes more northerly directed transport along the entire coast, in front of Senegambia this northern transport is less and north of Kololi Point the northern transport is clearly higher again, causing a larger transport gradient.

- A so-called ‘morphological zero point’ is computed in front of the Senegambia area. According to the feasibility study in 2000 this ‘morphological zero point’ was situated between Kololi and Bald Cape. The modelling study for this research shows that the sediment transport direction changes from southerly to northerly transport in front of the Senegambia area; sediment is thus transported away to both directions causing large erosion at Kololi Beach. Adjusting the coastline equilibrium orientation, can cause this transport reversal point to move along the coast.

7. MITIGATION MEASURES

For the erosion problem in front of the Senegambia area various solutions can be considered. This chapter focuses on different measures to mitigate this erosion problem; these measures are evaluated reflected on the present situation in The Gambia. Therefore in section 7.1 the zero-option is discussed when no measures are taken. Some hard and soft solutions are discussed in section 7.2 and 7.3 respectively. Finally some recommendations regarding the coastal protection of the Senegambia area are presented in section 7.4.

7.1 ZERO OPTION

The erosion problem at Kololi beach has been indicated as an urgent matter by The Gambian government early 2010. The present erosion rate at Kololi beach is still in the order of magnitude of 3 m/year, which has also been observed during several visits in 2010. The modelling study shows that for the 2009 coastline orientation and both the overall and 2009 wave climate the erosion rates are high, see Figure E-17. Keep in mind that these erosion rates are an indication; the exact values are not reliable. Erosion of the coastal stretch in front of the Senegambia will take place until the coastline has reached his dynamic equilibrium orientation. If no short-term measures are taken and longer-term measures are examined, the beaches in front of the beach resorts will keep eroding until no beach is present anymore for recreation. For the short- and long-term this will have a large impact on the tourism industry in the Senegambia area and The Gambia.

Therefore a solution should be applied where to present beach is protected on short term and the presence of a sufficient beach width will be present in the future. In the following sections "hard" and "soft" solutions will be discussed.

7.2 "HARD" SOLUTIONS

The term "hard" in the title of this section refers to the materials that are used in the coastal defence solutions. It often refers to structures of concrete or stones. These are groynes, detached breakwaters and a sea wall or revetment. During the 2000 feasibility study a protection with structures was not recommended at Senegambia as the modelling study results indicated that northern transport was present in front of Senegambia, interruption of this transport by structures would have an adverse effect on the entire coast north of Kololi.

7.2.1 GROYNES

Groynes are constructed to maintain a minimum, dry beach width or to control the amount of sand moving alongshore as it interferes in the coastal processes close to the shore (e.g. currents; sediment transport processes). As illustrated schematically in Figure 7-1, for single and multiple groynes (groyne field), the shoreline adjusts to the presence of the obstruction in long shore sediment transport; Figure 7-2 shows an example of a groyne field. The groyne simply blocks a part of this normal transport of sand alongshore and causes it to accumulate in a fillet on the groynes updrift side, the side from which the sediment is coming. This accumulation reorients the shoreline and reduces the angle between the shoreline and the prevailing incident wave direction. The reorientation reduces the local rate of long shore sand transport to produce accumulation and/or redistribution of sand updrift of the groyne. The amount of sand transported past the groyne is greatly reduced or eliminated; conservation of sand mass therefore produces erosion and a decrease in beach width on the down drift side of the groyne. A scheme of structures aims at making the alongshore transport constant over a certain coastal stretch.

Groynes offer little or no reduction in wave energy to shore-normal waves during storms. Consequently, cross-shore sediment transport processes for natural beaches are similar to groyne field compartments. And, for near normal wave incidence, the groyne system can create strong local current and rip currents which add to the offshore movement of beach material during storms. When designing groynes, this should be taken into account.

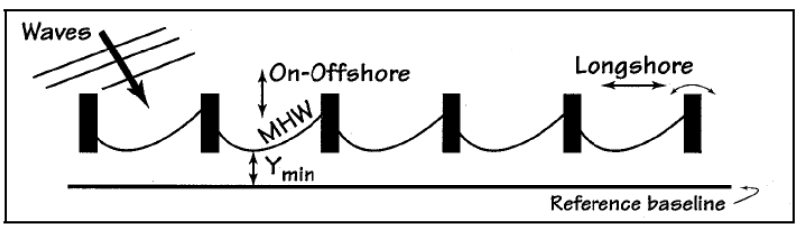

Figure 7-1: Schematic groyne scheme

Figure 7-2: Example of a groyne field

7.2.2 NEAR SHORE OR DETACHED BREAKWATERS

Near shore breakwaters are detached, generally shore-parallel structures that reduce the amount of wave energy reaching a protected area. They are similar to natural bars, reefs or near shore islands that dissipate wave energy. The reduction in wave energy slows the littoral drift, produces sediment deposition and a shoreline bulge or salient feature in the sheltered area behind the breakwater as can be seen in Figure 7-3. Some long shore sediment transport may continue along the coast behind the near shore breakwater. Figure 7-4 shows an example of the effect of detached breakwaters in front of a coastal stretch.

The breakwater shelters the coast immediately behind the structure and adjacent areas from the incoming waves. The acceleration of the littoral current updrift causes initial erosion of the beach on the updrift side. The same occurs in the area immediately down drift. These currents carry the eroded material towards the sheltered area, where it deposits. These mechanisms cause the patterns of deposition behind and erosion on either side which is observed in nature.

Protection afforded by the breakwater will limit erosion of the salient during significant storms. The exposed gap area will be eroded with sediment dragged offshore during storms. Breakwater height, length, wave transmission characteristics and distance from shore contribute to its effectiveness to provide a minimum dry beach width.

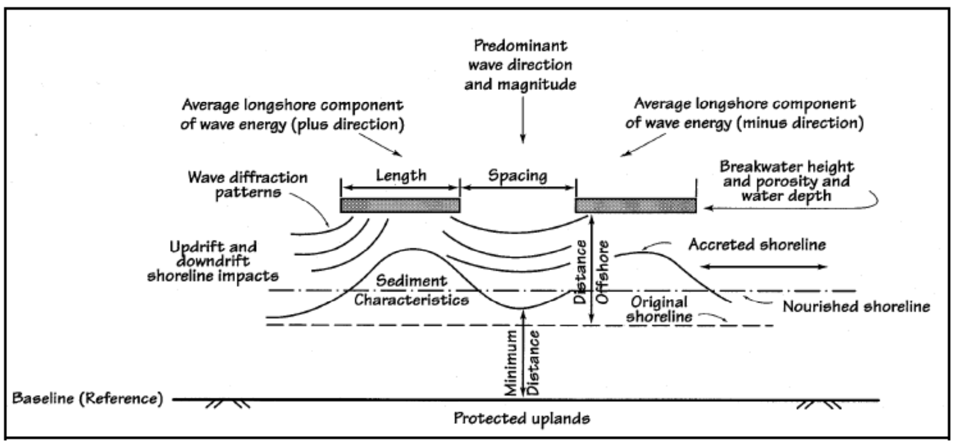

Figure 7-3: Schematic sketch of near shore breakwaters

Figure 7-4: Detached breakwaters in front of the English coast near Middleton

7.2.3 REVETMENT OR SEA WALL

A revetment or sea wall is a (sloping) structure placed parallel to the shoreline to absorb the energy of incoming waves. The main differences between a seawall and a revetment are that a revetment has a distinct slope (e.g. 1: 2 or 1: 4), that the surface of a revetment might be either smooth or rough and that the height of a revetment does not necessarily fill the total height difference between beach and mainland. Stones and possibly also concrete units of a revetment are placed on a bank to protect the coastline behind the structure from erosion. A revetment placed on an erosive coastline is vulnerable to collapsing due to extensive scouring in front of the structure. Use of a revetment for coastal protection is only a solution for storm surge problems to protect the mainland. If structural erosion occurs along the stretch of a coast under consideration, revetments or seawalls can in no way be selected as the only protection measure.

Figure 7-5: Revetment along a coast

7.3 "SOFT" SOLUTIONS

The term "soft" refers to the application of soil as a counter measure to a coastal defence problem. The principle of "soft solutions" is to counterbalance the volume of eroded material along a coastal stretch. This can be done via beach or foreshore suppletions.

A “soft” solution is a capital Beach Nourishment, including optional future repetitive re-nourishments since nourished beaches tend to erode faster than natural beaches. Generally, the sands will be borrowed from offshore sources and brought into the scheme by dredging vessels. The main advantages of beach nourishment are that the capital investment is relatively cheap; the result is aesthetically pleasing, the impact on adjacent coastline structures is generally positive since they benefit from the importation of sand as well and the option is very flexible and easy to implement. See Figure 7-6 for a beach nourishment in progress.

Figure 7-6: Beach nourishment in progress

COMBINATION OF BEACH STABILISATION STRUCTURES AND NOURISHMENT

Structural measures such as groynes and detached breakwaters may be combined with initial beach fills to reduce coastal impacts down drift of the protected stretch. The combination mitigates downdrift impacts and increases the fill life of the nourished beach. A groyne field combined with initial nourishment enables sand to immediately begin to bypass the groyne field. Together, their life-cycle costs and environmental impact may be less than if selectively implemented. Construction of the beach stabilization structures without fill is likely to damage adjacent coastal cells.

7.4 RECOMMENDATIONS

All the “hard” solutions will have an adverse effect on the adjacent coast as the scheme interferes into the occurring sediment processes. The protection measure reduces the sediment transport, decreasing local transport gradients to provide a more stable beach. Downdrift of the protection scheme the original transport rates do occur which leads to large gradients causing erosion. According to the modelling results a so-called ‘morphological zero point’ is probably present in front of the Senegambia area; sediment is then transported away both to the north and to the south. North of Senegambia the developed area of Kotu is situated, south of Senegambia lays Bijilo Park. As can be seen in Figure 6-18 the computed transport is southerly directed for the largest part of the nourishment area for the present situation. The area south of the nourishment has been accreting for the last 5 years. Blocked sediment transport by a hard structure would first cause erosion south of the protection scheme, which is then spread out over the adjacent area. As the computed sediment transport around Sheraton is northerly directed, zero transport at Bijilo would still give a positive sediment balance for the coastal stretch in between. This means that in general no erosion but even small accretion will still be present. As no data is available for calibration, the model contains a certain degree of uncertainty.

North of Senegambia the sediment transport is northerly directed. A hard protection measurement will thus cause structural erosion north of Kololi Point if sediment transport will be blocked at Senegambia. If the trend of the changing wave climate continues, the sediment transport along the complete coast will shift to more northern transport as can be seen in Figure 6-26. Blocked sediment transport by the protection scheme will then have a larger adverse impact on the coastal stretch north of Kololi.

The application of a series of groynes in front of the Senegambia area for the present situation could be a mitigation measure to consider against the ongoing erosion at Kololi beach. The groyne field would trap the sediment and a stable beach will be formed in front of the beach resorts. Erosion would occur north of the measure as described above. The construction of groynes is rather expensive; also no rocks for the construction of groynes are present in The Gambia, making the construction more expensive and complicated. Groyne system can create local currents and rip currents; the appearance of a groyne system is also aesthetically less pleasing.

Detached breakwater(s) in front of the Senegambia area could also be a possible measure to consider for the same reasons as a groyne field. As this is also a “hard” measure it would have an adverse effect on the coastal stretch north of Kololi. Unlike groynes a detached breakwater influences the sediment transport by reducing the wave energy. Adverse secondary currents are present around the breakwater and have less influence on the currents at the beach. The detached breakwater is also aesthetically more pleasing then a series of groynes.

A revetment or sea wall will be no solution for the protection of Kololi Beach in front of the Senegambia area. This kind of measure would only protect the structures on the mainland, the beach in front of the sea wall or revetment would erode and disappear completely.

Beach nourishments will again be a good mitigation measure for the erosion problem at the Senegambia area. It is of importance that the state and spread of the nourishment is monitored along the coast and re-nourishment would be necessary as the erosion rates at Senegambia are still very high. This means that beach nourishment will therefore be a temporary solution. Beach nourishments are relatively cheap and easy to implement. The lifetime of a re-nourishment with the same volume of 1,000,000 m^3 will be longer for the present situation as the sand deficit south of Senegambia has been decreased. The coastline south of Kololi is approaching its dynamic equilibrium which means the sediment transport will diminish which leads to a decrease in transport gradients. The complexity of the reef area and the uncertainty of the future wave climate make the future difficult to predict.

A Combination of a “hard” structure with initial nourishment in front of the Senegambia area may be considered to solve the short-term problem and to guarantee a sufficient beach width for lifetime of the nourishment. Re-nourishment in combination with a “hard” protection scheme would solve the short-term erosion problem; interruption of the alongshore sediment transport could maintain a stable beach. Furthermore coastal impacts down drift will be reduced by the initial nourishment as sediment has been added to the sand balance.

8. CONCLUSIONS AND RECOMMENDATIONS

The conclusions will first be discussed by answering both the research questions. Then the hypothesis will be discussed as formulated in section 1.6. The conclusion regarding the research questions are presented in section 8.1. In sections 8.2 the hypotheses are discussed and the recommendations resulting from this thesis are presented in section 8.3

8.1 CONCLUSIONS BASED ON THE RESEARCH QUESTIONS

- What happened to the nourished sand, where has it been transported to?

As can be concluded from the field data analysis and modelling study, eroded material from the nourished beach has for a large part been transported to the stretch south of the nourishment area. The sediment transport modelling substantiates these observed trends in shoreline movement. See Figure 4-6, Figure 6-6 and Figure 6-7, un-calibrated sediment transport shows high erosion inside the nourishment area and an overall trend of small accretion between Sheraton and the southern part of the nourishment. The accreted volume along the coast south of the nourishment area is approximately 50% of the total nourished volume; a small part has been transported north. Eroded shell fractions from the nourishment are likely to have been transported off-shore. Computed sediment transport show southern transport from the beach resorts to Sheraton, see Figure 6-18; these transports were much higher for the 2003 and 2004 coastline orientations as can be seen in Figure 6-25. Initially also large accretion was present north of Kololi Point, see Figure 4-5, due to local flow patterns caused by the reef area and the outcrop. This effect has been reinforced due to the relatively high amount of nourished sediment in the northern part of the nourishment. Large accretion north of Kololi Point was only present during the first year after nourishment; during the 2004-2009 period erosion was present between Kololi and Kotu point with accretion behind Kotu Point.

- Which processes cause the high erosion rate at Kololi Beach?

The cause of the high erosion rate at Kololi Beach is an enumeration of multiple processes. The modelling study on which the conclusions have been based is performed using the present bathymetry and the wave climate from 2000 to 2009. Data for observed trends are available and have been used from 1964 on. It is possible that both the bathymetry and/or wave climate have changed over time but this has not been taken into account and could cause the large difference between observed trends for 1964-1983 and the present erosion.

The combinations of the following processes have probably enforced the higher erosion rate at Senegambia than was first expected. In 2010 still a higher erosion rate is present than during the undisturbed period 1964-1983, even though the coastlines are similar.

- The large amount of shell fractions in the nourished sediment has a negative influence on the stability of the sediment. Small shell fractions wash away very easily like fine sediments, resulting in an off-shore sediment loss, and do not contribute to the total volume of sediment when erosion is present. Therefore the erosion rate is the percentage of present shell fractions higher along an eroding coastal stretch. In front of the Senegambia Beach resort even sediment with more than 30% shell fractions and fine sediments is present. The dent in front of the Senegambia beach resorts is probably enforced due to additional erosion caused by this effect.

- The water level has a high influence on the sediment transport along the coastal stretch within the research area. During low water the transport is much lower due to additional friction on the waves offshore, resulting in low transport gradients. During high water the bottom friction on the waves is less causing higher sediment transports along the coast; furthermore the influence and sheltering effect of the reef area is greatly reduced. Therefore gradients in transport are larger, especially behind the reef area, causing high erosion rates as can be seen in Figure 6-23. Because sea level rise causes a higher water level, the influence can be relatively large for a large time scale. In case of a sea level rise of 0.2 m/century the water level has risen with 10 cm from 1964, causing higher transports and erosion rates for the present situation. This effect would be the same or even larger when the reefs would be slowly eroding or subsiding.

- The last 3 years the wave climate in front of The Gambia has been changing. This was not clearly visible in the wave roses but the resulting sediment transports increased in northern direction. From 2000-2006 the overall trend was the same, which changed in 2007 to a different trend for 2008 and 2009, see Figure 6-12. This changing wave climate causes alongshore transport to be more northerly directed and possibly larger erosion in front of the Senegambia area.

- A part of the sediment has been placed adjacent to the designed target area; therefore the nourishment had an initial spread. This caused the nourishment to become less effective than could be expected.

8.2 CONCLUSIONS ON THE HYPOTHESES

The hypotheses which have been formulated in section 1.6 will be discussed and either approved or rejected in the following section. First the hypothesis is repeated after which the conclusion regarding the hypothesis is given.

Hypothesis 1: *The waves which attack Kololi Beach are rougher than in the surrounding areas. North of Kololi Beach two reefs are present and the wave climate is calmer there. Because of direct wave impact from the sea and a steep foreshore, the waves break close to the coast and therefore the breaker zone is rough and the rate of erosion is high.*

The nearshore wave climate south of Kololi beach, in front of Bijilo Park, is rougher than the waves in front of the beach resorts, see Figure 5-17. The wave climate around the reef area is remarkable due to shoaling and refraction caused by the local bathymetry. This influences the nearshore wave heights which changes along the coast, possibly causing secondary flows. Due to the sheltering effect of the reefs the wave climate is calmer there. The foreshore is steep along the entire coast; in front of Senegambia the foreshore is steepest as can be seen in Figure 3-18. The breaker zone in front of Bijilo Park and Senegambia is rough so sediment is stirred up and comes in suspension, possibly transported away by a current. As the wave incidence in front of Bijilo is close to normal and the angle of wave incidence at Senegambia is increasing, the erosion in front of the Senegambia area is higher. The rate of erosion is therefore influenced by the local angle of wave incidence and not because of the direct wave impact from the sea which is even higher south of the nourishment area.

Hypothesis 2: *Between approximately 1980 and 1996 high volumes of sand have been mined from coastal stretches south of Kololi. Because of this, the coast has a shortage of sand. Nourished sand has been transported south with the alongshore current to supplement the deficit.*

A large part of the nourished sediment has been transported to the south by alongshore sediment transport. This transport was first caused by high gradients in sediment transport due to construction of the nourishment. Illegal sand mining caused spatial variations of the shoreline orientation unlike the dynamic equilibrium. With an addition of sediment into the system these spatial variations cause gradients in the sediment transport creating accretion. The alongshore transport to the south is enhanced due to the shortage of sand, but also the existing coastline orientation causes southern transport and accretion between Sheraton and Bijilo Park.

Hypothesis 3: *The amount of shells in the nourished sediment has a negative effect on the beach stability and will therefore erode more easily. The nourished sand contains a large amount of broken and sometimes whole shells. These shell fractions have a negative influence on the sediment characteristics.*

Sieving of sediment samples shows that the sediment contains approximately 15% shell fractions, with a maximum of 30% for the current stretch in front of Senegambia. The amount of shell fractions varies locally along the coast between 0 and 20%. These shell fractions tend to break and start to diminish due to (rough) wave action. Small shell fractions wash away very easily, like fine sediments, and do not contribute to the total volume of sediment when erosion is present. Therefore the shell fractions have to be removed from the sieving curves as they do not increase stability; shell fractions in the sieving curves cause a higher d_{50} which is not representative for the reality.

Hypothesis 4: *During the rainy season a large portion of the precipitation in the hinterland is drained on Kololi Beach by two drainage points. By the intensity of the rain, deep and wide gullies arise on the beach which wash away the sand and leave a gap in the beach which is filled up again. This will have effect on the erosion rate, although this will not be large.*

No adequate information or data are present on the effect of the drainage points on Kololi Beach. The sediment which is washed away comes in suspension in the ocean and becomes part of the sediment balance along the coast. The dent in Kololi beach which was thought to be caused by the drainage points has been enforced or caused by a rip current and the very low quality of sediment in front of the Senegambia area.

Hypothesis 5: *During the first days of construction, the sediment used for the nourishment was dredged in front of Kololi. Changes in bathymetry which arose during these activities could have influence on the waves, wave conditions and cross shore transport. A pit in the sea bottom that arises can cause nourished sediment to fill up that pit again, losing sediment to the ocean.*

The exact location of dredging sediment in front of Kololi is not known. Also the total volume is small compared to the total volume which is nourished at the beach. Also comparing the two different measurements in 2010 does not show a gap or a filled gap. Therefore no conclusion can be drawn on this matter. If sediment has been nourished close tot Kololi Beach, it is possible that cross-shore transport has filled this gap with sediment from the nourishment which would be a loss of sediment.

Hypothesis 6: *Checking the amount of nourished sediment was done by counting the hopper capacities. Some sediment remains in the hopper causing a deficit in the total amount of nourished sediment. Also the porosity of the sediment inside the hopper, just after the nourishment and after settlement can be different, causing a volume change.*

The porosity of sediment inside the hopper shortly after dredging is higher than consolidated sediment on the beach. This difference in porosity probably caused a change in total volume of approximately 5%. Checking the exact amount of nourished sediment was done during construction; no sufficient data is present on the exact amount of nourished sediment, which could be lower than 1,000,000 m^3 which should have been nourished. According to the sediment budgets based on the trends in shoreline movement the volume of nourished sediment was not considerably less than 1,000,000 m^3.

Hypothesis 7: *The reefs in front of Kololi and Kotu influence the nearshore wave climates which have caused the outcrops along the coast at Kololi and Kotu. Erosion or subsiding of these reefs would have a large effect on the area behind them which could cause locally high erosion rates.*

Unfortunately no adequate data are present to substantiate this hypothesis. Measured lines from the 2000 and 2010 measurement campaigns which are close to each other have been compared, where small changes in the bathymetry were visible. As no measured lines along the same locations for several periods are available, no conclusion can be drawn regarding the erosion of the reef area.

8.3 RECOMMENDATIONS

- The wave and current patterns inside the reef area are very complex and have not been taken into account during the modelling study. These secondary flows and local wave climates are of a great importance on the erosion in front of the Senegambia area. Therefore a 2-Dimensinal model has to be used to investigate the effects caused by the reefs and gain quantitative insight in the sediment transports in front of the Senegambia area. This model can then be used for more research on the application of a protection scheme.

- The nourished sediment contains a lot of shells and shell fractions. These shell fractions wash out of the sediment and do not contribute to the stability, no further information on shells in nourished sediment is present. The high beach scarp at Kololi Beach has also been caused by cementation of the shell fractions. More research is needed on the influence of the shells on the erosion and stability of Kololi Beach

- To gain more quantitative insight into the alongshore sediment transport it is suggested to collect more data along the coast at fixed times throughout the year. By measuring the exact location of the coastline and some cross-shore profiles along the coast the state of the beaches can be closely monitored and the data is very useful for future research.

- Further research on the changing wave climate would give more insight into the historical and possibly also future trends of the wave climates. The wind climate is clearly changing from 2007 and this has a large influence on the sediment transport along the coast.

BIBLIOGRAPHY

J.A. Battjes, Short Waves,Lecture notes for CT 4320, Delft University of Technololgy, 2006

Battjes and Stive (1985)

P. Bruun, Sea level rise as a cause of shore erosion, *Proceedings ASCE,* 1962

Coastal Protection Study, Feasibility report Coastal Protection Study, Royal Haskoning, Nijmegen, Banjul 2000.

Coastal zone management handbook for The Gambia, Royal Haskoning, Nijmegen, 2006

R.G. Dean, Equilibrium beach profiles: characteristics and applications, *Journal of Coastal Research*, pp 53-84, 1977

R. Deigaard, et al, Mathematical model for littoral drift, *J. Waterway. Port, Coastal an Ocean eng., ASCE*, pp. 351-369, 1986

Det Norske Veritas, *Environmental conditions and environmental loads*, 2007

DHI, Third Banjul Port Project, Mathematical modelling of hydrodynamics and sedimentation at Banjul Port, 1993

DHI, LITPACK *User manual*, 2007

DHI, *User manual LITDRIFT*, 2007

J. van de Graaff, Coastal Morphology and Coastal Protection, Lecture notes for CT5309, Delft University of Technololgy, 2009

Hallermeijer, R.J. (1978) Uses for a calculated limit depth for beach erosion, *Proceedings 16th Coastal Engineering Conference,* ASCE, pp. 1493-1512

SWAN. *SWAN Users Manual, SWANCycle III, version 40.81, 2010*

L.H. Holthuijsen, Introduction to physical oceanography. Lecture notes CT5317, Delft University of Technololgy, 2007

L.H. Holthuijsen, Waves in oceanic and coastal waters, 2007

Babu P. Jallow, M.K.A. Barrow, S.P. Leatherman, Vulnerability of the coastal zone of The Gambia to sea level rise and development of response strategies and adaptation options, 1996

Pelnard-Considere (1956) Essai de theorie de lévolution des fomres de ravage en plages de sable et de galets, III (1) pp 289-298

Rubey, W. W., Settling velocities of gravel, sand and silt particles, *Amer. J. Sci. Sev. 5, 25, 325-338, 1933*

M.J.F. Stive, J.Bosboom. Coastal dynamics 1, lecture notes CT4305, Delft University of Technololgy, 2010

LIST OF FIGURES

Figure 1: Overview research area: from Bald Cape to Kotu ... vii
Figure 2: Measured shoreline movement for 1964-1983 and 2004-2009, the nourishment area is in front of the Senegambia area ... viii
Figure 3: Significant wave heights in front of the Beach resorts and at the reef area for southern waves (a) and northern waves (b) ... ix
Figure 4: Sediment transport for mean coastline and water level CD+1 ... x
Figure 5 Shoreline Movement for different water levels ... xi
Figure 6: Sediment transport for different wave climates ... xi

Figure 1-1: Map of Africa ... 1
Figure 1-2: Map of west-Gambia ... 2
Figure 1-3: Kololi Beach in front of Senegambia Beach Resort (2002) ... 3
Figure 1-4: Location Kololi Beach ... 4
Figure 1-5: Design nourishment at Kololi Beach ... 5
Figure 1-6: Finished nourishment at Kololi beach, Senegambia Beach Resort (December 2003) ... 5
Figure 1-7: Kololi Beach in front of Senegambia Beach Resort (April 2010) ... 6

Figure 2-1: Sand balance 2000 (Source: CZM Handbook) ... 12
Figure 2-2: Wave output locations ... 13
Figure 2-3: S-phi curves for location 7, 8 and 9. ... 13
Figure 2-4: Prediction of coastal development ... 14
Figure 2-5: Prediction of coastal development after nourishment ... 15
Figure 2-6: Beach nourishment profiles ... 18
Figure 2-7: Design of the nourishment ... 18
Figure 2-8: Kololi area before nourishment ... 18
Figure 2-9: Construction of Kololi Beach ... 19

Figure 3-1: Climate graph ... 21
Figure 3-2: Effect of sand mining ... 22
Figure 3-3: Coastal definitions ... 23
Figure 3-4: Streams near the research area ... 24
Figure 3-5: Available wind/wave points ... 25
Figure 3-6: Wind rose for all year climate ... 26
Figure 3-7: Offshore wave rose for sea waves ... 26
Figure 3-8: Offshore swell wave rose, peak direction ... 27
Figure 3-9: Offshore swell wave rose, principal wave direction ... 27
Figure 3-10: Offshore wave rose (total), peak direction ... 29
Figure 3-11: Offshore wave rose (total), principal wave direction ... 29
Figure 3-12: Wave height against peak period ... 29
Figure 3-13: Tide level in front of the Senegambia Area ... 30
Figure 3-14: Offshore Bathymetry ... 31
Figure 3-15: Data point measurement 2000 + 2003 ... 32
Figure 3-16: Data point measurement September 2010 ... 33

Figure 3-17: Location of beach profiles 34
Figure 3-18: Beach profiles 34
Figure 3-19: Gaps in the beach due to drainage problems 37
Figure 3-20: Circulation patterns for different angles of wave incidence, A: typical longshore transport due to obliquely incident waves, B: rip current pattern in case of approximately normal wave incidence, C: combination of previous two cases for slightly oblique waves. 38

Figure 4-1: Coastline data points along research area 41
Figure 4-2: Coastline estimation in Google Earth 42
Figure 4-3: Shoreline movement from 1964 to 1983, derived from aerial photographs 43
Figure 4-4: Shoreline movement from 1983 to 2002, derived from aerial photographs 44
Figure 4-5: Shoreline movement from 2002 to 2004, derived from aerial photographs 45
Figure 4-6: Shoreline movement from 2004 to 2009, derived from aerial photographs 46
Figure 4-7: Shoreline movement from 1964 to 1983, derived from aerial photographs 47
Figure 4-8: Shoreline movement from 1983 to 1993, derived from aerial photographs 47
Figure 4-9: Sediment budget between 1964 and 1983 49
Figure 4-10: Sediment budget between 2004 and 2009 49
Figure 4-11: Kololi beach September 2010 51
Figure 4-12: sediment characteristics 52
Figure 4-13: Comparison profiles 2000 and 2010 53
Figure 4-14: Comparison profiles 2003, April 2010 and September 2010 53
Figure 4-15: Northern part of the (a) in-survey and (b) out-survey 54
Figure 4-16: Spreading of a nourishment 55
Figure 4-17: Rip-current in front of the Senegambia area 56
Figure 4-18: Used profiles, Coastline and Swan data point 58

Figure 5-1: computational grids 60
Figure 5-2: (a and b): Off-shore bathymetry 61
Figure 5-3: Nearshore bathymetry 61
Figure 5-4: Wind direction versus wave direction 62
Figure 5-5: Density plot for swell conditions 63
Figure 5-6: Density plot for wind0wave conditions 63
Figure 5-7: Significant wave height for south-western waves for large grid (a) and nearshore grid (b) 67
Figure 5-8: Significant wave height for north-western waves for large grid (a) and nearshore grid (b) 68
Figure 5-9: Refractive pattern for south-western swell waves 69
Figure 5-10: Nearshore wave roses in front of Senegambia (a) principal wave direction and (b) peak direction 69
Figure 5-11: Nearshore wave roses for principal wave direction 70
Figure 5-12: Nearshore wave roses for peak direction 70
Figure 5-13: Significant wave height for wind generated waves for the large grid 71
Figure 5-14: Significant wave height for wind generated waves for the nearshore grid 72
Figure 5-15: Refractive pattern for wind generated waves. 72
Figure 5-16: Wave roses for wind generated waves at (a) Senegambia area and (b) Point Sheraton 73
Figure 5-17: Significant wave height for high water level (a) and low water level (b) 74

Figure 6-1: Single line theory 79
Figure 6-2: Bathymetry of profile 14 80

Figure 6-3: Sieving curves for sediment in front of Beach resorts 81
Figure 6-4: Computed fall velocities as function of the grain diameter 81
Figure 6-5: Used coastline angles 83
Figure 6-6: Computed Sediment transport capacity for mean coastline and water level CD +1m, note that the results presented have not been calibrated 86
Figure 6-7: Computed Shoreline movement for mean coastline and water level CD +1m, note that the results presented have not been calibrated 86
Figure 6-8: Computed Sediment transport capacity for mean coastline and different water levels, note that the results presented have not been calibrated 87
Figure 6-9: Computed Shoreline movement for mean coastline and different water levels, note that the results presented have not been calibrated 88
Figure 6-10: Computed Sediment transport capacity for different coastlines at mean sea level, note that the results presented have not been calibrated 89
Figure 6-11: Computed Shoreline movement for different coastlines at mean sea level, note that the results presented have not been calibrated 89
Figure 6-12: Accumulated sediment transport for total time series 90
Figure 6-13: Sediment transport capacity for 2004 and 2009 wave climate, note that the results presented have not been calibrated 91
Figure 6-14: Shoreline movement for 2004 and 2009 wave climate, note that the results presented have not been calibrated 91
Figure 6-15: Cross-shore distribution of the alongshore transport for MSL 92
Figure 6-16: S-ϕ curves for different profiles along the coast, note that the results presented have not been calibrated 93
Figure 6-17: C-values along the coast, note that the results presented have not been calibrated 93
Figure 6-18: Sediment transport for mean coastline and water level CD+1 96
Figure 6-19: Shoreline movement for mean coastline and water level CD+1 96
Figure 6-20: Sediment transport for principal wave and peak direction 98
Figure 6-21: Shoreline movement for principal wave and peak direction 98
Figure 6-22: Sediment transport for different water levels 100
Figure 6-23: Shoreline movement for different water levels 100
Figure 6-24: Sediment transport for different coastlines 102
Figure 6-25: Shoreline movement for different coastlines 102
Figure 6-26: Sediment transport for 2004 coastline with changing wave climates 104
Figure 6-27: Shoreline movement for 2004 coastline with changing wave climates 104

Figure 7-1: Schematic groyne scheme 108
Figure 7-2: Example of a groyne field 108
Figure 7-3: Schematic sketch of near shore breakwaters 109
Figure 7-4: Detached breakwaters in front of the English coast near Middleton 109
Figure 7-5: Revetment along a coast 110
Figure 7-6: Beach nourishment in progress 111

Figure A-1: Raw and smoothened measured profile 132
Figure A-2: Predicted tide level during measurement 132
Figure A-3: Location of 200, 2003 and April 2010 measurements 132

Figure B-1: Sample locations sand search 2000 135
Figure B-2: Sample locations sand search 2001 136
Figure B-3: Overview sample locations sand search 2002 138
Figure B-4: Sample locations Kololi sand search 2002 138

Figure B-5: Sample properties and locations for the 2002 sand search 140

Figure C-1: monthly wave roses for total wave height, principal wave direction 141
Figure C-2: Monthly wave roses for swell waves, principal wave direction 142
Figure C-3: Monthly wave roses for total wave height, peak direction 143
Figure C-4: Monthly wave roses for swell waves, peak direction 144
Figure C-5: Annual wave roses for total wave height, principal wave direction 145
Figure C-6: Annual wave roses for swell waves, principal wave direction 146
Figure C-7: Annual wave roses for total wave height, peak direction 147
Figure C-8: Annual wave roses for swell waves, peak direction 148
Figure C-9: Monthly wave roses for sea waves, principal wave direction 149
Figure C-10: monthly wave roses for sea waves, peak direction 150
Figure C-11: Annual wave roses for sea waves, principal wave direction 151
Figure C-12: Annual wave roses for sea wave height, peak direction 152

Figure D--1: Significant wave height for western waves 153
Figure D-2: Significant wave height and refractive pattern inside the reef area for western waves 154
Figure D-3: Significant wave height and refractive pattern inside the reef area for north-western waves 155
Figure D-4: Significant wave height and refractive pattern inside the reef area for south-western waves 156
Figure D-5: Significant wave height for north-western waves with steepness = 0.003 157
Figure D-6: Significant wave height for north-western waves with steepness = 0.012 157
Figure D-7: Refractive pattern for north-western waves 158
Figure D-8: Refractive pattern for wind-generated waves inside the reef area 158
Figure D-9: Significant wave high inside reef area for high and low water level 159

Figure E-1 Aerial photograph of Senegambia area, 2003: before nourishment 161
Figure E-2 Aerial photograph of Senegambia area, 2004: after nourishment 161
Figure E-3 Aerial photograph of Senegambia area, February 2011 162
Figure E-4: Reef area Bathymetry 162
Figure E-5: Overview of 2000 and 2010 compared profiles 163
Figure E-6: Overview of 2003 and 2010 compared profiles 164
Figure E-7: Comparison of the 2000 and 2010 profiles 165
Figure E-8: Comparison of the 2003 and 2010 profiles 166
Figure E-9: Sediment budget for 1983 - 1993 167
Figure E-10: Sediment budget for 1993 - 2002 167
Figure E-11: 2003 in-survey 168
Figure E-12: 2004 out-survey 169
Figure E-13: Accumulated sediment transport for peak direction 170
Figure E-14: Computed sediment transport for 2004 and 2009 wave climate for 2009 coastline 171
Figure E-15: Computed shoreline movement for 2004 and 2009 wave climate for 2009 coastline 171
Figure E-16: Sediment transport for mean and 2009 wave climate for 2009 coastline 172
Figure E-17: Shoreline movement for mean and 2009 wave climate for 2009 coastline 172
Figure E-18: Cross-shore distribution of alongshore transport for low water level (CD +0.3m) 173
Figure E-19: Cross-shore distribution of alongshore transport for high water level (CD +1.7m) 173

LIST OF TABLES

Table 2-1: Nourishment design profiles 17
Table 3-1: Minimum and maximum temperature 22
Table 3-2: Sediment supply to the coast by rivers in the research area (Source: CZM Handbook) 24
Table 3-3: characteristic tidal water levels at Kololi (MHWS/N = Mean High Water Spring/Neap tide) 30
Table 4-1: Shoreline movement according to 2000 Feasibility Study 47
Table 4-2: Locations sediment samples 51
Table 5-1: Computational resolution 60
Table 5-2: Range of values for boundary conditions for swell conditions 63
Table 5-3: Range of values for boundary conditions for wind conditions 63
Table 5-4: SWAN Physical parameter settings for swell conditions 65
Table 5-5: SWAN Physical parameter settings for wind conditions 65
Table 6-1: Overview of sediment transport calculations 84
Table B-1: sediment properties sand search 2000 135
Table B-2: Results sand search 2001 137
Table B-3: Sediment properties sand search 2002 139

Appendices

APPENDIX A: BATHYMETRIC SURVEY

APRIL 2010

In the beginning of the project a mission of one month to The Gambia was planned to meet the secretary's from the government which are responsible for the coastal protection and to get to know the research area. During this mission also a low-cost bathymetric survey was conducted to obtain recent data. The survey in April 2010 was conducted with a Valeport Midas Surveyor GPS echo sounder. The transducer of the echo sounder was mounted fit to a fishery boat with a self-made frame at approximately 30 cm below sea level. The equipment measured the depth from the transducer to the bottom of the sea. The position was measured by an external GPS, every second the position and depth was logged 6 times.

The transducer was fitted at the bottom of a long pole with the GPS receiver on top so that the measured locations correspond with the measured depths. The pole was mounted fit to the fishery boat with a frame which was detachable. Before sailing out on the ocean the equipment was calibrated. The draft of the transducer was measured and entered into the surveyor which adds the draft to the measured depth; the stored depth is the distance between the water level and the bottom. A bar check was performed by lowering a steel plate to a known depth and adapting the velocity of sound in water inside the equipment, this was done for a number of depths. The bar check was again carried out offshore.

After the calibration the measurement was conducted in the Kololi area as shown in Figure A-3. The sailed track was monitored by handheld GPS so that the sailed lines were fairly close to each other. The distance between sailed lines is between 25 to 50 meters. The measurement was conducted during high tide so the depth could be measured as close to the beach as possible.

There were some problems with the equipment as it was arranged at the last moment and the equipment was relative old and not used for a long time. During the first measurement day the equipment had a lot of problems with logging the data and the measurement contained a lot of error data and was not accurate. This measurement was still useful because we could get acquainted with the equipment and get used to perform a bathymetric survey. During the second measurement day the equipment was performing better but there were still some problems with the equipment: nearshore the measured depth sometimes went towards zero, these error data was filtered out later during the processing. The locations were automatically stored in the local geodetic system. The parameters of the system are summarized below.

The available equipment had no sensor to correct for heave and tide so the data had to be processed after the measurement. In The Gambia there is no registration of the tide, the Banjul Port however makes a tidal prediction for each year; given tidal heights are with respect to chart datum. The data from this prediction is used to make an assumption of the tide during the measurement day. The heights and times are taken from the Tide Prediction by the GPA and an assumption was made by combining a semi-diurnal and a diurnal tidal component. Because Kololi is south of Banjul, there is also a small shift in time. See Figure A-2 for the used tidal data to process the measurement data.

Because of error data in the measurement, the data has been filtered to depth values between 20 and 2 meters. It is certain that all measured depths are between these values. The raw data has a lot of fluctuations caused by the waves. This is corrected by taking an average of the measured depths, see Figure A-1.

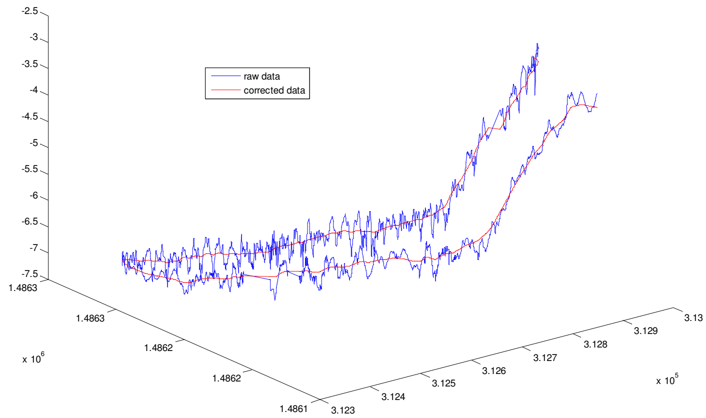

Figure A-1: Raw and smoothened measured profile

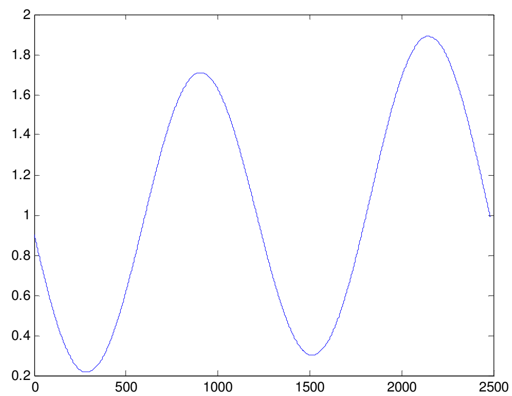

Figure A-2: Predicted tide level during measurement

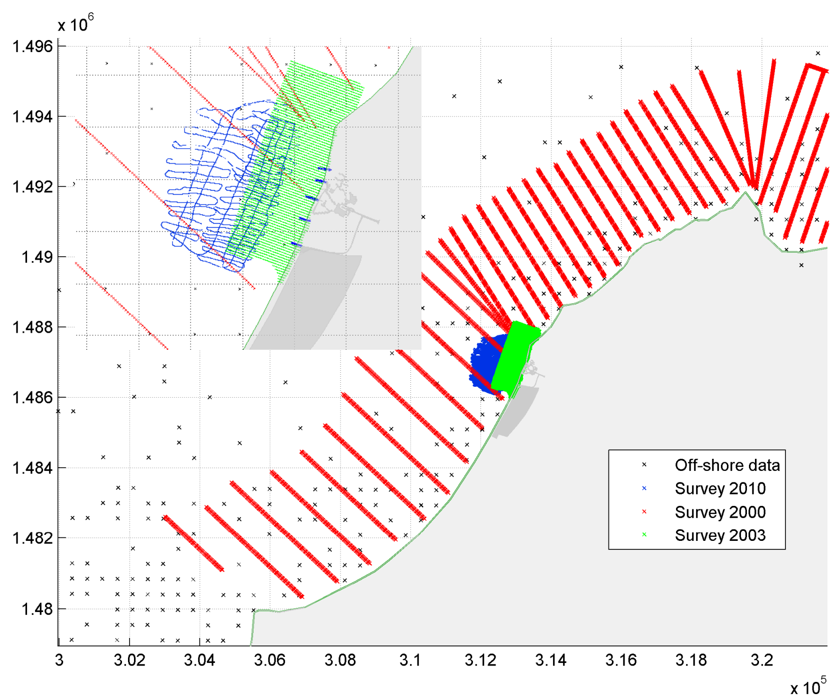

Figure A-3: Location of 200, 2003 and April 2010 measurements

GPS GEODETIC PARAMETERS

The measured data was stored in the local datum. The grid co-ordinates are quoted in universal Transverse Mercator projection (UTM), Zone 28. The applicable geodetic parameters are summarised as follows:

Datum: World Geodetic System 1984 (WGS 84)
Spheroid: World Geodetic System 1984 (WGS 84)
a = 6378137.000 meter
e^2 = 0.006694379

Local Datum

Datum: Bathurst Base East End
Spheroid: Clarke 1880 (modified)
a = 6378249.14 meter
e^2 = 0.0068035110

Projection

U.T.M. zone 28
Central Meridian: 15° West
Latitude of Origin: 0° North
False Easting: 500,000 meter
False Northing: zero
Scale factor on CM: 0.9996

Datum shift parameters

The following datum shift, rotation and scale parameters have been used for the conversion of the WGS 84 co-ordinates to the Local Datum co-ordinates are as follows:

Delta X = 162.775 meter
Delta Y = 11.694 meter
Delta Z = -203.021 meter

Rotation X = 0.1099 seconds
Rotation Y = -0.1067 seconds
Rotation Z = 0.0215 seconds

Scale factor = 0.242 parts per million

The measured data is eventually transformed to the universal WGS ’84 datum. This was done because the data was available with different datum’s, some of them with errors. After correction of these errors all the data was transformed to the WGS ’84 datum with UTM projection.

SEPTEMBER 2010

During the study it became clear that the reefs offshore of Kololi are of great importance for the wave and coastline modelling and were not measured properly yet. There was also an error in the locations of the 2000 and 2003 measurements, making the bathymetric data unreliable. Therefore a new and extensive bathymetric survey is conducted in September 2010. During this survey also the error in the DEEP 2000 and 2003 measurement was found and corrected.

The bathymetric survey in September 2010 has been conducted in collaboration with DEEP from Amsterdam which also conducted the measurements in 2000 and 2003. The measurement has been conducted using an RTK-GPS station which gives an accuracy of approximately 2 cm in X, Y and Z direction. The RTK-GPS base station has been set up at a known point with a known corresponding height. The measurement was conducted with respect to this base station, from the station it was possible to measure in a range of 6 kilometres if clear view was available.

The frame of the April 2010 measurement has been used for the measurement in September. The transducer had a draught of approximately 40 cm and the GPS receiver had a clear view and was exactly in top of the transducer. Measured depth has been is corrected for tide and heave by means of the RTK-GPS receiver. Measured values are corrected with the exact know height from the base station.

APPENDIX B: SAND SEARCH CAMPAIGN LOCATIONS AND RESULTS

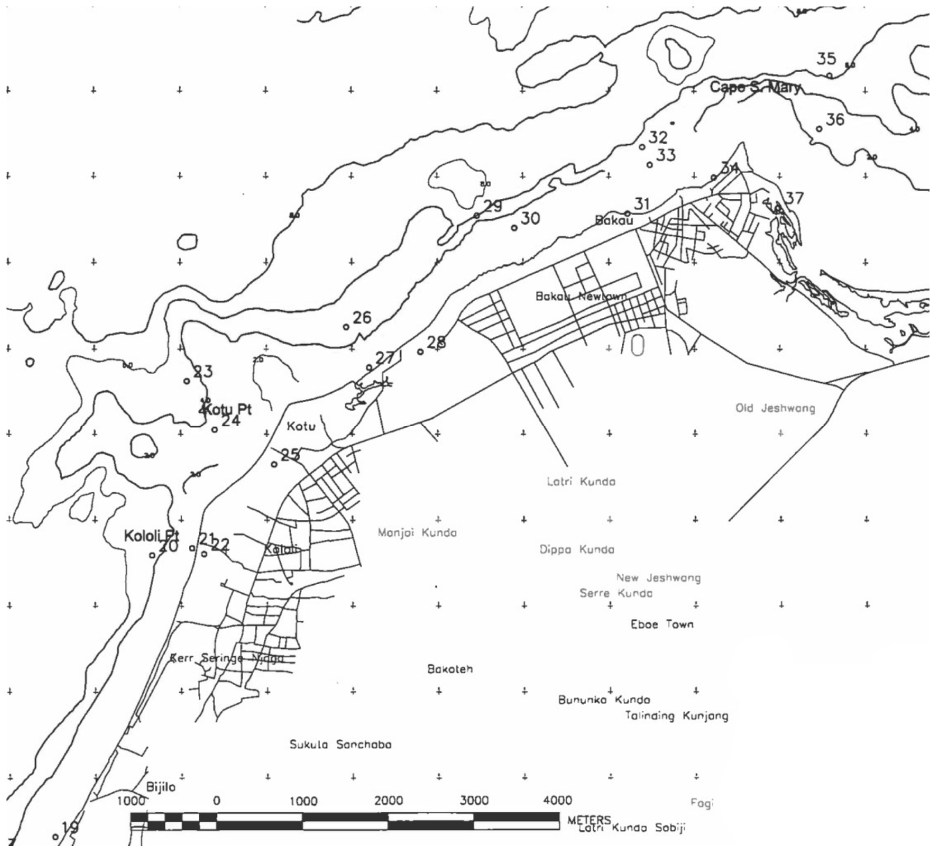

Figure B-1: Sample locations sand search 2000

Sample no	Depth below water level (m)	D50 (mm)	D10 (mm)	D90 (mm)
19	0	0.21	0.10	0.49
20	4.9	0.12	0.09	0.25
21	2.5	0.12	0.09	0.22
22	8.0	0.22	0.16	0.42
23	8.0	0.17	0.08	0.29
24	5.9	0.18	0.09	0.28
25	0	0.19	0.10	0.28
26	7.2	0.46	0.18	2.30
27	5.6	0.13	< 0.07	0.35
28	0	0.20	0.13	0.28
29	9.8	0.37	0.17	0.85
30	6.8	0.15	< 0.07	3.10
31	0	0.28	0.16	0.50
32	2	0.23	0.16	0.43
33	6.9	0.15	0.09	0.60
34	0	0.43	0.18	0.85
35	8.5	0.43	< 0.07	1.20
36	3.9	0.17	0.09	0.28
37	0	0.43	0.16	3.20
38	10	0.60	0.19	5.70
39	5	0.30	0.10	4.20

Table B-1: sediment properties sand search 2000

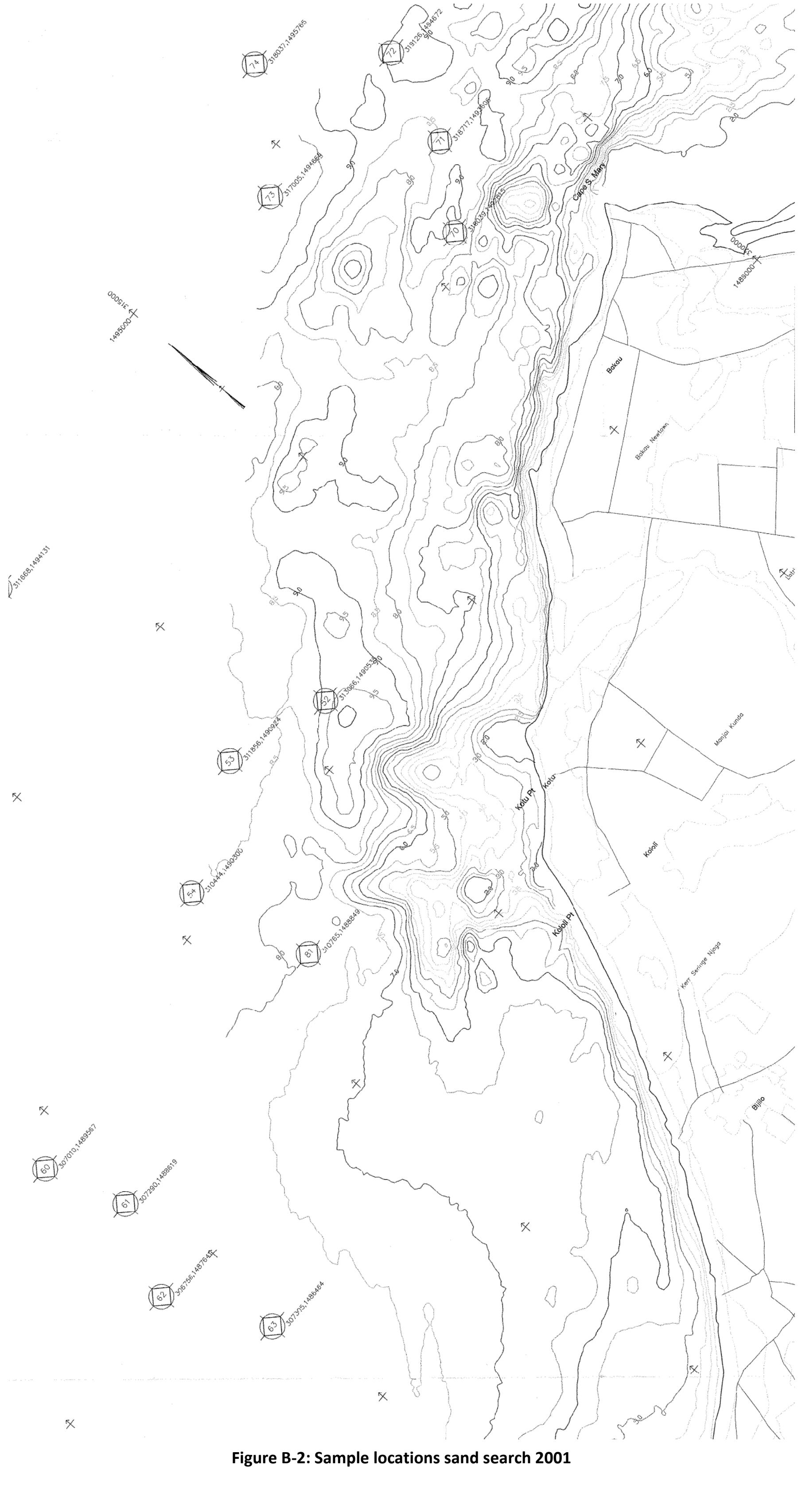

Figure B-2: Sample locations sand search 2001

DEEP ref	Depth [m]	Description	Sample No.	Sample Depth [m]	D50 [micron]
52	0.0-0.1	Silt and shell	Grab	0.0-0.1	
53	0.0-0.1	Silt and shell	Grab	0.0-0.1	
54	0.0-0.1	Shell and silt			
	0.1-2.2	Silt	54A	0.4-0.8	250
61	0.0-0.2	Silt with some fine sand			
	0.2-2.5	Silt	61A	0.1-0.5	225
	2.5-2.6	Rock and sand			
70	0.0-0.8	Stone and clay			
	0.8-2.6	Very fine sand	70A	0.9-1.3	12000
71	0.0-0.1	Gravel			
	0.1-1.0	Clay			
	1.0-2.6	Stone, shells and fine sand / clay	71A	1.0-1.4	1200
72	0.0-0.3	Gravel and shell			
	0.3-1.3	Clay with some fine sand			
	1.3-2.9	Sand	72A	1.3-1.7	375
73	0.0-1.0	Shells and sand	73A	0.6-0.9	400
	1.0-2.5	Layers of clay and fine sand			
80	0.0-1.5	Silt (some shells in the top 200mm)	80A	0.2-0.6	250
	1.5-2.3	Clay			225
81	0.0-2.2	Silt and fine sand (some shells in the top 200mm)	81A	0.2-0.6	

Table B-2: Results sand search 2001

For the 2002 sand search the following indicators correspond with their locations:

AT2 – AT8 are taken in front of Kotu.

AT9 – AT16 and AT20 – AT25 are taken in front of Kololi

AT17 – AT19 are taken north of Cape point

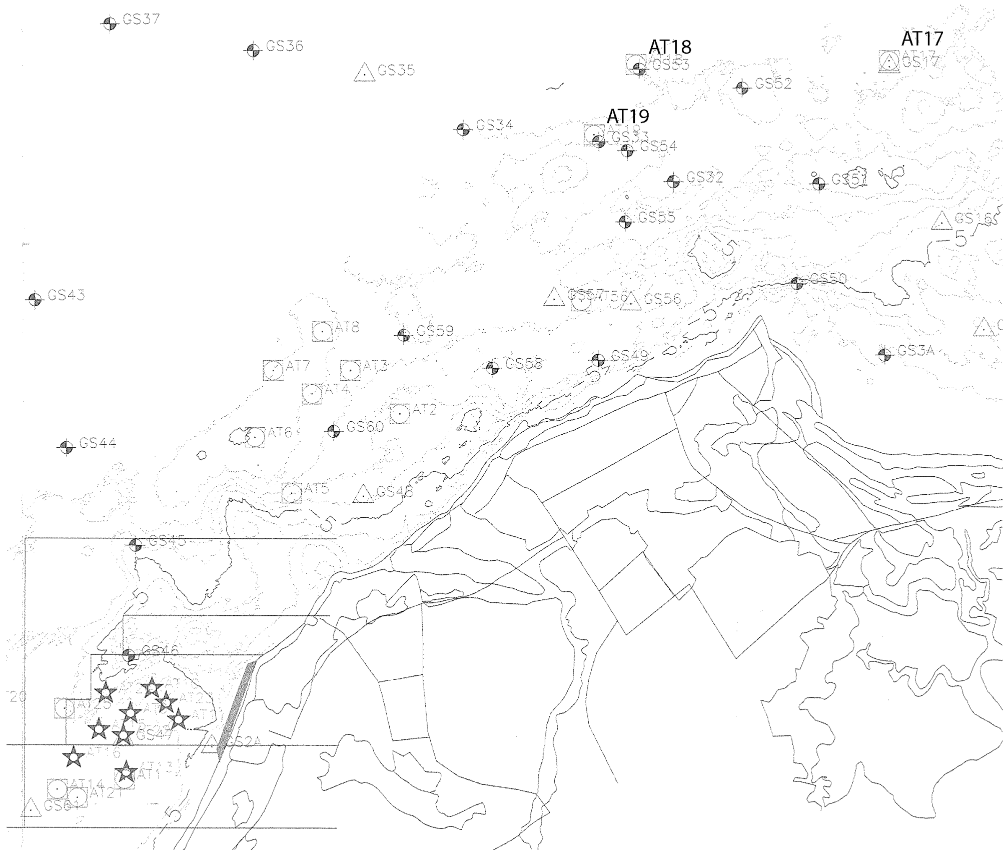

Figure B-3: Overview sample locations sand search 2002

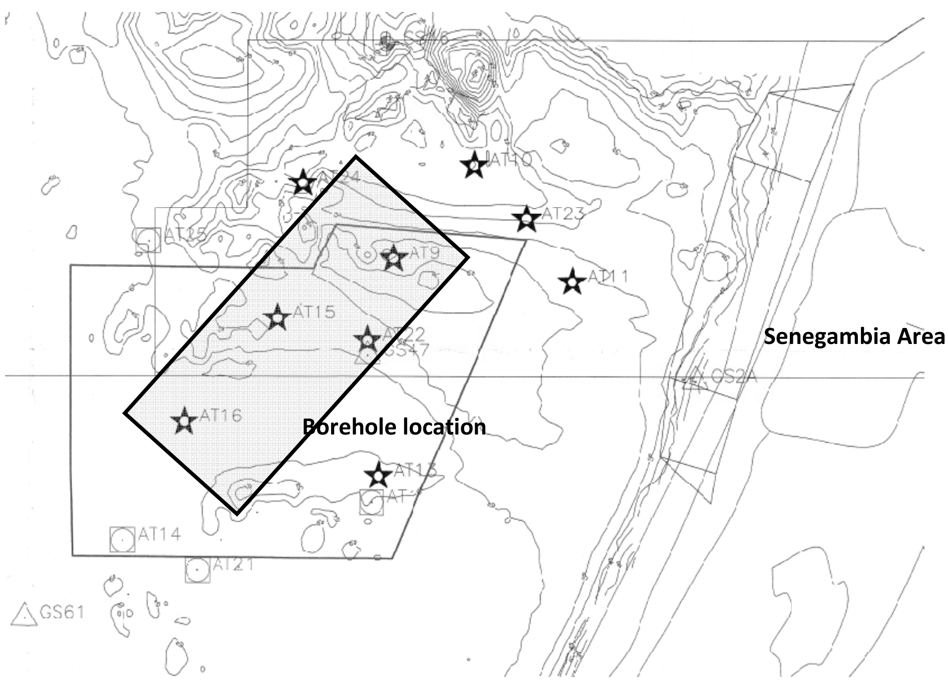

Figure B-4: Sample locations Kololi sand search 2002

#	Depth	D_{50}	D_{mf}	D_{msk}
AT09	0.3 – 1.1	186	184	191
	1.1 – 2.5	299	570	473
AT10	0.6 – 1.5	193	197	207
	1.5 – 3.0	184	182	186
AT11	0 – 0.8	273	762	575
	0.8 – 3.0	306	671	545
AT12	0 – 0.4	996	1748	1074
	0.4 – 1.0	243	269	271
	1.0 – 2.0	242	252	255
AT13	1.5 – 3.0	228	251	256
AT15	0 – 1.0	147	149	149
	1.0 – 2.0	163	170	175
	2.0 – 3.0	393	422	423
AT16	1.5 – 3.0	200	197	204
AT22	0 – 1.0	159	187	205
	1.0 – 2.0	509	580	580
AT23	1.0 – 3.0	382	388	388
AT24	0 – 0.3	175	181	188
	0.3 – 1.5	377	421	426
AT35	0 – 0.3	853	1585	1007
	0.3 – 2.0	334	628	514
AT36	0 – 0.8	539	895	719
	1.2 – 2.4	721	1213	911
AT42	0 – 0.6	434	545	530
	0.6 – 1.7	345	480	463
AT43	0 – 2.5	232	244	247
AT44	0 – 0.7	517	868	709
	0.7 – 1.4	465	623	584
AT45	0.4 – 1.2	776	1347	950
AT47	0 – 1.2	403	523	498

Table B-3: Sediment properties sand search 2002

AT8	13	29.223	15	43.054	1	0 - 0.15	mix of shels sand gravel and clay	NS
						0.15 - 1.0	reddish brown / light grey sandy stiff CLAY, weatherec soil with black gravels (0.5 - 1.0 cm)	NS
AT7	13	28.963	16	43.381	1.2	0 - 0.3	fine black SAND with lot of small shell particles	NS
						0.3 - 1.2	mix of shels sand gravel and clay (weathered rock)	NS
AT6	13	28.524	16	43.499	2.9	0 - 2.9	light grey SILT, very wet with plasticity	NS
AT5	13	28.16	16	43.25	0.6	0 - 0.6	mix of sand gravel and clay (weathered rock), light grey / reddish brown	NS
AT4	13	28.811	16	43.119	2	0 - 0.4	mix of fine black SAND, light grey medium SAND, shell particles	S
						0.4 - 2.0	light brown CLAY with gravel and sand, plasticity	NS
AT3	13	28.968	16	42.863	1.3	0 - 0.1	fine SAND and shells	S
						0.1 - 1.0	mix of sand gravel and clay (weathered rock), light grey / reddish brown	NS
AT2	13	28.686	16	42.53	1.8	0 - 0.8	fine black SAND with a lot of shells (>50%)	S
						0.8 - 1.4	very clayey SAND, plsticity	NS
						1.4 - 1.8	mix of sand gravel and clay (weathered rock), light grey / reddish brown	NS
AT17	13	31.041	16	39.274	3	0 - 0.1	SHELLS	NS
						0.1 - 0.6	soft light grey sandy CLAY	NS
						0.6 - 1.5	light grey clayey SAND, clay content decreasing with depth	NS
						1.5 - 3.0	yellowish brown medium coarse SAND	VS
AT18	13	30.999	16	40.572	3	0 - 0.4	light brown quartz SAND with shells (50%)	S
						0.4 - 1.2	interchanging layers of light grey SAND with clayey SAND	NS
						1.2 - 2.0	sandy CLAY embedded with clay layers	NS
						2.0 - 3.0	yellowish brown medium coarse quartz SAND	NS
AT19	13	30.534	16	41.248	2.7	0 - 0.2	Shells with sand and clay	NS
						0.2 - 1.8	light grey sandy CLAY	NS
						1.8 - 2.7	yellow brown / light grey CLAY	NS
AT22	13	26.598	16	44.392	3	0 - 1.0	fine dark grey SAND (150 mu)	S
	E	311694	N	1486618		1.0 - 3.0	yellowish brown medium coarse quartz SAND (400 - 700 mu)	VS
AT23	13	26.814	16	44.107	3	0 - 1.0	fine dark grey SAND (150 mu)	S
	E	312212	N	1487013		1.0 - 3.0	yellowish brown medium coarse quartz SAND (400 - 700 mu)	VS
AT24	13	26.875	16	44.512	1.5	0 - 0.3	fine dark grey SAND (150 mu) with some shells	S
	E	311431	N	1487131		0.3 - 1.5	yellowish brown medium coarse quartz SAND (400 - 700 mu)	VS
AT25	13	26.731	16	44.757	3	0 - 2.5	dark grey clayey fine SAND with some shells	NS
	E	311037	N	1486868		2.5 - 3.0	yellowish brown medium coarse quartz SAND (400 - 700 mu)	VS
Wednesday November 27th								
AT9	13	26.743	16	44.346	2.8	0 - 0.3	dark grey fine SAND with thin clayey sand layers	S
	E	311779	N	1486885		0.3 - 1.1	medium yellowish brown quartz SAND	VS
						1.1 - 2.8	fine to medium yellowish brown quartz SAND (lost 50 cm of sample)	VS
AT10	13	26.909	16	44.203	3	0 - 0.6	dark grey fine SAND with some clay and shells in bottom of sample	S
	E	312040	N	1487189		0.6 - 3.0	yellowish brown medium SAND	VS
AT15	13	26.635	15	44.556	2.8	0 - 0.2	very loose wet dark grey fine to medium SAND	S
	E	311399	N	1486689		0.2 - 1.8	dark grey fine to medium SAND (no shells, no clay)	VS
						1.8 - 2.8	yellowish brown medium SAND	VS
AT16	13	26.45	15	44.723	3	0 - 0.2	very loose wet dark grey fine SAND	S
	E	311095	N	1486350		0.2 - 1.5	dark grey fine SAND with little plasticity and some shells (10%)	S
						1.5 - 3	yellowish brown medium SAND	VS
AT13	13	26.357	15	44.37	3	0 - 0.8	dark grey fine to medium SAND, (no shells no clay)	VS
	E	311731	N	1486174		0.8 - 1.5	dark grey silty fine SAND, with little plasticity and 5% shells	S
						1.5 - 3.0	yellowish brown medium SAND	VS
AT1	13	26.27	15	44.35	0.5	0 - 0.15	fine SAND with COBBLES	NS
	E	311766	N	1486013		0.15 - 0.5	hard yellowish brown CLAY	NS
AT11	13	26.704	15	44.024	3	0 - 0.9	very loose wet dark grey fine SAND, with some shells in bottom of sample	S
	E	312360	N	1486809		0.9 - 3.0	yellowish brown medium SAND	VS
AT14	13	26.2	15	44.3	1.75	0 - 1.75	clayey whitish very fine SAND	NS
	E	310953	N	1485890				

Figure B-5: Sample properties and locations for the 2002 sand search

APPENDIX C: WAVE DATA

Monthly wave roses for total significant wave height point N, principal wave direction.

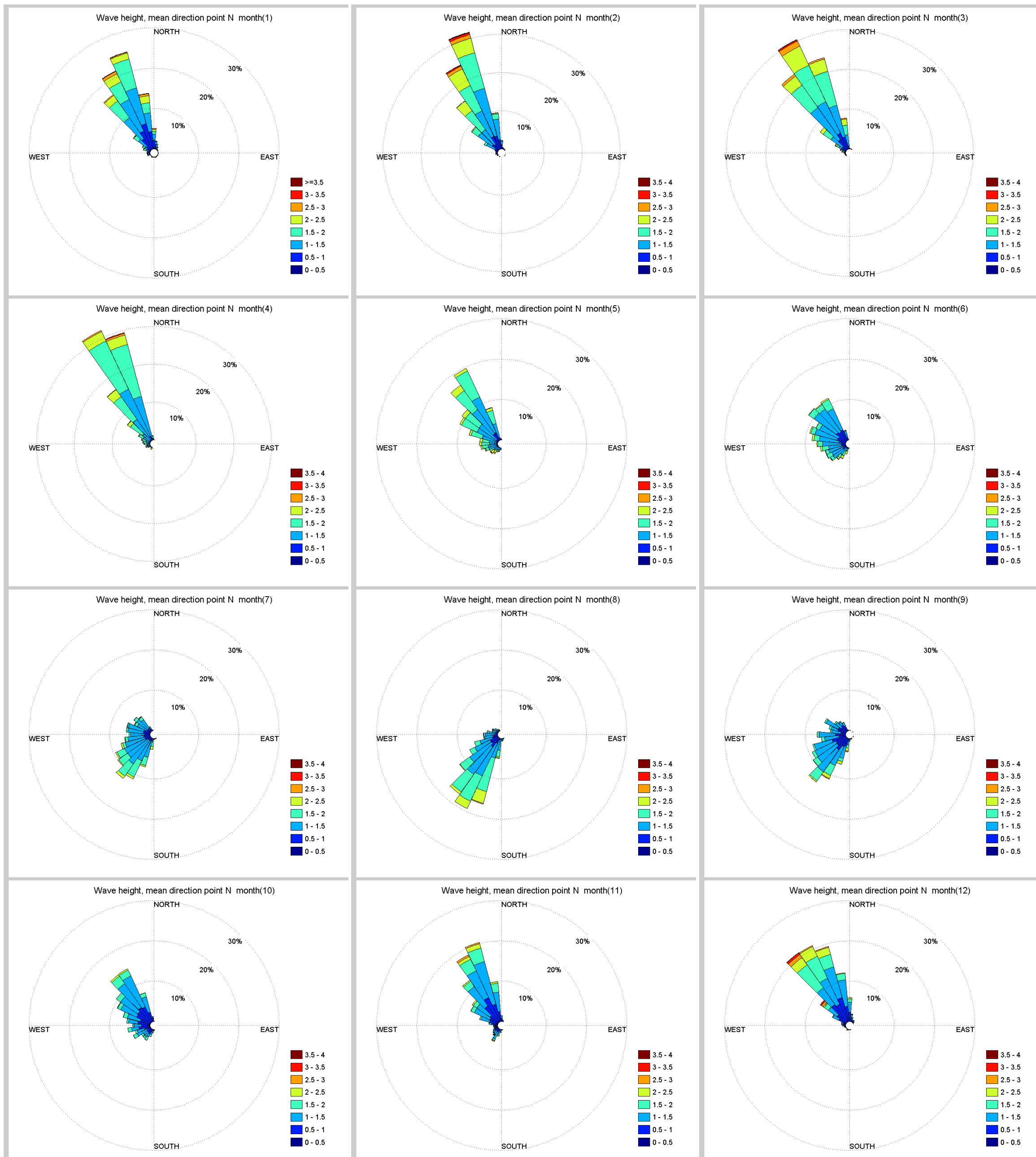

Figure C-1: monthly wave roses for total wave height, principal wave direction

Monthly wave roses for significant swell wave height point N, principal wave direction.

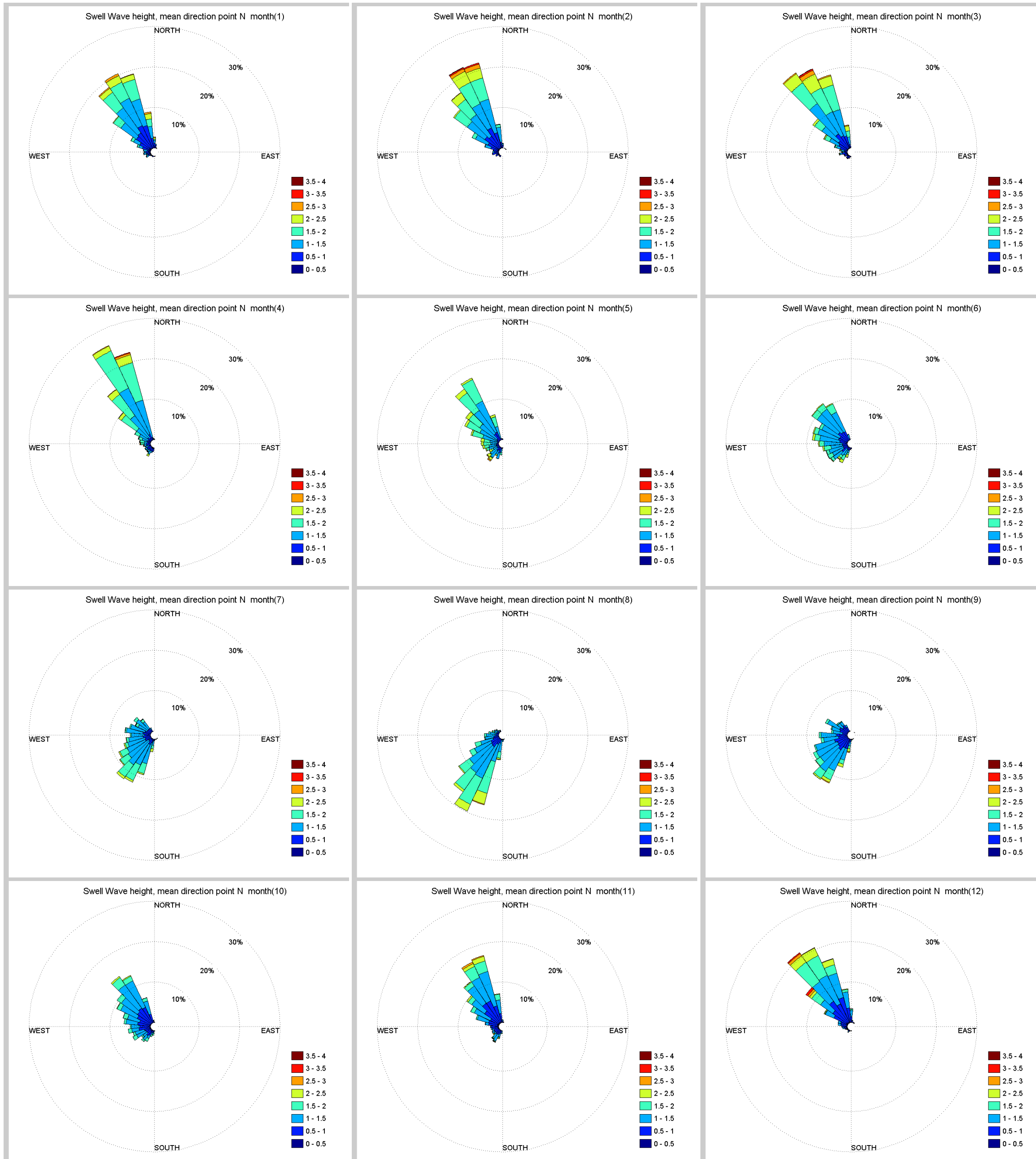

Figure C-2: Monthly wave roses for swell waves, principal wave direction

Monthly wave roses for total significant wave height, peak direction.

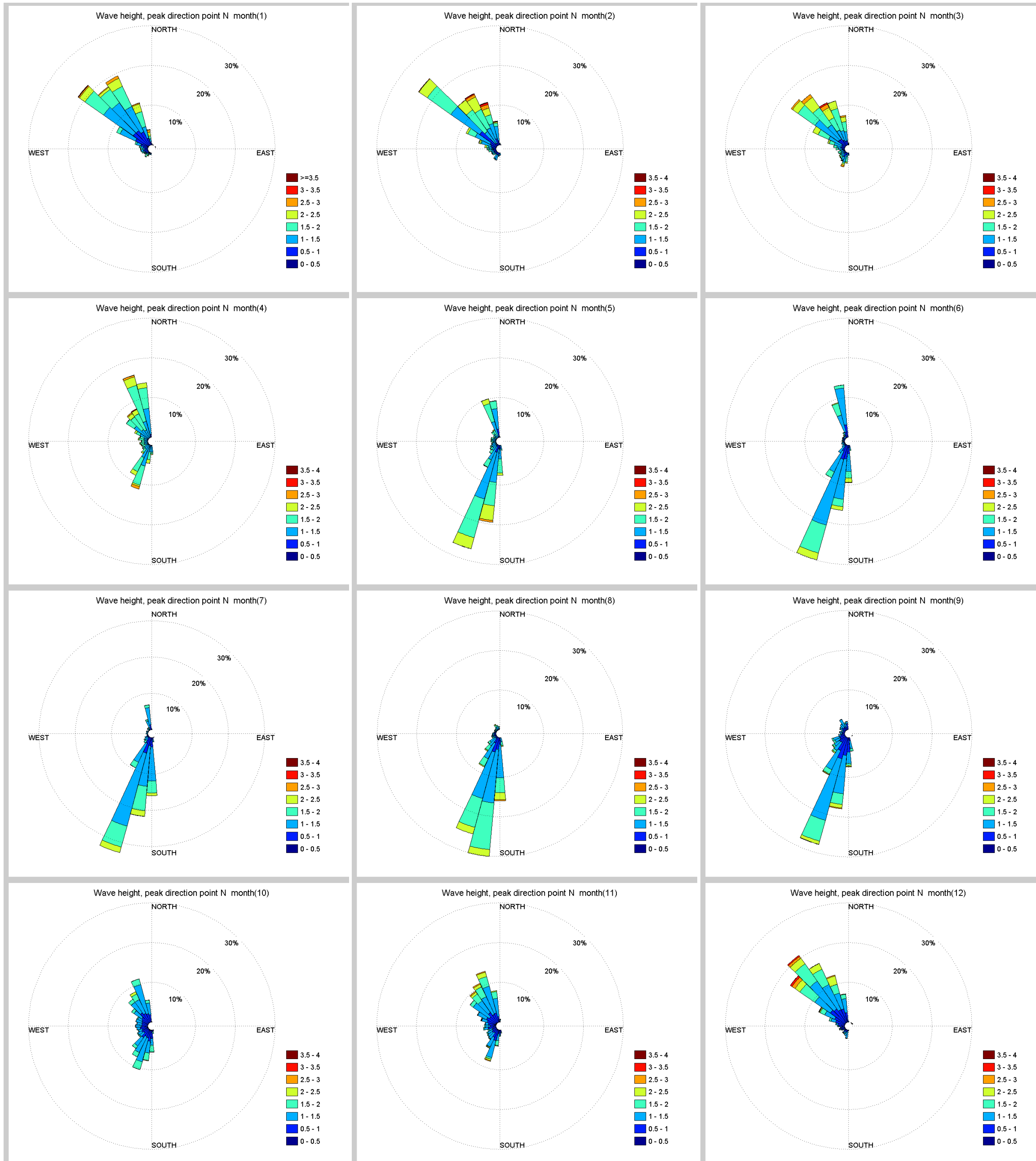

Figure C-3: Monthly wave roses for total wave height, peak direction

Monthly wave roses for significant swell wave height, peak direction.

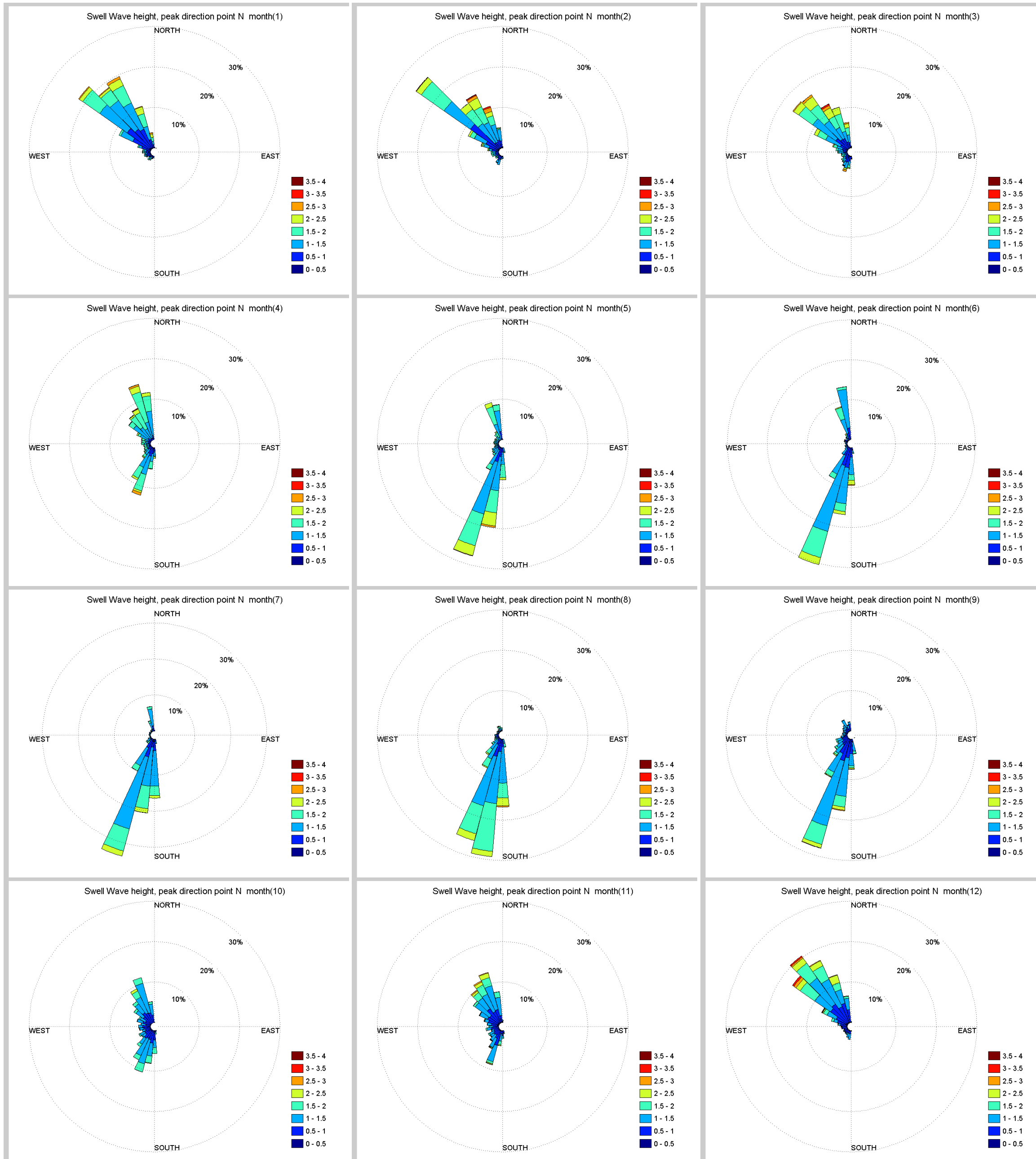

Figure C-4: Monthly wave roses for swell waves, peak direction

Annual wave roses for total significant wave height, principal wave direction.

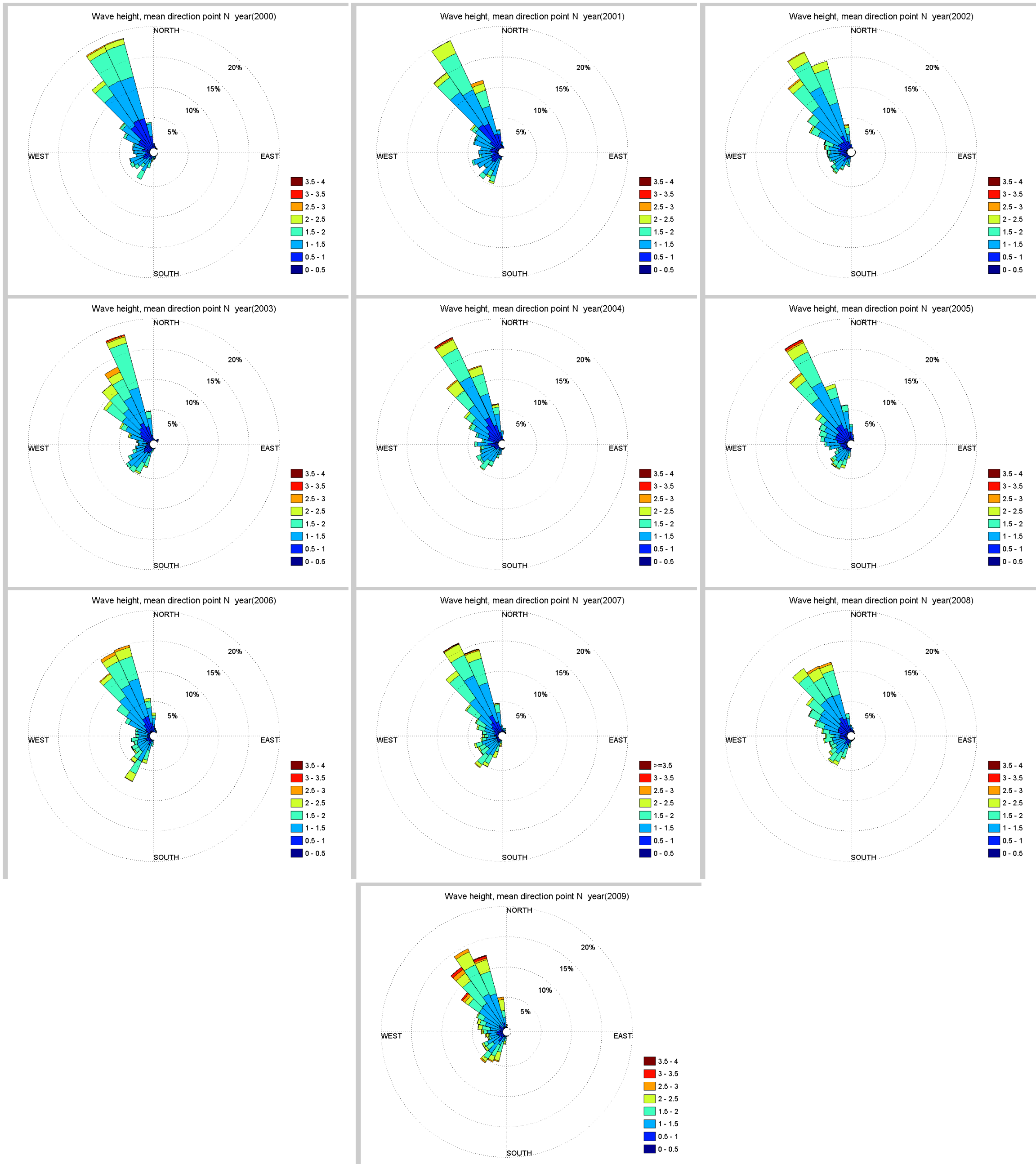

Figure C-5: Annual wave roses for total wave height, principal wave direction

Annual wave roses for significant swell wave height, principal wave direction.

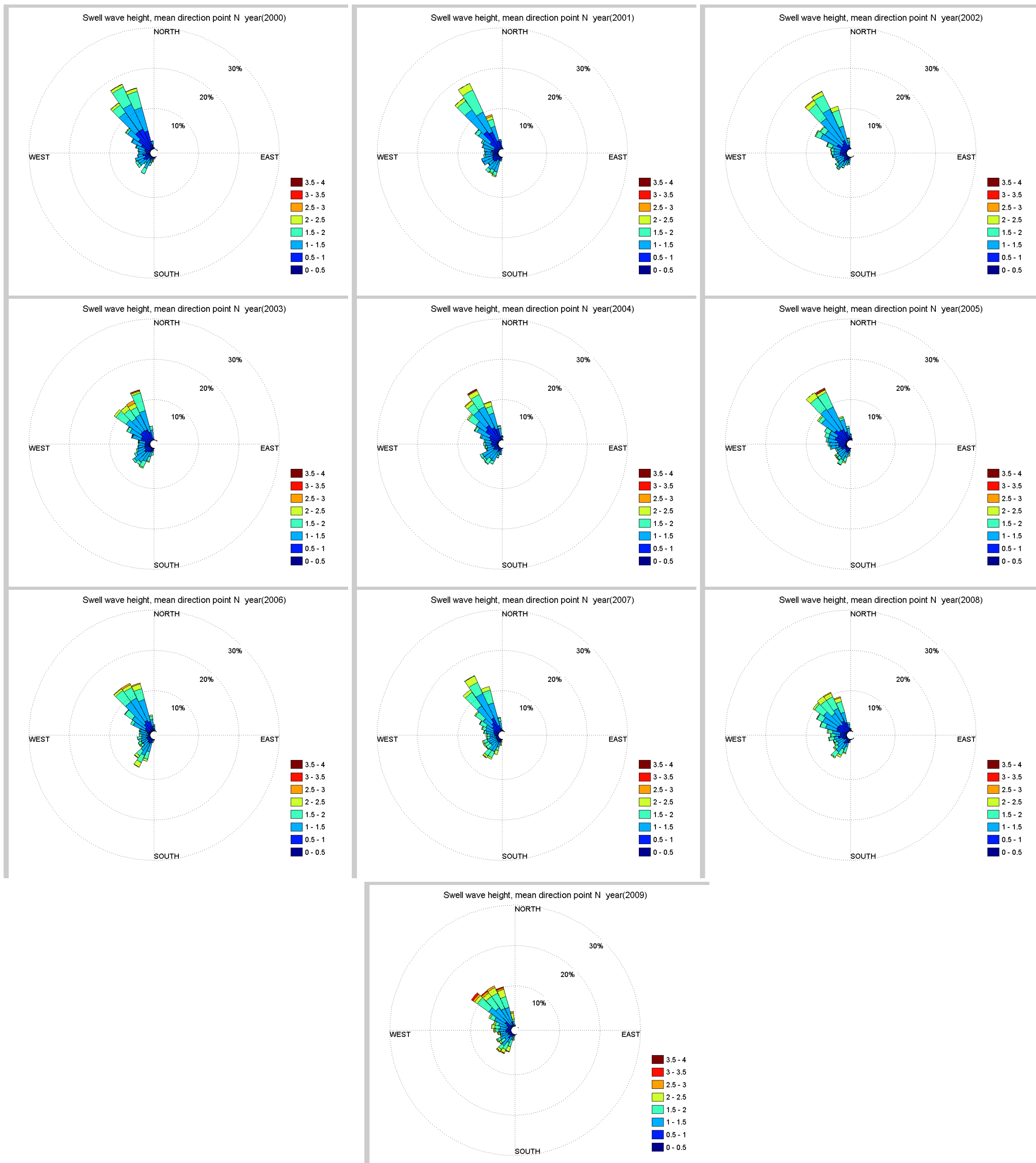

Figure C-6: Annual wave roses for swell waves, principal wave direction

Annual wave roses for total significant wave height, peak direction.

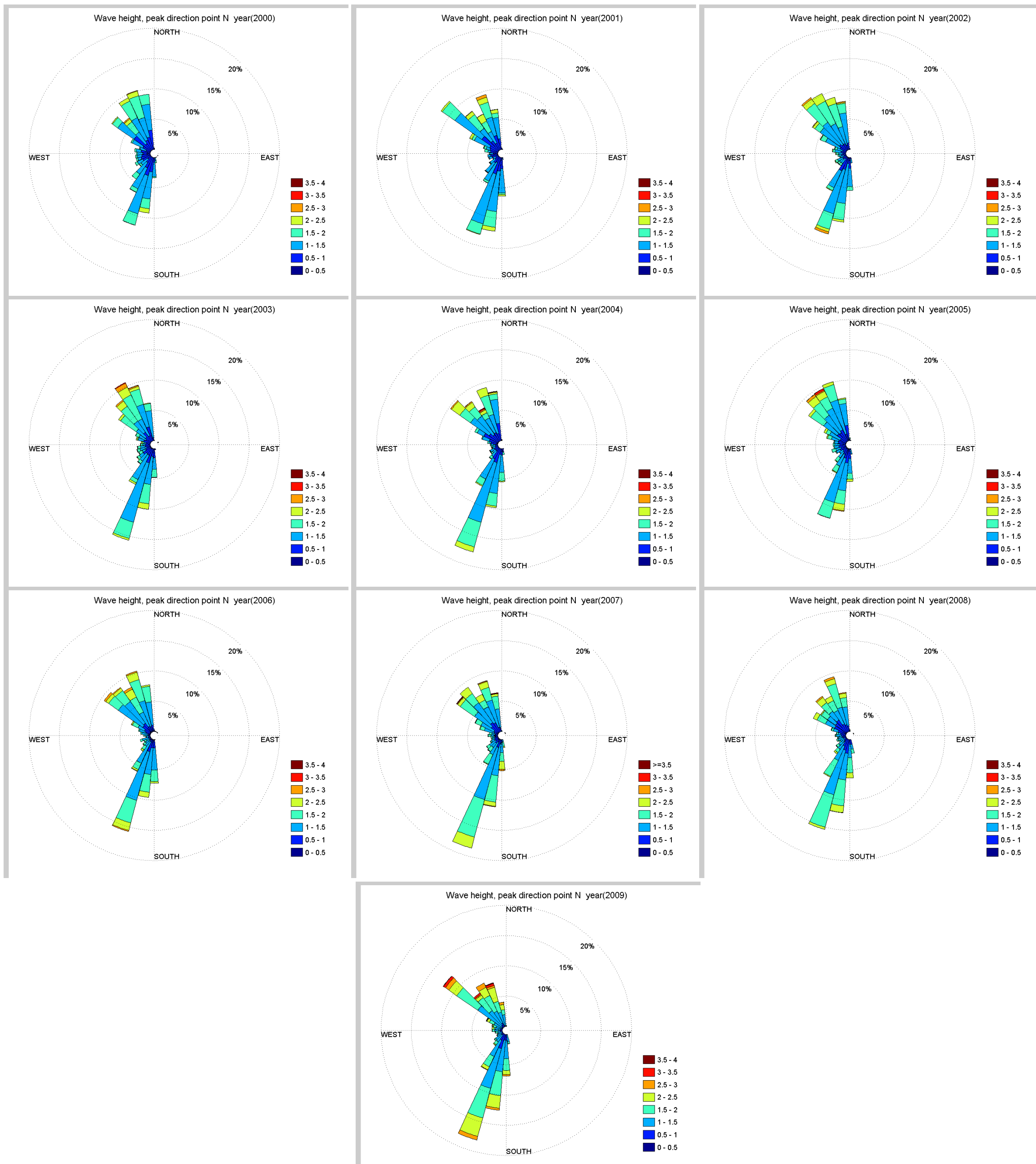

Figure C-7: Annual wave roses for total wave height, peak direction

Annual wave roses for significant swell wave height, peak direction.

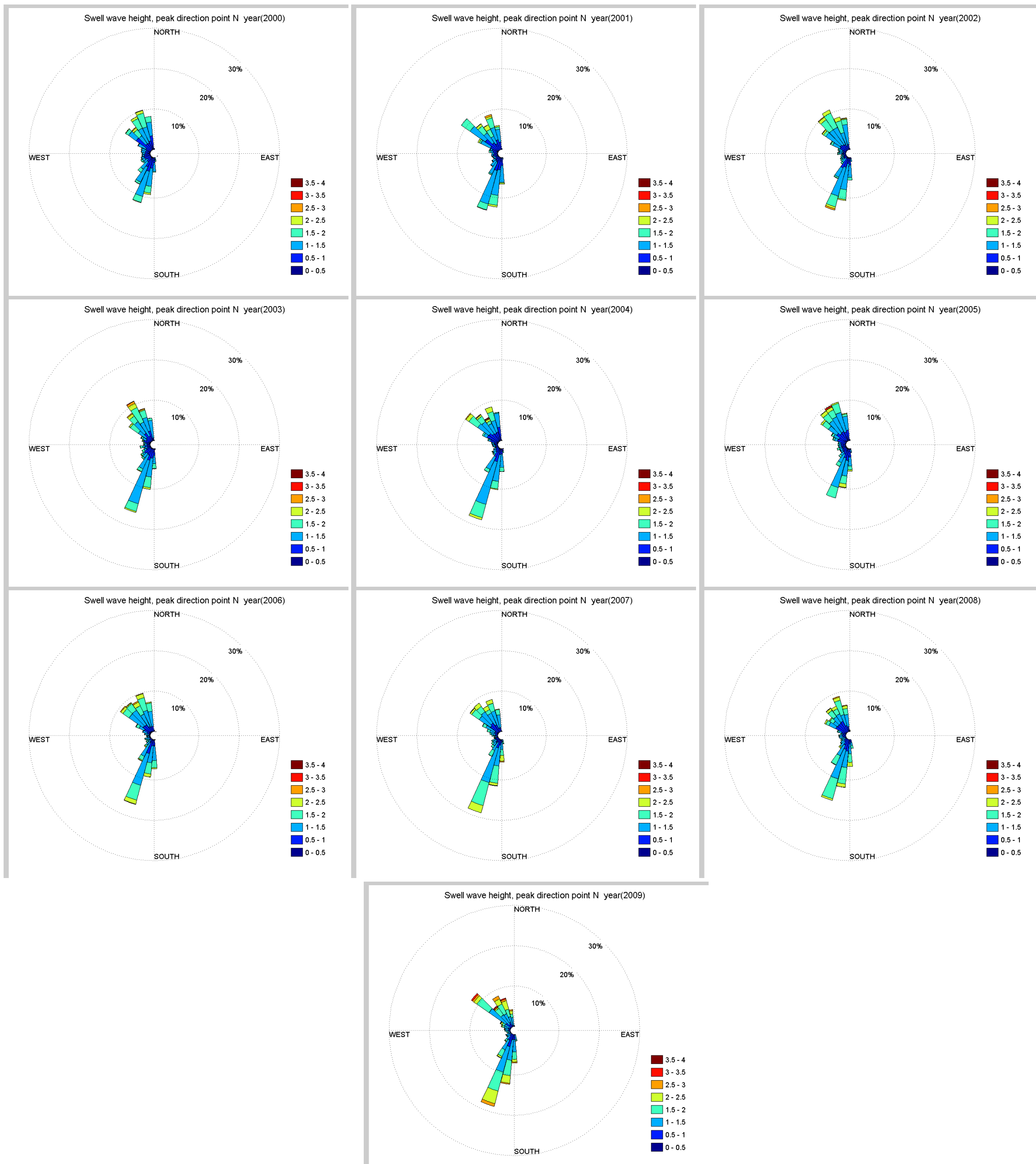

Figure C-8: Annual wave roses for swell waves, peak direction

Monthly wave roses for significant sea wave height, principal wave direction.

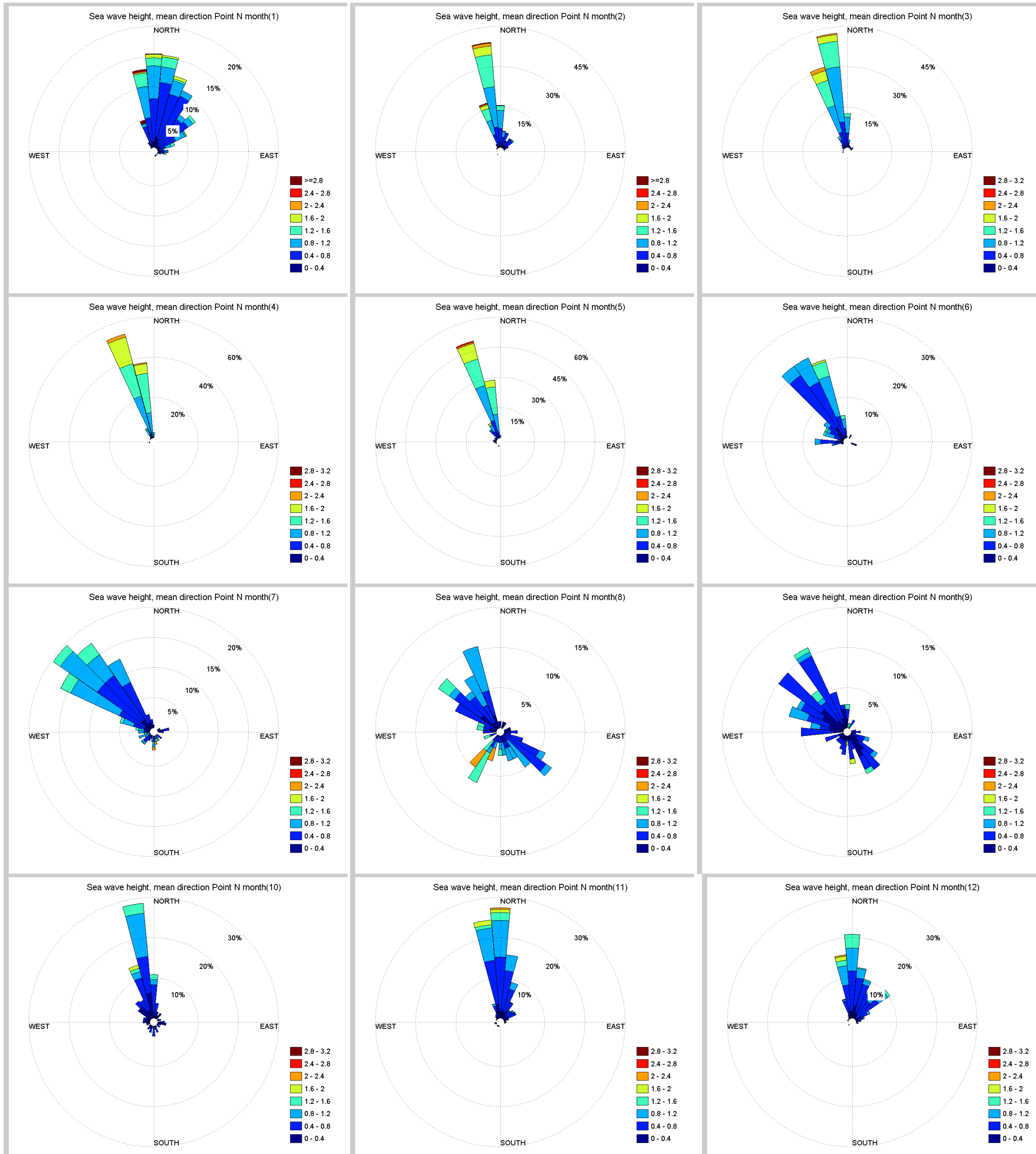

Figure C-9: Monthly wave roses for sea waves, principal wave direction

Monthly wave roses for significant sea wave height, peak direction.

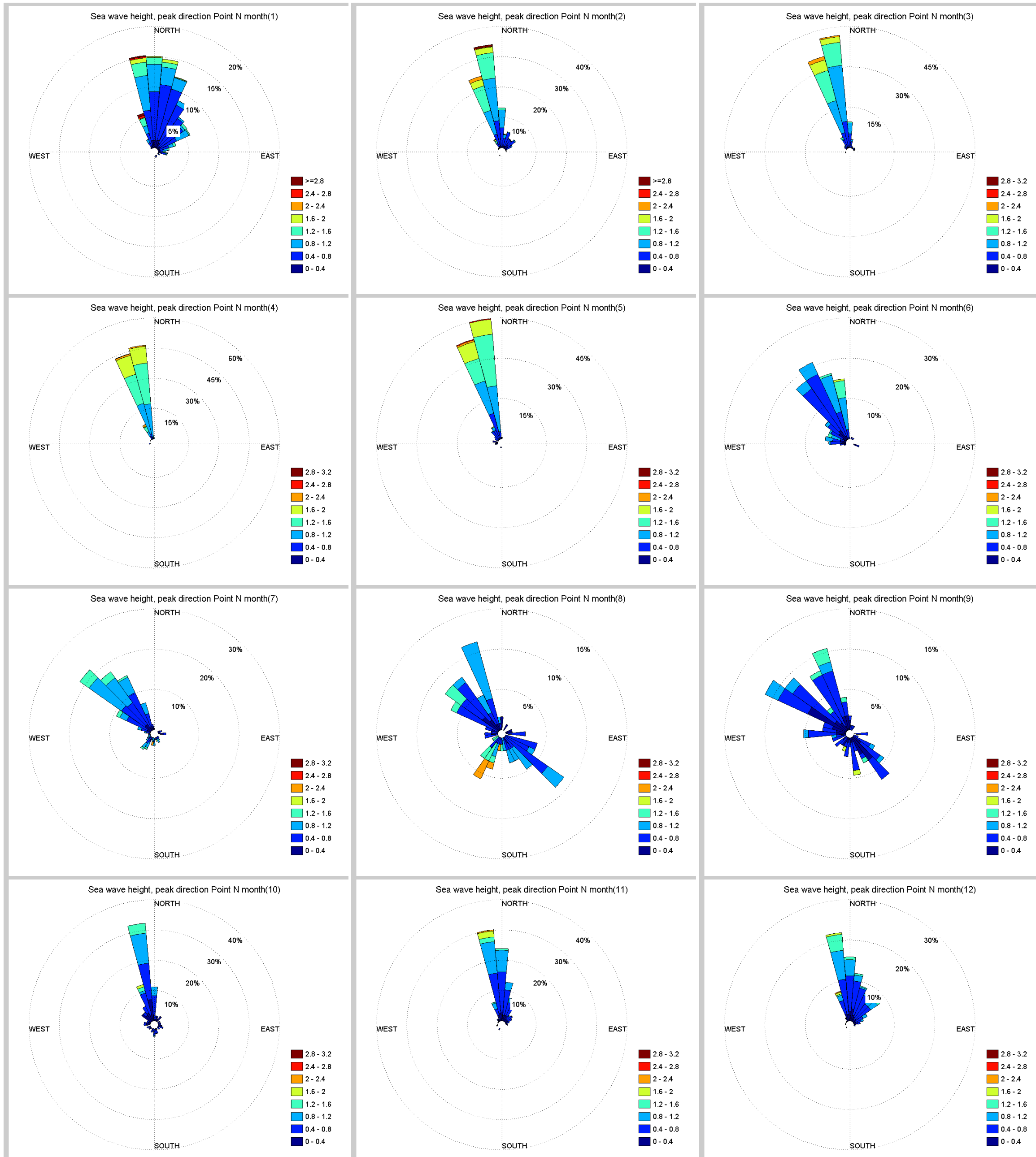

Figure C-10: monthly wave roses for sea waves, peak direction

Annual wave roses for significant sea wave height, principal wave direction.

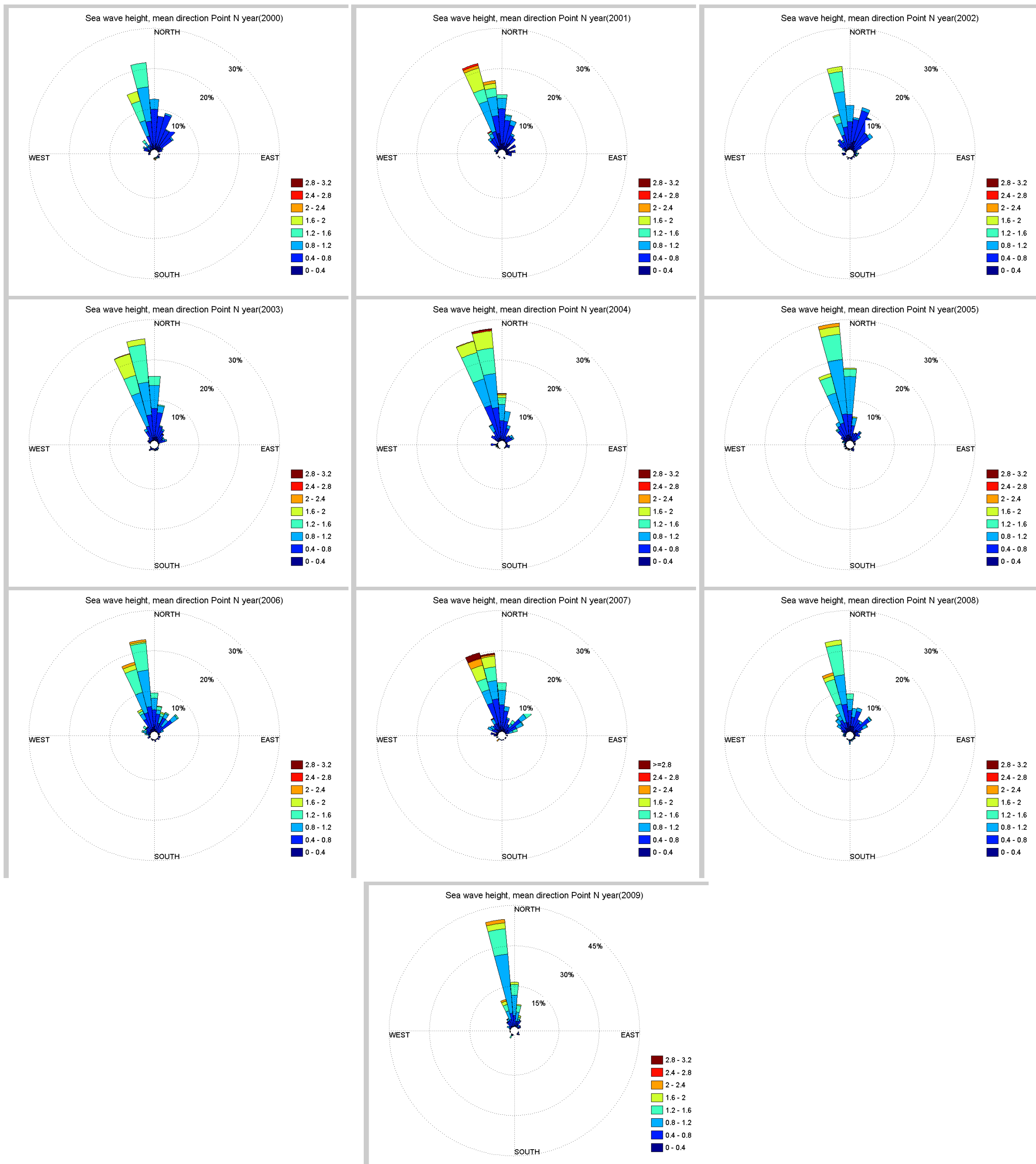

Figure C-11: Annual wave roses for sea waves, principal wave direction

Annual wave roses for significant sea wave height, peak direction.

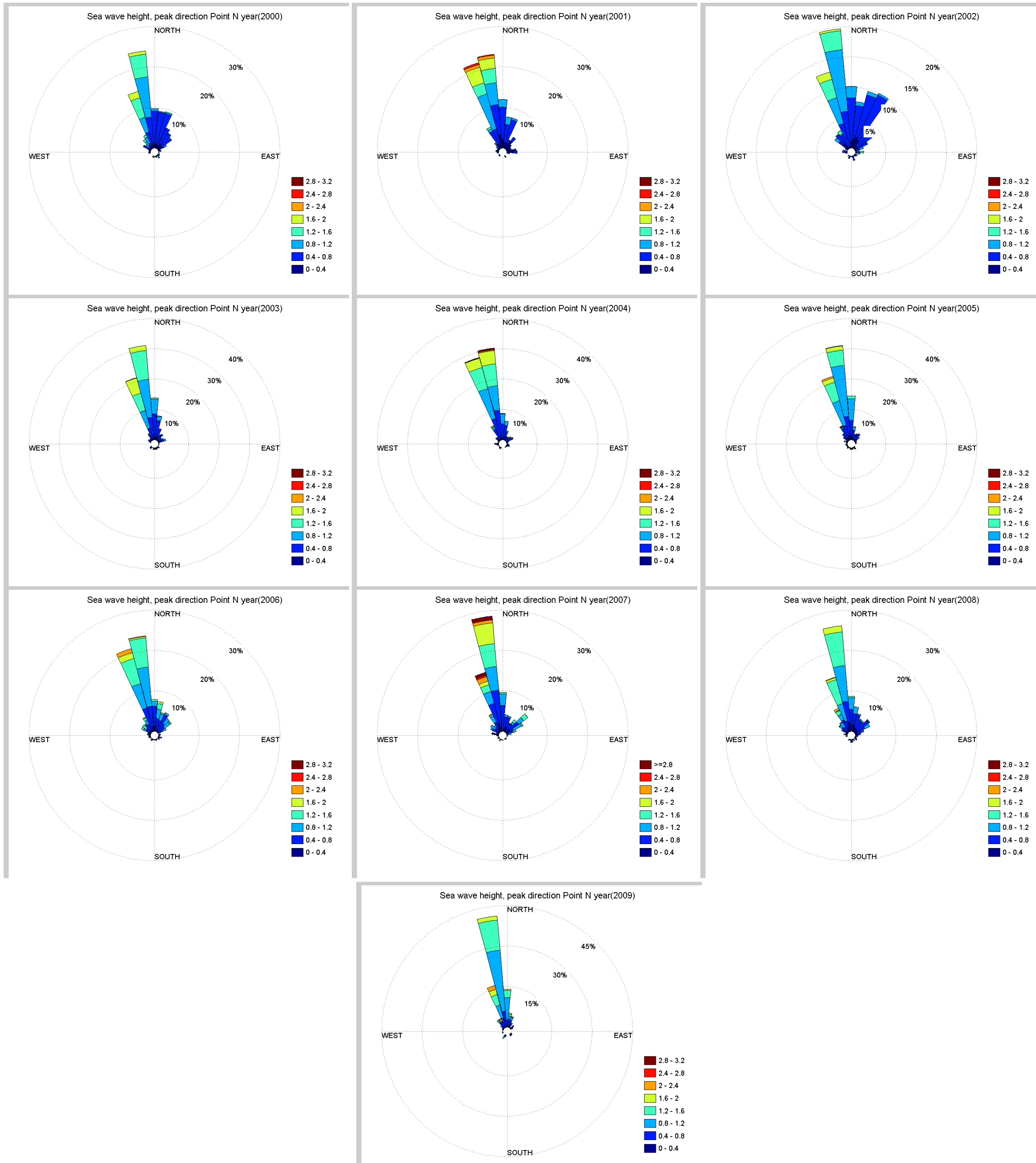

Figure C-12: Annual wave roses for sea wave height, peak direction

APPENDIX D: SWAN RESULTS

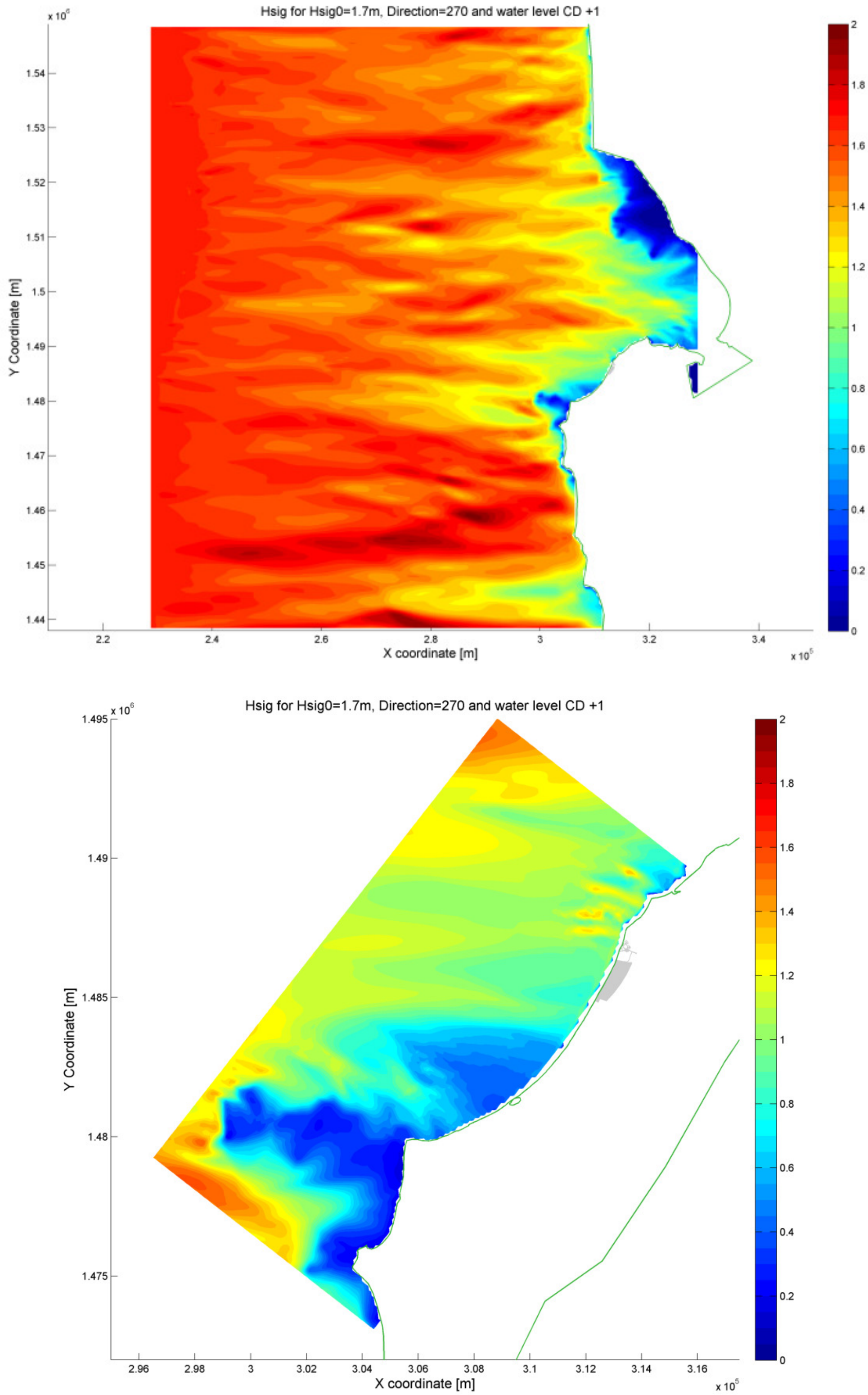

Figure D--1: Significant wave height for western waves

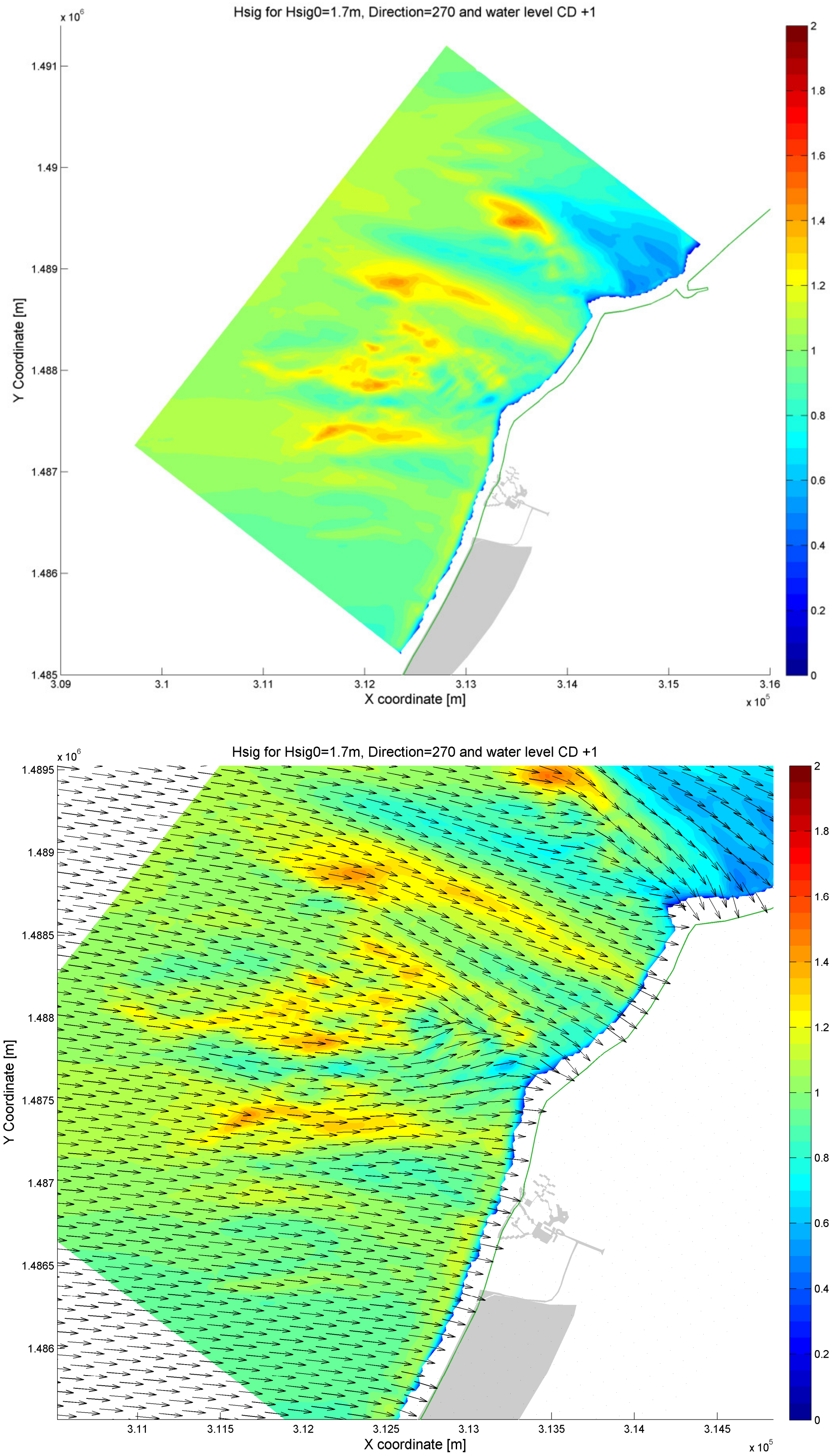

Figure D-2: Significant wave height and refractive pattern inside the reef area for western waves

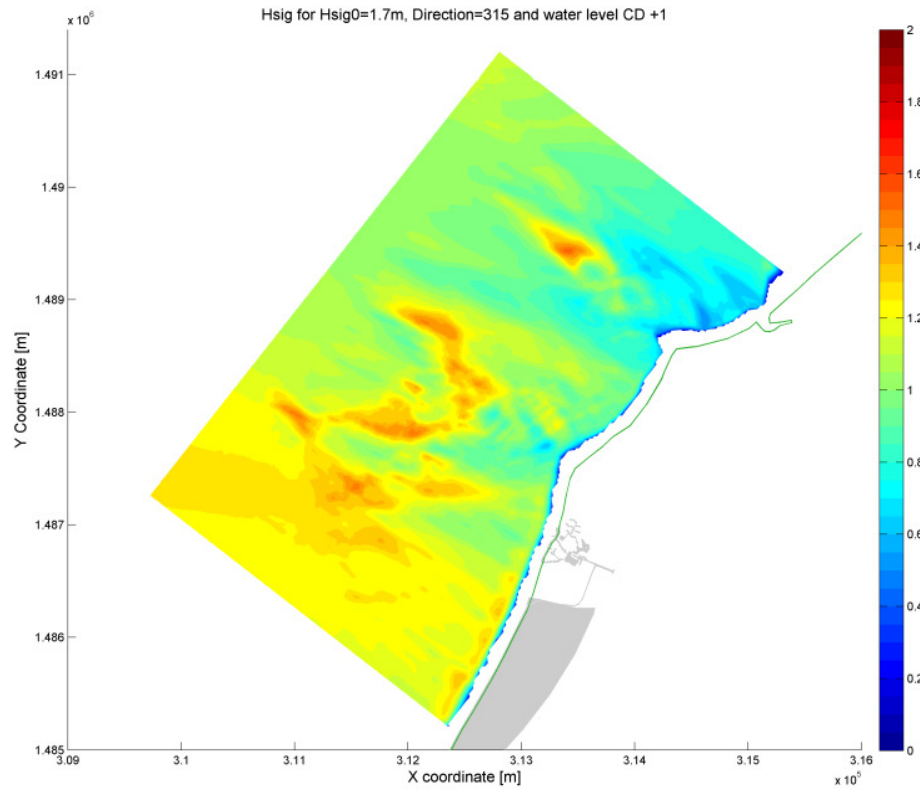

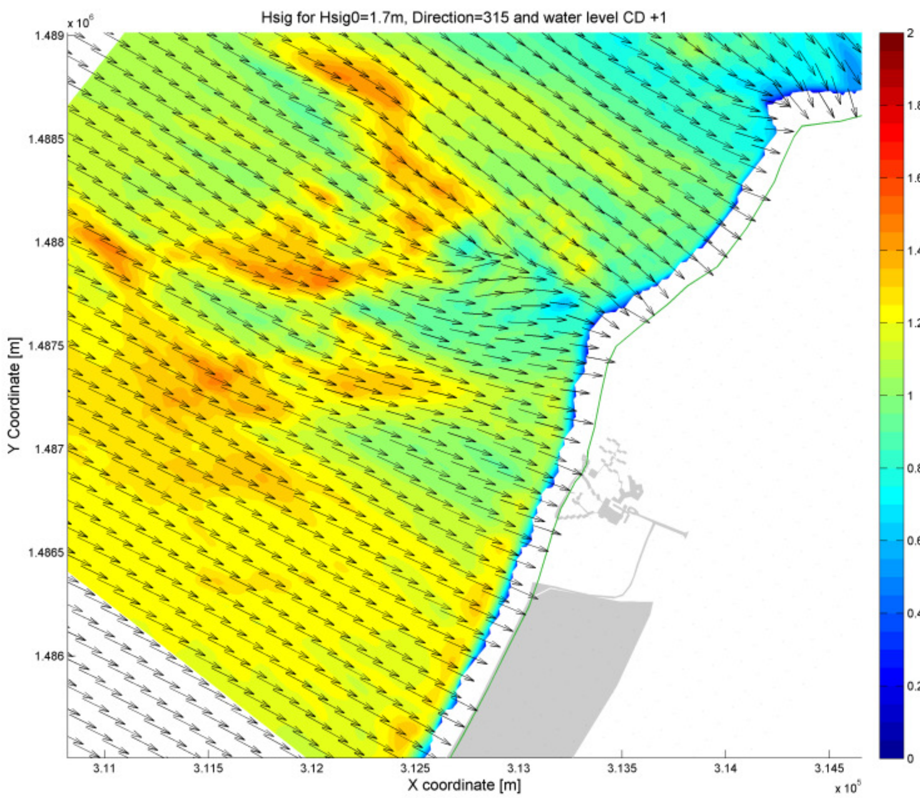

Figure D-3: Significant wave height and refractive pattern inside the reef area for north-western waves

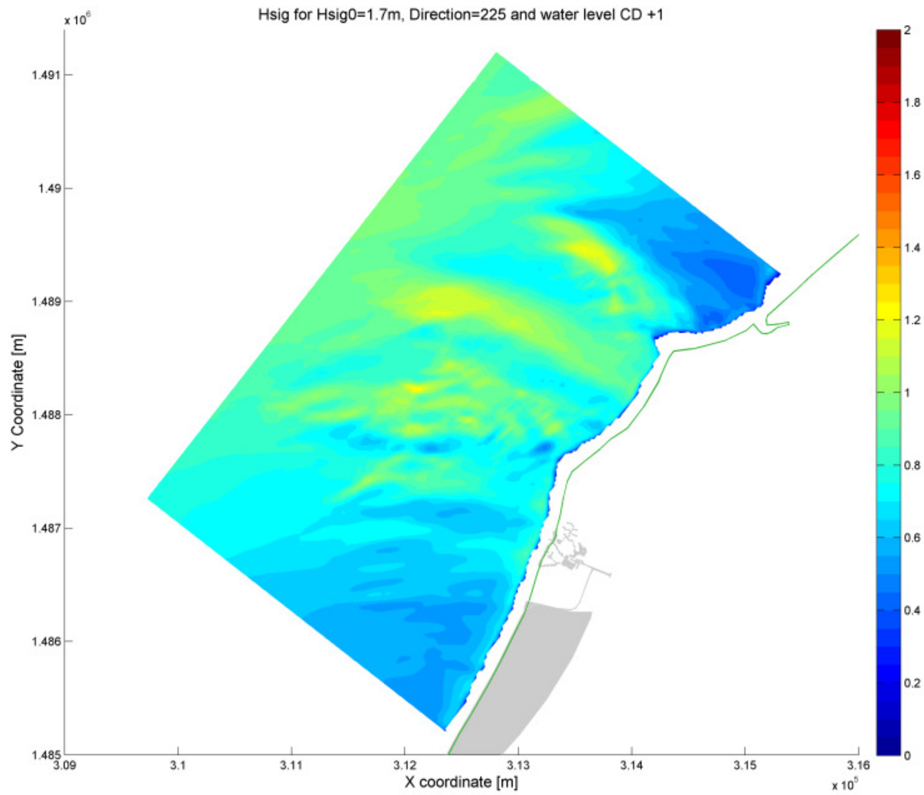

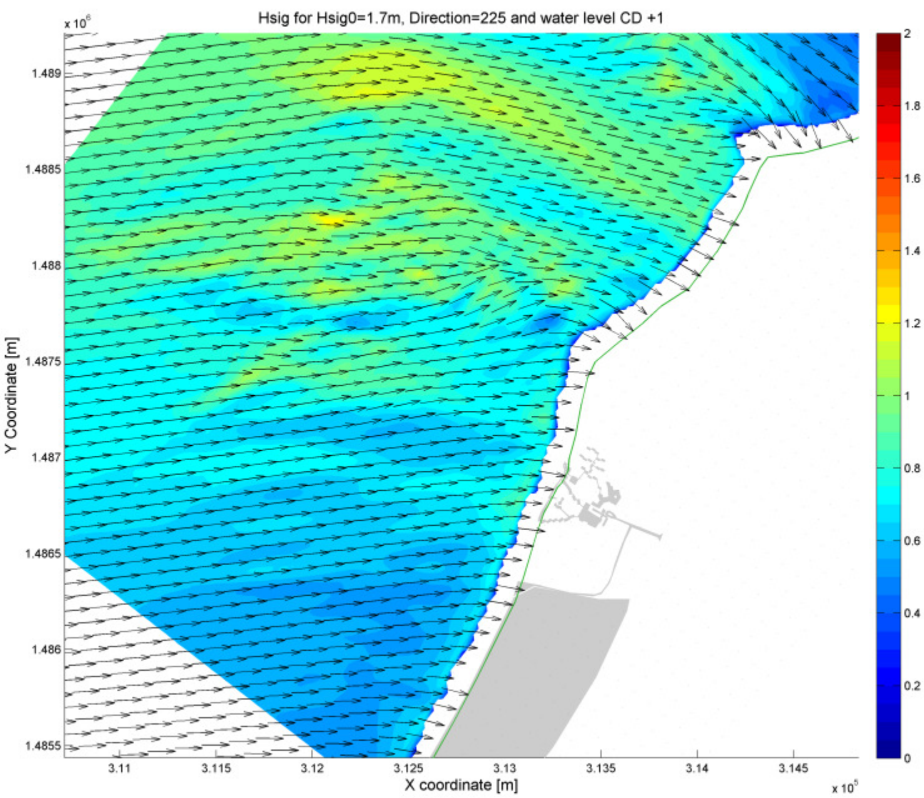

Figure D-4: Significant wave height and refractive pattern inside the reef area for south-western waves

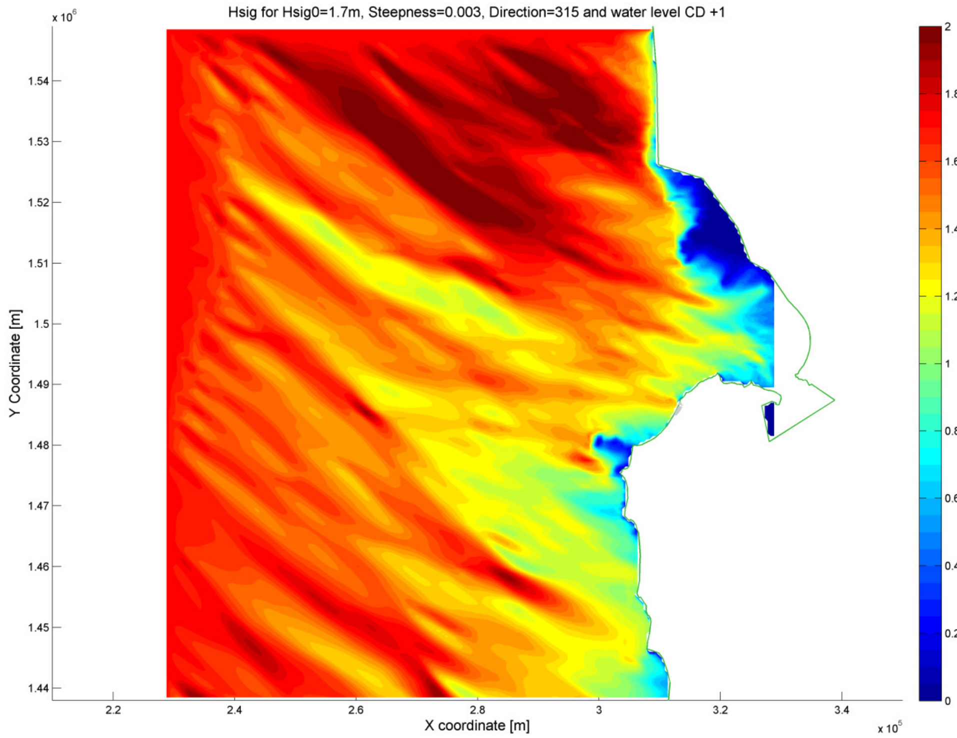

Figure D-5: Significant wave height for north-western waves with steepness = 0.003

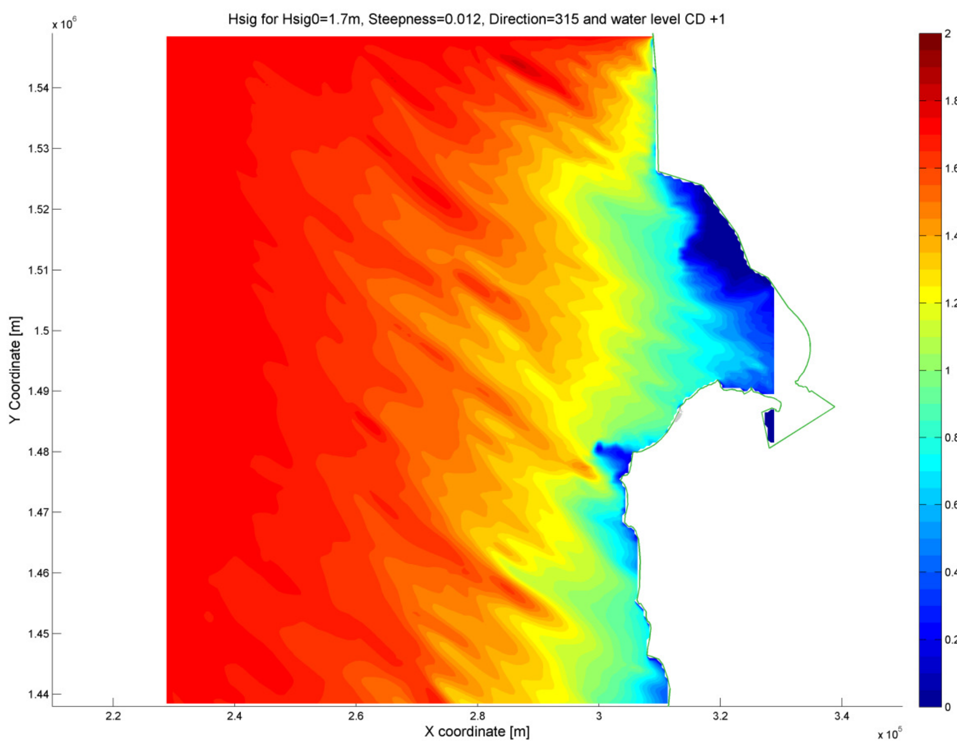

Figure D-6: Significant wave height for north-western waves with steepness = 0.012

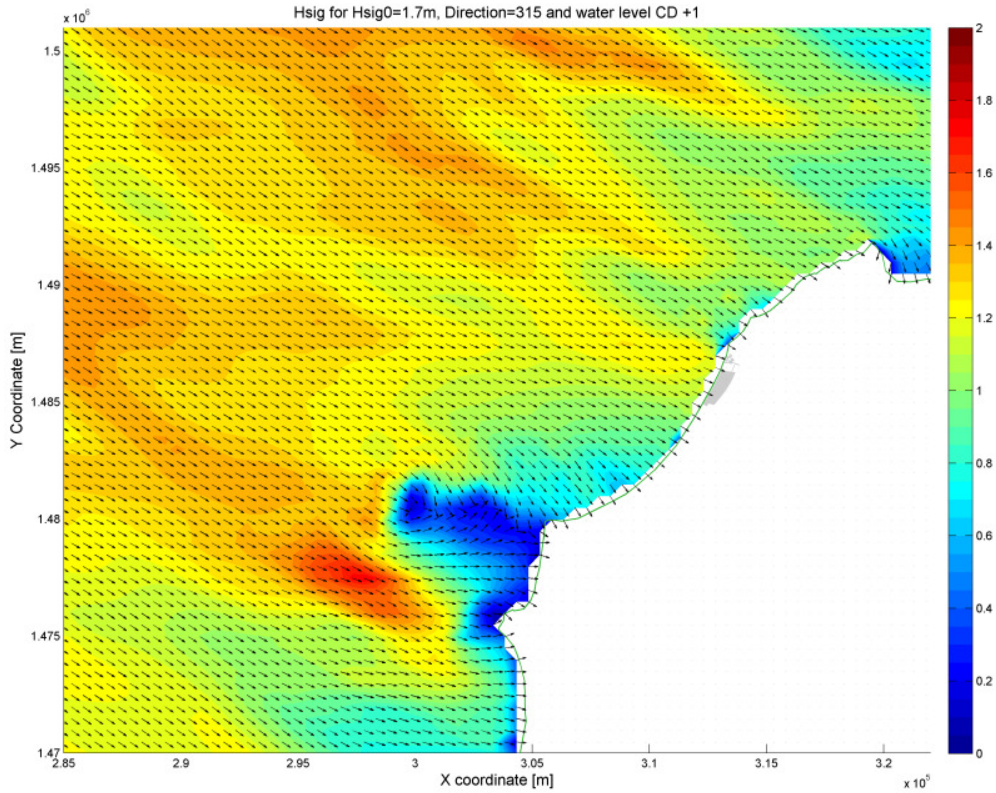

Figure D-7: Refractive pattern for north-western waves

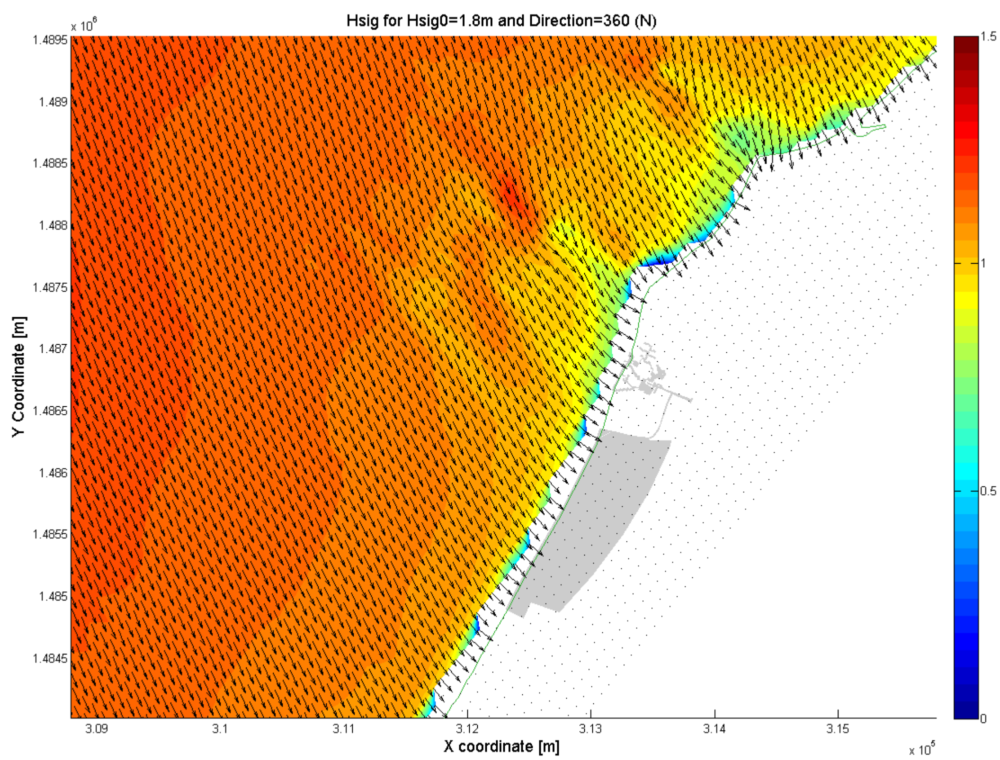

Figure D-8: Refractive pattern for wind-generated waves inside the reef area

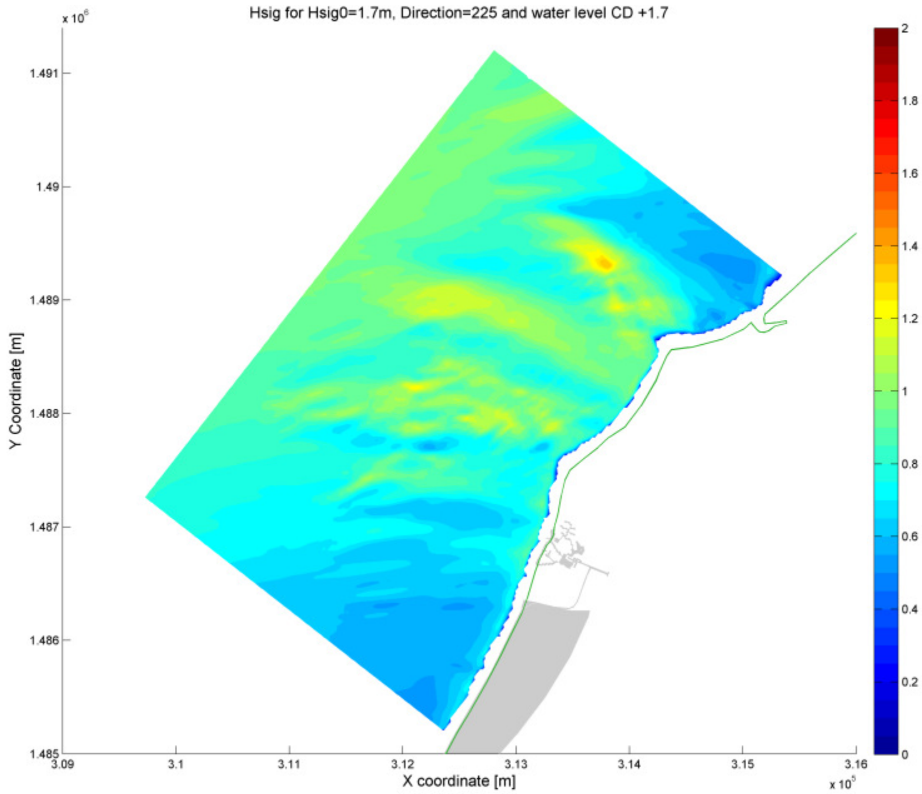

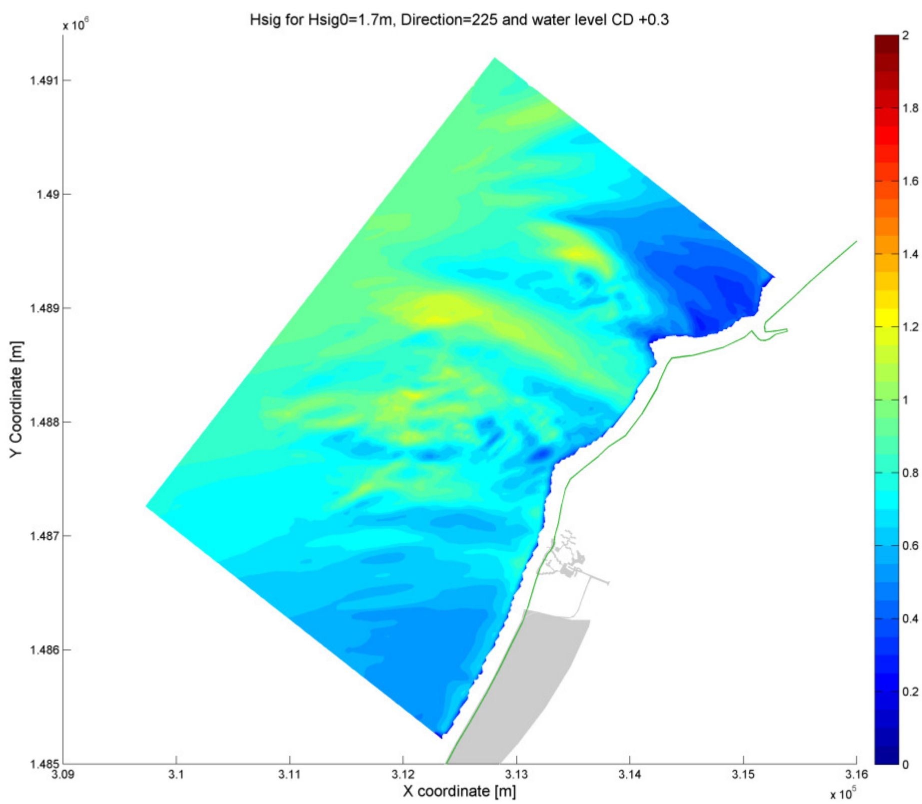

Figure D-9: Significant wave high inside reef area for high and low water level

APPENDIX E: REPORT FIGURES

Figure E-1 Aerial photograph of Senegambia area, 2003: before nourishment

Figure E-2 Aerial photograph of Senegambia area, 2004: after nourishment

Figure E-3 Aerial photograph of Senegambia area, February 2011

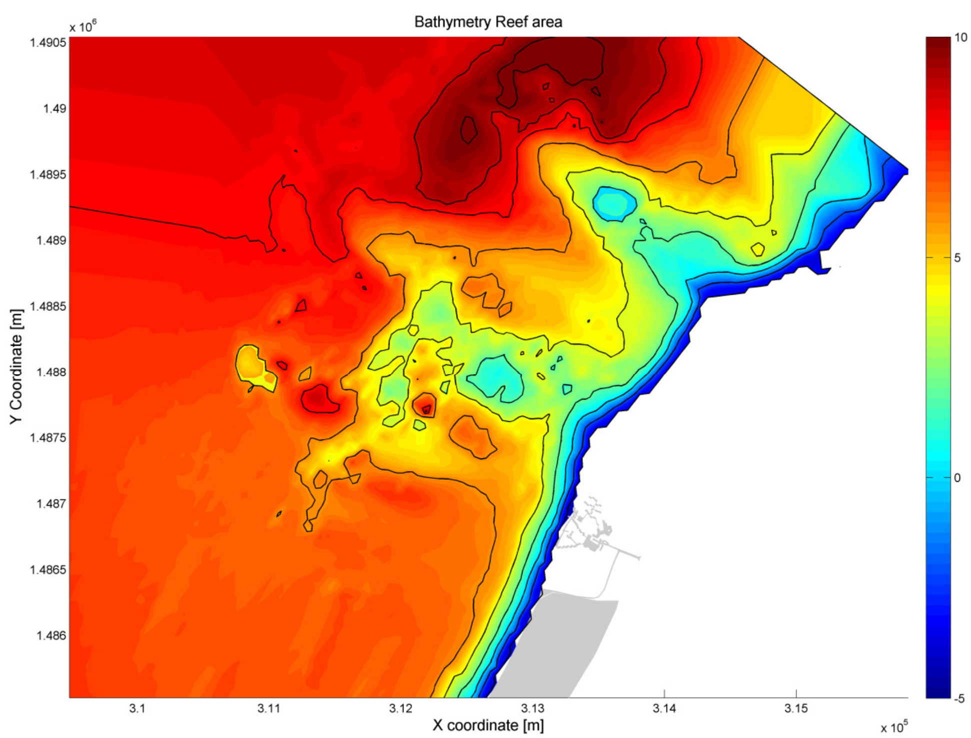

Figure E-4: Reef area Bathymetry

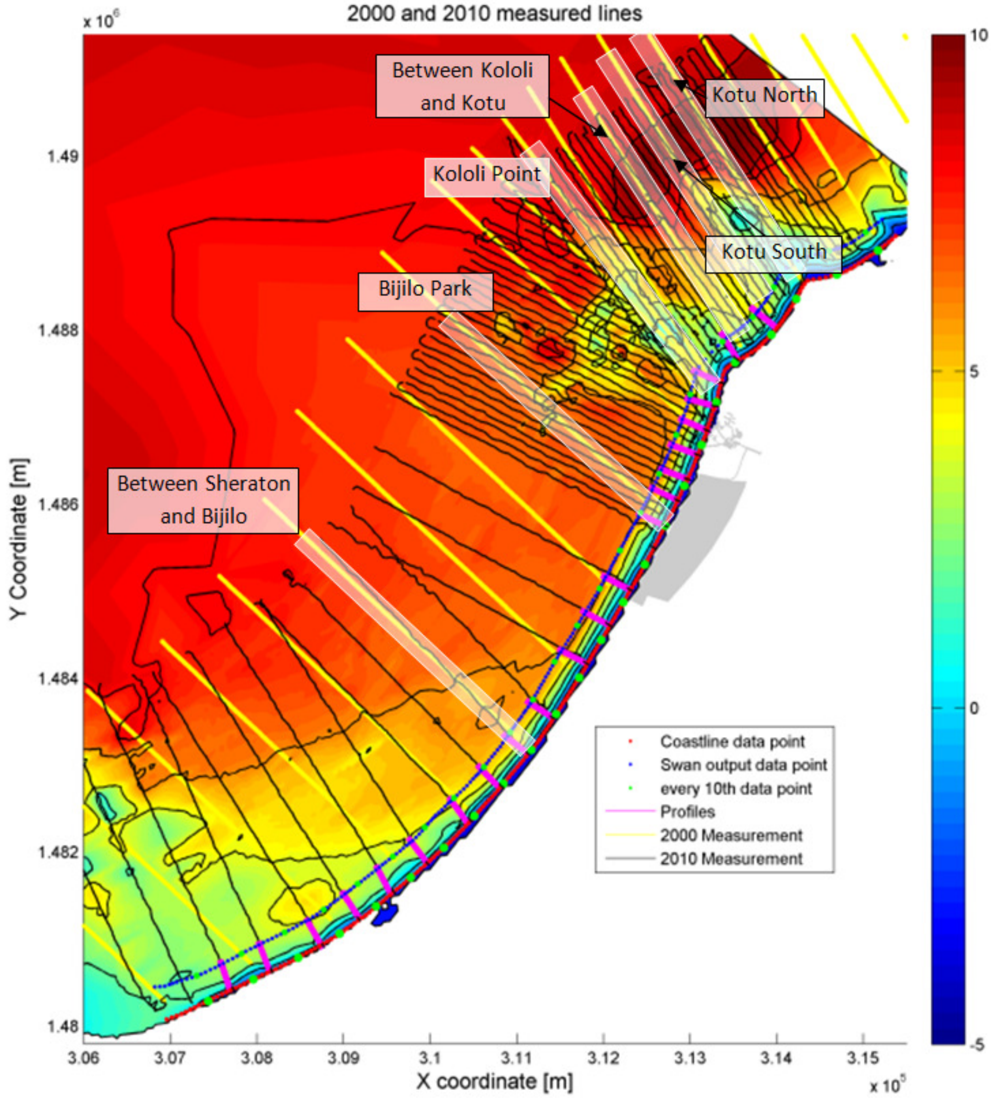

Figure E-5: Overview of 2000 and 2010 compared profiles

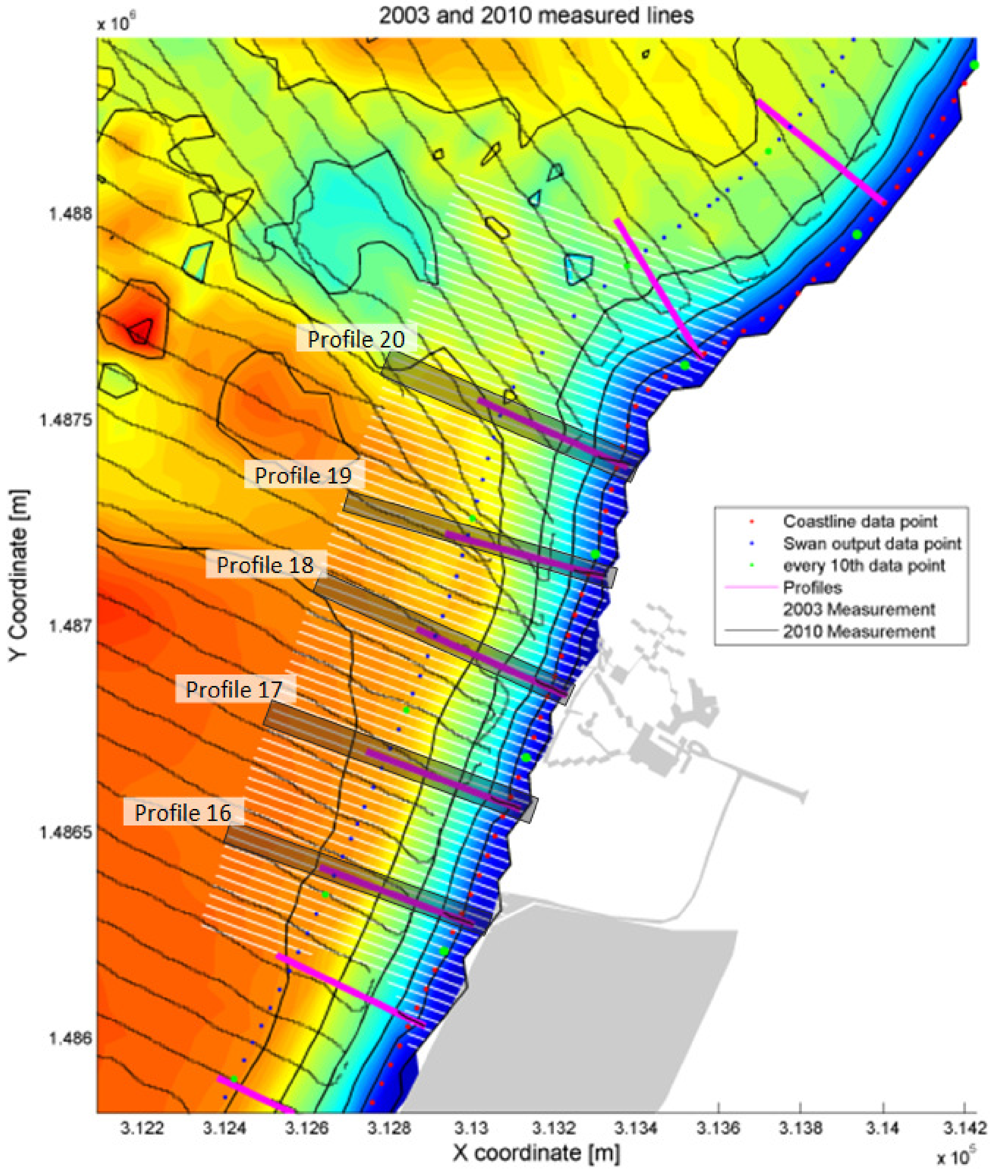

Figure E-6: Overview of 2003 and 2010 compared profiles

The profiles from 2000 and 2010 are shown in Figure E-7 for 4 locations along the coast:

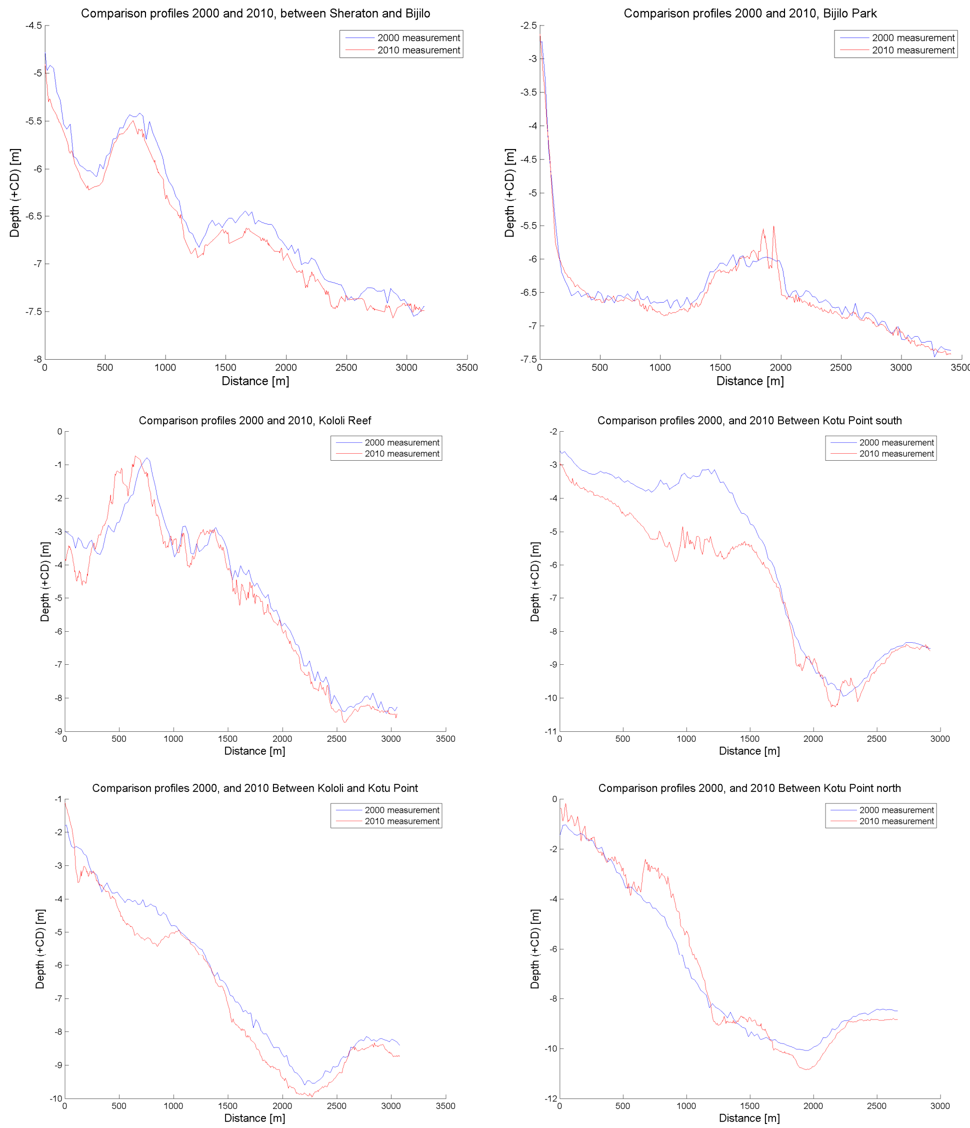

Figure E-7: Comparison of the 2000 and 2010 profiles

The profiles in from 2003 and 2010 in front of Senegambia are shown in Figure E-8:

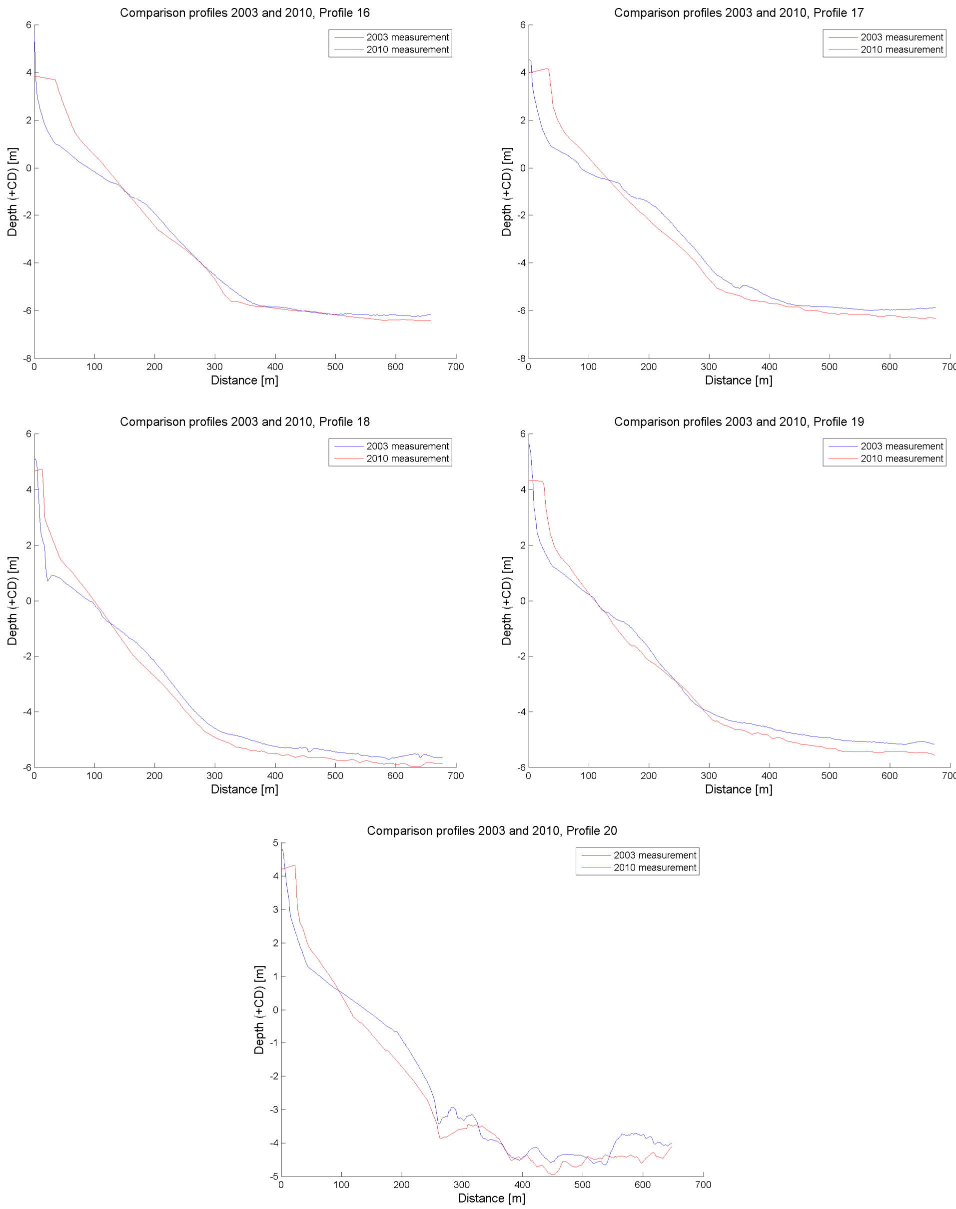

Figure E-8: Comparison of the 2003 and 2010 profiles

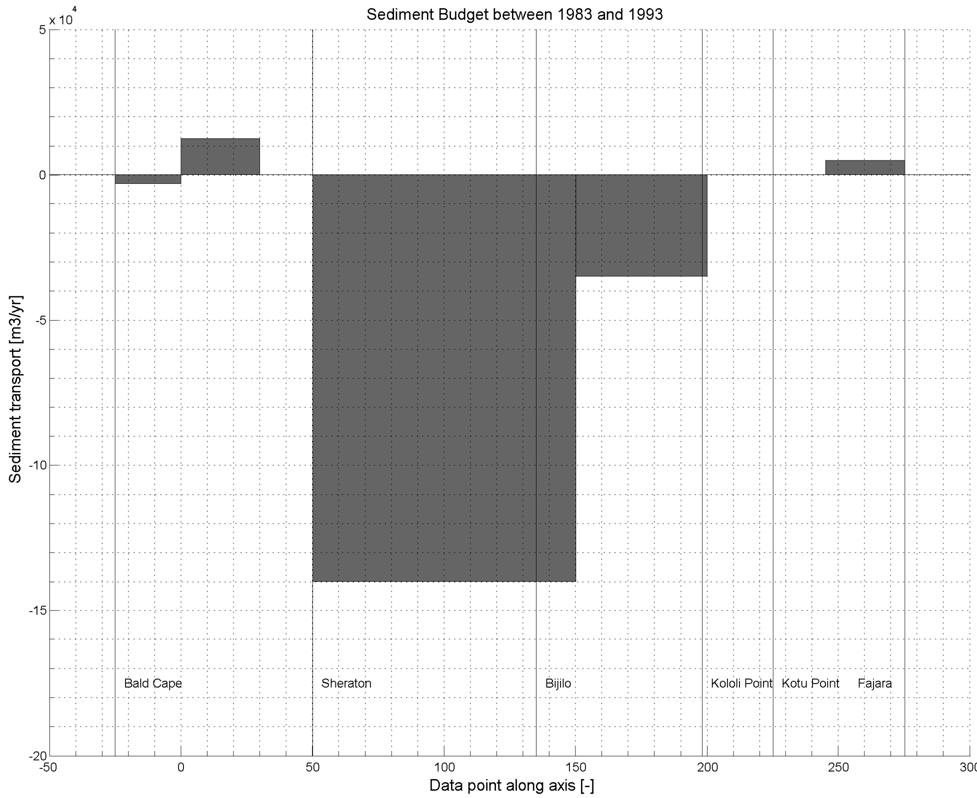

Figure E-9: Sediment budget for 1983 - 1993

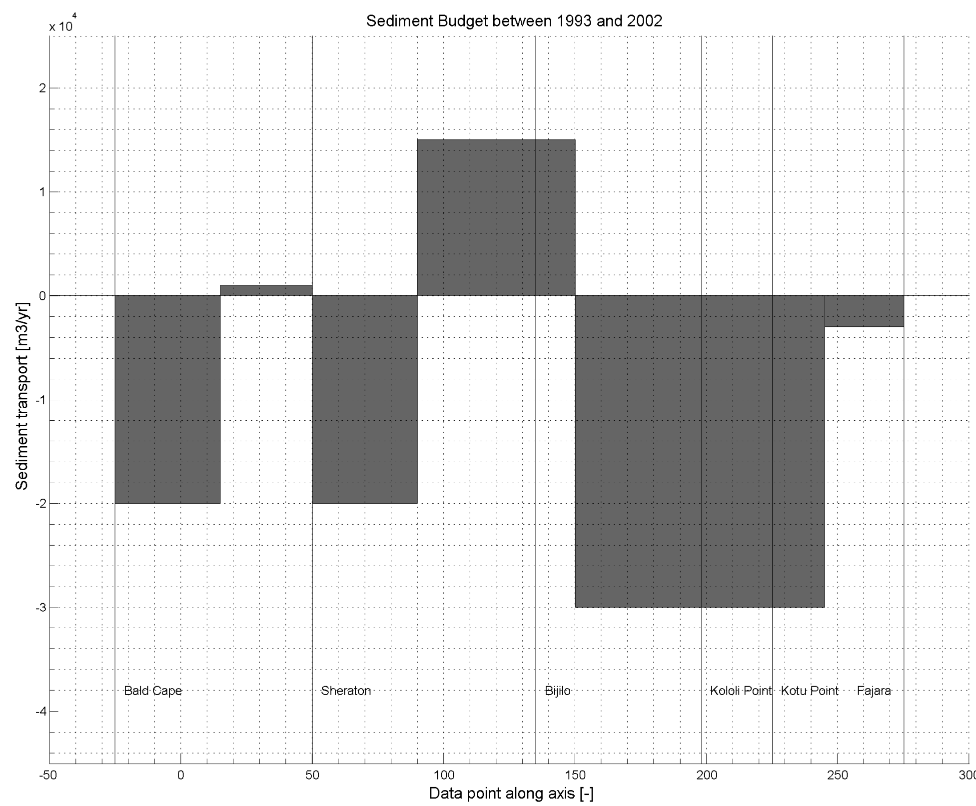

Figure E-10: Sediment budget for 1993 - 2002

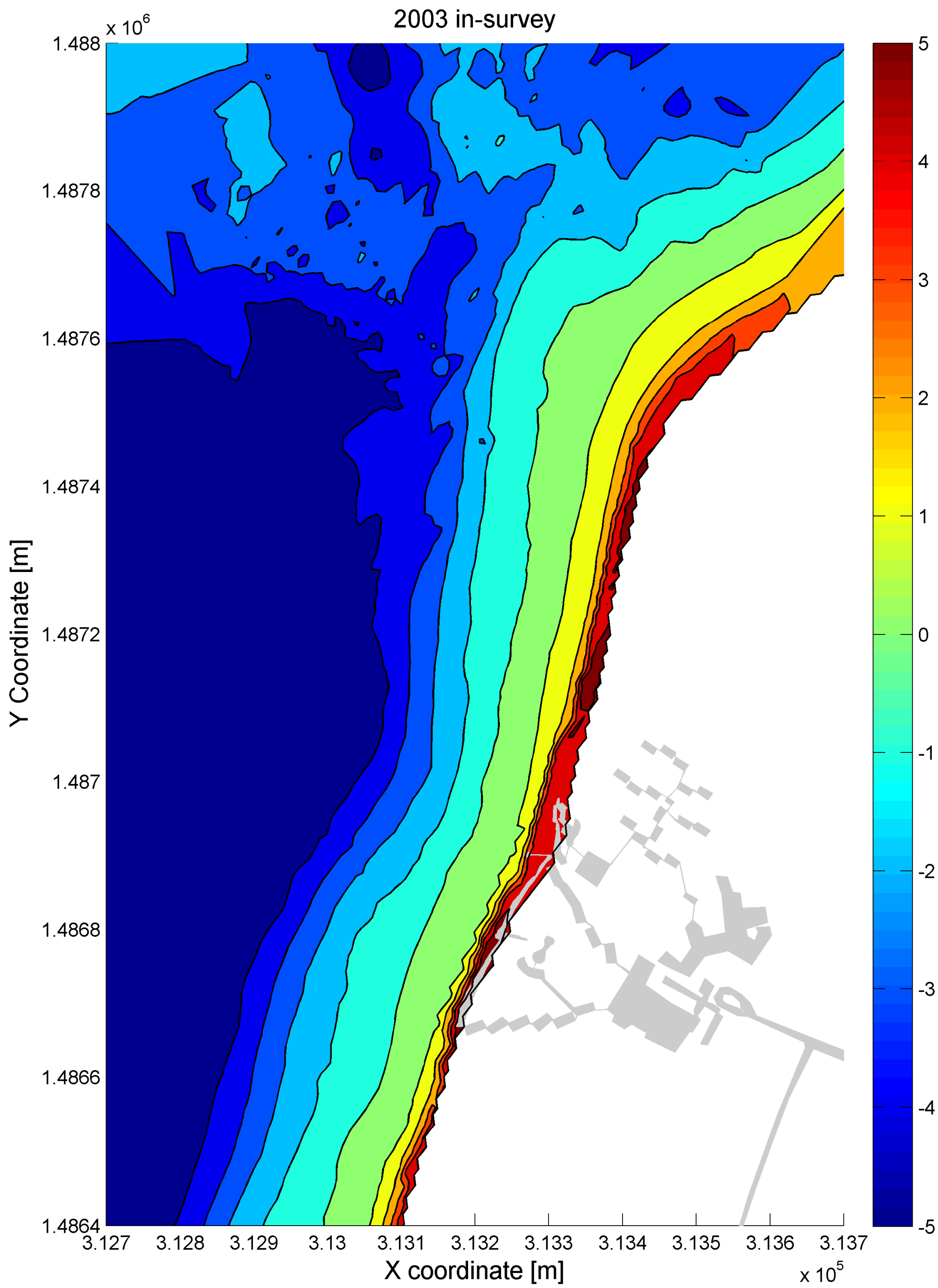

Figure E-11: 2003 in-survey

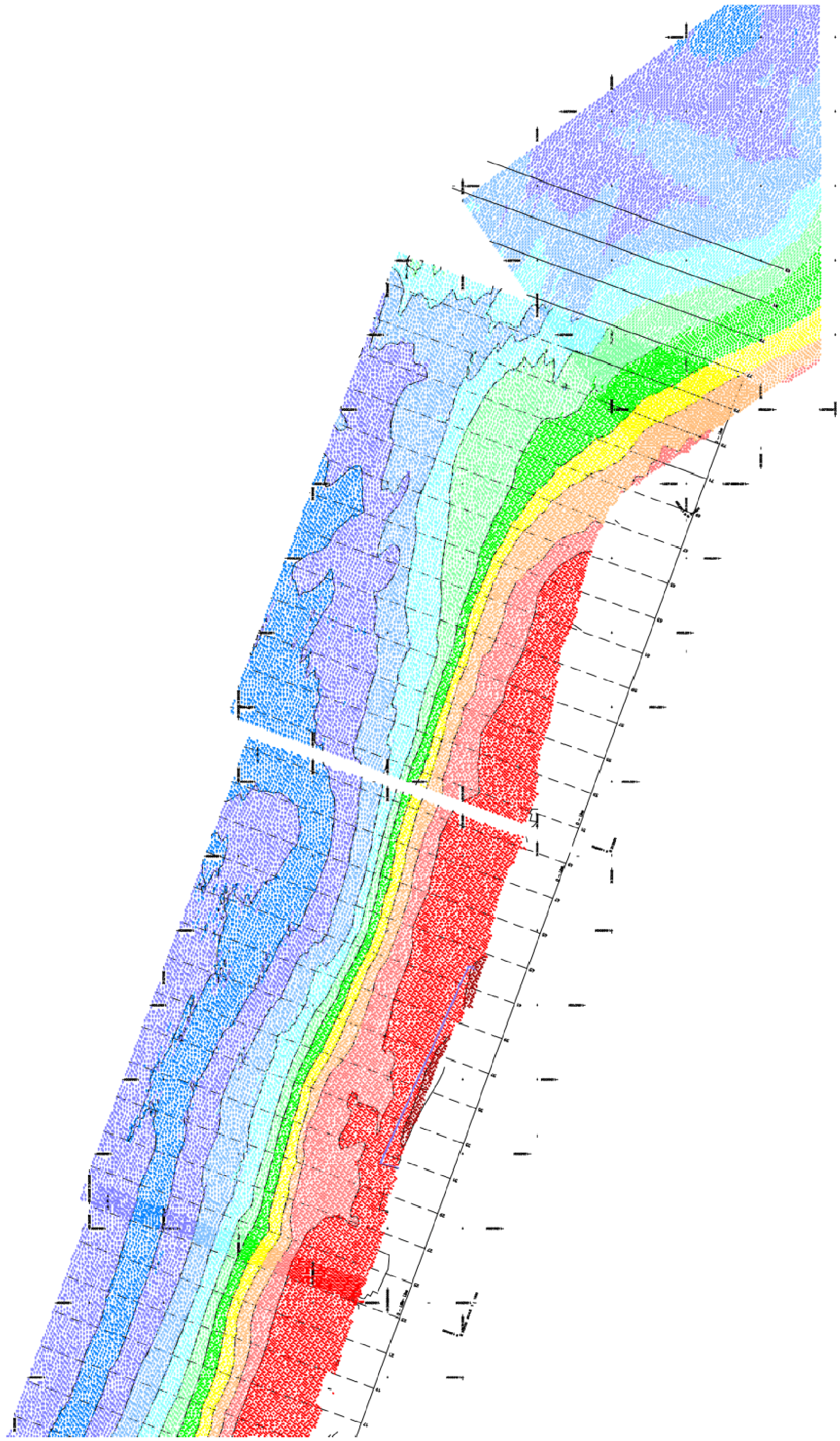

Figure E-12: 2004 out-survey

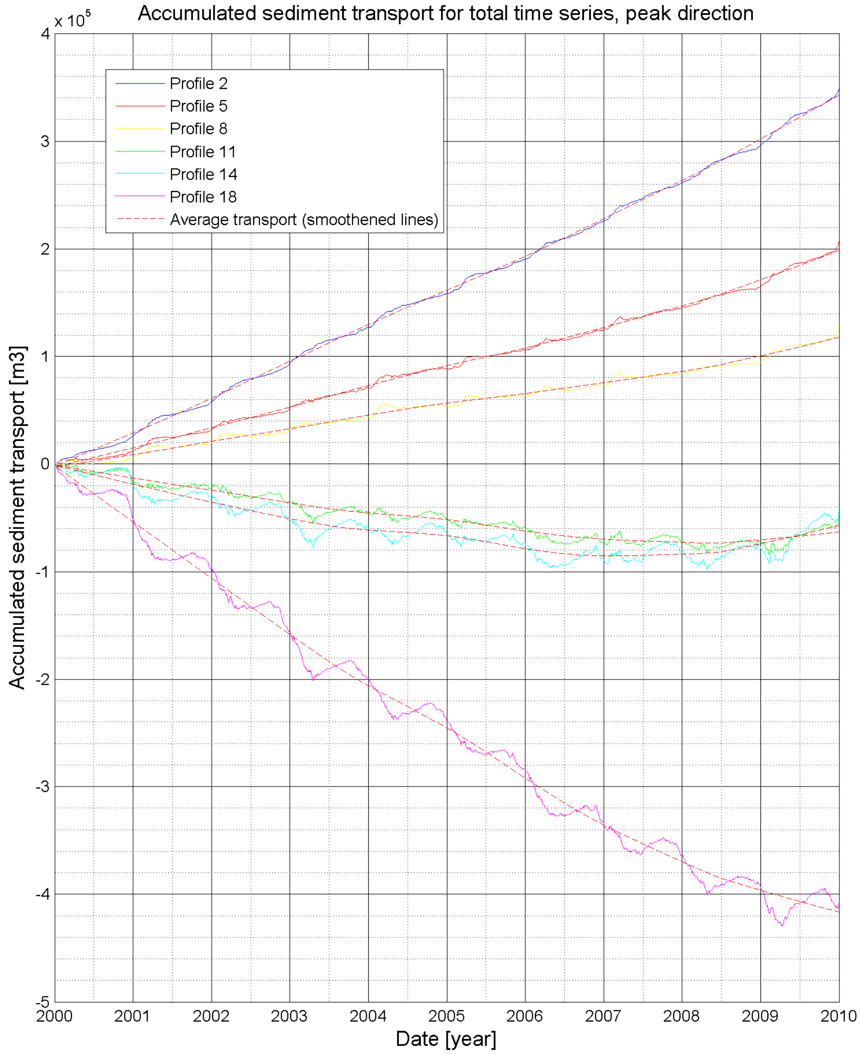

Figure E-13: Accumulated sediment transport for peak direction

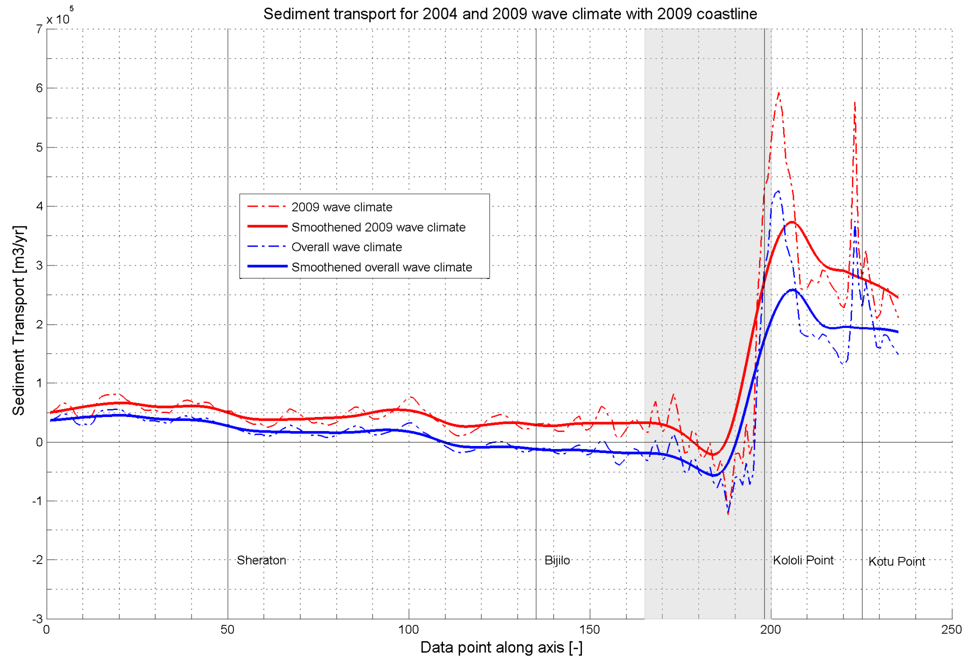

Figure E-14: Computed sediment transport for 2004 and 2009 wave climate for 2009 coastline

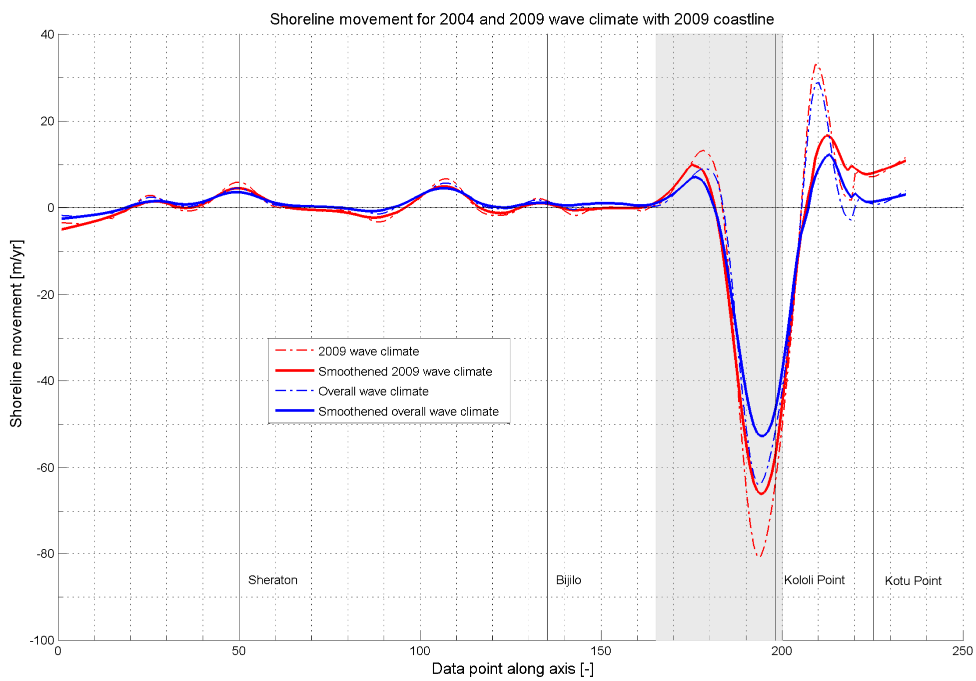

Figure E-15: Computed shoreline movement for 2004 and 2009 wave climate for 2009 coastline

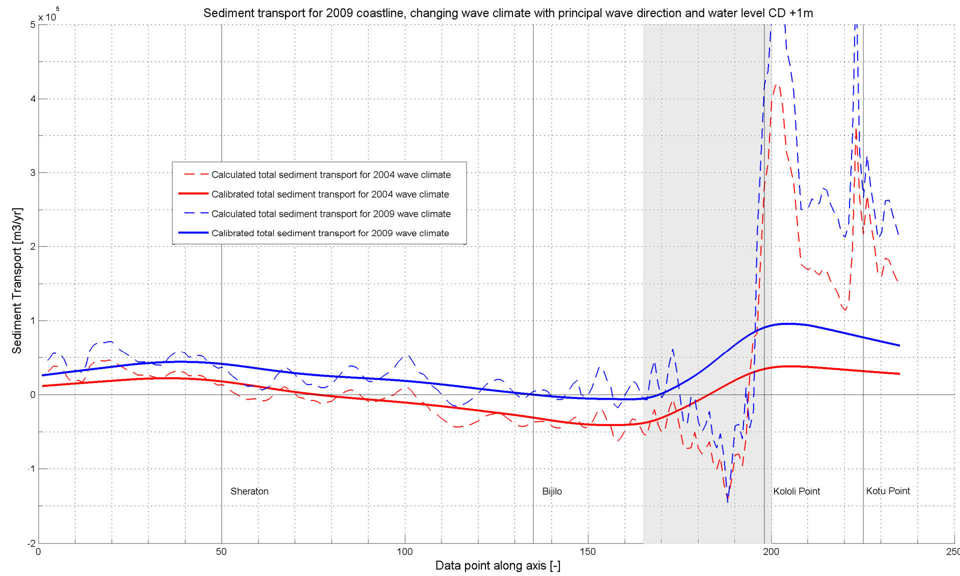

Figure E-16: Sediment transport for mean and 2009 wave climate for 2009 coastline

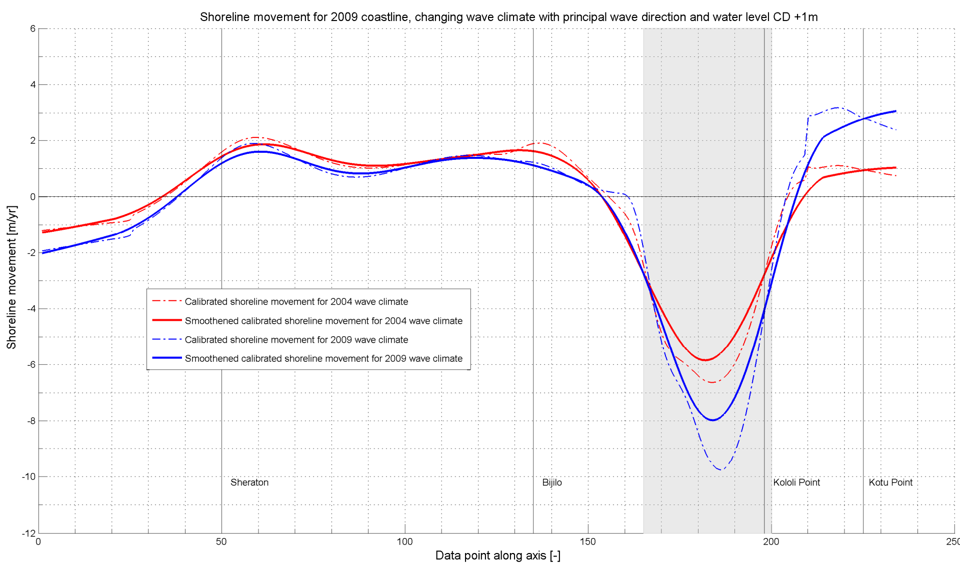

Figure E-17: Shoreline movement for mean and 2009 wave climate for 2009 coastline

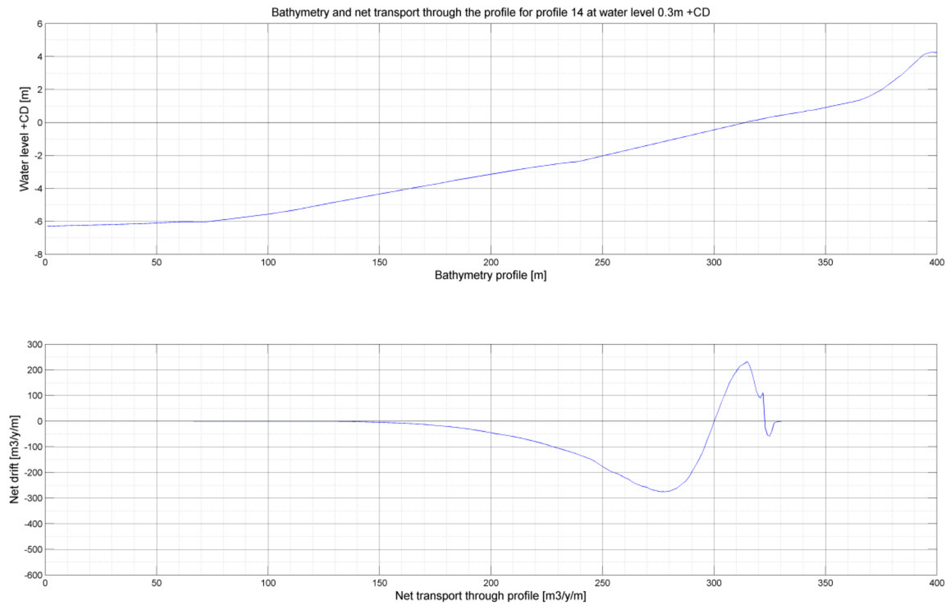

Figure E-18: Cross-shore distribution of alongshore transport for low water level (CD +0.3m)

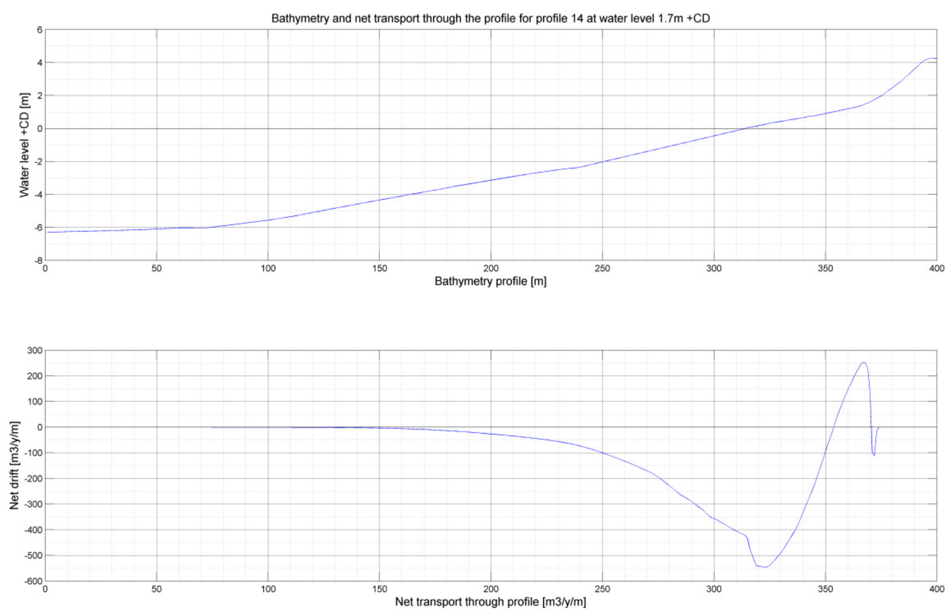

Figure E-19: Cross-shore distribution of alongshore transport for high water level (CD +1.7m)